

Domino Azide-Metallo-carbene Coupling and Nucleophilic Trapping: Synthetic
Applications and Mechanistic Studies.

by

Bren Jordan Perez Atienza

A thesis submitted in partial fulfillment of the requirements for the degree of

Doctor of Philosophy

Department of Chemistry
University of Alberta

©Bren Jordan Perez Atienza, 2016

Abstract

Metallo-carbenes are a class of reactive intermediates used in many strategic and complementary carbon-carbon and carbon-heteroatom bond forming reactions. The Stevens [1,2]-rearrangement of ammonium ylides is an example of a transformation typically involving metallo-carbenes. The replacement of the amine with azide in this metallo-carbene-mediated process results to the formation of an electron-deficient imine; this imine can then be trapped with variety of nucleophiles.

During the course of our study using electron-rich arenes as nucleophilic traps, a key step in the proposed total synthesis of isatisine A, we began to have issues with regioselectivity. In an effort to trouble-shoot this process, we encountered some seemingly anomalous results. Highly inquisitive, mechanistic studies were then undertaken to understand the progress of the reaction. These mechanistic studies resulted in the elucidation of a novel dual catalysis mechanism for this domino process. A library of compounds (truncated analogs of isatisine A) was then made using the newly developed reaction conditions. The mechanism was then used as a guide to develop asymmetric versions of the transformation.

While attempting to apply the newly developed reaction transformation to the synthesis of isatisine A, another opportunity arose. We began exploring the possibility of expanding the existing chemical library through umpolung (reversal of polarity) reactivity. Although we were unable to induce umpolung reactivity of nucleophiles with our rigid electrophilic *C*-acylimines, a different regiodivergent functionalization was developed, opening the door to a greater variety of compounds. This library of new

compounds was then submitted to be screened for potential antiviral activity. After several rounds of structure activity relationship studies, new lead structures were found. This dissertation has many important implications: (1) the potential of the western fragment of isatisine A as a novel antiviral lead, (2) a novel dual catalysis in metallocarbene chemistry utilizing the concept of electrophilic metalation.

Preface

A significant portion of Chapter Two was published in RSC Advances as: Bott, T. M.; Atienza, B. J.; West, F. G. *RSC Adv.*, **2014**, *4*, 31955-31959. Portion of Chapter Three and antiviral assay results will be published as Atienza, B. J.; Jensen, L. D.; Marchant, D.; West, F. G., “Dual Catalytic Synthesis of Antiviral Compounds Based on Click Chemistry,” *Manuscript in preparation*. I was responsible for the preparation and characterization of compounds and preparing the manuscript. Lionel Jensen was responsible for the antiviral assay. Dr. Frederick West and Dr. David Marchant were the supervisory authors and were involved with concept formations and manuscript composition. The remaining portion of Chapter Three will be published as Atienza, B. J.; West, F. G., “Enantioselective Synthesis of Indolinones via Dual Catalysis”, *Manuscript in preparation*. I was responsible for the characterization of compounds and preparing the manuscript. Dr. Frederick West is the corresponding author and was involved in concept formation and manuscript composition. Chapter Four will be published as Zeer-Wanklyn, I.; Atienza, B. J.; West, F.G. “Regiodivergent Functionalization of Rigid *C*-acylimines: Total Synthesis of Halichrome A”. I was responsible for the preparation of the adducts described explicitly in Chapter Four. Issac Zeer-Wanklyn was responsible for the preparation of other compounds that are not described here. Dr. Frederick West is the corresponding author and was involved in concept formation and manuscript composition.

*To my loving grandfather, Daniel, for teaching me the value of hardwork, grit and
patience. May you rest in peace.*

Acknowledgements

Firstly, I would like to thank my advisor, Dr. Frederick “Boss” West, for his endless patience, support and mentorship. Boss, I don’t know if I am going to be able to find an advisor more than capable of tolerating my attitude, stubbornness, curiosity and independence than you did. You are a perfect example of an advisor willing to give your time and guidance during the occasions I needed perspective and boundless space during the instances I wanted to be left alone to cultivate my curiosity. My years in graduate school are full of fond memories and scientific learning, all because you were an excellent team leader. I will forever remember the times when: (1) you told me I have a “nose” for chemistry and (2) you asked me thought-provoking questions, (it made me stronger!). These were all extraordinary.

Secondly, I would like to acknowledge all the previous members of the West group whom I had the chance of working with. My labmates, Yong, Verner and Tom: you guys are awesome and I will forever value the oftentimes-dirty conversations, yet enough to make our days in the lab fun. The serious diazo people: Christine, Nargess and Mandy, I will forever remember the times I talked to you about chemistry, during the subgroup meetings when I was a second year, the “corridor” and group meeting discussions about chemistry and just plain chat about life in general. Christine, I owe you a great deal for proofreading the entirety of my thesis, thank you. You are the real MVP and I hope to see you in Vancouver soon. To the person I consider my chemistry friend Pavan: I am not sure if you hate me or you were just being a complete asshole all the time, but thank you for the “not so boring” trash talk. To my good friend and extremely talented student, Issac, you are a great undergrad and I had fun mentoring you. Not only are you a bloody smart kid but you also have an incredible, down-to-earth attitude. I hope to see you in US (if they still allow a Filipino there! Oh. I still hate the immigration. Boss is one of the few exceptions, though) and please finish your graduate school, get a PhD (or MD), teach and kick some ass with your future amazing publication record and pedigree (make your mentors and supervisors proud).

Thirdly, I would like to thank my examining committee members: Dr. Eric Rivard, Dr. Rylan Lundgren, Dr. Derrick Clive, Dr. Todd Lowary and Dr. Huw Davies (Emory University). These people are specially selected to examine each facets of my dissertation, broad knowledge in the discipline and for that I am truly grateful. I want to single out Dr. Eric Rivard for the amazing discussions and time you extended when I needed the perspective of an inorganic chemist. I am sure that you read my thesis from start to finish, hence I needed heck a lot of time to include your edits but I thank you for the suggestions during my final defense. To the amazing faculty and support staff of University of Alberta, Department of Chemistry, in particular, Dr. Angie Moralez-Izquierdo thank you for all the assistance you stretched for my graduate career. To our collaborators, Dr. David Marchant and Lionel Jensen, thank you for the amazing time in LKS.

Finally, I want to express my deep, sincere gratitude to my family in the Philippines and Canada for the help, guidance and encouragement during my five years in graduate school. To my people, my mom (Guada), dad (Ben), three siblings (Geleen, Gleenah, Brian), granma Lydia and granma Behing, granpa Daniel and grandpa Juan, auntie Nori and auntie Mely, my other uncles and aunties, and all my cousins: thank you! All these years of boundless patience and hardwork from my parents and grandparents is now starting to pay off.

Table of Contents

Chapter One	1
1.1 Overview.....	1
1.2 Introduction.....	2
1.3 Completed syntheses of isatisine A	4
1.3.1 Kerr's total synthesis of (+)-isatisine A: the first total synthesis	5
1.3.2 Panek's total synthesis of (+)-isatisine A: the annulation strategy.....	8
1.3.3 Liang's total synthesis of (-)-isatisine A.....	11
1.3.4 Xie's total synthesis of (-)-isatisine A	14
1.3.5 Ramana's total synthesis of (-)-isatisine A	18
1.4 Conclusion	20
1.5 Proposed Retrosynthesis of Isatisine A	21
1.6 References.....	23
Chapter Two	25
2.1 Introduction.....	25
2.2.1 Preparation of diazocarbonyl compounds and carbene reactive intermediates ...	28
2.2.2 Structure and reactivity of free carbenes	29
2.2.3 Structure and reactivity of metallocarbenes or carbenoids	30
2.2.4 Reactivity of metallocarbenes with nitrogen nucleophiles	33
2.2.4.1 Reactions of metallocarbenes with amines	35
2.2.4.2 Reactions of metallocarbenes with imines.....	37
2.2.4.3 Reactions of metallocarbenes with nitriles	37
2.2.4.4 Reactions of metallocarbenes with amides	38

2.3 Reactions of metallocarbenes with azides	39
2.3.1 Intramolecular rhodium (II) carbene interception with an azide.	40
2.3.2 Intermolecular rhodium (II) carbene interception with an azide.	42
2.3.3 Intramolecular copper(I) carbene interception with an azide.	44
2.4 Results and Discussion	45
2.4.1 Preparation and Stability of Starting Materials.....	46
2.3.2 Survey of reaction conditions	50
2.3.3 Scope of the optimized reaction conditions	52
2.3.4 Formation of a <i>C</i> -acylimine intermediate from dicarbonyl-stabilized diazo and subsequent trapping with nucleophiles	54
2.3.5 Proposed mechanism for the transformation	60
2.4 Summary	61
2.5 Experimental	62
2.5.1 General Information.....	62
2.6 References.....	80
Chapter Three	85
3.1 Introduction.....	85
3.2.1 Pertinent precedents in metallocarbene chemistry.....	87
3.2.2 Known representative precedents on electrophilic metalation	90
3.2.3 Hypothetical solution to the current problem	94
3.3 Results and discussion	95
3.3.1 Survey of reaction conditions	95
3.3.2 Mechanistic considerations	100

3.3.2.1 What is the copper oxidation state in the catalytic cycle?	100
3.3.2.2 How does the copper (I) form in solution from a copper (II) pre-catalyst?	103
3.3.2.3 Which species catalyzes the Friedel- Crafts alkylation?.....	106
3.3.2.4 Combining all the information: the proposed catalytic cycles.....	110
3.3.3 Scope of the reaction.....	111
3.4. Part II: asymmetric preparation of indol-3-one adducts	116
3.4.1 Asymmetric preparation of indol-3-one adducts using chiral auxiliary.	117
3.4.2 Asymmetric preparation of adducts using chiral phosphoric acid co-catalyst: attempts to correlate pKa with the enantioselectivity.	122
3.4.3 Product isomerization experiment	128
3.5 Conclusions.....	130
3.6 Experimental.....	131
3.6.1 General Information.....	131
3.7 References:.....	165
Chapter Four	169
4.1 Introduction.....	169
4.2 Results and discussion	170
4.2.1 Strategy using a late stage azide metallocarbene coupling/indole addition.....	170
4.2.2 Strategy using early stage azide metallocarbene coupling/indole addition	173
4.4 Experimental.....	189
4.4.1 General Information.....	189
Chapter Five.....	204
Summary and Future Directions.....	204

Bibliography	207
Chapter Three:	213
Appendix I: X-ray Crystallographic Data for compound 29d . (Chapter Two)	219
Appendix II: X-ray Crystallographic Data for compound 22 (Chapter Three)	231
Appendix III: X-ray: Crystallographic Data for compound 55a . (Chapter Three).....	244
Appendix IV: X-ray Crystallographic Data for compound 59a (Chapter Three).....	260
Appendix V: Selected NMR Spectra (Chapter Three)	277
Appendix VI: Mechanistic studies (Monitoring Decomposition of Diazo Azide in the Presence of Copper (I) catalyst, Using NMR Spectroscopy) (Chapter Three).....	285
Appendix VII: Mechanistic studies (Comparison of Diazo Azide Decomposition In the Presence of Copper(II) and Copper(I) Catalyst) (Chapter Three)	287
Appendix VIII: Mechanistic studies (Detection of Dimer, Indicative of Formation of Triflic Acid) (Chapter Three).....	290
Appendix IX: Mechanistic Studies (UV-VIS Detection of Copper Complex) (Chapter Three)	292
Appendix X: Determination of Diastereomeric Ratio Using HPLC	294
Appendix XI: Selected NMR Spectra (Chapter Four).....	297

List of Tables

Table 2.1: Cyclization and trapping of diazo azide 26	53
Table 2.2: Cyclization and trapping of diazo azide 29	56
Table 3.1: Survey of reaction conditions	99
Table 3.2: Scope of the reaction.	115
Table 3.3: Survey of chiral phosphoric acid (CPA) co-catalyst.	126
Table 3.4: Scope of the chiral phosphoric acid (CPA) co-catalyzed reaction.	128

List of Figures

Figure 1.1: Structure of (+)-isatisine A and its acetonide derivative.....	3
Figure 2.1: Representative examples of classic and modern reactive intermediates.....	25
Figure 2.2: Electronic structure of carbene (methylene).	30
Figure 2.3: Fischer metallocarbene vs. Schrock metallocarbene.....	31
Figure 2.4: Differential scanning calorimetry (DSC) report for 29a	48
Figure 2.5: Thermogravimetric analysis (TGA) report for 29a	49
Figure 2.6: ORTEP diagram, derived from X-ray diffraction data of 29d	58
Figure 3.1: Schematic representation of the different mechanisms for C-H activation....	86
Figure 3.2: Reactivity of the diazo with varying number of flanking carbonyl groups and approximated temperature range to initiate the decomposition.	88
Figure 3.3: ORTEP diagram, derived from X-ray diffraction data of the desired regioisomer 22	96
Figure 3.4: Reaction monitoring using IR spectroscopy.	102
Figure 3.5: ORTEP diagram, derived from X-ray diffraction data of the major diastereomer of 55 (55a).	119
Figure 3.6: Structure of the major conformer of the intermediate <i>C</i> -acyliminium ion...	122
Figure 3.7: Other chiral Brønsted acids tested.....	123
Figure 4.1: rOe correlation of the alcohol with the C-H on the indole moiety (23a).	180
Figure 4.2: The structure of halichrome A and metagenebiindole A.	181

List of Schemes

Scheme 1.1: The key Johnson [3+2] cycloaddition	6
Scheme 1.2: Elaboration of tetrahydrofuran 5	6
Scheme 1.3: Introduction of the diol moiety on the allyl ester 7	7
Scheme 1.4: Kerr's endgame on the total synthesis of (+)-isatisine A	8
Scheme 1.5: The key Mukaiyama [3+2] annulation strategy	8
Scheme 1.6: Conversion of intermediate aldehyde 12 to diol protected ester 15	9
Scheme 1.7: Conversion of intermediate carbonate 15 to the hemiaminal 17	10
Scheme 1.8: Conversion of the intermediate lactone 17 to the (+)-isatisine A	11
Scheme 1.9: Aldol reaction with the protected keto triol 19	12
Scheme 1.10: Intramolecular <i>C</i> -glycosylation of 21	12
Scheme 1.11: Oxidative ring contraction of 22	13
Scheme 1.12: Elaboration of the lactam 23	13
Scheme 1.13: Liang's endgame synthesis of (-)-isatisine A	14
Scheme 1.14: Proposed biogenic pathway for (-)-isatisine A	15
Scheme 1.15: Xie's key nucleophilic enolate addition on the <i>C</i> -acylimine 32	16
Scheme 1.16: Xie's key benzylic ester rearrangement	17
Scheme 1.17: Xie's endgame photodeprotection and cyclization	17
Scheme 1.18: Ramana's synthesis of the lactone 37	18
Scheme 1.19: Ramana's synthesis of nitro-alkyne 39	18
Scheme 1.20: Ramana's key nitro-alkyne isomerization of 39	19
Scheme 1.21: Ramana's endgame oxidative lactamization and deprotection of 41	20
Scheme 1.22: Bott's indolinone synthesis	21

Scheme 1.23: Our initial retrosynthesis	22
Scheme 2.1: Illustration of a diverted metallocarbene reaction.....	27
Scheme 2.2: General reactivity of metallocarbene	27
Scheme 2.3: Approaches to diazocarbonyl compounds	29
Scheme 2.4: Mechanism of metallocarbene formation.....	31
Scheme 2.5: Reactivity and selectivity of metallocarbenes.....	33
Scheme 2.6: General reactivity of nitrogen-based nucleophiles on metallocarbene	34
Scheme 2.7: Reaction of metallocarbenes with amines.....	35
Scheme 2.8: Possible mechanisms of Stevens rearrangement.....	36
Scheme 2.9: An example of [2,3]-shift pathway.	36
Scheme 2.10: Reactions of azomethine ylides.....	37
Scheme 2.11: Reactions of nitrile ylides.....	38
Scheme 2.12: Reactions of metallocarbenes with amides.	39
Scheme 2.13: Hypothetical reaction of metallocarbene with azide	39
Scheme 2.14: Wee's interception of metallocarbene with azide	41
Scheme 2.15: Lecourt and Micouin's interception of metallocarbene with azide.....	41
Scheme 2.16: Doyle's interception of metallocarbene with azide.....	42
Scheme 2.17: Doyle's b-lactam synthesis	43
Scheme 2.18: Doyle's multicomponent reaction	43
Scheme 2.19: Doyle's tetrahydropyrimidine synthesis	44
Scheme 2.20: Gu's stereoselective desymmetrization of diazides	44
Scheme 2.21: Gu's diastereoselective desymmetrization of meso diazides	45
Scheme 2.22: Synthesis of monostabilized diazocarbonyl substrate 26	46

Scheme 2.23: Synthesis of dicarbonyl stabilized diazo substrate 29a	47
Scheme 2.24: Synthesis of dicarbonyl stabilized diazo substrate 32	47
Scheme 2.25: Copper-catalyzed decomposition of 26	50
Scheme 2.26: Intermolecular trapping of <i>C</i> -acylimine with 34a	51
Scheme 2.27: Optimized reaction condition for intermolecular trapping of <i>C</i> -acylimine with 34a	51
Scheme 2.28: Further oxidation of 33c	52
Scheme 2.29: Possible equilibration and alternate structure for 29a	57
Scheme 2.30: Synthesis of tryptanthrin from 26 and 37	59
Scheme 2.31: Synthesis of tryptanthrin from 26 and 39	59
Scheme 2.32: Proposed reaction mechanism.....	61
Scheme 3.1: Kochi's cyclopropanation experiment and isolation of Cu(I) complex.....	89
Scheme 3.2: Catalytic electrophilic metalation experiments.....	90
Scheme 3.3: Reisman's concise total synthesis of naseaezine A and B.....	92
Scheme 3.4: Xia's concise total synthesis of protubonine A.....	93
Scheme 3.5: Diazo azide decomposition in the presence of different copper catalyst. ..	101
Scheme 3.6: Proposed mechanism for the reduction of Cu(II) precatalyst.	104
Scheme 3.7: Addition of pyridine and imidazole as catalyst poison.	105
Scheme 3.8: Addition of di <i>tert</i> -butylpyridine poison.....	106
Scheme 3.9: Attempts to isolate the <i>C</i> -acylimine 26 and sequential addition reaction..	108
Scheme 3.10: Comparison of the reactivity of the stable <i>C</i> -acylimine with Cu(I) or Brønsted acid catalyst.....	109
Scheme 3.11: Proposed mechanism of the reaction.....	111

Scheme 3.12: Diastereoselective preparation of bis(indole) adducts using menthol chiral auxiliary.	118
Scheme 3.13: Preparation of (<i>R</i>)-8-phenylmenthol.	120
Scheme 3.14: Diastereoselective preparation of the bis(indole) adducts 58 and 59 using (<i>R</i>)-8-phenylmenthol chiral auxiliary.	121
Scheme 3.15: Enantioselective preparation of 22 using D-CSA chiral co-catalyst.	123
Scheme 3.16: Synthesis of chiral phosphoric acid (CPA) co-catalyst.	125
Scheme 3.17: Kerr and You's indol-3-one synthesis.	129
Scheme 4.1: Proposed late stage Friedel-Crafts alkylation	171
Scheme 4.2: Attempts on initial <i>C</i> -glycosylation	172
Scheme 4.3: Successful attempts to induce <i>C</i> -glycosylation	173
Scheme 4.4: Proposed second retrosynthesis.	174
Scheme 4.5: Representative examples of amide formation	175
Scheme 4.6: Amidation of <i>o</i> -allylaniline with protected ribonolactone	176
Scheme 4.7: Deprotonation of indole 18	177
Scheme 4.8: Attempts to induce Steglich amidation	177
Scheme 4.9: Partial reduction of 18	178
Scheme 4.10: Proposed mechanism for the formation of 23 , 25 , and 26	179
Scheme 4.11: Literature examples of α -iminocarbonyl umpolung reactivity.	183
Scheme 4.12: Regiodivergent reactivity of σ -type nucleophiles	184
Scheme 4.13: Total synthesis of halichrome A	185
Scheme 4.14: Diversity with the Grignard reagents	186
Scheme 4.15: Other <i>C</i> -acylimines amenable to regiodivergent functionalization	187

Scheme 4.16: Potential domino umpolung functionalization	187
Scheme 4.17: Kinetic and thermodynamic addition of siloxyfuran	188
Scheme 5.1: More comprehensive SAR and SSAR analysis	205
Scheme 5.2: Another potential retrosynthesis	206

List of Symbols and Abbreviations

^1H	proton
^{13}C	carbon-13
Å	angstrom
Ac	acetyl
Ac ₂ O	acetic anhydride
$[\alpha]_{\text{D}}^{20}$	specific rotation at 20°C and wavelength of sodium D line
app.	apparent (spectral)
aq	aqueous solution
Ar	aryl
B:	unspecified base
Bn	benzyl
BOM	benzyloxymethyl
br	broad (spectral)
Bu	butyl
<i>c</i>	concentration
°C	degrees Celsius
ca.	approximately
calcd	calculated
cat.	indicates that the reagent was used in a catalytic amount
CDI	1,1-carbonyldiimidazole
cm ⁻¹	wave numbers
COSY	H-H correlation spectroscopy

conc.	concentrated
CPA	chiral phosphoric acid
CSA	camphorsulfonic acid
d	day(s); doublet (spectral)
DBU	1,8-diazabicyclo[5.4.0]undec-7-ene
DCC	N,N'-dicyclohexylcarbodiimide
DCE	1,2-dichloroethane
DCM	dichloromethane
δ	chemical shift (NMR)
dd	doublet of doublets (spectral)
ddd	doublet of doublet of doublets (spectral)
dddd	doublet of doublet of doublet of doublets (spectral)
dba	dibenzylideneacetone (ligand)
DFT	density functional theory
DIAD	diisopropyl azodicarboxylate
DIBAL-H	diisobutylaluminum hydride
DIPEA	diisopropylethylamine (Hunig's Base)
DMAP	4-dimethylaminopyridine
DMF	N,N-dimethylformamide
DMSO	dimethylsulfoxide
DMP	Dess-Martin periodinane
d.r.	diastereomeric ratio
dt	doublet of triplets (spectral)

dtbpy	di <i>tert</i> -butylpyridine
dtd	doublet of triplets of doublets (spectral)
E ⁺	unspecified electrophile
EC ₅₀	50% effective concentration
EDG	electron-donating group
e.e.	enantiomeric excess
EI	electron impact (mass spectrometry)
ent	enantiomer
e.r.	enantiomeric ratio
ESI	electrospray ionization (mass spectrometry)
Et	ethyl
EtOAc	ethyl acetate
EtOH	ethanol
equiv.	equivalent(s)
EWG	electron-withdrawing group
g	gram(s)
h	hour(s)
Hex	hexyl
HMBC	heteronuclear multiple bond coherence (spectral)
HMPA	hexamethylphosphoramide
HOBt	1-hydroxybenzotriazole
HPLC	high-pressure liquid chromatography
HSQC	heteronuclear single quantum coherence (spectral)

HRMS	high resolution mass spectrometry
$h\nu$	light
Hz	hertz
IC ₅₀	50% inhibitory concentration
<i>i</i> -Pr	isopropyl
IR	infrared
<i>J</i>	coupling constant
kcal	kilocalories
L	litre(s); unspecified ligand
LA	Lewis acid
LDA	lithium diisopropylamide
LHMDS	lithium bis(trimethylsilyl)amide
L _n *	chiral ligand
M	molar
m	multiplet (spectral)
M ⁺	generalized Lewis acid; molecular ion
Me	methyl
Mes	mesityl
mg	milligram(s)
MHz	megahertz
ML _n	unspecified metal-ligand pair
μL	microlitre(s)
μW	microwave(s)

min	minute(s)
mL	millilitre(s)
mm	millimeter(s)
mmol	millimole(s)
mol	mole(s)
Me	methyl
mg	milligram(s)
MOM	methoxymethyl
<i>m</i> -CPBA	<i>meta</i> -chloroper(oxy)benzoic acid
mp	melting point
min	minute(s)
mL	milliliter(s)
μM	micromolar
μW	microwave
mM	millimolar
MS	molecular sieves
Ms	methanesulfonyl
m/z	mass to charge ratio
<i>n</i> -Bu	normal butyl
nm	nanometer
N	normality (concentration)
NMO	<i>N</i> -methylmorpholine N-oxide
NMR	nuclear magnetic resonance

NOE	nuclear overhauser effect
<i>n</i> -Pr	normal propyl
Nuc	unspecified nucleophile
OMOM	methoxymethyl ether
ORTEP	oak ridge thermal-ellipsoid plot
Ph	phenyl
ppm	parts per million
Pr	propyl
PTAB	phenyltrimethylammonium perbromide
R	generalized alkyl group of substituent
rds	rate determining step
R_f	retention factor (in chromatography)
rOe	rotating-frame Overhauser enhancement
rt	room temperature
s	singlet (spectral)
sat'd	saturated
t	triplet (spectral)
T	temperature
TBS	tert-butyldimethylsilyl
TBA	tetrabutylammonium (TBAF or TBAI)
<i>t</i> -Bu	tert-butyl
TEA	triethylamine
TEMPO	(2,2,6,6-tetramethylpiperidin-1-yl)oxidanyl

TES	triethylsilyl
Tf	trifluoromethanesulfonyl
TFA	trifluoroacetic acid
TFAA	trifluoroacetic anhydride
THF	tetrahydrofuran
TIPS	triisopropylsilyl
TLC	thin layer chromatography
TMS	trimethylsilyl; tetramethylsilane (spectral)
Tol	tolyl
TROESY	transverse rotating-frame overhauser enhancement spectroscopy
Ts	p-toluenesulfonyl
TsOH	p-toluenesulfonic acid
X	variable substituent (alkyl, heteroatom, proton, etc.)
δ	chemical shift
Δ	heated to reflux

Chapter One

Isatisine A: the complex architecture and bioactivity that marvels many.

“Nature continues to be exceedingly generous to the synthetic chemist in providing ample opportunity for discovery and creative endeavor of highest magnitude and in surrounding him with an incredible variety of fascinating and complicated structures.”

--E. J. Corey--

1.1 Overview

This dissertation covers an extensive array of topics compiled through the course of a graduate career, from synthesis of highly energetic compounds containing both azide and diazo functional groups to reactions with transition metals and domino trapping with nucleophiles. From elucidation of novel dual catalysis to extension in asymmetric synthesis, and from total synthesis of natural products to uncovering lead compounds with encouraging antiviral activities. Despite the mixture of disparate topics in fundamental and applied chemistry that dissects each chapter of this dissertation, the common string that binds them together and makes it uniquely cohesive is the author’s desire to build pieces of isatisine A using novel fundamental reactions, and consequently to understand the molecular structure and its application bequeathed by nature. In this chapter, a narrative covering the isolation of isatisine A and its subsequent total synthesis by five research groups is imparted. A review covering the reactivity of carbenes and metallocarbenes – generated from the exposure of base metals with diazo compounds – with nitrogen nucleophiles is presented in the introduction of Chapter Two. The presentation of two reviews is a conduit, to guide the reader, connecting our retrosynthetic analyses, using a disconnection approach, to the heart of this dissertation – the synthesis.

The focal content of Chapter Two is our journey to the successful construction of the 3-indolinone skeleton of isatisine A using novel copper catalyzed azide-metallocarbene coupling and subsequent trapping of *C*-acylimines, mainly with Mukaiyama-type nucleophiles and active methylenes. The work of this chapter was pioneered by Dr. Tina Marie Bott, a previous alumna of the West group, and has been extended by the author of this dissertation.

Chapter Three illustrates the effective execution of novel dual catalysis utilizing byproducts of electrophilic metallation of copper and electron-rich arenes to assemble approximately two-thirds of the carbon skeleton (the western fragment) of Isatisine A in one pot. Studies on the mechanism and an asymmetric version of this methodology employing a binary combination of transition metal catalyst and organocatalyst are equally highlighted in this chapter.

Finally, Chapter Four narrates the application of some of the adducts described in Chapters Two and Three in the total synthesis of a marine alkaloid with indolinone skeleton exploiting regiodivergent reactivity of several σ - and π -type nucleophiles under controlled conditions. The attempt to efficiently implement chelation effects via telescoped synthesis to access umpolung reactivity of *C*-acylimines is also briefly discussed in this chapter. The author gratefully acknowledges the significant contributions of an undergraduate researcher, Issac Zeer-Wanklyn, to the work highlighted in this chapter.

1.2 Introduction

Isatis indigotica Fort. (Cruciferae) is a terrestrial, herbaceous plant species broadly cultivated in China, and has been widely used as a traditional Chinese medicine for the treatment of several viral infections.¹ In 2007, Chen and co-workers reported the isolation of isatisine A **1**

from *Isatis indigotica* Fort. collected from Anhui province in China; apparently, it is the only alkaloid among 12 compounds isolated previously from *I. Indigotica*. In the initial isolation foray, the natural products chemists obtained 64 mg of crystalline isatisine A as its acetonide derivative **2** from 50 kg of air-dried powdered leaves (0.000128 wt. %), and the basic skeleton was deduced using extensive 1D and 2D NMR experiments. X-ray crystallographic analysis further confirmed the structural assignment, as well as the relative stereochemistry of **2**. The solid state structure, derived from X-ray diffraction data, revealed that the isatisine A acetonide **2**, is comprised of an indol-3-one scaffold with two distinct substituents at the C-2 position, a branching indole and a D-ribose derived moiety in the furanose form. The carbon next to the anomeric centre of the D-ribose moiety and the nitrogen of the indol-3-one are also locked through an additional carbonyl group to form the lactam ring structure.

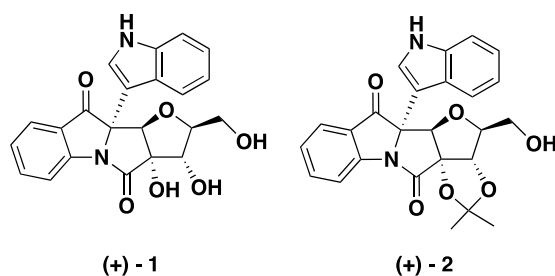


Figure 1.1: Structure of (+)-isatisine A and its acetonide derivative.

Incidentally, the rarity with which acetonide functionality such as that found in **2** occurs in nature encouraged the isolation chemists to further examine whether **2** is a real natural product or a resultant artifact after chromatographic purification of **1** due to the use of acetone as part of the eluent system. The natural products chemists hydrolyzed **2** under acidic conditions to afford **1**, then, using the HPLC profile of the crude leaf extract and the retention time obtained for **1** and **2**, Chen and co-workers were able to prove that **2** is indeed an artifact and **1** is the real natural product.

Although the relative stereochemistry of **1** was unambiguously established by NMR and X-ray crystallography, the absolute configuration of **1** remained unknown. After the first total synthesis of (+)-isatisine A by the Kerr group,² at the Western University, it was postulated that the absolute configuration originally published by the Chen group is structurally antipodal to the isolated alkaloid. Synthetically, the challenging structural features posed by isatisine A **1** include: a fused tetracyclic framework containing a regioselectively oxidized indole derivative, indol-3-one, and a densely functionalized furan subunit with a five contiguous stereocentres, which include two tetrasubstituted carbon centers entrenched in the core. It is also interesting to note that the acetonide derivative **2** also exhibited a moderate cytotoxicity against C8166 with $CC_{50} = 302 \mu\text{M}$ (cytotoxic concentration at which cell viability is reduced by half) and anti-HIV activity with an $EC_{50} = 37.8 \mu\text{M}$ (effective concentration at which viral replication is reduced by half) making it an attractive target for further drug development. Due to the insufficiency of the amount of the real natural product for complete bioassay, the full bioactivity of the natural product isatisine A **1** remained unknown.¹

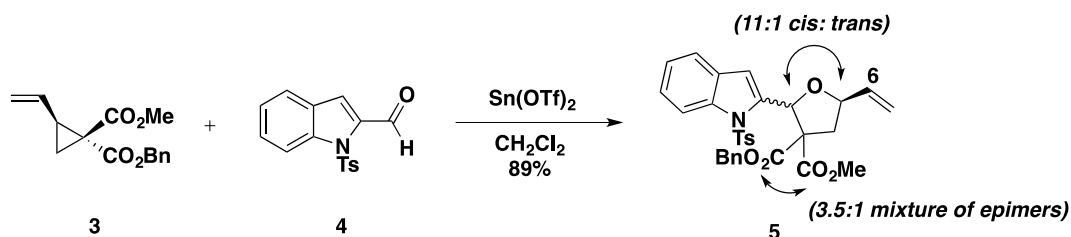
1.3 Completed syntheses of isatisine A

The unique architecture of isatisine A, which features a fused-tetracyclic skeleton, a branching indole, and a highly hydroxylated tetrahydrofuran, as earlier stated, stimulates creative strategies to assemble these pieces. The structural challenges of this target also provide an ideal testing ground for the application of synthetic methodologies developed by different research groups. Equally important is the antiviral activity and moderate cytotoxicity exhibited by this compound using cell-based assays. In this vein, it is not surprising that several research groups finished the synthesis of isatisine A. To date there have been five completed total syntheses of isatisine A.

In 2010, the Kerr group reported the first total synthesis of (+)-isatisine A. Their pioneering total synthesis included the reassignment of the absolute configuration depicted in the initial report by natural products chemist.² The successful total synthesis by the Kerr group was immediately followed by the two separate total syntheses by the Panek group (2011)³ at Boston University and a total synthesis by the Liang group (2011)⁴ at Nankai University. The Panek group employed a silyl-directed Mukaiyama [3+2] cycloaddition, while the Liang group elaborated a known carbohydrate member of the “chiral pool” – D-ribose –, to assemble the challenging tetrahydrofuran core. A year later, the Xie group (2012) at Lanzhou University disclosed a biogenesis proposal concerning the origin of isatisine A together with their version of the biomimetic synthesis.⁵ Soon after, the Ramana group (2012) at the CSIR-National Chemical Laboratory in India reported another total synthesis of isatisine A and its derivatives utilizing impressive combination of various metal-mediated reactions.⁶ In each of these syntheses, creative synthetic approaches to construct the densely functionalized tetrahydrofuran and 3-indolinone cores were the main highpoints.

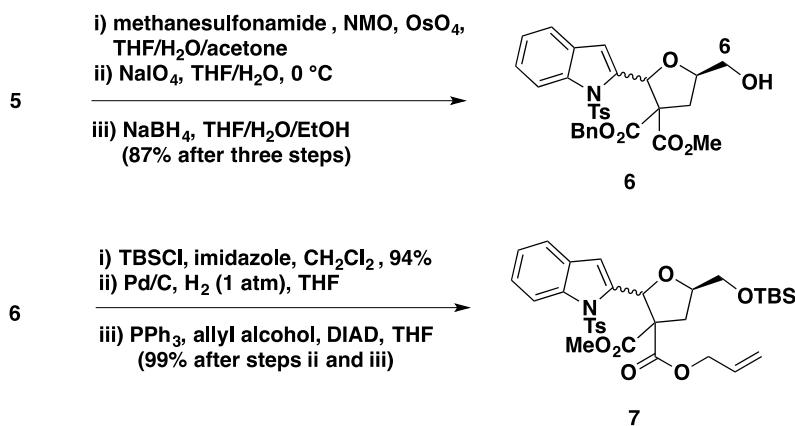
1.3.1 Kerr’s total synthesis of (+)-isatisine A: the first total synthesis²

In 2010, Kerr and Karadeolian strategically employed the Johnson [3+2] cycloaddition,⁷ in the synthesis of (+)-isatisine A, to form the tetrahydrofuran moiety from a donor-acceptor cyclopropane **3**⁸ and an aldehyde **4**. The Johnson [3+2] cycloaddition reaction of cyclopropane **3** with aldehyde **4** was achieved using catalytic amount of Sn(OTf)₂ to provide the tetrahydrofuran **5** in 89% yield as a useful mixture of 2,5-*cis* and 2,5-*trans* diastereomers (11:1) in favor of the desired *cis* diastereoisomer (Scheme 1.1).



Scheme 1.1: The Johnson [3+2] cycloaddition.

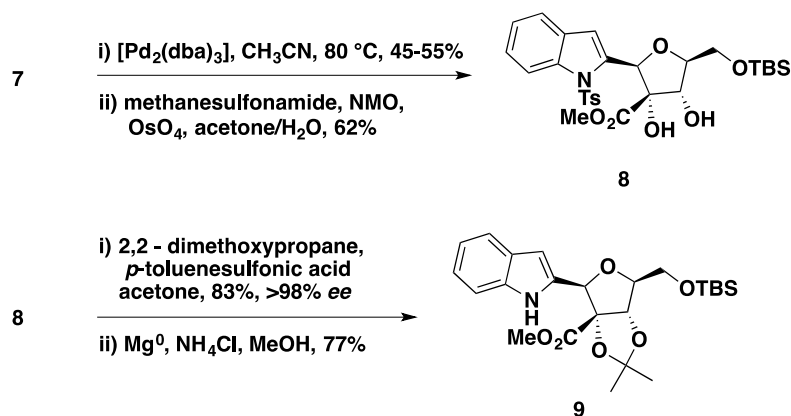
The alcohol at the C-6 position of **1** was installed in a three-step synthesis from the pendent alkene moiety utilizing a combination of OsO₄ and NMO, followed by cleavage of the diol by NaIO₄ and subsequent reduction by NaBH₄ to afford the intermediate tetrahydrofuran **6** in an 87% overall yield. In order to attach the requisite diol, **6** was protected as a silyl ether and debenzoylation of the benzyl ester was carried out prior to the introduction of allyl ester moiety under Mitsunobu conditions. The isolated yield of allyl ester **7** after three steps was reportedly 99% (Scheme 1.2).



Scheme 1.2: Elaboration of tetrahydrofuran 5.

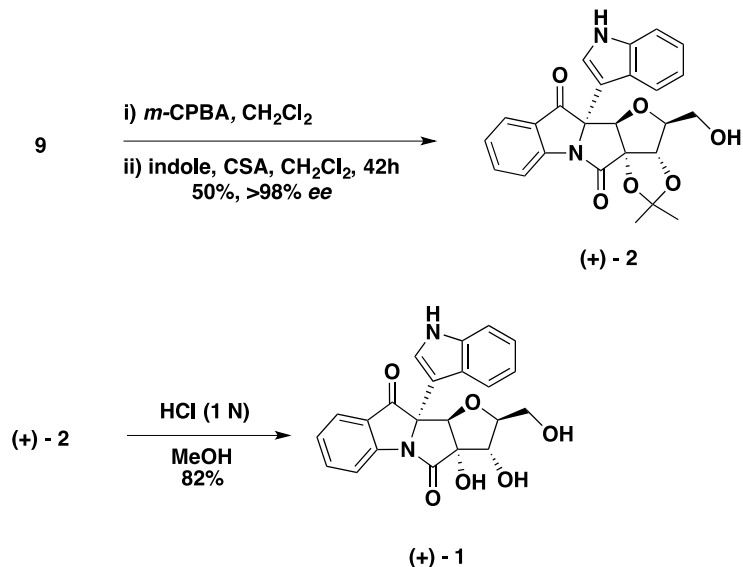
The enone precursor to the *cis*-diol methyl ester, was synthesized through a Pd-catalyzed deallylation and decarboxylation of the allyl ester **7**. Diastereoselective dihydroxylation of the intermediate from the less sterically encumbered β -face of the olefin to introduce the required hydroxyl groups was completed using OsO₄ and NMO, giving a moderate 62% yield from the

allyl ester **7**. The diol was then protected as its acetonide in 83% yield, and a greater than 98% enantiomeric excess. This step was followed by deprotection of the *N*-tosyl group by a dissolving metal reduction to produce the desired indole **9** in 77% yield (Scheme 1.3).



Scheme 1.3: Introduction of the diol moiety on the allyl ester **7.**

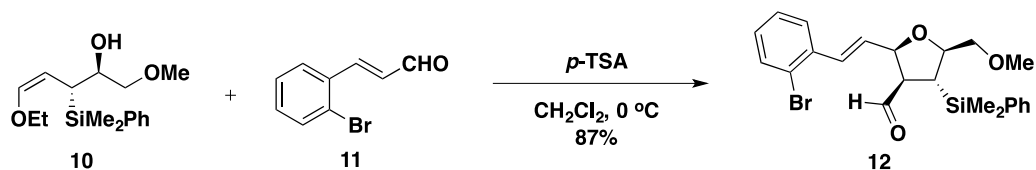
The indole branch present in **1**, was then introduced through the oxidation of intermediate indole **9** using *m*-CPBA oxidation and a subsequent Friedel-Crafts alkylation reaction. Finally, the deprotection of the acetonide group under mild acidic conditions successfully furnished the desired isatisine A (+)-**1** in a 5.8% yield, over a total of 14 formal steps. Furthermore, the synthetic isatisine A, of which the absolute configuration was ensured using optically pure starting materials in the total synthesis, showed the opposite optical rotation of the reported value, indicating that the synthetic isomer was the enantiomer of the structure depicted in the isolation paper by Chen and coworkers (Scheme 1.4).



Scheme 1.4: Kerr's endgame on the total synthesis of (+)-isatisine A.

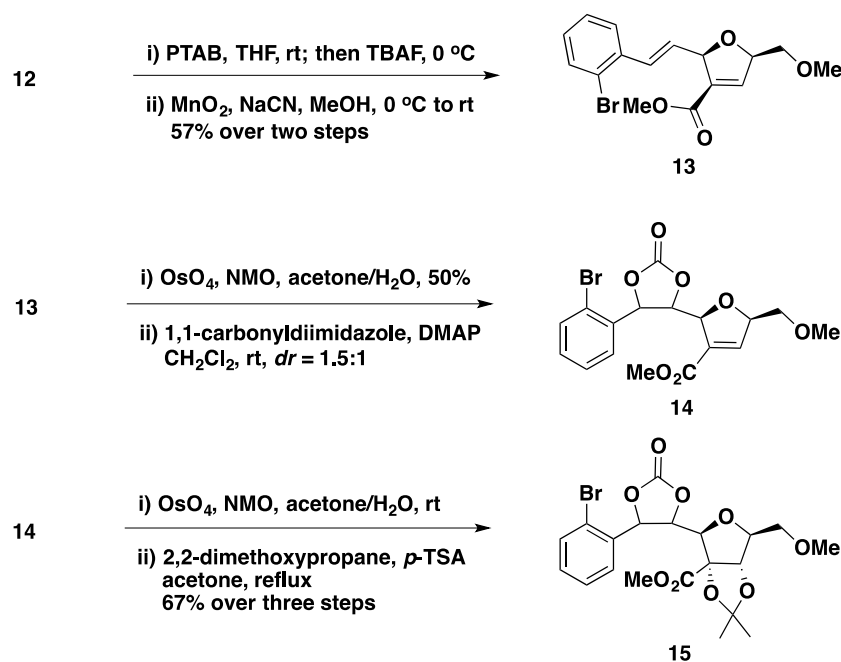
1.3.2 Panek's total synthesis of (+)-isatisine A: the annulation strategy³

The key element of the successful total synthesis of (+)-isatisine A by Panek and Lee was the silyl-directed Mukaiyama-type [3+2] annulation strategy to access the substituted tetrahydrofuran core. This exquisite methodology to provide the tetrahydrofuran core with the right stereochemistry in place was developed in the laboratory of James Panek at Boston University.⁹ Panek initiated the synthesis of the natural product with the successful reaction of silane **10**, which was readily prepared using a literature procedure developed by the same group in 2006,¹⁰ with 2-bromocinnamyl aldehyde **11** to readily furnish the desired tetrahydrofuran **12** in an 87% yield (Scheme 1.5).



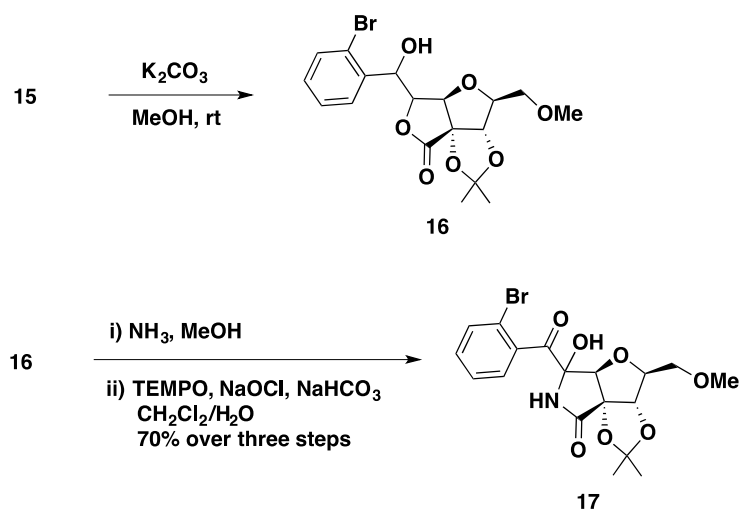
Scheme 1.5: The key Mukaiyama [3+2] annulation strategy.

Subsequent conversion of the aldehyde **12** to the enone **13** using PTAB followed by TBAF,¹¹ and then Corey-Ganem oxidation using MnO₂ in MeOH,¹² successfully secured ester intermediate **13** in a 57% yield over two steps. To synthesize the required protected diol intermediate **15**, Panek and Lee used OsO₄/NMO combination to furnish the desired adduct in a modest 50% yield, and a poor diastereomeric ratio of 1.5:1. The stereochemistry of the diol, however, was inconsequential, since the chiral centre would be oxidized to introduce the required aminal in the next step. The mixture was protected as a carbonate using 1,1-carbonyldiimidazole and DMAP to afford enone carbonate **14**. The mixture was carried forward to the next reaction without further purification. The carbonate **14** was oxidized again with OsO₄ and NMO to afford the required diol, which was immediately protected as acetonide, in a 67% yield over three steps (Scheme 1.6).



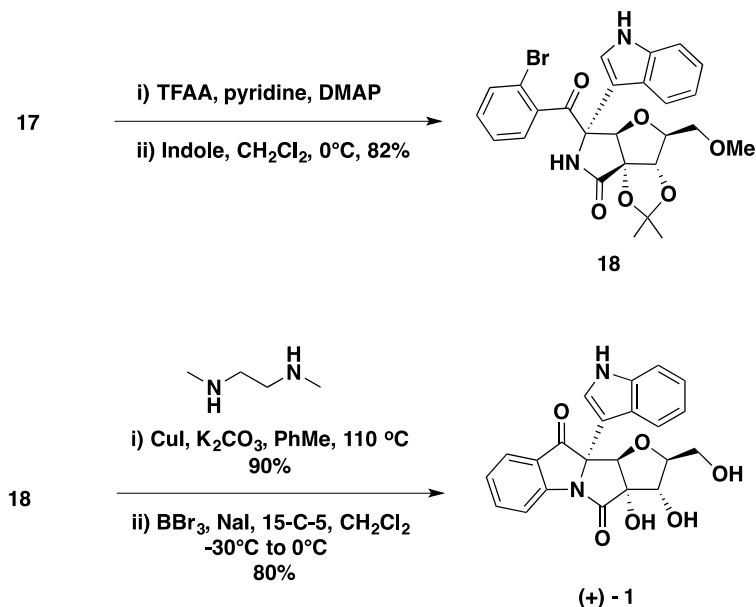
Scheme 1.6: Conversion of intermediate aldehyde 12 to diol protected ester 15.

Treatment of protected diol **15** with potassium carbonate in MeOH readily afforded lactone **16**. Use of ammonia in MeOH, followed by oxidation using TEMPO and NaOCl under Pinnick's reaction conditions over three separate steps afforded the hemiaminal **17** in a 70% yield. At this point, the author did not comment on the stereochemistry of the hemiaminal **17** (Scheme 1.7).



Scheme 1.7: Conversion of intermediate carbonate 15 to the hemiaminal 17.

The desired indole branch was stereoselectively introduced by converting the alcohol in **17** to triflate using TFAA and DMAP in pyridine, and then adding indole to the convex face of the ensuing *N*-acyliminium intermediate. The synthesis was completed through a CuI-mediated coupling in a 90% yield, followed by a BBr₃ mediated cleavage of the primary methyl ether and the acetonide to the corresponding alcohol present in (+)-**1** in an 80% yield (Scheme 1.8).

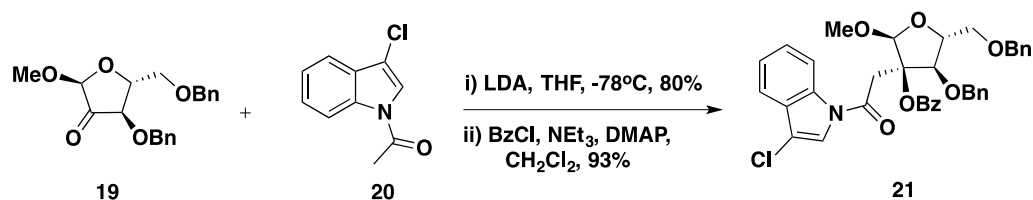


Scheme 1.8: Conversion of the intermediate lactone 17 to the (+)-isatisine A.

The total synthesis of (+)-**1** by Panek and Lee was achieved in 13 steps with a 6.9% overall yield, utilizing a silyl-directed Mukaiyama-type [3+2] annulation strategy and CuI-mediated amidation to secure the desired lactam ring in (+)-**1**.

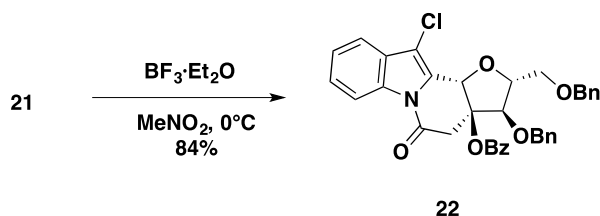
1.3.3 Liang's total synthesis of (-)-isatisine A⁴

The key features in Liang's total synthesis of (-)-isatisine A are the unprecedented intramolecular C-glycosylation and oxidative ring contraction to construct the densely substituted tetrahydrofuran moiety. Liang and co-workers initiated their synthesis using a protected keto-triol **19**, which was readily synthesized in four steps using a literature procedure.¹³ An aldol reaction between **19** and the lithium enolate of 3-chloro-*N*-acetyl indole **20**, followed by benzylation of the resulting alcohol furnished indole **21** (Scheme 1.9).



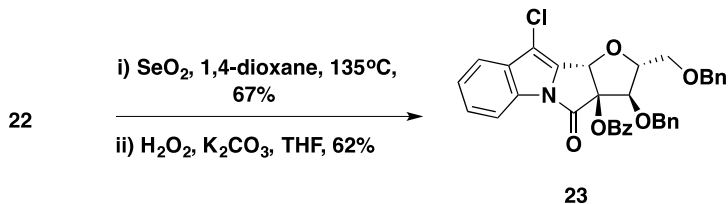
Scheme 1.9: Aldol reaction with the protected keto triol 19.

The indole **21** then underwent intramolecular *C*-glycosylation in the presence of BF₃·OEt₂ to furnish lactam **22** in 84% yield. It is important to note that this transformation is the first demonstration of *C*-glycosylation at the 2-position of an indole with an unactivated anomeric furanose centre. With compound **22** in hand, Liang and co-workers proceeded to examine the α -oxidation reaction of the lactam **22** (Scheme 1.10).



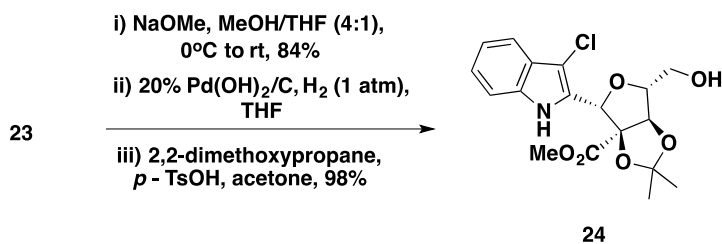
Scheme 1.10: Intramolecular C-glycosylation of 21.

Treatment of **22** with SeO₂ directly afforded the desired intermediate dicarbonyl compound, which easily underwent oxidative ring contraction in the presence of hydrogen peroxide to furnish the advanced tetracyclic lactam **23** in 67% and 62% yield respectively (Scheme 1.11).



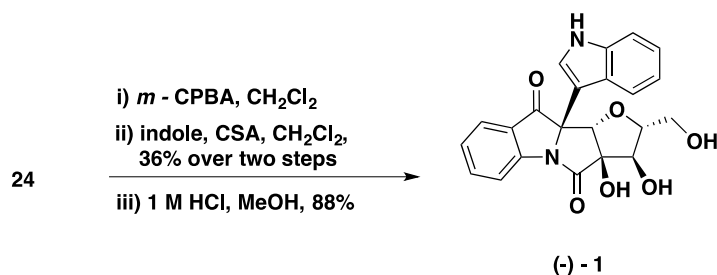
Scheme 1.11: Oxidative ring contraction of 22.

Lactam **23** was debenzoylated using NaOMe, which also opened the amide to the corresponding ester and amine. The benzyl group was readily deprotected using conventional hydrogenolysis conditions. The intermediate diol was then protected to furnish ester **24** in a greater than 80% yield over three steps (Scheme 1.12).



Scheme 1.12: Synthetic elaboration of the lactam 23.

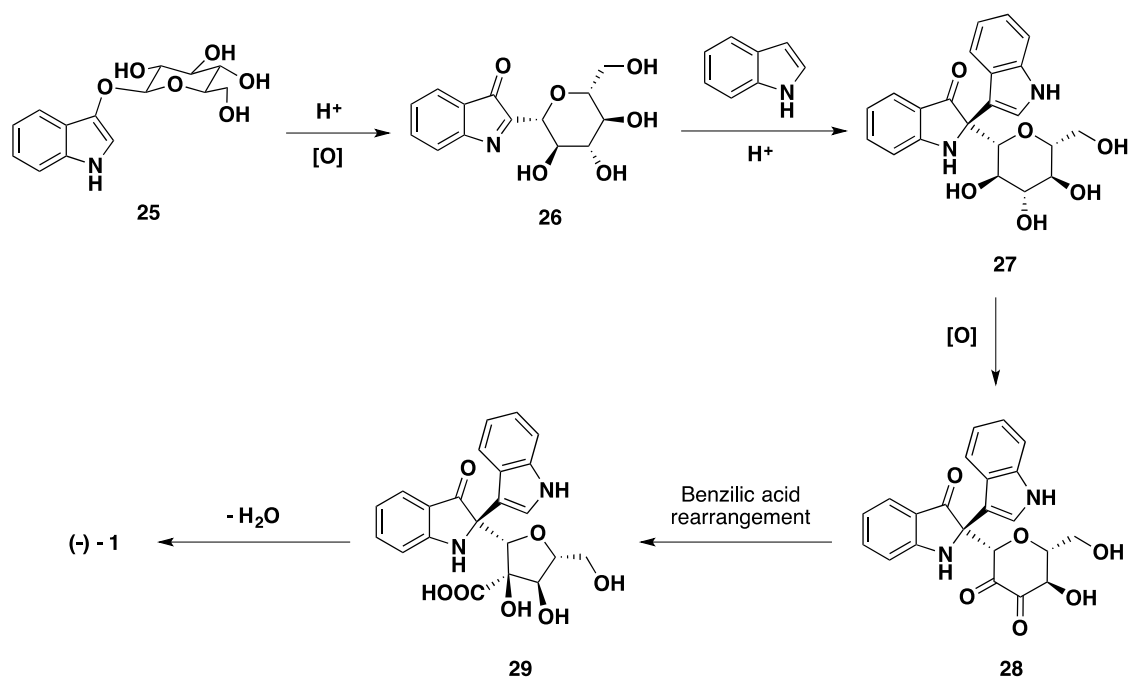
Following the oxidation protocol employed by Kerr and Karadeolian using *m*-CPBA and subsequent indole addition of the resulting aminal,² ester **24** was transformed into the acetonide derivative of (-)-isatisine A (**1**), which was previously made as an advanced intermediate in Kerr's total synthesis (Scheme 1.13).



Scheme 1.13: Liang's endgame synthesis of (-)-isatisine A.

1.3.4 Xie's total synthesis of (-)-isatisine A⁵

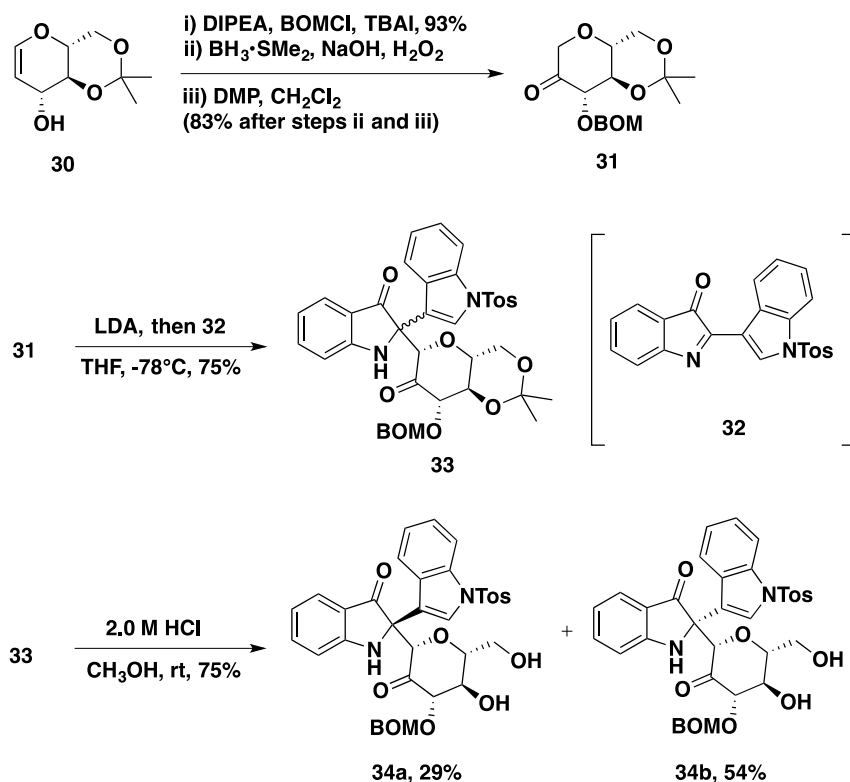
A year after Liang's and Panek's successful total synthesis, Xie and coworkers disclosed a biomimetic total synthesis of (-)-isatisine A. The key step in Xie's successful total synthesis of isatisine A was the benzilic acid rearrangement. Their proposed biogenic pathway starts from indican **25**, which is a common compound found in higher concentrations in the young leaves of *Isatis indigotica*.¹⁴ Compound **25** is first converted to the imine **26** through a proton-mediated rearrangement and then an acid-catalyzed Friedel-Crafts alkylation with indole to secure indol-3-one **26**. After further oxidation, indol-3-one **27** can give diketone **28**, presumably through an enzyme-catalyzed selective oxidation. Under the influence of an oxidant and an equivalent of water, **28** can spontaneously rearrange to substituted tetrahydrofuran **29**. Compound **29** can then undergo a facile dehydration to afford (-)-1. It is important to note that the indican **25** has also been isolated in other related plant species of *Isatis indigotica* Fort¹⁸ (Scheme 1.14).



Scheme 1.14: Proposed biogenic pathway for (-)-isatisine A.

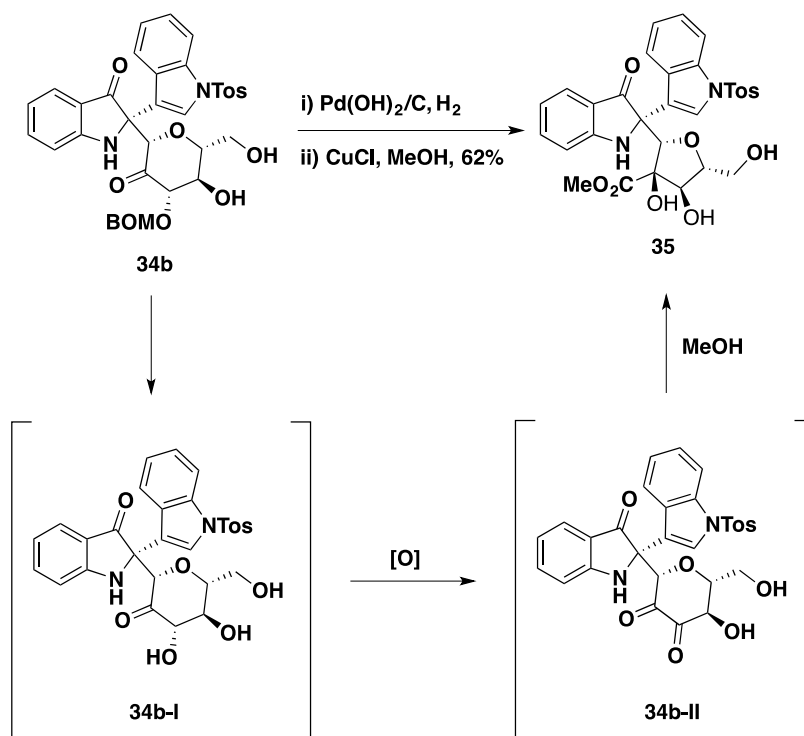
Guided by the biogenic pathway, Xie and coworkers commenced the total synthesis from the literature compound **30**, which was easily prepared from triacetyl-D-glucal in two steps.¹⁵ The enol ether **30** was protected using BOMCl and DIPEA, and subsequently oxidized to ketone **31** using a classic hydroboration/oxidation reaction to produce a secondary alcohol, followed by a Dess-Martin periodinane oxidation of the alcohol in DCM, with 77% yield in three successive steps. The ketone **31** was coupled to *N*-tosyl protected indolyimine **32** using a conventional aldol reaction mediated by strong LDA as a base to afford **33** in 75% yield. It is important to note that the indolyimine **32** was previously made via oxidative dimerization of indole¹⁶ followed by protection with tosyl chloride. Hence, the modularity of this procedure is, in our opinion, limited. Nonetheless, the reaction generated two diastereomers, which after acid-mediated deprotection of acetonide, yielded a separable mixture of diastereomers **34a/34b** in a 83% yield and *ca.* 2:1

diastereomeric ratio favoring the undesired diastereomer. This proved to be inconsequential, however, since Kerr found that the major undesired diastereomer readily and thermodynamically isomerized under acid catalysis at room temperature (Scheme 1.15).

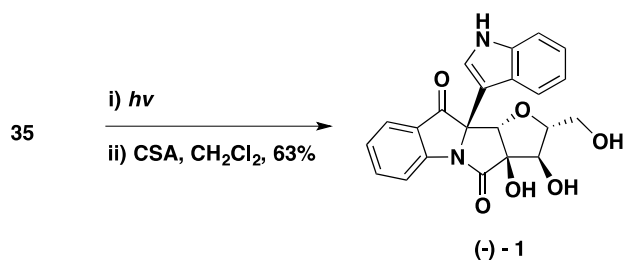


Scheme 1.15: Xie's nucleophilic enolate addition on the C-acylimine 32.

Based on this precedent, Xie decided to test Kerr's findings and used compound **34b** for further steps in the total synthesis. Compound **34b** was subjected to benzyl deprotection to generate intermediate **34b-I**, followed by α -hydroxy oxidation to generate intermediate **34b-II**. The intermediate **34b-II** underwent diketo rearrangement mediated by $\text{Pd}(\text{OH})_2$ followed by the addition of CuCl to generate **35** in a 62% yield without intermediate isolation (Scheme 1.16).

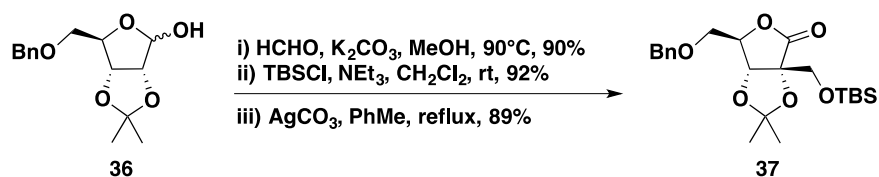


The tosyl-protected compound **35** was subjected to photoinduced deprotection to reveal the unprotected indole in a 46% isolated yield, which was subsequently isomerized and underwent acid mediated ring closure to form the desired (-)-**1**. Using Kerr's observation in which the diastereoselectivity of the indole branch was be equilibrated to the desired product under acidic conditions, Xie and coworkers were able to convert the major undesired diastereomer **34b** to (-)-isatisine A in an 8.6% overall yield (Scheme 1.17).



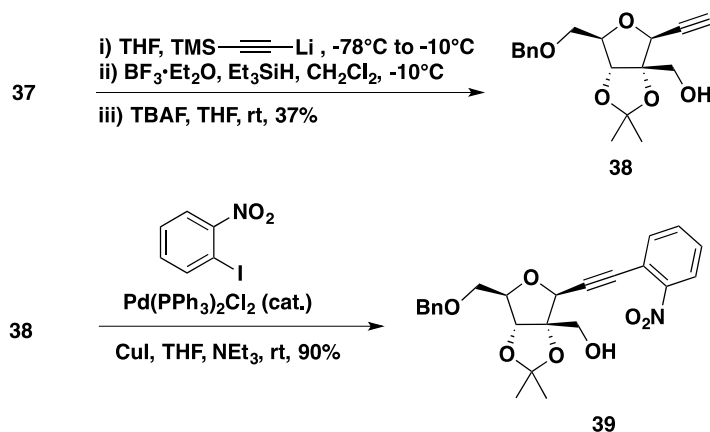
1.3.5 Ramana's total synthesis of (-)-isatisine A⁶

The newest addition to the repertoire of total syntheses of isatisine A was reported by Ramana and coworkers using a series of four impressive metal-mediated transformations – all of which have been developed in the laboratory of the Ramana group. Ramana and coworkers commenced their synthesis by the preparation of alkyne **38**. The starting material, protected D-ribose **36**, underwent an aldol reaction with formaldehyde, followed by protection to form a TBS ether, and direct oxidization of anomeric alcohol afforded lactone **37** (Scheme 1.18).



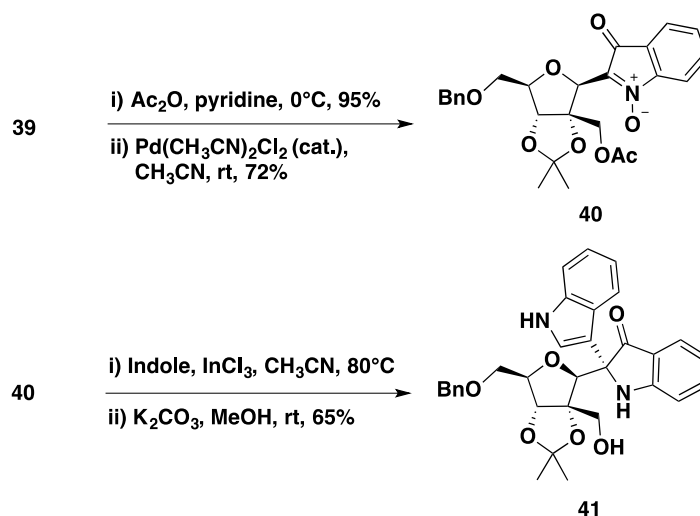
Scheme 1.18: Ramana's synthesis of the lactone 37.

The lactone **37** was then subjected to addition of TMS-ethynyllithium, followed by reduction of tertiary alcohol using triethylsilane in ethereal boron trifluoride¹⁷ and silyl-deprotection with TBAF to afford alkyne **38**. The alkyne **38** was subjected to traditional Sonogashira coupling with 2-iodonitrobenzene to synthesize the nitro-alkyne **39** (Scheme 1.19).



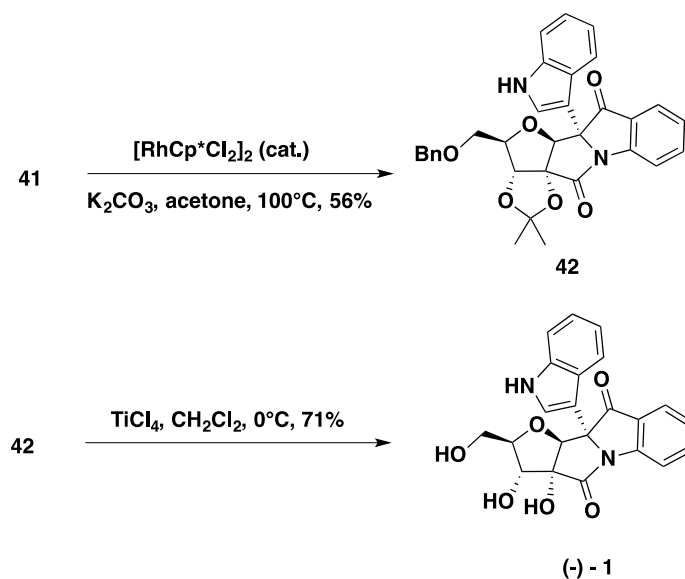
Scheme 1.19: Ramana's synthesis of nitro-alkyne 39.

The primary alcohol on nitro-alkyne **39** was protected as an acetate. The key nitro-alkyne cycloisomerization of **39** in the presence of $\text{Pd}(\text{MeCN})_2\text{Cl}_2$ gave the isatogen **40** in a 72% isolated yield. The N-O bond in compound **40** was subsequently reduced in the presence of InCl_3 ,¹⁸ followed by a facile indole addition, presumably mediated by an equivalent amount of HCl generated from the reduction of N-O bond. The intermediate was directly subjected to acetate deprotection to generate indolinone **41** in a 65% yield over two steps (Scheme 1.20).



Scheme 1.20: Ramana's nitro-alkyne isomerization of 39.

The indolinone **41** was next exposed to the oxidative lactamization protocol¹⁹ using $[\text{RhCp}^*\text{Cl}_2]_2$ at 100°C to furnish the benzyl and acetonide protected isatisine A **42** in 56% yield. Finally, the compound **43** was globally deprotected using TiCl_4 to release the desired (-)-isatisine A in 71% yield (Scheme 1.21).



Scheme 1.21: Ramana's endgame oxidative lactamization and deprotection of 41.

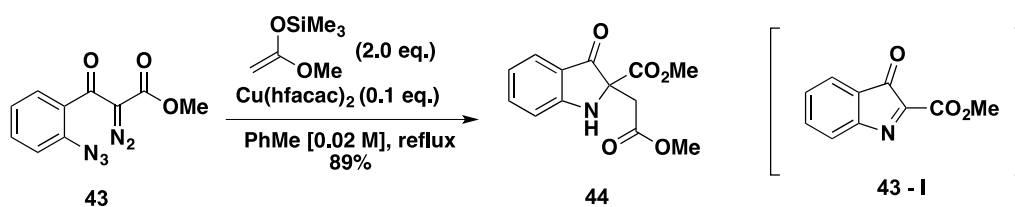
1.4 Conclusion

Five total syntheses of isatisine A have demonstrated that it serves well as a testing ground for creative strategies. New methodologies developed by several research groups to construct the key fragments of isatisine A, the highly substituted 3-indolinone and tetrahydrofuran cores, have shown that further manipulations of the adducts obtained from these reactions could expedite the synthesis of the natural product. The construction of the branched indol-3-one ring of the natural product was typically accomplished using conventional oxidation of indole moiety with *m*-CPBA and subsequent indole addition (Kerr, Liang and Xie). Panek used a known cross coupling procedure, while Ramana employed a novel nitroalkyne cycloisomerization. On the other hand, the used of compounds from the “chiral pool” – for example, D-glucose or D-ribose – and subsequent transformations were the typical approach to assemble the highly substituted furan moiety (Liang, Xie and Ramana). In this case, Kerr employed their well-developed Johnson [3+2] cycloaddition, while Panek used a silyl-directed

Mukaiyama [3+2] annulation strategy. All of these tools are characterized by unique approaches by each research group to construct the key fragments of the natural product. In the following two chapters, a novel construction of 3-indolinones and subsequent nucleophilic interception will be discussed. The last two chapters will be devoted to the discussion of attempts to make isatisine A, and the application of the adducts to develop lead compounds against Respiratory Syncytial Virus.

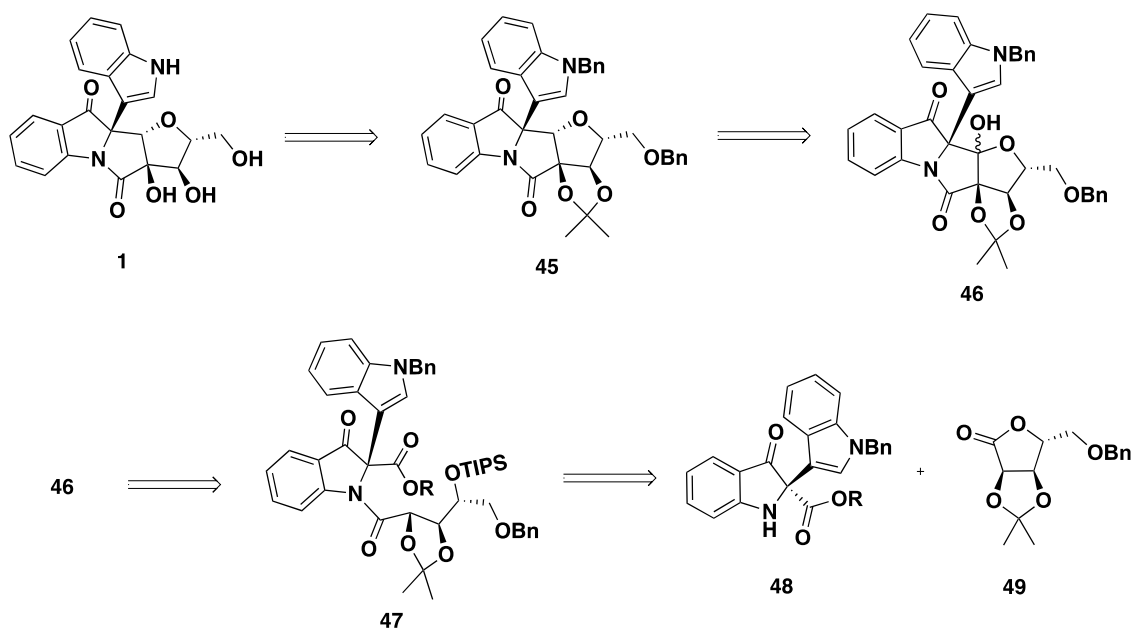
1.5 Proposed Retrosynthesis of Isatisine A

Our interest from this natural product stems from the previous result reported by Dr. Tina Bott,²⁰ an alumna of the West group, the efficient synthesis of the indolinone skeletal fragment of isatisine A. Starting from a compound containing azide and diazo functional groups, **43**, and treatment with a copper catalyst subsequently generates a C-acylimine intermediate *in situ*. The putative C-acylimine intermediate **43-I** could then be trapped by addition of a nucleophile to form 3-indolinone **44** (Scheme 1.22).



Scheme 1.22: Bott's indolinone synthesis.

With this earlier precedent in the West group, a retrosynthetic analysis of isatisine A was proposed and is shown in Scheme 1.23. In Scheme 1.23, it was envisioned that isatisine A could come from the benzyl and acetonide deprotection of tetrahydrofuran **45**. Tetrahydrofuran **45** could be envisaged as an adduct of hemiketal **46** after a deoxygenation reaction. Hemiketal **46** was pictured to come from an amide **47** after a Dieckmann-like cyclization of the α -C of the amide and a further cyclization of a deprotected secondary alcohol to the resultant ketone. Amide **47** could then be traced back to 3-indolinone **48** and furanone **49**. The 3-indolinone **48** was then envisioned to come from the reaction reported by Dr. Tina Bott but using benzyl indole as the nucleophile instead of the silyl ketene acetal.



Scheme 1.23: Our initial retrosynthesis.

With this retrosynthesis in mind, our project commenced with the elaboration of the methodology originally developed by Dr. Tina Bott (Chapter Two) and the preparation of compound **48** (Chapter Three) and the analogs of this compound.

1.6 References

1. Liu, J. F.; Jiang, Z. Y.; Wang, R. R.; Zheng, Y. T.; Chen, J. J.; Zhang, X. M.; Ma, Y. B., *Org. Lett.* **2007**, *9*, 4127-4129.
2. (a) Karadeolian, A.; Kerr, M. A., *J. Org. Chem.* **2010**, *75*, 6830-6841 (and citations therein); (b) Karadeolian, A.; Kerr, M. A., *Angew. Chem. Int. Ed.* **2010**, *49*, 1133-1135 (and citations therein).
3. (a) Lee, J.; Panek, J. S., *Org. Lett.* **2011**, *13*, 502-505 (and citations therein); (b) Lee, J.; Panek, J. S., *J. Org. Chem.* **2015**, *80*, 2959-2971 (and citations therein).
4. Zhang, X.; Mu, T.; Zhan, F.; Ma, L.; Liang, G., *Angew. Chem. Int. Ed.* **2011**, *50*, 6164-6166 (and citations therein).
5. Wu, W.; Xiao, M.; Wang, J.; Li, Y.; Xie, Z., *Org. Lett.* **2012**, *14*, 1624-1627 (and citations therein).
6. Patel, P.; Ramana, C. V., *J. Org. Chem.* **2012**, *77*, 10509-10515 (and citations therein).
7. Pohlhaus, P. D.; Sanders, S. D.; Parsons, A. T.; Li, W.; Johnson, J. S., *J. Am. Chem. Soc.* **2008**, *130*, 8642-8650.
8. Carson, C. A.; Kerr, M. A., *Angew. Chem. Int. Ed.* **2006**, *45*, 6560-6563.
9. (a) Huang, H.; Panek, J. S., *J. Am. Chem. Soc.* **2000**, *122*, 9836-9837; (b) Lowe, J. T.; Panek, J. S., *Org. Lett.* **2005**, *7*, 3231-3234.
10. Lowe, J. T.; Youngsaye, W.; Panek, J. S., *J. Org. Chem.* **2006**, *71*, 3639-3642.
11. Ager, D. J.; Fleming, I.; Patel, S. K., *J. Chem. Soc., Perkin Trans. 1* **1981**, 2520-2526.
12. Corey, E. J.; Gilman, N. W.; Ganem, B. E., *J. Am. Chem. Soc.* **1968**, *90*, 5616-5617.
13. Li, N. S.; Lu, J.; Piccirilli, J. A., *Org. Lett.* **2007**, *9*, 3009-3012.

14. (a) Kokubun, T.; Edmonds, J.; John, P., *Phytochemistry* **1998**, *49*, 79-87; (b) Maugard, T.; Enaud, E.; Choisy, P.; Legoy, M. D., *Phytochemistry* **2001**, *58*, 897-904.
15. Dötz, K. H.; Otto, F.; Nieger, M., *J. Organomet. Chem.* **2001**, *621*, 77-88.
16. Astolfi, P.; Panagiotaki, M.; Rizzoli, C.; Greci, L., *Org. Biomol. Chem.* **2006**, *4*, 3282.
17. Lewis, M. D.; Cha, J. K.; Kishi, Y., *J. Am. Chem. Soc.* **1982**, *104*, 4976-4978.
18. Ilias, M.; Barman, D. C.; Prajapati, D.; Sandhu, J. S., *Tetrahedron Lett.* **2002**, *43*, 1877-1879.
19. Gunanathan, C.; Ben-David, Y.; Milstein, D., *Science* **2007**, *317*, 790-792.
20. Bott, T. M.; Atienza, B. J.; West, F. G., *RSC Adv.* **2014**, *4*, 31955-31959.

Chapter Two

Azide Trapping of Metallocarbenes: Generation of Reactive C-Acylimines, Domino Trapping with Nucleophiles, and a Novel Route to the 3-Indolinone Skeleton of Isatisine A.

2.1 Introduction

Strategic and complementary carbon-carbon and carbon-heteroatom bond forming reactions are vital to the evolution of organic synthesis. With the exceptions of pericyclic¹ and other concerted reactions, most organic transformations are based on harnessing charged species or neutral radical species with fleeting timespans, known as high-energy reactive intermediates.² Beyond the useful subsequent unimolecular elimination reactions (E1 for cations and E1_{cb} for anions with a leaving group nearby) or bimolecular dimerization reactions (self recombination for radicals) ascribed as a common termination pathway for some of these reactive intermediates,² trapping with suitable functional groups has opened the door to numerous synthetic transformations. Figure 2.1 lists some of these species used in modern day organic synthesis, for example, metallocarbenes,³ oxyallyl cations⁴ and cyclic allenes,⁵ which have all been shown to be amenable to trapping.

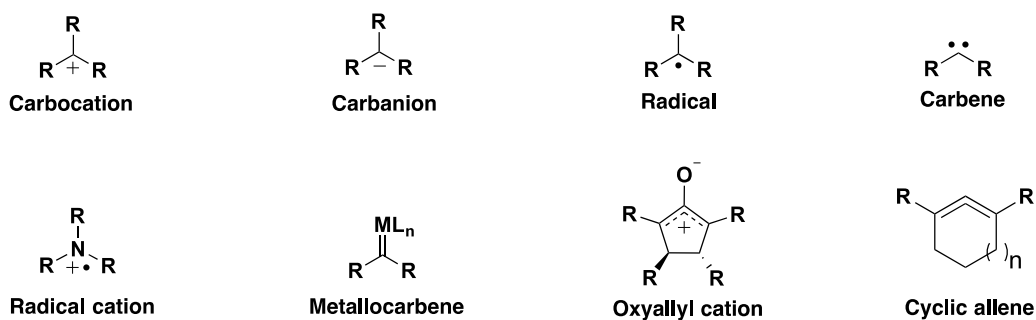
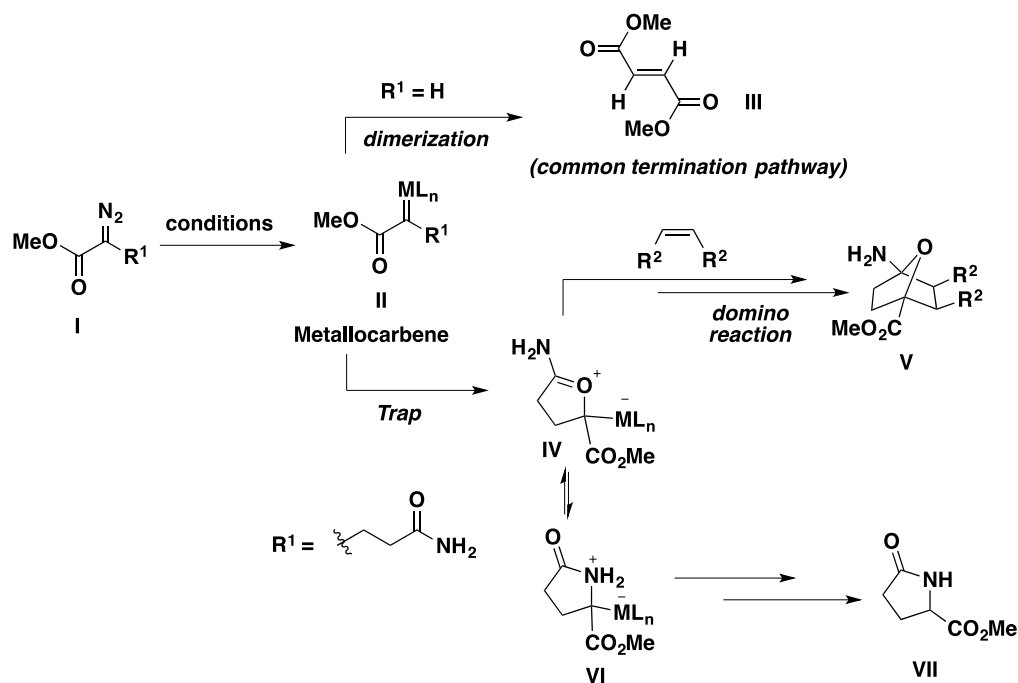


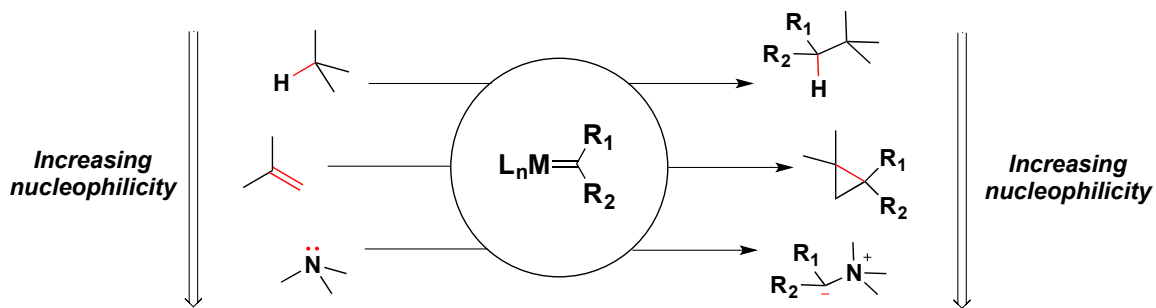
Figure 2.1: Representative examples of classic and modern reactive intermediates.

Domino reactions⁶ are regarded as an elegant and highly efficient approach for the synthesis of complex molecule scaffolds. These sequential transformations comprise of two or more bond-forming reactions under identical reaction conditions (one-pot). The latter transformations take place at the functionalities obtained in the former bond-forming reactions.⁶ Thus, high-energy reactive intermediates are one of the key elements to domino reactions.

In the list known reactive intermediates, free carbenes, generated from the photolytic or thermolytic extrusion of nitrogen from diazo precursors, are particularly difficult to control and have the tendency to undergo non-selective C-H insertion and dimerization reactions.⁷ Cognizant of this limitation, chemists found that addition of a transition metal was beneficial to generate a more controllable equivalent of carbene, the metallocarbene. This metallocarbene could then be trapped with variety of nucleophiles,⁸ which could then undergo subsequent domino reactions. For example (Scheme 2.1), a general diazocarbonyl **I** could be converted to metallocarbene **II** upon reaction with transition metals. If the R group on metallocarbene **I** does not contain a pendent nucleophile, the common termination pathway would be a dimerization⁹ to furnish alkene **III**. However, when the R group in **II** contains a nucleophilic oxygen or nitrogen, for instance, amide functional group, it could form two distinct ylides in dynamic equilibrium. The carbonyl ylide **IV** could engage in a domino [3+2] cycloaddition reaction with a dipolarophile to afford bicycle **V**. Alternatively, it could also afford pyrrolidone **VII** *via* a rearrangement pathway from ammonium ylide **VI**.



Weak C-H bonds are also potential reaction partners with metallocarbene,¹⁰ allowing for the concerted migration of hydrogen atom to the carbene carbon. Alkenes and alkynes are likewise competent nucleophiles. This latter process, however, typically results in ring closure, as opposed to an atom migration (Scheme 2.2).⁹



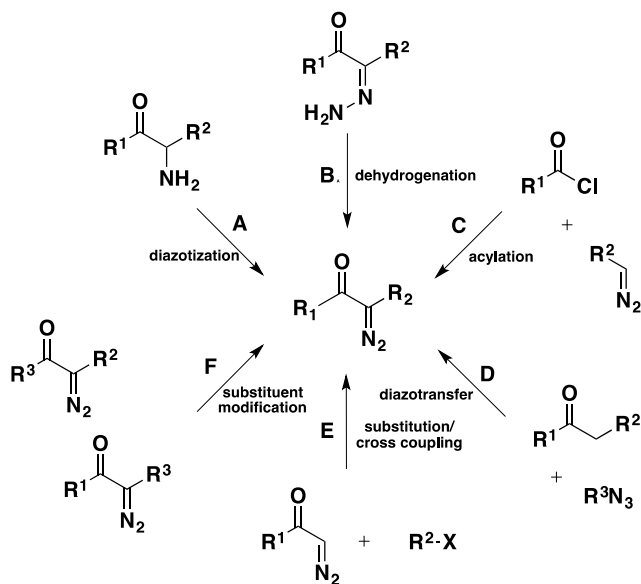
This chapter documents the development of azide trapping of metallocarbenes, generation of reactive C-acylimines and subsequent domino trapping with nucleophiles. To help appreciate this domino transformation, a review covering the aspects of the preparation of starting materials for carbene and metallocarbene generation, and structure and common reaction pathways of the carbene and of the metallocarbene intermediate are imparted. Particular emphases on the nitrogen-based functional groups as nucleophilic traps for metallocarbenes are included at the end of this chapter to aid in understanding the inspiration of this domino transformation.

2.2.1 Preparation of diazocarbonyl compounds and carbene reactive intermediates

Whether the reaction is done under photolytic, thermal, or metal-catalyzed conditions, stable diazo compounds are the typical precursors to make a carbene or a metallocarbene *in situ*. The extrusion of an equivalent of nitrogen from the diazo moiety, which requires an activation energy of about 30 kcal/mol in gas phase,¹¹ is typically the rate-determining step in most of its reactions (e.g., cyclopropanation);¹² this generates a fleeting carbene.

Diazo compounds can be made in a handful of ways, and Maguire and McKervey have compiled the most up to date review regarding the preparations α -diazocarbonyl compounds.¹³ For instance, α -diazocarbonyls can be made through a diazotization reaction of α -aminocarbonyls (path A, Scheme 2.3), or through dehydrogenation of hydrazones (path B, Scheme 2.3). Addition of diazo alkanes to acid chloride or mixed anhydride (path C, Scheme 2.3), and Regitz diazo transfer reactions of active methylenes with sulfonyl azides and organic bases (path D, Scheme 2.3) are also popular ways of making stable diazo compounds. More recently, substitution accompanied by cross-coupling on the ipso carbon of the diazo (path E,

Scheme 2.3) or a substituent modification on the ipso or β carbon of the α -diazocarbonyl compounds (path F, Scheme 2.3) have also been shown to be feasible.



Scheme 2.3: Approaches to diazocarbonyl compounds.

2.2.2 Structure and reactivity of free carbenes

Carbenes¹⁴ are charge neutral, divalent carbon species with only six electrons in their valence shell, two electrons in each σ bond, and two nonbonding electrons. Because the non-bonding electrons can be paired or unpaired, with their spins oriented parallel or antiparallel, there is the possibility of four electronic arrangements or spin states for simple cases like the methylene carbene (Figure 2.2).¹⁵ The singlet carbene has its non-bonding electrons paired or unpaired, and the spins must always be opposite. Since the σ -orbital is a hybrid, containing a substantial contribution from the carbon 2s atomic orbital, whereas π or p-orbitals consist of pure carbon 2p atomic orbitals, the electron pair typically occupies the lower energy σ - or sp^2 -orbital (Structure A, Figure 2.2). However, in rare cases that have only been documented

computationally, which presumably occur in the excited state of the carbene reactive intermediate, the electron pair also can exist in the higher energy, unhybridized p-orbital (Structure D, Figure 2.2), or the electrons can each separately occupy the σ - and the p- orbitals, but with opposite spin (Structure C, Figure 2.2). In triplet carbenes, the two non-bonding electrons have parallel spins located on the σ - and p- orbital of the carbene (Structure B, Figure 2.2). As a result of their high reactivity, the C-H insertion reactions of free carbenes tend to be unselective.¹¹ It is for this reason that the chemistry of free carbenes has lagged behind compared to other classical reactive intermediates, in particular in the context of domino reactions.

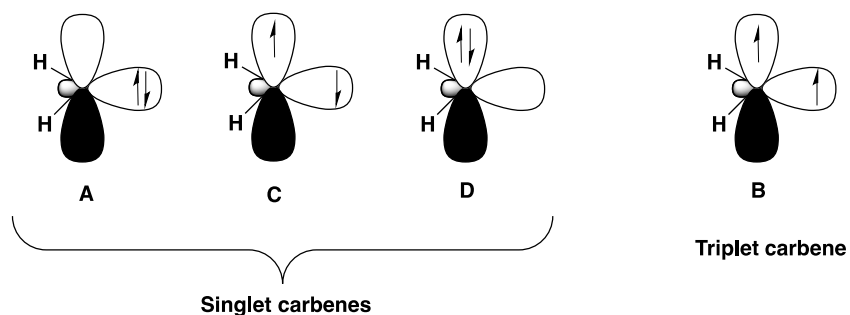
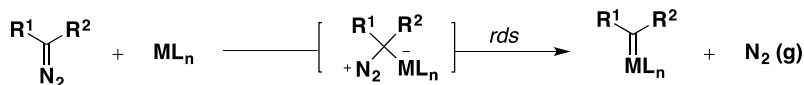


Figure 2.2: Electronic structure of carbene (methylene).

2.2.3 Structure and reactivity of metallocarbenes or carbenoids

Upon generation of a carbene *in situ* from the diazo precursor, the reaction of this intermediate is difficult to control as the carbene intermediate has the proclivity to undergo non-selective reactions.⁷ In order to mitigate this problem, a catalytic amount of a transition metal is often added to generate a more selective equivalent of a carbene, the metallocarbene. The mechanism for metal-mediated diazo decomposition is thought to proceed through nitrogen extrusion, the rate-determining step (an expanded discussion is found in Chapter Three), which results from nucleophilic attack of the diazo compound onto the transition metal. The typical

transition metals (salts) use to initiate the formation of a metallocarbene are $\text{Cu}(\text{hfacac})_2$, $\text{Cu}(\text{tfacac})_2$, $\text{Cu}(\text{acac})_2$, or $\text{Rh}_2(\text{OAc})_4$.



Scheme 2.4: Simplified mechanism of metallocarbene formation.

Metallocarbene, carbenoid or metallocarbenoid, refers to the transition-metal bound carbene. Properties that are inherent to the metal salts or complexes, such as electron count, oxidation state, ligand and number of open coordination sites, influence the reactivity of the bound carbene,^{9, 16} in addition to the observed chemo-, regio-, and stereoselectivity of the reaction. Carbenes bound to high oxidation state, electron poor, early transition metals (e.g. Ti(IV) or Ta(V)), typically react as nucleophiles, and are referred to as Schrock metallocarbenes. In the same way, carbenes bound to low oxidation state, electron rich, late transition metals (e.g. Pd(II), Cu(I) or Rh(II)), react as electrophiles and are referred to as Fischer metallocarbenes (Figure 2.3). Although not always accurate, it is also thought that Fischer metallocarbenes have a carbene in its paired singlet state while Schrock metallocarbenes have a carbene in its triplet state.

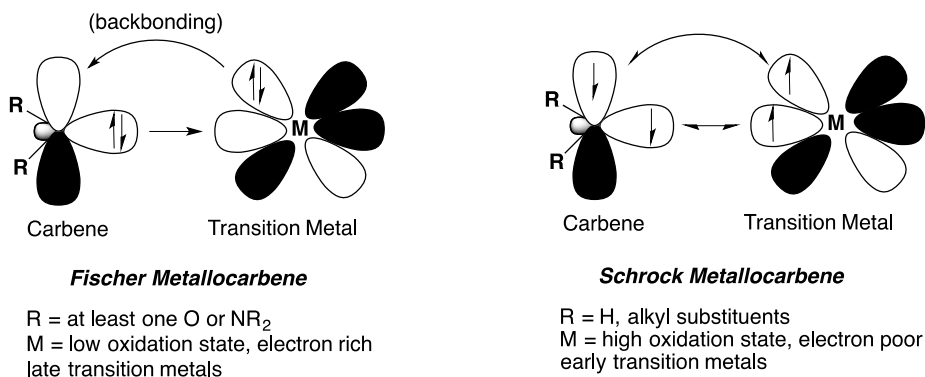
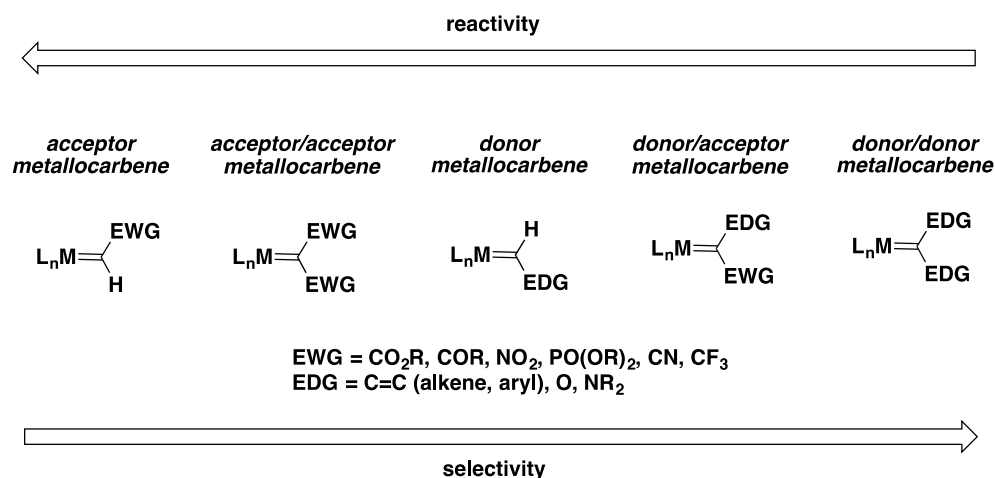


Figure 2.3: Fischer metallocarbene vs. Schrock metallocarbene.

An additional way of analyzing the reactivity of a metallocarbene is to look at the substituents bound to the carbon. The capacity of the substituent(s) to donate electrons to the nearly vacant p orbital of the metallocarbene or accept electrons from the filled orbital of the carbene can perturb the kinetic reactivity and selectivity of the metallocarbene. Carbenes with two substituents with a lone pair, or unsaturated C=C, that are capable of electron donation or conjugation, like O, NR₂, alkenyl C=C, aryl C=C, are known as donor/donor carbenes. Likewise, carbenes conjugated to two electron acceptors such as C=O, N=O, P=O are known as acceptor/acceptor carbenes. In general, metallocarbenes with two donor substituents are the least reactive for further functionalization at the carbene carbon, whereas metallocarbenes conjugated to two electron acceptors are highly reactive, and thus are difficult to isolate compared to the former.¹⁷ Their reaction selectivities are also affected by the substituents. Donor/acceptor metallocarbenes (metallocarbenes with one donor and one acceptor substituents) are, in general, the most selective for cyclopropanations followed by the acceptor/acceptor metallocarbenes and then by the acceptor metallocarbenes (Scheme 2.5).¹⁷ Although, one characteristic feature of a true Fischer metallocarbene is the presence of a donor (O, NR₂) substituent on the carbene, due to the electrophilicity of carbon on acceptor metallocarbene and acceptor/acceptor metallocarbene, these are also referred to as Fischer-like metallocarbenes.



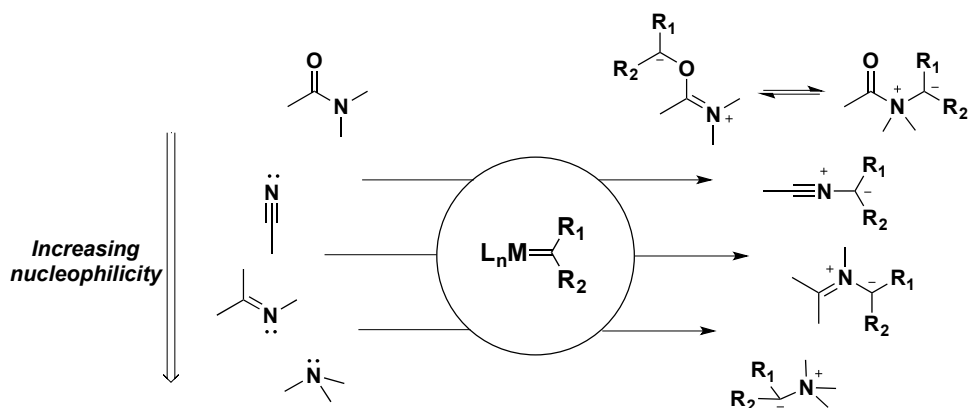
Scheme 2.5: Reactivity and selectivity of metallocarbenes.

Recent literature on the X-ray characterization of donor/donor and donor/acceptor carbenes bound with Rh(II) were published by Fürstner.¹⁸ Berry and Davies managed to characterize donor/acceptor carbenes using NMR and optical spectroscopy techniques.¹⁹ Together, they have shown that there is a substantial covalent character in the interaction of the donor/acceptor carbene itself and the transition metal used to generate them. As such, metallocarbenes cannot be treated as true free carbenes. Regardless of the true nature of the metallocarbenes, organic chemists have long acknowledged that these reactive intermediates can be very good alternatives to free carbenes in many of the reactions to which carbenes are linked.

2.2.4 Reactivity of metallocarbenes with nitrogen nucleophiles

Aside from the area of the “Interrupted Nazarov reaction”, the West group has a long history of research on the reactivity of Fischer-like metallocarbenes with pendent nitrogen nucleophiles. There are reviews covered by West,²⁰ Padwa,²¹ and McKervey,²² regarding this area and the unique reactivity of Fischer-like metallocarbenes with other heteroatoms. As such, only selected examples are presented here.

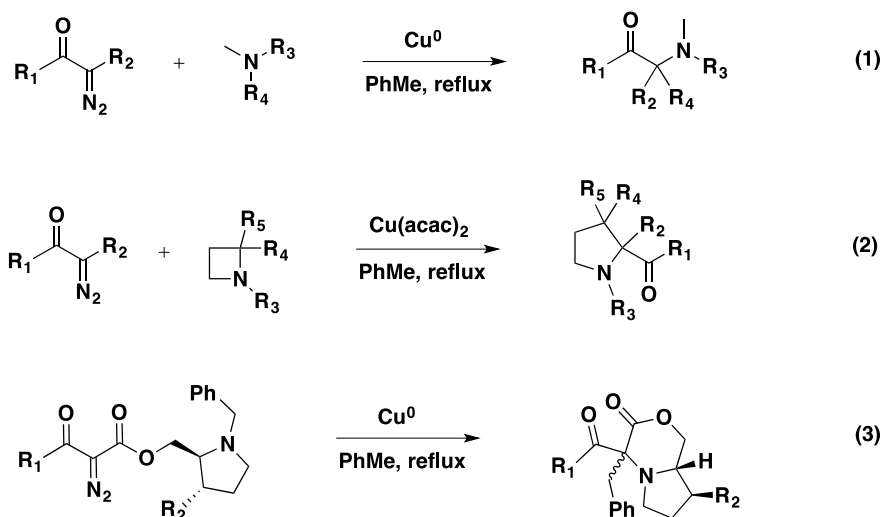
It has been observed that the addition of certain rhodium and copper salts to solutions of mono (precursor to acceptor metallocarbenes) and dicarbonyl (precursor to acceptor/acceptor metallocarbenes) stabilized diazo compounds leads to the evolution of nitrogen gas and the formation of products of the same general type as those formed in the thermal and photochemical decomposition of diazoalkanes.⁹ One particular class of nucleophiles that tends to divert metallocarbenes from their typical dimerization course, is nitrogen-based nucleophiles. The reactive metallocarbene intermediate, once formed, can react with the lone pair of the nearby nitrogen and form an ylide. Depending on the nitrogen based functional group that intercepts the metallocarbene, these are called ammonium ylides for amines, azomethine ylides for imines, and nitrile ylides for nitriles. Certain ambident nucleophilic functional groups, such as amides, can also react with metallocarbenes in two possible sites, either on the oxygen portion forming a carbonyl ylide or on the nitrogen portion forming another case of an ammonium ylide (Scheme 2.6).



Scheme 2.6: General reactivity of nitrogen-based nucleophiles on metallocarbene.

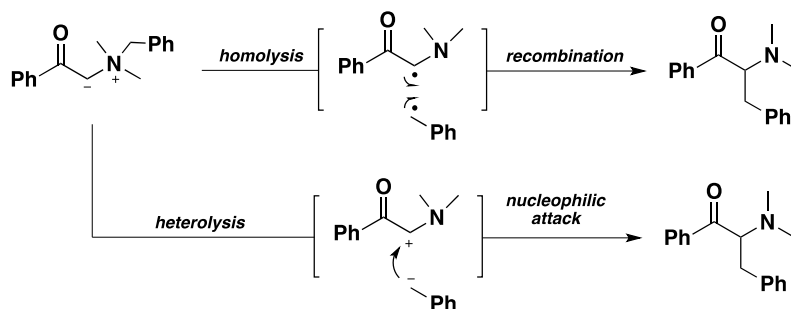
2.2.4.1 Reactions of metallocarbenes with amines

Owing to the nucleophilic lone pair present in amines, these functional groups react with the metallocarbenes to generate an intermediate known as an ammonium ylide. Typically, the common reaction pathways observed with ammonium ylides are the Stevens [1,2]-shift pathway (Scheme 2.7) and the [2,3]-rearrangement pathway (Scheme 2.9).



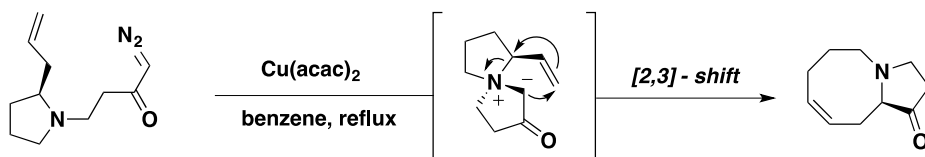
Scheme 2.7: Reaction of metallocarbenes with amines.

Mechanistically, the Stevens [1,2]-rearrangement reaction pathway involves the formation of an ammonium ylide intermediate, followed by a homolytic or heterolytic cleavage of one of the C-N bonds to give a radical pair or an ionic pair (Scheme 2.8).²³ The identity of the migrating group is the deciding factor whether the cleavage of the C-N bond is homolytic or heterolytic,²⁴ however the topic is still debated. Regardless of the nature of the reacting pair, these intermediates can recombine to form the [1,2]-shift product. Stevens [1,2]-rearrangement reaction pathway was successfully used as the key steps in the total syntheses of several natural products,²⁵ as well as the preparation of complex heterocycles²⁶ and simple acyclic amines.²⁷



Scheme 2.8: Possible mechanisms of Stevens rearrangement.

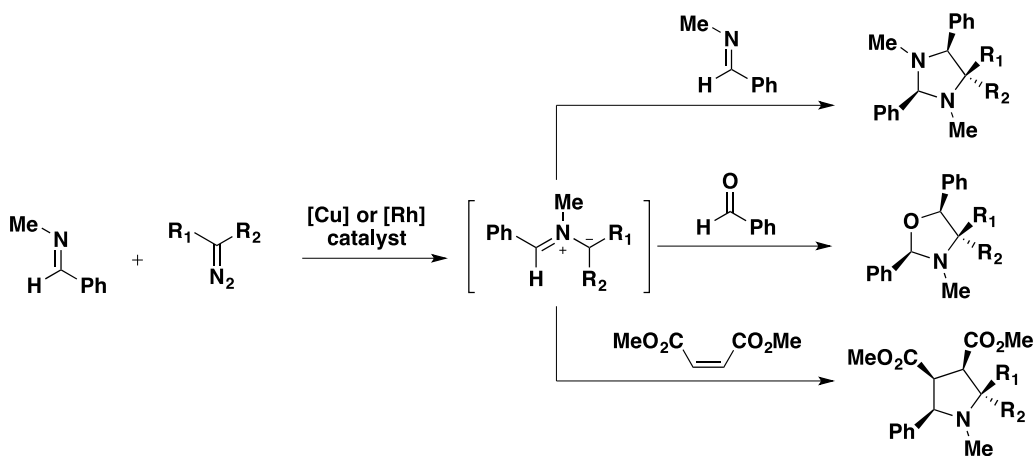
The [2,3]-sigmatropic rearrangement is another pathway typically observed with nitrogen nucleophiles bearing an allyl, propargyl or allenyl functionality (Scheme 2.9).^{8c} Usually, this reaction affords a mixture of compounds arising from the competition of [1,2]-reaction and [2,3]-reaction pathways. Singleton has shown computationally that these pathways originate from the partitioning of dynamic trajectories passing through a single [2,3]-rearrangement transition state.²³ As such, the distribution of products emanating from a given reactant is difficult to control and oftentimes relies on a trial and error basis to obtain the desired product with high selectivity. However, there are notable examples of successful attempts to induce the desired pathway. Unsurprisingly, these reaction pathways have also been used in the preparation of complex heterocycles with varied ring sizes, similar to the Stevens [1,2] – shift pathway.^{8c}



Scheme 2.9: An example of [2,3]-shift pathway.

2.2.4.2 Reactions of metallocarbenes with imines

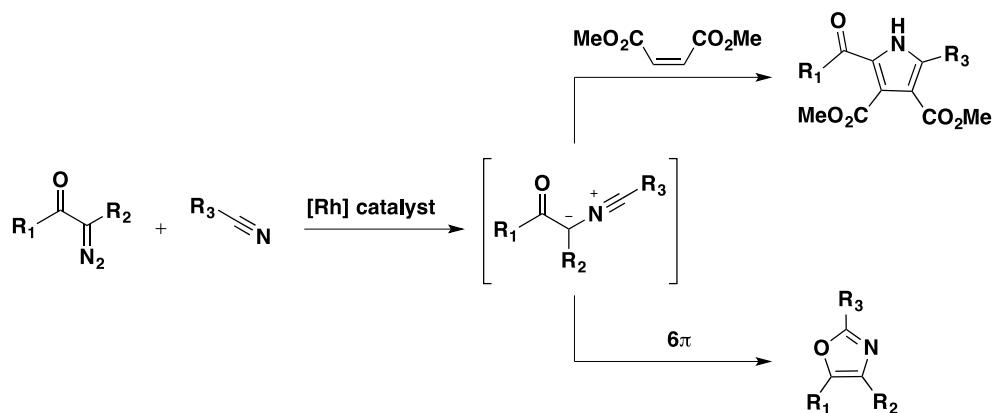
The lone pair on imine functional groups, although less nucleophilic than amines, is also known to react with metallocarbenes to form intermediates known as azomethine ylides.^{8c} Azomethine ylides can subsequently undergo a unimolecular [3+2]-cycloaddition with a pendent p-bond moiety forming an azacycle. Bimolecular [3+2]-cycloadditions of azomethine ylides with other molecules containing p-bonds are also known, and have been used to make valuable heterocycles in one step, for example, imidazolines, oxazoles or pyrrolidines (Scheme 2.10).



Scheme 2.10: Reactions of azomethine ylides.

2.2.4.3 Reactions of metallocarbenes with nitriles

The lone pair of a nitrile, in the same manner as amines and imines, also reacts with diazocarbonyls through its lone pair in the presence of copper or rhodium salts to form a nitrile ylide.^{8c} Similar to the azomethine ylide, the nitrile ylide intermediate can participate in [3+2]-cycloaddition reactions with a p-bond containing partner forming, for example, pyrroles, oxazoles and other heterocycles containing extra unsaturation (Scheme 2.11).



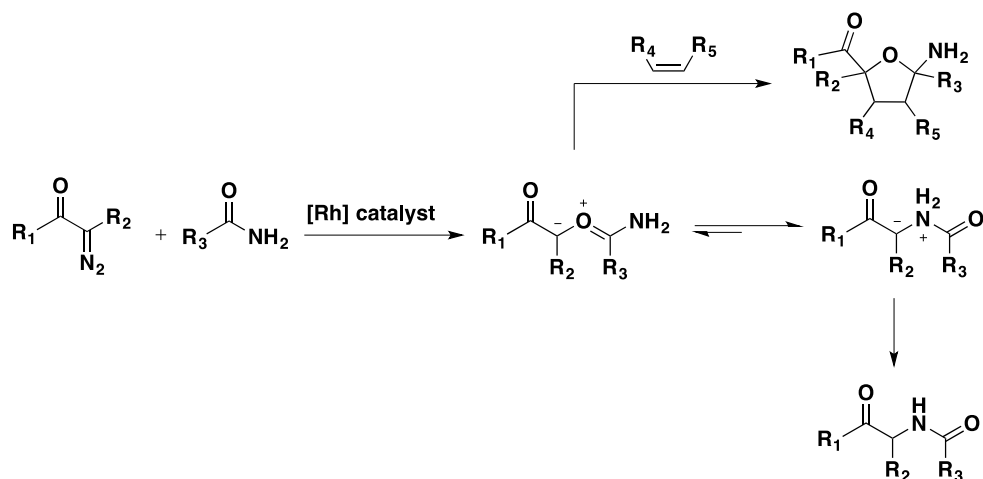
Scheme 2.11: Reactions of nitrile ylides.

2.2.4.4 Reactions of metallocarbenes with amides

Ambident nucleophiles, like amides, are also known to react with diazocarbonyls in the presence of copper and rhodium salts.^{8c} When the metallocarbene, derived from the diazocarbonyl, reacts with the nitrogen portion of an amide, an ammonium ylide results. This distinct ammonium ylide can undergo reaction pathways involving a [1,2]-shift or, if possible, a [2,3]-shift.

When the metallocarbene reacts with the oxygen portion of the amide, a different type of ylide results, which is known as a carbonyl ylide. This carbonyl ylide can further react with a p-bond containing moiety (dipolarophile), forming a cyclic compound with nitrogen substituents. This subtle change in reactivity with ambident nucleophiles like amides suggests that there is a dynamic equilibrium between the ammonium ylide and carbonyl ylide (Scheme 2.12). Depending on the solvent, reaction concentration and temperature, the distribution of the products arising from these two competing pathways can be controlled. However, the distribution of the ammonium ylide versus the carbonyl ylide is controlled thermodynamically, and Kappe and co-workers have shown that ammonium ylides are more stable, and even

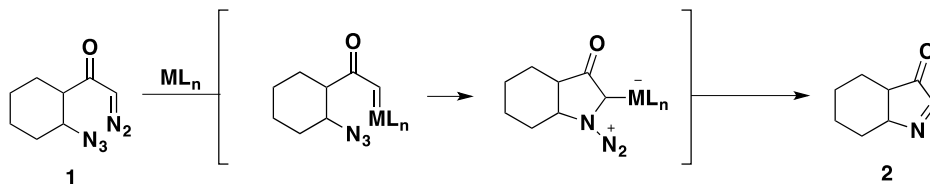
sometimes isolable.²⁸ Thus, if the transition state for further transformations of the carbonyl ylide is higher in relative energy than that of the ammonium ylide, then the rearranged product from the ammonium ylide is ultimately the major product (Curtin-Hammett principle).²⁹



Scheme 2.12: Reactions of metallocarbenes with amides.

2.3 Reactions of metallocarbenes with azides

Organic azides can intercept a variety of electrophilic species in a synthetically useful fashion,³⁰ such as aziridination of electron-deficient alkenes³¹ or Schmidt rearrangements. In this vein, we have speculated that replacement of basic amines with azides in the Stevens rearrangement reaction sequence, for instance **1**, might permit cyclization to a betaine or a zwitterion, which is expected to undergo facile loss of nitrogen gas to form the cyclic *C*-acylimine **2** (Scheme 2.13).



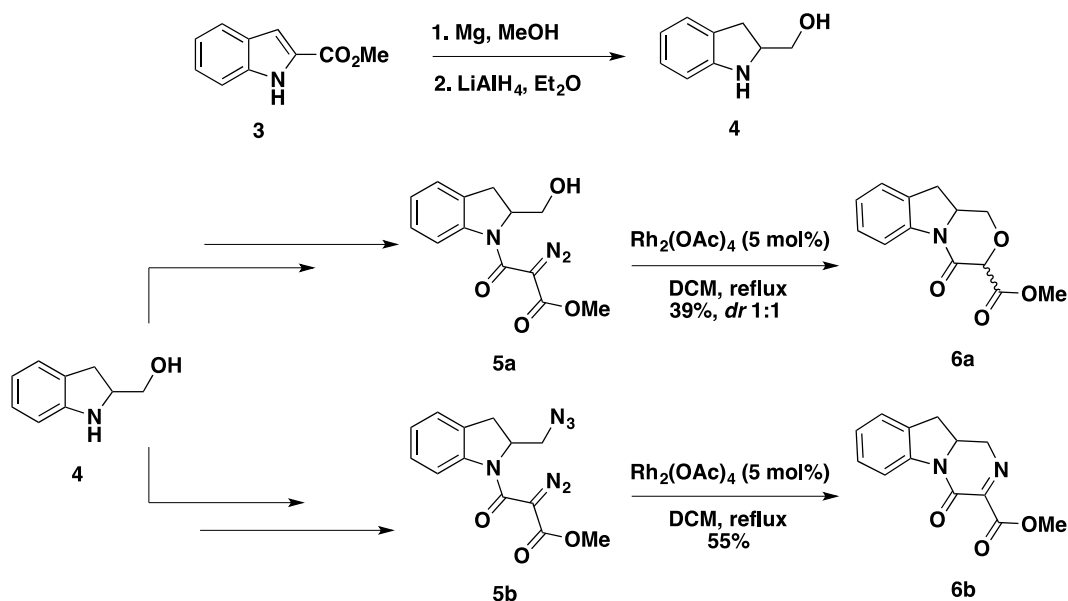
Scheme 2.13: Hypothetical reaction of metallocarbene with azide.

Reactions of azides with diazocarbonyls in the presence of copper and rhodium salts have been reported in the literature. For instance, Wee,³² Micouin and Lecourt³³ and others have reported that rhodium(II) salts can effectively catalyze the formation of imines from diazocarbonyls and azides. During the course of our study and the initial publication of our results,³⁴ concurrent publications from Doyle³⁵ and Gu³⁶ have also appeared in the literature and are described herein.

2.3.1 Intramolecular rhodium (II) carbene interception with an azide.

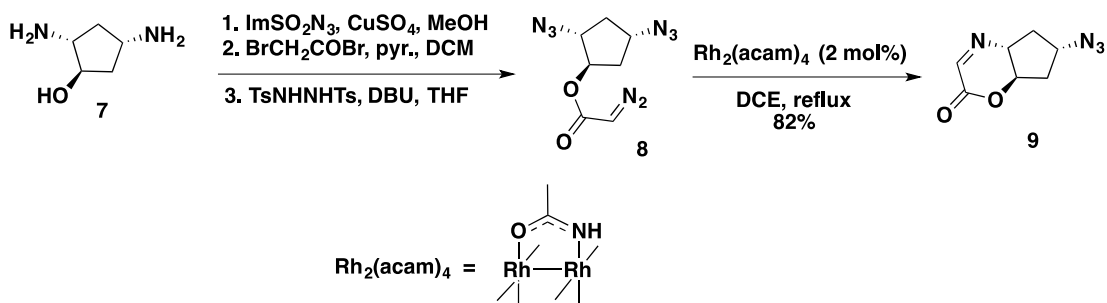
In 1996, Wee and Slobodian from the University of Regina disclosed a rhodium catalyzed reaction of indoline diazoamides **5a** and **5b**, to afford tetrahydropyrrolo[1, 2-a] indole derivatives **6a** and **6b**, generally in moderate to good yields. The starting material **5a** was readily synthesized from indole methyl ester **3**. Using standard dissolving metal reduction conditions, compound **3** can be reduced to indoline **4**. Indoline **4** can subsequently be manipulated to make compounds **5a** and **5b** using conventional functional group transformations, which are summarized in Scheme 2.14.

Under typical Rh(II) catalyzed metallocarbene formation, substrate **5a** can be expected to undergo C-H or O-H insertion. Indeed, Wee and Slobodian only isolated **6a** arising from O-H insertion in a modest 39% yield as a 1:1 mixture of *syn* and *anti* diastereomers. In the case of indoline diazoamide **5b**, where the pendent R group was azide, interception of the metallocarbene from the azide was observed, instead of the anticipated C-H insertion. This unexpected formation of a C-acylimine **6b**, in modest 55% yield, is the first example of an azide-metalcarbene coupling (Scheme 2.14). Formation of adduct **6b** can still be increased in 76% yield by changing the solvent to toluene and heating the reaction mixture to 110 °C.



Scheme 2.14: Wee's interception of metallocarbene with azide.

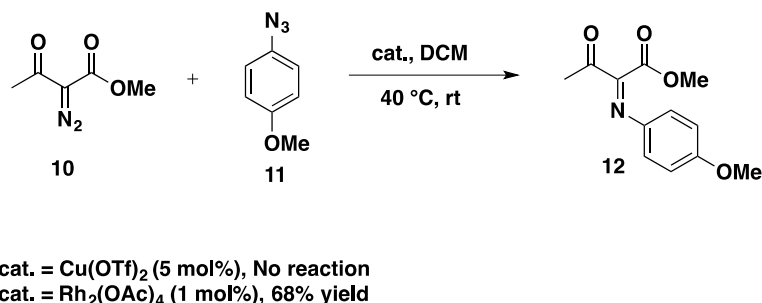
A French group from Laboratoire de Chimie Thérapeutique in Paris, France, led by Laurent Micouin and Thomas Lecourt, reported a similar observation in 2011. The authors disclosed a Rh₂(OAc)₄-catalyzed decomposition of the diazoester **8** to afford the C-acylimine adduct **9** in a very good (82%) yield. Diazoester **8** can be readily synthesized from amino alcohol **7** in three steps, following the transformation depicted Scheme 2.15.



Scheme 2.15: Lecourt and Micouin's interception of metallocarbene with azide.

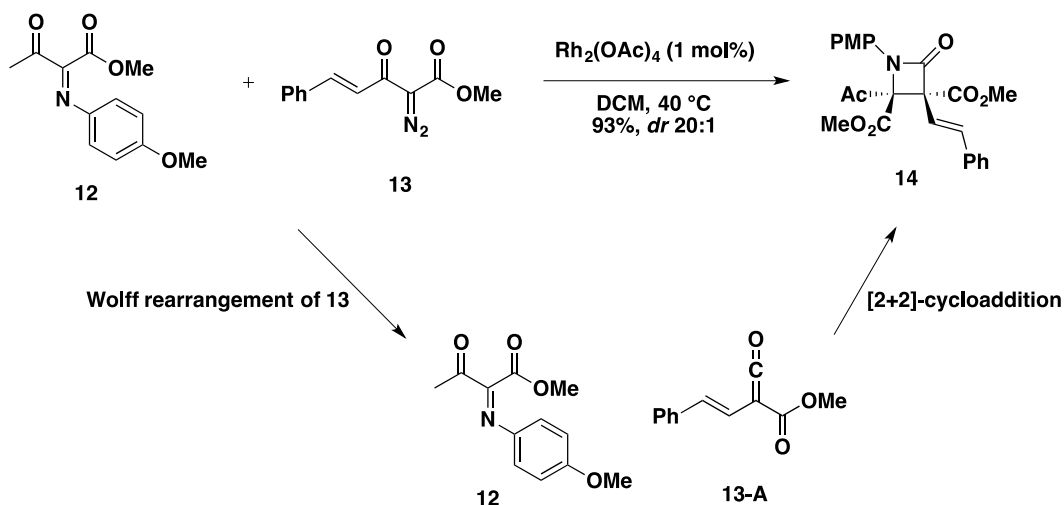
2.3.2 Intermolecular rhodium (II) carbene interception with an azide.

Three years after Micouin and Lecourt's published report, Michael Doyle and co-workers from the University of Maryland disclosed their version of a mild and chemoselective process for the synthesis of *C*-acylimine **12**. Using **10** and **11** as the model compounds, the authors optimized the formation of the imine using a variety of rhodium and copper catalysts (Scheme 2.16).



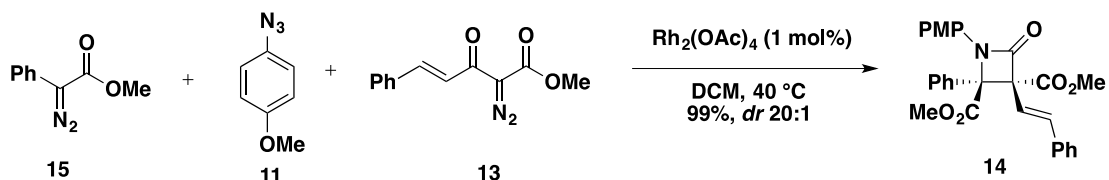
Scheme 2.16: Doyle's interception of metallocarbene with azide.

All of the rhodium and copper catalysts tested were found to decompose their model diazo compound **10**, indicating kinetic reactivity over the azide when mixture was heated to 40 °C in DCM or to 84 °C in DCE solvents over 24 hours, but interestingly only rhodium catalysts were effective in coupling with aryl azides. Using 1 mol % Rh₂(OAc)₄ as the catalyst, and the mixture heated to 40 °C in DCM over 24 hours was found to be the best set of conditions to afford **12**, albeit in a moderate (68%) yield. Adduct **12** can be used in the synthesis of a variety of β -lactams, one example being **14**. Following a stepwise Wolff rearrangement of enone diazoacetate **13**, ketene **13-A** was formed *in situ* and subsequently underwent a [2+2] cycloaddition (Scheme 2.17) with **12** in one-pot to form **14**.



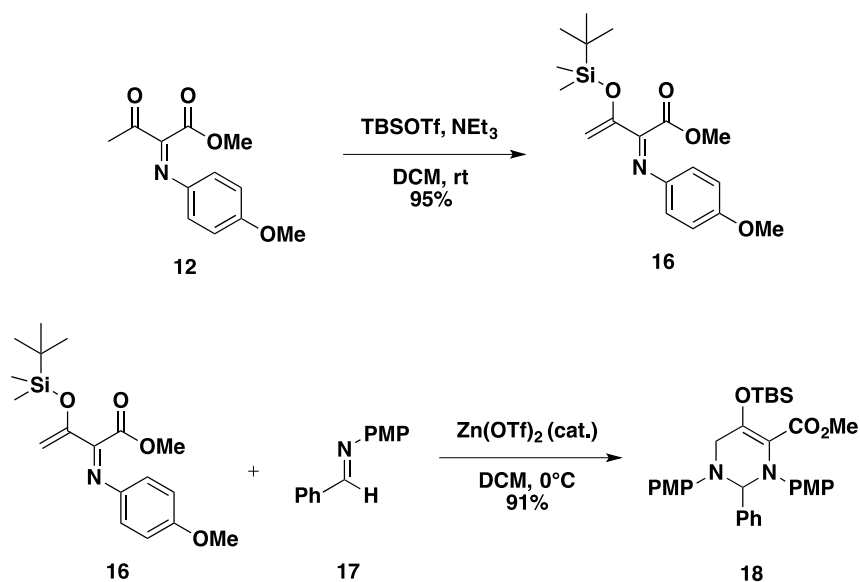
Scheme 2.17: Doyle's b-lactam synthesis.

An impressive multicomponent version of the synthesis was also demonstrated. Using the diazocarbonyl compound **15**, azide **11**, and enone diazoacetate **13**, with $\text{Rh}_2(\text{OAc})_4$ present in 1 mol% as the catalyst, an alternate route to b-lactam **14** is also feasible (Scheme 2.18). The authors noted that this reaction begins with the formation of the imine from **15** and **11**, followed by the Wolff rearrangement with **13**, which subsequently undergoes [2+2]-cycloaddition.



Scheme 2.18: Doyle's multicomponent reaction.

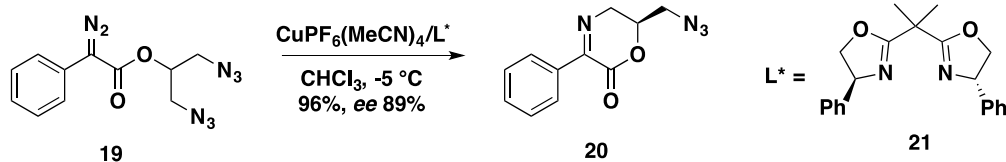
In a related process, imine **12** can also be used in the formation of tetrahydropyrimidine **18**. Imine **12** was initially converted to azadiene **16** using TBSOTf and triethylamine. The resulting azadiene then underwent a [4+2]-cycloaddition with aldimine **17** using catalytic $\text{Zn}(\text{OTf})_2$ (Scheme 2.19).



Scheme 2.19: Doyle's tetrahydropyrimidine synthesis.

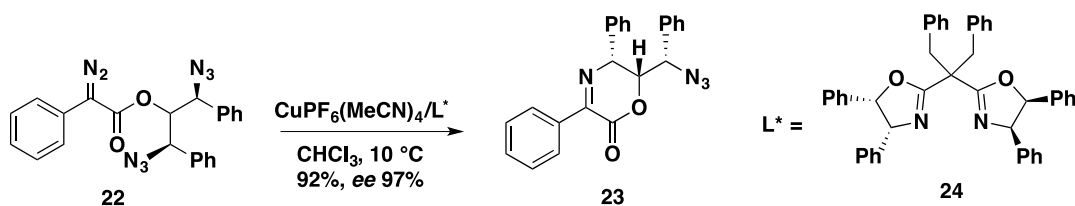
2.3.3 Intramolecular copper(I) carbene interception with an azide.

In the same year as Doyle's publication, collaborative efforts by Yan Su, from Ningxia University, and Peiming Gu, from Lanzhou University, resulted in an efficient enantioselective and diastereoselective desymmetrization of 1,3-diazido-2-propanol with aryldiazoacetate to make *C*-acylimines with nearby stereocentres (Scheme 2.20). One example of this was the enantioselective desymmetrization of diazide **19** to afford imine **20** using chiral bisoxazoline **21** and a copper (I) catalyst, which unbelievably resulted in 96% yield and 89% enantiomeric excess.



Scheme 2.20: Gu's stereoselective desymmetrization of diazides.

Diastereoselective desymmetrization of meso diazide **22**, however, needed a slightly higher temperature and a bulky chiral bisoxazoline ligand **24** to afford imine **23**, presumably because of steric influence imposed by heavily substituted diazide **22**. Nonetheless, the reaction proceeded with an excellent 92% yield and 97% enantiomeric excess (Scheme 2.21). As noted by the authors, the domino reaction described herein and Gu's enantioselective desymmetrization of diazide are the only reports in the literature on the interception of a copper carbene with an azide.



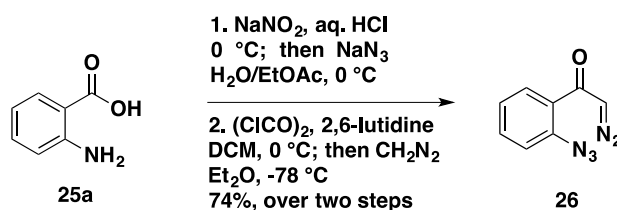
Scheme 2.21: Gu's diastereoselective desymmetrization of meso diazides.

2.4 Results and Discussion

With the necessary background from Wee's and Micouin and Lecourt's initial reports, for the hypothetical reaction in hand, we decided to make the model substrate necessary for our proposed transformation. The following sections cover the successful design of the substrate, a preliminary stability study of starting materials, and optimization of the desired transformation, along with the scope of the test reactions with silyl ketene acetals, silyl enol ethers, electron rich 1,3 dienes, *N*-methyl indole and tethered ammonium acid chloride, resulting in the short synthesis of the natural product tryphantrin.

2.4.1 Preparation and Stability of Starting Materials

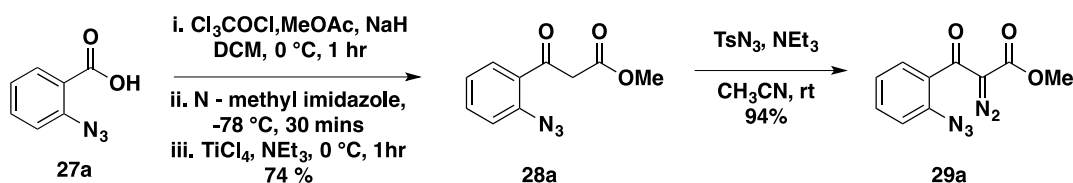
Intramolecular reactions are known to be faster in general than their intermolecular counterparts. This is thought to stem from the high local concentration of the reactive intermediate, favoring more successful collisions with the reacting pendent functional group. Guided by this impression and the goal to assemble the indolinone moiety of isatisine A (Chapter One), we designed a starting material containing diazoketone and azide moieties in close proximity, and a molecular formula whose ratio of (carbon + oxygen) atoms to nitrogen atoms would result in the material being safe to handle. Dr. Tina Marie Bott found that monostabilized diazocarbonyl substrate **26** can be easily prepared in two steps from anthranilic acid **25a**, and was amenable to handling and purification on small scales (*ca.* 1.0 g) (Scheme 2.22).



Scheme 2.22: Synthesis of monostabilized diazocarbonyl substrate 26.

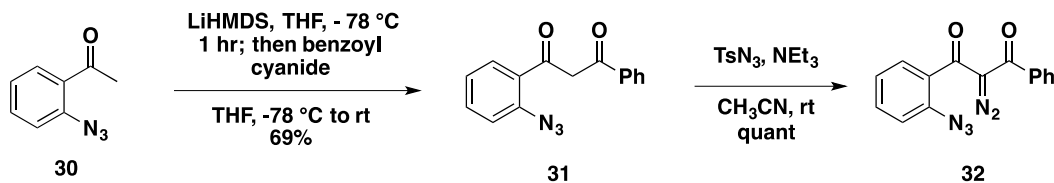
Substrate **28a**, bearing an additional carboxyl stabilizing group in the form of an ester, was directly prepared from **27a** through a cross-Claisen reaction protocol reported by Tanabe³⁷ and a subsequent Regitz diazotransfer reaction to afford the dicarbonyl stabilized diazo **29a** (Scheme 2.23) on small scales (*ca.* 1.0 g). After I stepped in with this project, we found that this reaction is highly amenable to multi gram-scale (*ca.* 20 g) preparation and was used routinely to prepare the desired starting material for the next test reactions (**caution: unless really necessary, limit the scale of the reaction to the suggested scale found in the experimental section**). As a

testament to the robustness of this preparation, an experienced undergrad researcher Isaac Zeer-Wanklyn was able to repeat the procedure with identical yields albeit in *ca.* 5 g scale.



Scheme 2.23: Synthesis of dicarbonyl stabilized diazo substrate 29a.

A substrate bearing a carbonyl stabilizing group, in the form of a ketone, was prepared through a lithium enolate formation of **30**, followed by addition to benzoyl cyanide to afford diketo **31**. A Regitz diazotransfer reaction employing 1,3-diketone **31** furnished diazodicarbonyl **32** (Scheme 2.24). Similar to diazo **29a**, this substrate is also highly amenable to multi gram-scale (*ca.* 5 g) preparation.



Scheme 2.24: Synthesis of dicarbonyl stabilized diazo substrate 32.

All of these types of substrates are relatively stable to decomposition over a certain period of time. For example, diazo **26**, which has no additional carboxyl stabilizing group, could be stored at -4°C over a period of two weeks with no decomposition and was generally stable at room temperature for a week. After longer time periods, this compound produced an intractable mixture of coloured products visible on TLC. Substrate **29a**, bearing an additional carboxyl stabilizing group was stable to decomposition over a period of three months or so at room temperature, and generally showed no evidence of sensitivity to heat or impact.

The decomposition stability trend was largely visible in differential scanning calorimetry (DSC) and thermo gravimetric analysis (TGA) experiments. An example of a DSC experiment for compound **29a** is shown in Figure 2.4. This data shows the temperature at which the crystals began to melt (endotherm, positive peak) and began to decompose (exotherm, negative peak). Shown in Figure 2.5 is an example of a TGA experiment; this data shows the weight variation of the solid **29a** as a function of temperature.

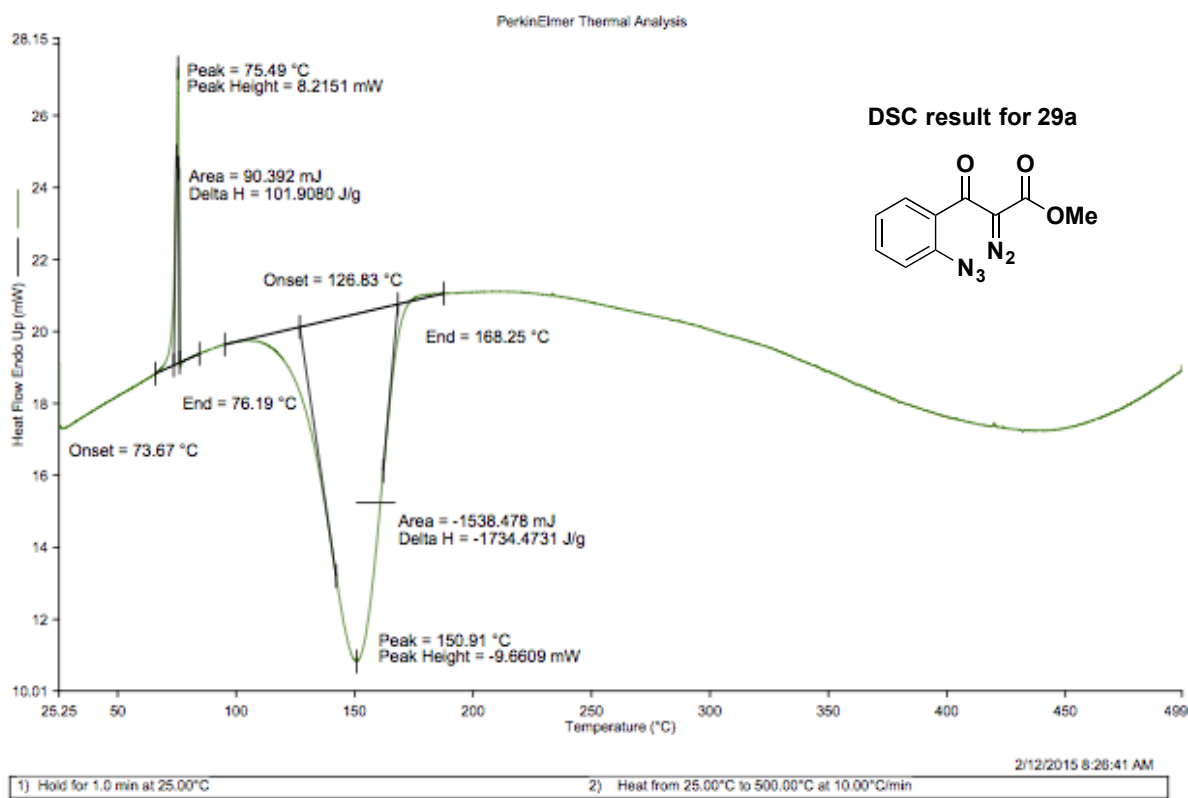


Figure 2.4: Differential scanning calorimetry (DSC) report for 29a.

Compounds with no additional carbonyl began to decompose at 70 °C under neat conditions, due to reduced stabilization. On the other hand, compounds with added stabilization, either through additional ketone or ester electron delocalization, decompose at temperatures higher than 120 °C under neat conditions.

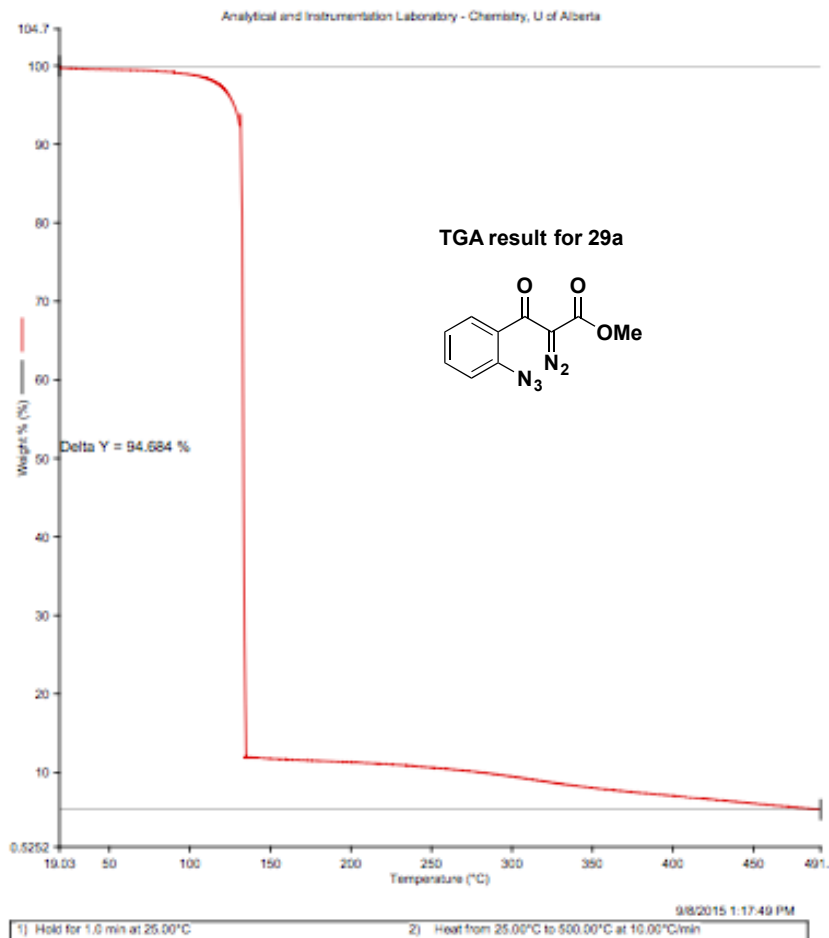


Figure 2.5: Thermogravimetric analysis (TGA) report for 29a.

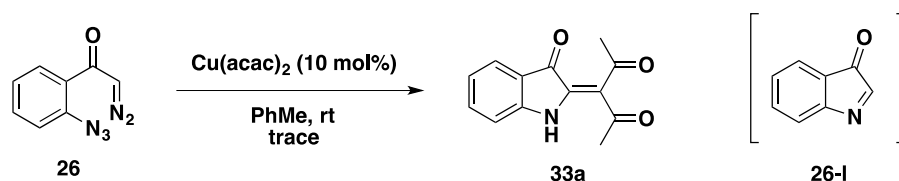
The decomposition pattern was monitored using a TGA experiment. We found that dicarbonyl stabilized diazo crystals generally exhibited one sharp inflection point, starting at temperatures at around 130 °C, consistent with the temperature posted by the DSC experiment. These experiments alone should, however, not be treated as an indication that the material is completely safe for handling. Other parameters, for example shock sensitivity, are equally important.³⁸ Similar to other common potentially explosive material typically used in organic synthesis laboratories, such as peroxides, we cautioned the potential users to treat the starting material with due care and respect. In our hands, we did not observe any detonation of these diazo azide starting materials and we performed most of our large-scale reactions involving these

substrates in a well-ventilated fume hood equipped with a blast shield. We also suggest wearing Kevlar® laboratory coat and earplug as an added safety precaution especially for relatively large-scale reactions.

2.3.2 Survey of reaction conditions

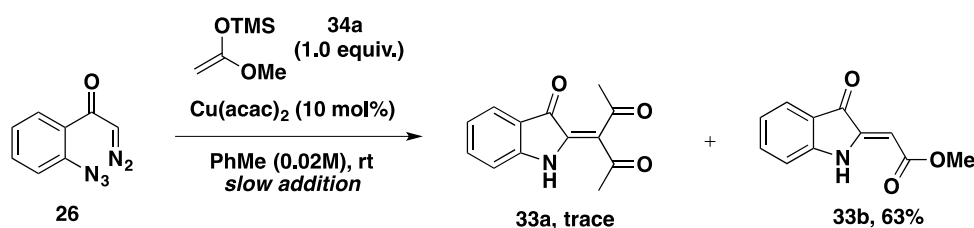
Copper carbenes, in general, favor the formation of ylides over competing C-H insertion or cyclopropanation reactions.³⁹ They are, in a way, complementary to rhodium carbenes, which favor the C-H insertion or cyclopropanation.⁹ Additionally, since the main the goal was to demonstrate the feasibility of the reaction on a large scale, it was necessary to use copper salts for preliminary optimization to minimize costs.

With the necessary starting materials in hand, examination of the reactivity of simple diazoketone **26** was initiated. Treatment of **26** with 10 mol% Cu(acac)₂ in toluene at room temperature with no added nucleophile led to rapid consumption of **26** and the formation of multiple, highly-colored products. Purification of this mixture yielded small quantities of a bright red solid, which was identified as alkylideneindolone **33a**, apparently formed via nucleophilic trapping of the intermediate **26-I** by the acetylacetonate ligand from the catalyst, followed by autoxidation to form adduct **33a**. Importantly, 3*H*-indole-3-one **26-I** was not isolated in this, or any subsequent experiment (Scheme 2.25).⁴⁰



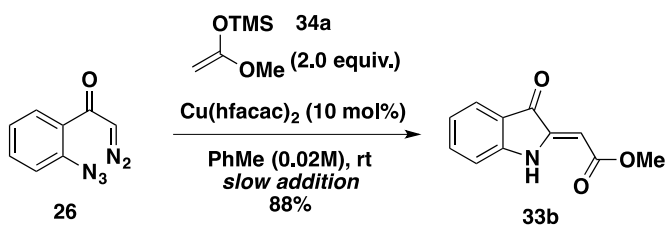
Scheme 2.25: Copper-catalyzed decomposition of 26.

The ready formation of **33a** in the presence of catalytic amounts of acetylacetonate nucleophile indicates the high reactivity of this intermediate.⁴¹ With this in mind, we carried out the same reaction, this time in the presence of 1 equiv of silyl ketene acetal **34a**. In this case, known alkylidene indolone **33b**⁴² was obtained in good yield, along with traces of **33a**. Notably, no evidence was seen for competing reaction of **34a** with the intermediate metallocarbene, indicating that intramolecular capture by azide to generate **26-I** is kinetically favored (Scheme 2.26).



Scheme 2.26: Intermolecular trapping of C-acylimine with 34a.

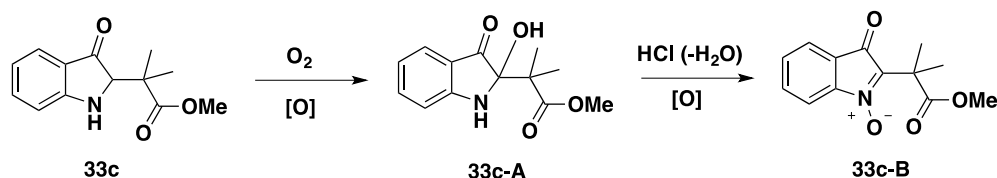
Several other catalysts were screened, and copper(II) bis(hexafluoroacetylacetonate) (Cu(hfacac)_2) was found to give the optimal results, affording the desired product in good yield, with no competing trapping by the ligand (Scheme 2.27).



Scheme 2.27: Optimized reaction condition for intermolecular trapping of C-acylimine with 34a.

2.3.3 Scope of the optimized reaction conditions

After a useful amount the desired **33b** adduct in the optimization study was obtained, a variety of traps were examined using identical reaction conditions (Table 2.1). To avoid potential catalyst deactivation, we focused on carbon nucleophiles as opposed to heteroatom nucleophiles that could bind tightly to the copper complex. Efficient trapping was seen with tetrasubstituted silyl ketene acetal **34b**, affording indolone **33c** (entry 2). A dehydrogenated product analogous to **33a** and **33b** could not be formed in this case due to the exocyclic quaternary center; however, slow oxidation to a different product was observed (Scheme 2.28). Upon prolonged exposure to air, **33c** produced 2-hydroxyindolone **33c-A**. Further oxidation was observed when **33c-A** was allowed to stand in CDCl₃, presumably the result of elimination due to traces of acid.⁴³ Notably, the further oxidation of **33c** to **33c-A** and then to nitron **33c-B** was consistent with the pathway implied for the formation of dehydrogenated product **33a** and **33b**.



Scheme 2.28: Further oxidation of 33c.

Deliberate inclusion of Na(acac) **34c** afforded adduct **33a** in good yield; acetyl acetone **34d** itself also provided this product, but at a disappointingly slow rate (entries 3 and 4). Alternatively, diethyl bromomalonate **34e** did afford **33d** in good yield without the need for added base (entry 5); in this case, the exocyclic alkylidene group is presumably formed via elimination rather than autoxidation. *N*-Methyl indole **34f** gave known indolyindolone **33e**⁴⁴ (entry 6) and use of the Danishefsky diene **34g** led to the tricyclic 4-pyridone **33f** in good yield

(entry 7), presumably via a stepwise Mannich/Michael process with **26-I**,⁴⁵ followed by autoxidation.

Table 2.1: Cyclization and trapping of diazo azide **26^a**

Entry	Substrate	Nucleophile	Product	Yield ^b (%)
<div style="text-align: center;"> <p> $\text{26} \xrightarrow[\text{PhMe (0.02M), rt, slow addition}]{\text{trap 34 (1.0 equiv.)}, \text{Cu(hfacac)}_2 \text{ (10 mol\%)}} \text{33}$ </p> </div>				
1	26	34a 	33b 	96
2	26	34b 	33c 	93
3	26	34c 	33a 	78
4	26	34d 	33a	— ^c
5	26	34e 	33d 	83
6	26	34f 	33e 	53
7	26	34g 	33f 	75

^aStandard procedure: a solution of **26** in PhMe (0.04 M) was added dropwise over 1 hr by syringe pump to a solution of Cu(hfacac)₂ (10 mol%) and the trap (2 equiv.) in PhMe (0.04 M) at rt. ^bAll yields given are for isolated product after chromatographic purification. ^cSmall quantities of **33a** were obtained, but yield was not determined.

2.3.4 Formation of a C-acylimine intermediate from dicarbonyl-stabilized diazo and subsequent trapping with nucleophiles

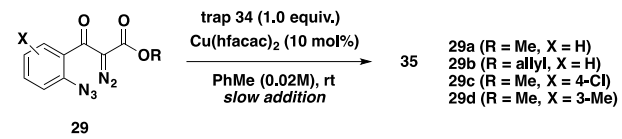
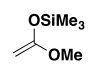
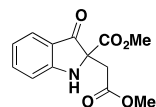
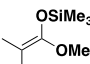
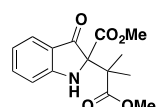
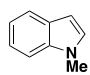
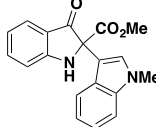
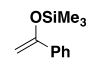
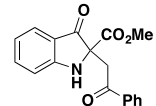
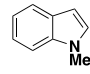
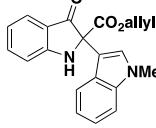
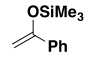
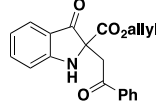
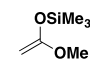
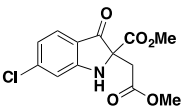
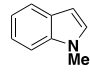
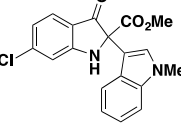
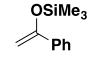
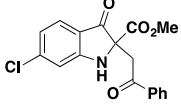
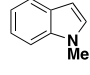
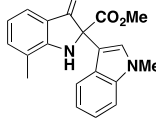
As previously noted, a second substrate **29a** bearing an additional carboxyl stabilizing group was prepared. This compound could also be subjected to the domino azide coupling/nucleophilic trapping process, though higher temperatures were required to consume the starting material. Treatment with Cu(hfacac)₂ in toluene at reflux in the presence of silyl ketene acetals **34a** and **34b** furnished adducts **35a** and **35b** (Table 2, entries 1 and 2). Diminished yields of **35b** can be attributed to the steric demand encountered during the formation of two contiguous quaternary centers. Given the lack of hydrogens at C-2 of the indolone ring, no autoxidation of **35a** was observed.

As stated in Chapter One, we wanted to extend the methodology to access one of our possible starting materials in the synthesis of isatisine A by using electron rich arenes, more specifically, indole as the trap. In Kerr and coworkers' synthesis, indole was reported to undergo a bimolecular reaction with a malonate-derived diazo in the presence of a copper catalyst, forming a compound with malonate on the C-3 position of the indole.⁴⁶ A similar transformation was reported by Davies and co-workers⁴⁷ using a rhodium catalyst.⁴⁸ We viewed this reaction as a potential problem for the desired domino cyclization and nucleophilic trapping. A competing N-H insertion with an unprotected indole and cyclopropanation were also foreseen problems. All of these side reactions could contribute to yield erosion of the desired adduct. However, as previously noted, our substrate design was guided by the idea that unimolecular reaction between metalcarbene and azide is a competent elementary step and more likely to occur before a bimolecular reaction. Thus, as predicted, treatment of **29a** with Cu(hfacac)₂ in toluene at reflux

in the presence of *N*-methyl indole **34f** gave the desired **35c** in good yield (entry 3), along with a substantial amount of the C-2 substituted side product. No formal C-H insertion or cyclopropanation between the *N*-Methyl indole and the ensuing metallocarbene was detected, indicating that trapping of the metallocarbene with the azide is kinetically faster than any formation of impurities. Using unprotected indole, however, resulted in a drastic reduction of the yield of the desired adduct (Chapter Three) and the formation of intractable highly-coloured compounds on TLC. Attempts to characterize the side products were met with failure. In Chapter Three, we will address these encountered problems using milder conditions to access the desired bis(indole) adducts.

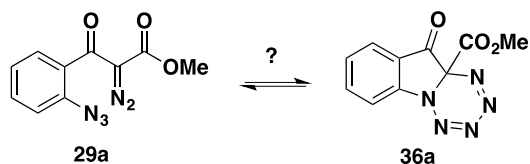
Other traps were also effective, including the trimethylsilyl enol ether of acetophenone **34h** (entry 4). The corresponding allyl ester **29b** also furnished the desired adducts, albeit in slightly diminished yields (entries 5 and 6). Interference with the intermediate metallocarbene by the pendent allyl group may contribute to yield erosion, though we were unable to detect any cyclopropane-containing impurities. The effects of ring substitution were also briefly evaluated with substrates **29c** and **29d**. An electron-withdrawing chloro substituent was well tolerated, affording adducts **35g-i**, and **29d**, which contained a methyl group adjacent to the azide. Notably, compatibility with halo substituents suggests that further elaboration of the indolinone products via cross-coupling processes should be possible.

Table 2.2: Cyclization and trapping of diazo azide 29^a

Entry	Substrate	Nucleophile	Product	Yield ^b (%)
<div style="text-align: center;">  </div>				
1	29a	34a 	35a 	89
2	29a	34b 	35b 	48
3	29a	34f 	35c 	72
4	29a	34h 	35d 	71
5	29b	34f 	35e 	63
6	29b	34h 	35f 	52
7	29c	34a ^c 	35g 	73
8	29c	34f 	35h 	76
9	29c	34h 	35i 	76
10	29d	34h 	35j 	68

^a Standard procedure: a solution of **29** in PhMe (0.04 M) was added dropwise over 1hr by syringe pump to a solution of Cu(hfacac)₂ (10 mol%) and the trap (2 equiv.) in PhMe (0.04 M) at reflux. ^b All yields given are for isolated product after chromatographic purification. ^c The OTBS silyl ketene acetal was used in place of the OTMS version.

During the time this work was presented at the Canadian Society for Chemistry (CSC) conference held in Vancouver, British Columbia, Prof. André Beauchemin from the University of Ottawa posed an intriguing question on the possible alternate structure of **29a-d**. Out of curiosity, Prof. Beauchemin was contemplating whether an alternative charge neutral azaheptacycle **36a-d** was possible (Scheme 2.29), inspiring a more detailed investigation into the structure of substrates **29a-d**.



Scheme 2.29: Possible equilibration and alternate structure for 29a.

The NMR characterizations for the presumed compounds **29a-d** in CDCl₃ showed a distinct signature for one compound alone suggesting that in the NMR timescale this compound did not equilibrate with another structure. However, the chemical shifts could also be consistent with **36a**. Furthermore, the IR characterization done in cast film, apart from the carbonyl peaks for the ketone and ester, showed one broad and strong peak at *ca.* 2100 cm⁻¹. This was consistent with azide and diazo functional groups. Enthralled by this enquiry, and to avoid structure ambiguity, we sought to further answer this question by obtaining a crystal structure of **29d**. In the solid state crystal structure of **29d**, depicted in Figure 2.6, it was clear that the compound exists only in the open form, and our earlier assignment was indeed the correct one.

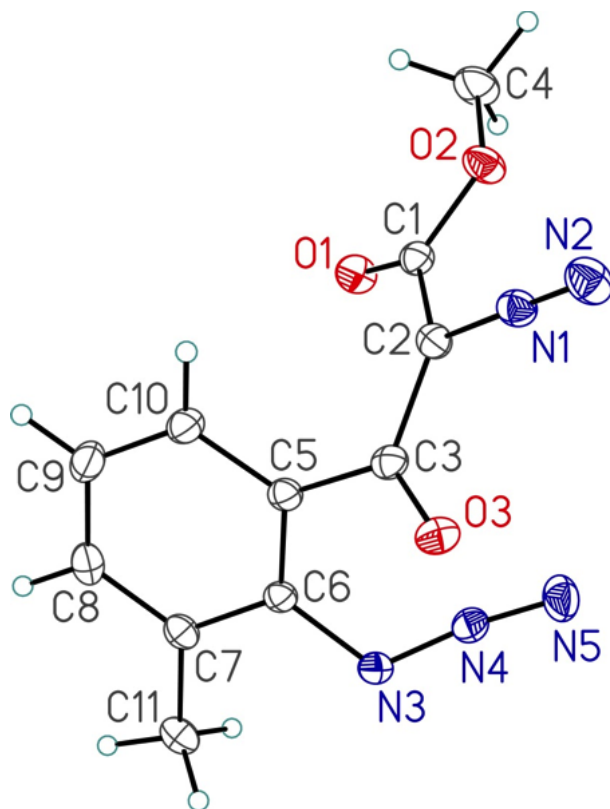
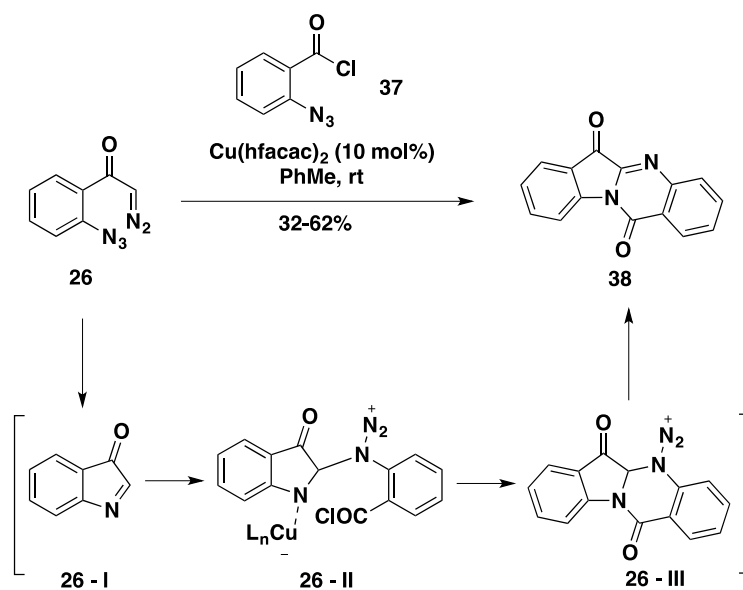


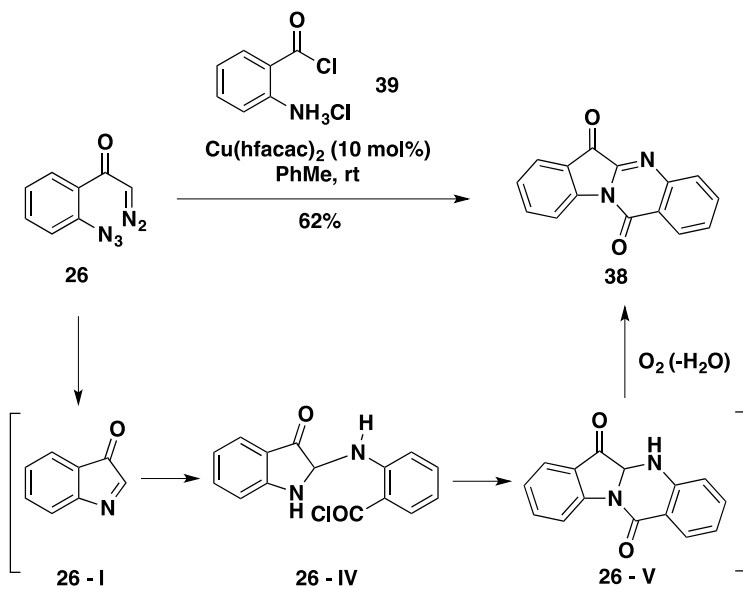
Figure 2.6: ORTEP derived from X-ray diffraction data of **29d**.

Finally, an interesting observation was made when **26** was treated with $\text{Cu}(\text{hfacac})_2$ in the presence of acid chloride **37** (Scheme 2.30). In this case, the tetracyclic product **38** was formed, but in variable yields. Compound **38** is the natural product tryptanthrin,⁴⁹ which possesses a number of promising biological activities.⁵⁰ This process is presumed to occur through sequential addition of the azido group of **37** to imine **26-I** (or its copper complex)⁵¹, followed by *N*-acylation from **26-II** and elimination of dinitrogen from **26-III**.



Scheme 2.30: Synthesis of tryptanthrin from 26 and 37.

Consistent yields could be obtained if ammonium chloride salt **39** was used in place of **37**. In this case, a dehydrogenation step from **26-V** must occur following assembly of the tetracyclic scaffold (Scheme 2.31).

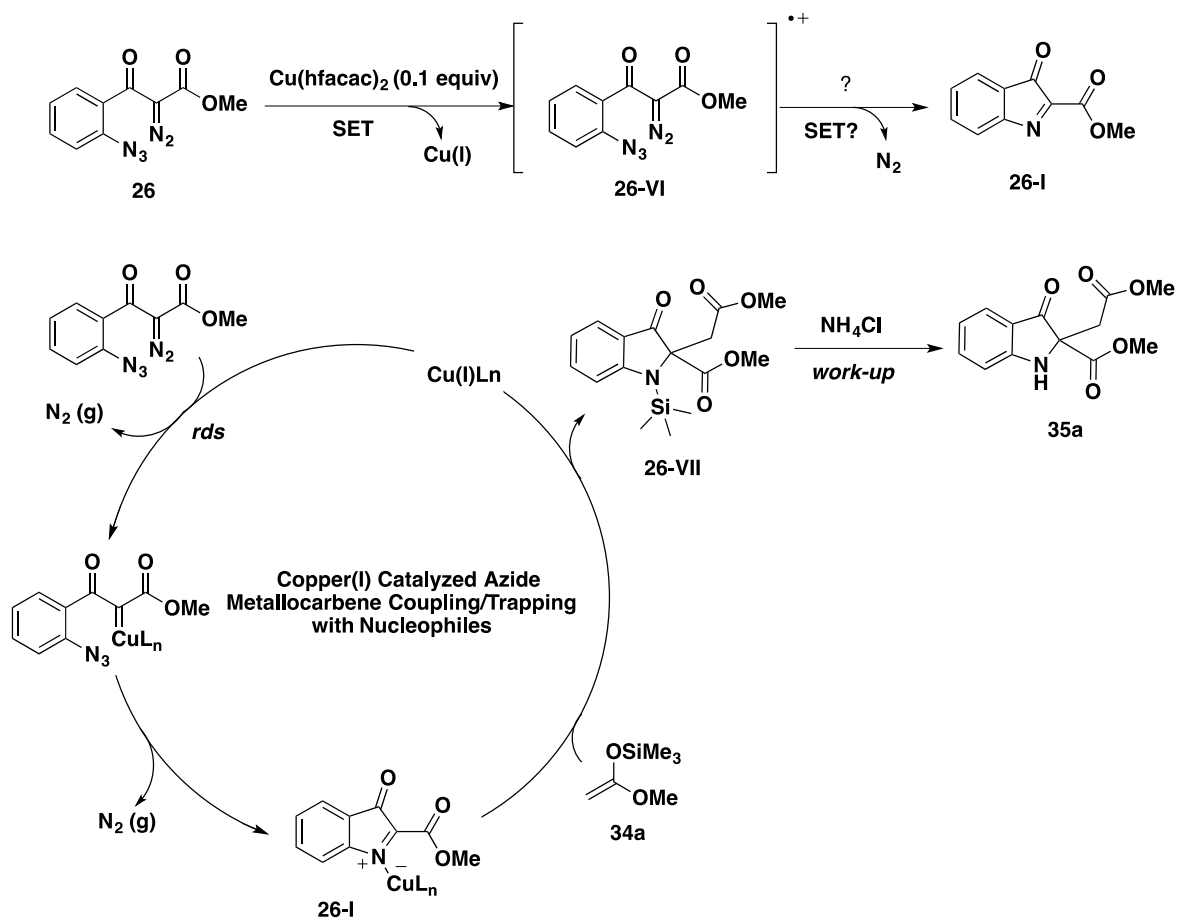


Scheme 2.31: Synthesis of tryptanthrin from 26 and 39.

2.3.5 Proposed mechanism for the transformation

Considering the previous precedents regarding the copper carbene chemistry studied by Salomon and Kochi,⁵² and the difference in the decomposition rate for a diazoketone and an azide observed by Doyle³⁵ and us, we constructed a proposed mechanism (Scheme 2.32). The first step involves a single electron transfer between a sacrificial quantity of the diazoketone **26** and the copper (II) catalyst, forming a copper (I) and radical cation **26-VI**. Copper (I) could then convert the remaining starting material **26** to the imine **26-I** (shown as coordinated with copper) *via* the immediate formation of a metallocarbene. Based on the kinetics and DFT calculations conducted by Nakamura and co-workers, the extrusion of nitrogen from the diazo-metal complex was likely the rate-determining step (*rds*) in the catalytic cycle.¹² This precedent from Nakamura reinforced our observations that dicarbonyl stabilized diazoketones were less prone to metal catalyzed decomposition compared to the monocarbonyl stabilized counterpart, presumably because of greater resonance stabilization of the former compared to the latter. The fate of the radical cation **26-VI** was not clear to us, but considering the maximal yield obtained on some of our substrates, it seemed that this could also be funneled to the intermediate imine **26-I** presumably *via* another single electron transfer and then extrusion of nitrogen. The intermediate imine could then be converted to the desired final product, likely *via* addition of the nucleophile on the copper (I) activated imine **26-I**, and silyl migration. The *N*-silyl protected indolinones **26-VII** could undergo facile desilylation to the desired amine during work-up using saturated ammonium chloride or saturated potassium carbonate. These *N*-silyl protected indolinones were difficult to isolate or to clearly ascertain on thin-layer chromatography (TLC) and attempts to do so were met with failure. However, after subjecting the crude reaction mixture before work-up to

electrospray mass spectrometry analysis, mass fragments corresponding to the proposed *N*-silyl intermediate **26-VII** were observed, reinforcing our proposal.



Scheme 2.32: Proposed reaction mechanism.

2.4 Summary

Domino azide trapping of highly reactive metalcarbenes and nucleophilic addition to the resulting *C*-acylimine has been achieved, forming substituted indolone systems by sequential formation of adjacent C–N and C–C bonds in one pot. With unsubstituted diazoketone precursors, a rapid autoxidation occurs after nucleophilic trapping. A variety of nucleophiles can be used, including active methylenes, silyl enol ethers, silyl ketene acetals, the Danishefsky

diene and *N*-methylindole. Use of 2-azido- or 2-aminobenzoyl chloride allows for the 1-step construction of the natural product tryptanthrin.

2.5 Experimental

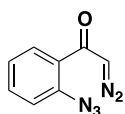
2.5.1 General Information

Reactions were carried out in an oven- (130 °C) or flame-dried glassware under a positive argon atmosphere unless otherwise stated. Transfer of anhydrous reagents was accomplished with oven-dried syringes or cannulae. Solvents were distilled before use: acetonitrile (CH₃CN), dichloromethane (DCM) and dichloroethane (DCE) from calcium hydride, toluene (PhMe) from sodium metal, diethyl ether (Et₂O) and tetrahydrofuran (THF) from sodium metal/benzophenone ketyl. Thin layer chromatography was performed on glass plates pre-coated with 0.25 mm silica gel with fluorescent indicator UV₂₅₄ (Rose Scientific). Flash chromatography columns were packed with 230-400 mesh silica gel (Silacyle). Proton nuclear magnetic resonance spectra (¹H NMR) were recorded at 300 MHz, 400 MHz, or 500 MHz and coupling constants (*J*) are reported in Hertz (Hz). Carbon nuclear magnetic resonance spectra (¹³C NMR) were recorded at 100 MHz or 125 MHz. The chemical shifts are reported on the δ scale (ppm) and referenced to the residual solvent peaks: CDCl₃ (7.26 ppm, ¹H; 77.06 ppm, ¹³C), *d*₆-DMSO (2.49 ppm, ¹H; 39.5 ppm, ¹³C).

Important safety precaution: While we did not observe any detonation during the preparation of 26 and 29a-d and their subsequent reactions with the catalysts and nucleophiles, and 29a-d are while amenable to gram-scale reactions, both azides and diazo groups are potentially explosive and must be handled with care, especially when the (C+O)/N ratio of the molecular formula is less than 3. In particular, for compound 26 we recommend limiting the scale of its preparation to ≤ 250 mg, although the procedure given is at a larger scale. Compounds 29a-d should be stored under argon or nitrogen at ≤ -20 °C and protected from exposure to light when not in use.

Distribution of credits: Dr. Tina Bott was responsible for the preparation **26**, **29a** and its ketoester **28a**, **33a-c**, **33f**, **35a-b**. I was responsible for the preparation of **29b-d** and its ketoester **28b-d**, **32**, **33c-d**, **35c-j**, **38**. Dr. Tina Bott was responsible for the optimization of the reaction using compound **26** and **29a**. She also observed the oxidation pathway of compound **33c** to **33c-A** and further to **33c-B**. Preliminary stability and decomposition studies using DSC and TGA experiments on **26**, **29a-d** and **32** were done by the author of this dissertation.

Compound 26:



Dichloromethane (35 mL) was added to a reaction flask containing 2-azidobenzoic acid (1.35 g, 8.3 mmol) and the suspension was cooled to 0 °C. Addition of 2,6-lutidine (1.4 mL, 16 mmol) resulted in a homogeneous reaction mixture that was subsequently treated with oxalyl chloride (1.9 mL, 16.4 mmol). The reaction was allowed to stir at 0 °C, with gradual warming to room temperature overnight. Removal of the solvent provided a deep red solid that was immediately dissolved in Et₂O and cooled to -78 °C. Once cooled, the acid chloride solution was transferred via cannula into an ethereal solution of diazomethane (~5 equivalents, prepared from Diazald®) at -78 °C. The reaction was allowed to warm from -78 °C to room temperature overnight. Excess diazomethane was quenched by drop-wise addition of glacial acetic acid. The solution was subsequently washed with an equal volume of water (2x), 1 M NaOH (3x) and brine. The combined organic layers were then dried over MgSO₄, filtered and concentrated to provide a yellow oil. Purification by flash chromatography, using a 9:1 mixture of hexanes:EtOAc, gave **26** in 74 % yield. To prevent decomposition, the product was stored under Ar in the freezer in a

foil wrapped flask. Under these conditions the compound was stable over several months.

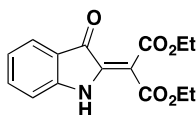
Inexperienced users should carry out this reaction at ~ 1/4 scale.

26: bright yellow crystalline solid; (m.p. = 66-67 °C), $R_f = 0.5$ (4:1 hexanes:EtOAc); IR (cast film) 3138, 2199, 2119, 1603, 1590, 1567, 1479, 1445, 1347, 1313, 1286 cm^{-1} ; ^1H NMR (300 MHz, CDCl_3) δ 7.79 (br d, $J = 6.3$ Hz, 1H); 7.50 (ddd, $J = 1.4, 7.0, 7.0$ Hz, 1H), 7.26-7.19 (m, 2H), 6.18 (br s, 1H); ^{13}C NMR (125 MHz, CDCl_3) δ 184.9, 137.9, 132.8, 130.2, 129.3, 125.0, 118.9, 58.0; HRMS calc'd for $\text{C}_8\text{H}_5\text{N}_5\text{ONa}$ $[\text{M} + \text{Na}]^+$ 210.0386, found 210.0385.

General procedure for the reaction of diazo-azide substrate 26 with external nucleophiles.

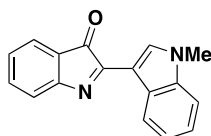
A solution of diazo-azide **26** in toluene (0.04 M) was added via syringe pump over 1h to a solution of the nucleophile **34** (2 equiv, 0.04 M in toluene) and $\text{Cu}(\text{hfacac})_2$ (10 mol %) at room temperature. The reaction mixture turned dark brown over the course of the addition. Once the addition was complete, the reaction was monitored by TLC for consumption of the diazo-azide starting material. The reaction was typically complete within 15 minutes of the conclusion of the syringe pump addition. In most cases, the reaction mixture was washed with an equivalent volume of 0.5 M aqueous solution of K_2CO_3 and brine. The combined organic layers were then dried over MgSO_4 , filtered, concentrated under reduced pressure and purified by flash chromatography. One exception is for the formation of **33f** using Danishefsky's diene (**34g**) as the nucleophile, which gave better results by evaporating the crude reaction mixture followed by direct column chromatography.

Compound 33d:



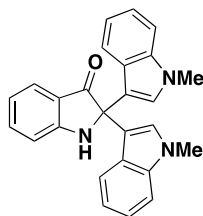
Isolated as a red/orange needle-like solid in 83 % yield; m.p. = 118-120°C; R_f = 0.50 (orange spot, 3:7 EtOAc:hexanes); IR (cast film) 3379, 2982, 2935, 1730, 1688, 1690, 1609, 1482, 1283, 1195, 1145, 754 cm^{-1} ; ^1H NMR (300MHz, CDCl_3) δ 9.17 (br s, 1H), 7.63 (d, J = 7.6 Hz, 1H), 7.48 (app t, J = 7.8 Hz, 1H), 6.98 (app t, J = 7.5 Hz, 1H), 6.91 (d, J = 8.1 Hz, 1H), 4.41 (q, J = 7.1 Hz, 2H), 4.29 (q, J = 7.1 Hz, 2H), 1.39 (t, J = 7.1 Hz, 3H), 1.32 (t, J = 7.1 Hz, 3H); ^{13}C NMR (125 MHz, CDCl_3) δ 185.6, 166.1, 164.7, 152.2, 142.4, 137.5, 125.6, 122.1, 119.9, 111.8, 102.2, 62.0, 61.7, 14.1, 13.9; HRMS calc'd for $[\text{C}_{15}\text{H}_{15}\text{NO}_5 + \text{Na}]^+$ 312.0842, found 312.0837.

Compound 33e:



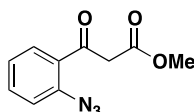
Isolated as purple solid with blue luster in 53 % yield; m.p. = 225-226 °C; R_f = 0.52 (purple spot, 3:7 EtOAc:hexanes); IR(cast film) 3051, 2924, 1719, 1610, 1558, 1457, 1368, 1291, 1157, 1141, 871, 771 cm^{-1} ; ^1H NMR (500 MHz, CDCl_3) δ 8.61 (m, 1H), 8.42 (s, 1H), 7.51 (m, 2H), 7.39 (m, 4H), 7.13 (ddd, J = 0.8, 7.5, 7.5 Hz, 1H), 3.90 (s, 3H); ^{13}C NMR (125 MHz, CDCl_3) δ 196.1, 163.7, 158.2, 137.6, 137.0, 136.2, 127.1, 126.1, 124.5, 123.8, 123.5, 122.9, 122.5, 121.1, 109.8, 106.8, 33.6; HRMS calc'd for $[\text{C}_{17}\text{H}_{12}\text{N}_2\text{O} + \text{H}]^+$ 261.1022, found 261.1023.

Bis(indole) adduct:



Upon extended stirring with N-methylindole **34f**, a 2:1 adduct was observed: isolated as light green crystals; m.p. > 250 °C (dec.), $R_f = 0.00$ (3:7 EtOAc:hexanes; insoluble in variety of solvents, minimal solubility in cold DMSO); IR (microscope) 3420, 3048, 2941, 1696, 1619, 1547, 1537, 1332, 746 cm^{-1} ; ^1H NMR (500 MHz, d_6 -DMSO) δ 8.13 (s, 1H), 7.49 (m, 1H), 7.46 (d, $J = 7.5$ Hz, 1H), 7.37 (d, $J = 8.0$ Hz, 2H), 7.31 (d, $J = 8.0$ Hz, 2H), 7.08 (m, 2H), 7.08 (br s (buried in m), 2H), 6.92 (d, $J = 8.5$ Hz, 1H), 6.86 (ddd, $J = 1.0, 7.5, 7.5$ Hz, 2H), 6.71 (ddd, $J = 0.5, 6.9, 6.9$ Hz, 1H), 3.70 (s, 6H); ^{13}C NMR (125 MHz, d_6 -DMSO) δ 201.5, 161.0, 138.0, 137.8, 128.7, 126.4, 125.0, 121.7, 121.1, 119.0, 118.1, 117.6, 113.5, 112.4, 110.3, 67.8, 32.8; HRMS cal'd for $[\text{C}_{26}\text{H}_{21}\text{N}_3\text{O} + \text{Na}]^+$ 414.1582, found 414.1575.

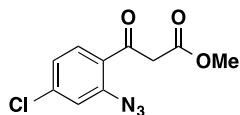
Compound 28a:



Dichloromethane (10 ml) was added to a conical flask containing 2-azidobenzoic acid (350 mg, 2.2 mmol) and the suspension was cooled to 0 °C before addition of methyl acetate (175 μL , 2.2 mmol) and trichloroacetyl chloride (290 μL , 2.6 mmol). This solution was slowly transferred *via* cannula to a suspension of NaH (60 % dispersion in oil, 105 mg, 2.6 mmol) in DCM (3 mL) at 0 °C. After stirring at 0 °C for 15 min, the solution was cooled to -45 °C before the addition of 1-methylimidazole (205 μL , 2.6 mmol). The solution was stirred for an additional 10 minutes at -

45 °C before slowly adding TiCl₄ (825 μ L, 7.5 mmol) followed by NBU₃ (2 mL, 8.4 mmol). The dark red/brown solution was kept at -45 °C for 30 minutes before being warmed to 0 °C and subsequently being quenched with water (10 mL). The organic layer was separated and the aqueous layer washed 3x with equal portions of Et₂O. The combined organic layers were washed with an equivalent volume of water and brine, dried over MgSO₄, filtered, and concentrated under reduced pressure. The crude product was purified by flash chromatography (silica gel, 1:4 hexanes:EtOAc) to afford 322 mg (68 %) of **28a** as a pale yellow oil: R_f = 0.60 (7:3 hexanes:EtOAc); IR (cast film) 2953, 2128, 1746, 1680, 1650, 1627, 1480, 1449, 1289, 1254, 1203 cm⁻¹; ¹H NMR (500 MHz, CDCl₃) *as a 4:1 mixture of keto:enol tautomers* δ (keto) 7.84 (ddd, J = 0.5, 1.6, 7.8 Hz, 1H), 7.59 (ddd, J = 1.7, 7.3, 8.1 Hz, 1H), 7.27-7.22 (m, 2H), 4.11 (s, 2H), 3.77 (s, 3H); δ (enol) 7.78 (dd, J = 1.6, 7.8 Hz, 1H), 7.48 (ddd, J = 1.6, 7.3, 8.1 Hz, 1H), 7.27-7.22 (m, 2H), 5.88 (s, 1H), 3.84 (s, 3H) *enol proton not detected*; ¹³C NMR (125 MHz, CDCl₃) *as a mixture of keto:enol tautomers* δ 192.9, 173.4, 168.7, 168.1, 139.1, 137.9, 133.9, 131.6, 131.1, 129.9, 129.4, 125.7, 125.0, 124.8, 119.2, 119.1 92.6, 52.3, 51.6, 49.6; HRMS calc'd for C₁₀H₉N₃O₃Na [M + Na]⁺ 242.0536, found 242.0536.

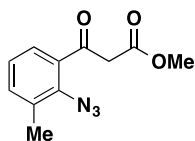
Compound **28c**:



Compound **28c** was prepared analogously to the procedure described for Compound **28a**, using 2-azido-4-chlorobenzoic acid as the starting material in place of 2-azidobenzoic acid. Isolated as a yellow oil in 76 % yield: R_f = 0.70 (7:3 hexanes:EtOAc); IR (cast film) 2953, 2115, 1745, 1680, 1589, 1249, 807 cm⁻¹; ¹H NMR (400 MHz, CDCl₃) *as a 5:2 mixture of keto:enol tautomers*

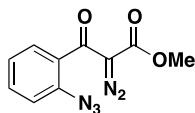
δ (keto) 7.66 (dd, $J = 0.4, 8.4$ Hz, 1H), 7.10-7.04 (m, 2H), 3.96 (s, 2H), 3.64 (s, 3H); δ (enol) 7.60(dd, $J = 0.8, 8.0$ Hz, 1H), 7.10-7.04 (m, 2H), 5.79 (s, 1H), 3.69 (s, 3H) *enol proton not detected*; ^{13}C NMR (125 MHz, CDCl_3) *as a mixture of keto:enol tautomers* δ 191.4, 173.2, 167.8, 167.0, 140.4, 139.8, 139.0, 137.2, 132.4, 130.9, 127.4, 125.3, 125.0, 123.7, 119.1(2x), 92.7, 52.2, 51.5, 49.3; HRMS calc'd for $\text{C}_{10}\text{H}_8^{35}\text{ClN}_3\text{O}_3\text{Na}$ $[\text{M} + \text{Na}]^+$ 276.0146, found 276.0144.

Compound 28d:



Compound **28d** was prepared analogously to the procedure described for Compound **28a**, using 2-azido-3-methylbenzoic acid as the starting material in place of 2-azidobenzoic acid. Isolated as a light yellow oil in 56 % yield: $R_f = 0.63$ (7:3 hexanes:EtOAc); IR (cast film) 2955, 2110, 1740, 1680, 1601, 1251, 807 cm^{-1} ; ^1H NMR (400 MHz, CDCl_3) *3:1 mixture of keto:enol tautomers* δ (keto) 7.53 (br d, $J = 7.9$ Hz, 1H), 7.34-7.30 (m, 1H), 7.14 (app t, $J = 7.5$ Hz, 1H), 4.00 (s, 2H), 3.71 (s, 3H), 2.37 (br s, 3H); δ (enol) 7.33-7.30 (m, 1H), 7.22 (br d, $J = 7.6$ Hz 1H), 7.09 (app t, $J = 7.7$ Hz, 1H), 5.49 (s, 1H), 3.78 (s, 3H), 2.32 (s, 3H) *enol proton not detected*; ^{13}C NMR (125 MHz, CDCl_3) *as a mixture of keto:enol tautomers* δ 193.7, 173.0, 170.9, 167.7, 137.2, 135.9, 135.3, 133.7, 133.1, 132.9, 131.6, 128.7, 128.0, 127.7, 125.4, 92.2, 52.9, 52.4, 51.5, 48.4, 40.5, 18.1; HRMS calc'd for $\text{C}_{11}\text{H}_{11}\text{N}_3\text{O}_3\text{Na}$ $[\text{M} + \text{Na}]^+$ 256.0693, found: 256.0695.

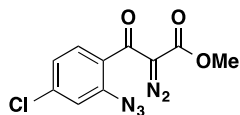
Compound 29a:



Triethylamine (715 μ L, 5.1 mmol) was added to a stirred solution of ketoester **28a** (1.02 g, 4.65 mmol) in CH₃CN (19 ml). Tosyl azide (916 mg, 4.65 mmol) in CH₃CN (9 mL) was transferred *via* cannula into the flask and the reaction was left to stir overnight. Concentration under reduced pressure followed by purified *via* flash chromatography (silica gel, 17:3 hexanes:EtOAc) resulted in a quantitative yield of **29a** (1.14 g) as a pale yellow solid. To prevent decomposition the product was stored under Ar in the freezer in a foil wrapped flask. Under these conditions the compound was stable over several months.

29a: m.p. = 76-78 °C; R_f = 0.54 (7:3 hexanes:EtOAc); IR (cast film) 2956, 2132, 1729, 1700, 1633, 1597, 1486, 1446, 1438, 1334, 1316, 1287 cm⁻¹; ¹H NMR (500 MHz, CDCl₃) δ 7.54-7.52 (m, 1H), 7.34 (dd, J = 1.5, 7.8 Hz, 1H), 7.28-7.21 (m, 2H), 3.79 (s, 3H); ¹³C NMR (125 MHz, CDCl₃) δ 185.7, 160.9, 137.7, 137.5, 131.9, 130.3, 128.4, 124.8, 118.3, 52.3; HRMS calc'd for C₁₀H₇N₅O₃ [M]⁺ 245.0549, found 245.0549.

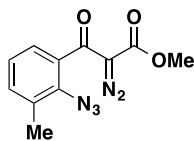
Compound 29c:



Compound **29c** was prepared analogously to the procedure described for Compound **29a**, using compound **28c** as the starting material in place of Compound **28a**. Isolated as a light orange oil in 94 % yield: R_f = 0.65 (7:3 hexanes:EtOAc); IR (cast film) 2956, 2113, 1729, 1633, 1591, 1318,

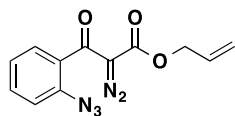
907 cm^{-1} ; ^1H NMR (400 MHz, CDCl_3) δ 7.25-7.23 (m, 1H), 7.17-7.15 (m, 2H), 3.76 (s, 3H); ^{13}C NMR (125MHz, CDCl_3) δ 184.6, 160.7, 139.2, 137.8, 129.7, 128.7, 125.1, 118.6, 52.4 (diazoketone ^{13}C signal was not detected due to broadening); HRMS calc'd for $\text{C}_{10}\text{H}_6^{35}\text{ClN}_5\text{O}_3\text{Na}$ $[\text{M} + \text{Na}]^+$ 302.0051, found: 302.0054.

Compound 29d:



Compound **29d** was prepared analogously to the procedure described for Compound **29a**, using compound **28d** as the starting material in place of Compound **28a**. Isolated as yellow oil in 88 % yield: $R_f = 0.59$ (7:3 hexanes:EtOAc); IR (cast film) 2956, 2122, 1725, 1630, 1455, 1306, 1200, 1126, 750 cm^{-1} ; ^1H NMR (500 MHz, CDCl_3) δ 7.31-7.29 (m, 1H), 7.18-7.16 (m, 2H), 3.79 (s, 3H), 2.43 (s, 3H); ^{13}C NMR (125 MHz, CDCl_3) δ 168.2, 160.8, 135.5, 133.7, 132.5, 132.4, 126.1, 125.4, 52.4, 17.9 (diazoketone ^{13}C signal was not detected due to broadening); HRMS calc'd for $\text{C}_{11}\text{H}_9\text{N}_5\text{O}_3\text{Na}$ $[\text{M} + \text{Na}]^+$ 282.0598, found: 282.0598. (Note: a crystalline **29d** can be prepared by slow evaporation of a saturated DCM solution overnight at room temperature, m.p. = 83-84 $^\circ\text{C}$)

Preparation of Compound 29b:

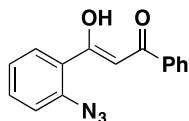


Dichloromethane (10 ml/ 350 mg acid) was added to a conical flask containing 2-azido benzoic acid (1.0-1.2 g, 6.3-7.5 mmol) and the suspension was cooled to 0 $^\circ\text{C}$ before addition of allyl acetate (1.0 equiv) and trichloroacetyl chloride (1.2 equiv). This solution was slowly transferred via cannula to a suspension of NaH (1.2 equiv) in DCM (3 mL/350 mg acid) at 0 $^\circ\text{C}$. After

stirring at 0 °C for 15 min, the solution was cooled to -45 °C before the addition of 1-methylimidazole (1.2 equiv). The solution was then stirred for an additional 10 minutes at -45 °C before slowly adding TiCl₄ (3.4 equiv) followed by NBU₃ (4.0 equiv). The dark red/brown solution was kept at -45 °C for 30 minutes before being warmed to 0 °C and subsequently quenched with water (10 mL/ 350 mg acid). The organic layer was separated and the aqueous washed 3x with equal portions of DCM. The combined organic layers were washed with an equivalent volume of water and brine, dried over MgSO₄, filtered, and concentrated under reduced pressure. The crude product **28b** was partially purified by flash chromatography to afford an orange oil whose R_f was about 0.7 (7:3 hexanes:EtOAc). The orange oil was concentrated and added to a stirred solution of triethylamine (1.2 equiv) in CH₃CN (20 mL/1.2 equiv). Tosyl azide (1.0 equiv) in CH₃CN (9 mL/1.0 equiv) was transferred via cannula into the flask and the reaction was left to stir overnight. Concentration under reduced pressure followed by purification via flash chromatography (silica gel, 8:2 hexanes:EtOAc→7:3 hexanes:EtOAc slowly added in gradient) furnished **29b** as a yellow oil in 46 % yield (from starting 2-azidobenzoic acid).

29b: R_f = 0.59 (7:3 hexanes:EtOAc); IR (cast film) 2956, 2122, 1725, 1630, 1455, 1306, 1200, 1126, 750 cm⁻¹; ¹H NMR (500 MHz, CDCl₃) δ 7.45 (ddd, *J* = 1.7, 8.0, 8.0 Hz, 1H), 7.31 (ddd, *J* = 0.6, 1.7, 8.0 Hz, 1H), 7.18-7.16 (m, 2H), 5.80 (app tdd, *J* = 5.8, 10.4, 17.2 Hz 1H), 5.22 (app tdd, *J* = 1.5, 1.5, 17.2 Hz, 1H), 5.21 (app tdd, *J* = 1.3, 1.3, 10.4 Hz, 1H), 4.62-4.60 (m, 2H); ¹³C NMR (125 MHz, CDCl₃) δ 185.6, 160.2, 137.7, 131.9, 131.3, 130.4, 128.5, 124.7, 119.0, 118.3, 65.9 (diazoketone ¹³C signal was not observed due to broadening); HRMS calc'd for C₁₂H₉N₅O₃Na [M+Na]⁺ 294.0598, found: 294.0594.

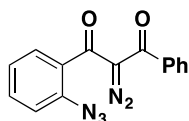
Compound 31:



A solution of LiHMDS (6.2 mL, 6.2 mmol, 1M THF) was added to a solution of 2-azidoacetophenone (1.0 g, 6.2 mmol) in 10 mL THF at -78 °C. The mixture was allowed to stir for 30 min. Then, a solution of benzoyl cyanide (822 mg, 6.2 mmol, dissolved in 10 mL THF) was added dropwise. The mixture was allowed to stir for 1 h. The reaction was quenched with satd. NH₄Cl (15 mL). The mixture was diluted with diethyl ether (10 mL). The organic layer was separated and washed with water (20 mL, 3x). The organic layer was washed with brine and dried with MgSO₄. The solution was concentrated under pressure to afford yellow oil. The yellow oil was purified using flash column chromatography eluting 10 % EtOAc in hexanes to furnish 1.13 g (69%) of **31** as a yellow oil.

31: R_f = 0.63 (7:3 hexanes:EtOAc); IR (cast film) 3064, 2420, 2125, 1599, 1281, 1604, 778, 1126, 750 cm⁻¹; ¹H NMR (500 MHz, CDCl₃) δ 8.01-7.87 (m, 3H), 7.59-7.48 (m, 4H), 7.28-6.99 (m, 2H), 7.00 (s, 1H); ¹³C NMR (125 MHz, CDCl₃) δ 185.5, 184.4, 138.3, 135.4, 132.6, 132.5, 130.4, 128.7, 128.3, 127.3, 125.0, 119.3, 98.3; HRMS calc'd for C₁₅H₁₁N₃O₂ [M]⁺ 265.0851, found: 294.0849. (Note: the enol H was not detected.)

Compound 32

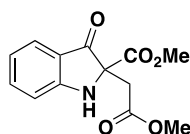


Triethylamine (715 μL, 5.1 mmol) was added to a stirred solution of ketoenol **31** (500 mg, 1.89 mmol) in CH₃CN (8 mL). Tosyl azide (400 mg, 2.00 mmol) in CH₃CN (5 mL) was transferred

via cannula into the flask and the reaction was left to stir overnight. Concentration under reduced pressure followed by purified *via* flash chromatography (silica gel, 7:3 hexanes:EtOAc) resulted in a quantitative yield of **32** (551 mg, quant) as a pale yellow oil. To prevent decomposition the product was stored under Ar in the freezer in a foil wrapped flask. Under these conditions the compound was stable over several months.

32: $R_f = 0.71$ (7:3 hexanes:EtOAc); IR (cast film) 3053, 2451, 2132, 1641, 1283, 1607, 779, 1136, 754 cm^{-1} ; ^1H NMR (500 MHz, CDCl_3) δ 7.55-7.53 (m, 2H), 7.43-7.28 (m, 5H), 7.13 (ddd, $J = 7.6, 7.6, 0.8$ Hz, 1H), 6.92 (d, $J = 8.0$ Hz, 1H); ^{13}C NMR (125 MHz, CDCl_3) δ 185.9, 184.9, 137.5, 136.7, 132.5, 132.5, 130.0, 129.5, 128.2, 128.0, 125.0, 118.2, 98.3; LC-MS calc'd for $\text{C}_{15}\text{H}_9\text{N}_5\text{O}_2$ $[\text{M}+\text{H}]^+$ 291.2, found: 291.2.

Representative procedure for reaction of **29a-d** with nucleophiles: Compound **35a**:

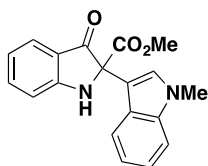


A solution of diazo-azide **29a** in toluene (0.04 N) was added to a solution of 1-methoxy-1-trimethoxysilyloxyethene **34a** (2 equiv, 0.04 N in toluene) and $\text{Cu}(\text{hfacac})_2$ (10 mol %) at reflux *via* syringe pump over 1h. The reaction mixture turned dark brown over the course of the addition. Once the addition was complete, the reaction was monitored by TLC for consumption of the diazo-azide starting material. Upon consumption of **29a**, the reaction mixture was cooled to room temperature and then washed with an equivalent volume of 0.5 M aqueous solution of K_2CO_3 and brine. The combined organic layers were then dried over MgSO_4 , filtered, concentrated under reduced pressure and purified by flash chromatography (silica gel, 4:1 hexanes:EtOAc) to yield 89 % of **35a** as a yellow oil: $R_f = 0.3$ (yellow spot, 7:3 hexanes:EtOAc); IR (cast film) 3377, 2955, 1743, 1617, 1488, 1469, 1214 cm^{-1} ; ^1H NMR (500

MHz, CDCl₃) δ 7.60 (br d, J = 7.8 Hz, 1H), 7.52-7.48 (m, 1H), 6.97 (dd, J = 0.7, 7.5 Hz, 1H), 6.91-6.88 (m, 1H), 5.61 (br s, 1H), 3.74 (s, 3H), 3.72 (s, 3H), 3.55 (d, J = 17.4 Hz, 1H), 2.57 (d, J = 17.4 Hz, 1H); ¹³C NMR (125 MHz, CDCl₃) δ 194.0, 171.5, 167.8, 161.8, 138.0, 125.4, 120.3, 119.2, 113.3, 71.53, 53.6, 52.2, 39.6; HRMS calc'd for C₁₃H₁₃NO₅ [M]⁺ 263.0794, found: 263.0794.

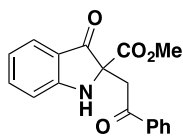
Similar procedures were followed in the preparation of **35b-j**.

Compound 35c:



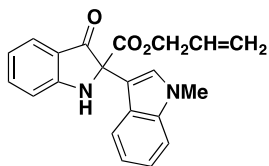
Isolated as a yellow solid in 72 % yield: m.p. = 80–81 °C (powder), m.p. = 165-166 °C (crystals); R_f = 0.31 (yellow spot, 7:3 hexanes:EtOAc); IR (cast film) 3366, 3051, 1744, 1702, 1616, 1485, 1293, 742 cm⁻¹; ¹H NMR (500 MHz, CDCl₃): δ 7.73 (d, J = 8.0 Hz, 1H), 7.60 (d, J = 8.0 Hz, 1H), 7.56 (app dt, J = 1.0, 8.0 Hz, 1H), 7.34 (d, J = 8.5 Hz, 1H), 7.30 (s, 1H), 7.26 (app dt, J = 0.5, 8.0 Hz, 1H), 7.14 (app dt, J = 0.5, 7.5 Hz, 1H), 7.02 (d, J = 8.5 Hz, 1H), 6.96 (app t, J = 8.0 Hz, 1H), 5.77 (br s, 1H), 3.84 (s, 3H), 3.79 (s, 3H); ¹³C NMR (125 MHz, CDCl₃): δ 195.2, 169.1, 161.0, 137.9, 137.4, 128.0, 126.0, 125.4, 122.3, 120.4, 120.0, 119.9, 119.5, 113.6, 109.8, 109.8, 72.4, 53.8, 32.9; HRMS calc'd for C₁₉H₁₇N₂O₃ [M + H]⁺ 321.1234, found: 321.1233.

Compound 35d:



Isolated as a yellow oil in 71 % yield: $R_f = 0.48$ (yellow spot, 7:3 hexanes:EtOAc); IR (cast film) 3379, 2953, 2919, 1745, 1702, 1619, 1487, 1221, 753 cm^{-1} ; ^1H NMR (500 MHz, CDCl_3): δ 8.00 (d, $J = 8.0$ Hz, 2H), 7.67-7.62 (m, 2H), 7.56-7.50 (m, 3H), 7.01 (d, $J = 8.0$ Hz, 1H), 6.93 (app t, $J = 8.0$ Hz, 1H), 5.81 (br s, 1H), 4.37 (d, $J = 18.0$ Hz, 1H), 3.77 (s, 3H), 3.22 (d, $J = 18.0$ Hz, 1H); ^{13}C NMR (125 MHz, CDCl_3): δ 197.7, 195.0, 168.1, 162.0, 138.1, 135.8, 133.9, 128.8, 128.3, 125.4, 120.1, 119.1, 113.2, 71.9, 53.6, 44.8; HRMS calc'd for $\text{C}_{18}\text{H}_{16}\text{NO}_4$ $[\text{M} + \text{H}]^+$ 310.1074, found: 310.1074.

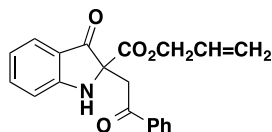
Compound 35e:



Isolated as a yellow powder in 63% yield: m.p. 92 $^{\circ}\text{C}$ (dec.); $R_f = 0.43$ (yellow spot, 7:3 hexanes:EtOAc); IR (cast film) 3371, 3051, 2919, 1742, 1703, 1615, 1485, 1225, 743 cm^{-1} ; ^1H NMR (500 MHz, CDCl_3): δ 7.72 (d, $J = 7.8$ Hz, 1H), 7.63 (d, $J = 8.1$ Hz, 1H), 7.52 (ddd, $J = 1.3$, 7.1, 8.3 Hz, 1H), 7.32-7.30 (m, 2H), 7.26 (ddd, $J = 1.1$, 7.0, 8.2 Hz, 1H), 7.12 (ddd, $J = 1.1$, 7.0, 8.0 Hz, 1H), 6.99 (d, $J = 8.2$ Hz, 1H), 6.94 (app t, $J = 7.8$ Hz, 1H), 5.88 (app tdd, $J = 5.6$, 10.5, 17.2 Hz, 1H), 5.83 (brs, 1H), 5.29 (app tdd, $J = 1.5$, 1.5, 17.2 Hz, 1H), 5.22 (app tdd, $J = 1.2$, 1.2, 10.4 Hz, 1H), 4.76 (app tdd, $J = 1.5$, 5.5, 13.5 Hz, 1H), 4.71 (app tdd, $J = 1.5$, 5.5, 13.5 Hz, 1H), 3.73 (s, 3H); ^{13}C NMR (125 MHz, CDCl_3): δ 194.7, 168.3, 161.0, 137.8, 137.4, 131.2, 128.1,

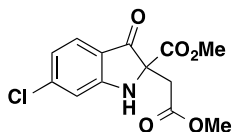
126.0, 125.4, 122.2, 120.2, 119.9(2x), 119.8, 119.1, 113.5, 109.8, 109.7, 72.5, 67.1, 32.9; HRMS calc'd for C₂₁H₁₉N₂O₃ [M + H]⁺ 347.1390, found: 347.1393.

Compound 35f:



Isolated as yellow oil in 52 % yield: $R_f = 0.55$ (yellow spot, 7:3 hexanes:EtOAc); IR (cast film) 3379, 2918, 1744, 1702, 1619, 1487, 1220, 753 cm^{-1} ; ¹H NMR (500 MHz, CDCl₃): δ 8.01-7.99 (m, 2H), 7.66 (br d, $J = 7.7$ Hz, 1H), 7.63 (m, 1H) 7.53-7.50 (m, 3H), 7.00 (d, $J = 8.5$ Hz, 1H), 6.92 (app t, $J = 8.0$ Hz, 1H), 5.85 (app tdd, $J = 5.5, 10.5, 17.2$ Hz, 1H), 5.85 (buried br s, 1H), 5.28 (app tdd, $J = 1.5, 1.5, 17.2$ Hz, 1H), 5.20 (app tdd, $J = 1.3, 1.3, 10.5$ Hz, 1H), 4.68 (app tdd, $J = 1.0, 5.5, 13.0$ Hz, 1H), 4.63 (app tdd, $J = 1.0, 5.5, 13.0$ Hz, 1H), 4.40 (d, $J = 18.2$ Hz, 1H), 3.22 (d, $J = 18.2$ Hz, 1H); ¹³C NMR (125 MHz, CDCl₃) δ 197.6, 195.0, 167.3, 162.0, 138.0, 135.9, 133.9, 131.3, 128.8, 128.2, 125.4, 120.0, 119.1, 118.6, 113.2, 72.0, 66.9, 44.8; HRMS calc'd for C₂₀H₁₈NO₄ [M + H]⁺ 336.1230, found: 336.1230.

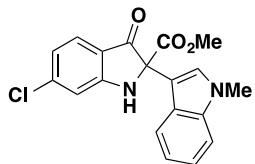
Compound 35g:



Isolated as a light yellow oil in 73 % yield: $R_f = 0.40$ (yellow spot, 7:3 hexanes:EtOAc); IR (cast film) 3368, 2955, 1746, 1716, 1612, 1438, 1214, 922 cm^{-1} ; ¹H NMR (500 MHz, CDCl₃): δ 7.55 (d, $J = 8.0$ Hz, 1H), 7.01 (d, $J = 1.9$ Hz, 1H), 6.90 (dd, $J = 1.6, 8.2$ Hz, 1H), 5.72 (br s, 1H), 3.79 (s, 3H), 3.77 (s, 3H), 3.58 (d, $J = 18.0$ Hz, 1H), 2.62 (d, $J = 18.0$ Hz, 1H); ¹³C NMR (125 MHz,

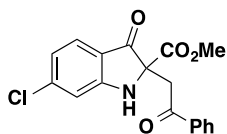
CDCl₃): δ 192.6, 171.4, 167.5, 161.9, 144.7, 126.4, 121.2, 117.7, 113.1, 71.9, 53.8, 52.3, 39.5;
HRMS calc'd for C₁₃H₁₃³⁵CINO₅ [M + H]⁺ 298.0477, found: 298.0474.

Compound 35h:



Isolated as bright yellow crystals in 76 % yield: m.p. = 194-195°C; R_f = 0.35 (yellow spot, 7:3 hexanes:EtOAc); IR (cast film) 3364, 3052, 2952, 1746, 1711, 1610, 1242, 741 cm⁻¹; ¹H NMR (400 MHz, CDCl₃): δ 7.61 (d, J = 8.0 Hz, 1H), 7.52 (ddd, J = 1.0, 1.8, 8.0 Hz, 1H), 7.31 (ddd, J = 1.1, 1.8, 8.3 Hz, 1H), 7.26-7.22 (m, 2H), 7.10 (ddd, J = 1.1, 7.0, 8.1 Hz, 1H), 6.99 (dd, J = 0.5, 1.7 Hz, 1H), 6.89 (dd, J = 1.7, 8.3 Hz, 1H) 5.80 (br s, 1H), 3.81 (s, 3H), 3.75 (s, 3H); ¹³C NMR (125 MHz, CDCl₃) δ 193.3, 168.6, 161.1, 144.5, 137.3, 128.0, 126.4, 125.8, 122.3, 121.1, 120.1, 119.3, 118.1, 113.3, 109.8, 109.3, 72.7, 53.9, 32.9; HRMS calc'd for C₁₉H₁₆³⁵ClN₂O₃ [M + H]⁺ 355.0844, found: 355.0846.

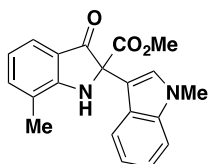
Compound 35i:



Isolated as a light yellow oil in 76 % yield: R_f = 0.43 (yellow spot, 7:3 hexanes:EtOAc); IR (cast film) 3394, 2955, 1747, 1709, 1612, 1221, 787 cm⁻¹; ¹H NMR (500 MHz, CDCl₃): δ 8.00 (dd, J = 1.0, 8.3 Hz, 2H), 7.65 (app dt, J = 1.3, 7.3 Hz, 1H), 7.59 (dd, J = 0.6, 8.4 Hz, 1H), 7.54-7.41 (m, 2H), 7.00 (dd, J = 0.5, 1.7 Hz, 1H), 6.90 (dd, J = 1.7, 8.3 Hz, 1H), 5.87 (br s, 1H), 4.37 (d, J

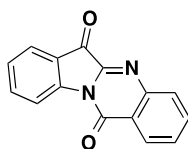
= 18.0 Hz, 1H), 3.77 (s, 3H), 3.22 (d, $J = 18.0$ Hz, 1H); ^{13}C NMR (125 MHz, CDCl_3) $\delta = 197.5$, 193.5, 167.7, 162.1, 144.7, 135.7, 134.0, 128.8, 128.3, 126.3, 120.9, 117.5, 113.0, 72.3, 53.7, 44.6; HRMS calc'd for $\text{C}_{18}\text{H}_{15}^{35}\text{ClNO}_4$ $[\text{M} + \text{H}]^+$ 344.0684, found: 344.0686.

Compound 35j:



Isolated as a yellow powder in 68 % yield: m.p. = 170-171 °C; $R_f = 0.35$ (yellow spot, 7:3 hexanes:EtOAc); IR(cast film) 3359, 3055, 2950, 1746, 1705, 1608, 1460, 1241, 743 cm^{-1} ; ^1H NMR (500 MHz, CDCl_3) δ 7.55-7.33 (m, 2H), 7.31-7.19 (m, 4H), 7.07 (app t, $J = 7.9$ Hz, 1H), 6.84 (app t, $J = 7.3$ Hz, 1H), 5.58 (br s, 1H), 3.77 (s, 3H), 3.72 (s, 3H), 2.26 (s, 3H); ^{13}C NMR (125 MHz, CDCl_3) δ 195.2, 169.2, 160.2, 137.9, 137.4, 128.1, 126.1, 122.8, 122.7, 122.2, 120.5, 119.9, 119.5, 119.5, 110.0, 109.8, 72.5, 53.8, 32.9, 15.8; HRMS calc'd for $\text{C}_{20}\text{H}_{19}\text{N}_2\text{O}_3$ $[\text{M} + \text{H}]^+$ 335.1396, found: 335.1388.

Tryptanthrin 38:



Anthranilic acid (2.0 equiv) in toluene (20 mL) solution was added with thionyl chloride (2.0 equiv) and the solution was heated at reflux for 2 h. The reaction mixture was allowed to cool to rt, then a toluene solution of $\text{Cu}(\text{hfacac})_2$ (0.1 equiv) was added and stirred for 30 mins. The solution was then allowed to warm to 40 – 50 °C before a toluene solution of **26** (49 mg, 0.26 mmol, 1.0 equiv, 0.04 M) was added via syringe pump over 1 h and then stirred for an additional

6 h. The reaction mixture was allowed to cool and was washed with equivalent volumes of 1.0 M aq K_2CO_3 and brine. The combined organic layers were dried over $MgSO_4$, filtered and concentrated under reduced pressure to afford a black crude material. The mixture was dissolved in small amount of DCM and purified by column chromatography using silica gel; 20%→30→40% EtOAc in hexane gradient elution to furnish 40 mg (62 %) of **38** as a fibrous yellow solid (minimal solubility in $CHCl_3$ and DMSO): m.p. 262-264 °C; $R_f = 0.72$ (yellow spot, 1:1 EtOAc:hexanes); IR(cast film) 2920, 1735, 1694, 1468, 1316, 775, 757 cm^{-1} ; 1H NMR (300 MHz, $CDCl_3$) δ 8.65 (d, $J = 8.1$ Hz, 1H), 8.46 (d, $J = 7.2$ Hz, 1H), 8.05 (d, $J = 8.1$ Hz, 1H), 7.78-7.94 (m, 3H), 7.69 (app t, $J = 7.5$ Hz, 1H) 7.44 (app t, $J = 7.5$ Hz, 1H); ^{13}C NMR (125 MHz, $CDCl_3$) δ 182.6, 158.2, 146.7, 146.4, 144.4, 138.3, 135.2, 130.8, 130.3, 127.6, 127.2, 125.4, 123.8, 122.0, 118.0; HRMS calc'd for $C_{15}H_8O_2N_2$ $[M]^+$ 248.0586, found 248.0585.

2.6 References

1. Fleming, I., *Pericyclic reactions*. Second edition. ed.; Oxford University Press: Oxford, 2015.
2. (a) Singh, M. S., *Reactive intermediates in organic chemistry : structure and mechanism*. (online resource); (b) Olah, G. A.; Prakash, G. K. S., *Carbocation chemistry*. Wiley-Interscience: Hoboken, N.J., 2004. (c) Parsons, A. F., *An introduction to free-radical chemistry*. Blackwell Science: Oxford; Malden, MA, 2000. (d) Perkins, M. J., *Radical chemistry: the fundamentals*. Oxford University Press: Oxford ; New York, 2000. (e) Buncl, E.; Dust, J. M., *Carbanion chemistry: structures and mechanisms*. American Chemical Society ; Oxford University Press: Washington, DC Oxford, 2003.
3. Bott, T. M.; Vanecko, J. A.; West, F. G., *J. Org. Chem.* **2009**, *74*, 2832-2836.
4. (a) Kwon, Y.; Schatz, D. J.; West, F. G., *Angew. Chem. Int. Ed.* **2015**, *54*, 9940-9943; (b) Wu, Y.-K.; McDonald, R.; West, F. G., *Org. Lett.* **2011**, *13*, 3584-3587.
5. Barber, J. S.; Styduhar, E. D.; Pham, H. V.; McMahon, T. C.; Houk, K. N.; Garg, N. K., *J. Am. Chem. Soc.* **2016**, *138*, 2512-2515.
6. Tietze, L.-F.; Brasche, G.; Gericke, K. M., *Domino reactions in organic synthesis*. Wiley-VCH: Weinheim, 2006.
7. Regitz, M.; Maas, G., *Diazo compounds properties and synthesis*. Academic Press: Orlando, 1986 (online resource).
8. (a) Davies, H. M.; Morton, D., *Chem. Soc. Rev.* **2011**, *40*, 1857-1869; (b) Davies, H. M.; Beckwith, R. E., *Chem. Rev.* **2003**, *103*, 2861-2904; (c) Padwa, A.; Weingarten, M. D., *Chem. Rev.* **1996**, *96*, 223-270; (d) Doyle, M. P.; Forbes, D. C., *Chem. Rev.* **1998**, *98*, 911-936.

9. Doyle, M. P.; McKervey, M. A.; Ye, T., *Modern catalytic methods for organic synthesis with diazo compounds : from cyclopropanes to ylides*. Wiley: New York, 1998.
10. Davies, H. M.; Du Bois, J.; Yu, J. Q., *Chem. Soc. Rev.* **2011**, *40*, 1855-1856.
11. Carey, F. A.; Sundberg, R. J., *Advanced organic chemistry. Part B, Reaction and synthesis*. 5th ed.; Springer: New York, 2007.
12. Nakamura, E.; Yoshikai, N.; Yamanaka, M., *J. Am. Chem. Soc.* **2002**, *124*, 7181-7192.
13. Ford, A.; Miel, H.; Ring, A.; Slattery, C. N.; Maguire, A. R.; McKervey, M. A., *Chem. Rev.* **2015**, *115*, 9981-10080.
14. von E. Doering, W.; Knox, L. H., *J. Am. Chem. Soc.* **1956**, *78*, 4947-4950.
15. Chen, B.; Rogachev, A. Y.; Hrovat, D. A.; Hoffmann, R.; Borden, W. T., *J. Am. Chem. Soc.* **2013**, *135*, 13954-13964.
16. Frenking, G.; Solà, M.; Vyboishchikov, S. F., *J Organomet. Chem.* **2005**, *690*, 6178-6204.
17. Davies, H. M. L.; Panaro, S. A., *Tetrahedron* **2000**, *56*, 4871-4880.
18. (a) Werlé, C.; Goddard, R.; Fürstner, A., *Angew. Chemie Int. Ed.* **2015**, *54*, 15452-15456;
(b) Werlé, C.; Goddard, R.; Philipps, P.; Farès, C.; Fürstner, A., *J. Am. Chem. Soc.* **2016**, *138*, 3797-3805.
19. Kornecki, K. P.; Briones, J. F.; Boyarskikh, V.; Fullilove, F.; Autschbach, J.; Schrote, K. E.; Lancaster, K. M.; Davies, H. M. L.; Berry, J. F., *Science* **2013**, *342*, 351-354.
20. Vanecko, J. A.; Wan, H.; West, F. G., *Tetrahedron* **2006**, *62*, 1043-1062.
21. Padwa, A.; Hornbuckle, S. F., *Chem. Rev.* **1991**, *91*, 263-309.
22. Ford, A.; Miel, H.; Ring, A.; Slattery, C. N.; Maguire, A. R.; McKervey, M. A., *Chem. Rev.* **2015**, *115*, 9981-10080.

23. Biswas, B.; Singleton, D. A., *J. Am. Chem. Soc.* **2015**, *137*, 14244-14247.
24. (a) Ollis, W. D.; Rey, M.; Sutherland, I. O., *J. Chem. Soc. Perkin Trans 1* **1983**, 1009-1027; (b) Eberlein, T. H.; West, F. G.; Tester, R. W., *J. Org. Chem.* **1992**, *57*, 3479-3482.
25. Vanecko, J. A.; West, F. G., *Org. Lett.* **2005**, *7*, 2949-2952.
26. (a) West, F. G.; Naidu, B. N., *J. Am. Chem. Soc.* **1993**, *115*, 1177-1178; (b) West, F. G.; Naidu, B. N., *J. Org. Chem.* **1994**, *59*, 6051-6056; (c) Bott, T. M.; Vanecko, J. A.; West, F. G., *J. Org. Chem.* **2009**, *74*, 2832-2836.
27. West, F. G.; Glaeske, K. W.; Naidu, B. N., *Synthesis* **1993**, 977-980.
28. Padwa, A.; Snyder, J. P.; Curtis, E. A.; Sheehan, S. M.; Worsencroft, K. J.; Kappe, C. O., *J. Am. Chem. Soc.* **2000**, *122*, 8155-8167.
29. Seeman, J. I., *J. Chem. Ed.* **1986**, *63*, 42.
30. (a) Bräse, S.; Gil, C.; Knepper, K.; Zimmermann, V., *Angew. Chemie Int. Ed.* **2005**, *44*, 5188-5240; (b) Rostami, A.; Wang, Y.; Arif, A. M.; McDonald, R.; West, F. G., *Org. Lett.* **2007**, *9*, 703-706.
31. Hong, K. B.; Donahue, M. G.; Johnston, J. N., *J. Am. Chem. Soc.* **2008**, *130*, 2323-8.
32. Wee, A. G. H.; Slobodian, J., *J. Org. Chem.* **1996**, *61*, 9072.
33. Blond, A.; Moumne, R.; Begis, G.; Pasco, M.; Lecourt, T.; Micouin, L., *Tetrahedron Letters* **2011**, *52*, 3201-3203.
34. Bott, T. M.; Atienza, B. J.; West, F. G., *RSC Adv.* **2014**, *4*, 31955-31959.
35. Mandler, M. D.; Truong, P. M.; Zavalij, P. Y.; Doyle, M. P., *Org. Lett.* **2014**, *16*, 740-743.

36. (a) Wu, X. P.; Su, Y.; Gu, P. M., *Org. Lett.* **2016**, *18*, 1498; (b) Qiao, J.-B.; Zhao, Y.-M.; Gu, P., *Org. Lett.* **2016**, *18*, 1984-1987; (c) Wu, X. P.; Su, Y.; Gu, P. M., *Org. Lett.* **2014**, *16*, 5339-5341.
37. Misaki, T.; Nagase, R.; Matsumoto, K.; Tanabe, Y., *J. Am. Chem. Soc.* **2005**, *127*, 2854-2855.
38. Göbel, M.; Klapötke, T. M., *Adv. Funct. Mater.* **2009**, *19*, 347-365.
39. (a) Doyle, M. P.; Griffin, J. H.; Chinn, M. S.; Vanleusen, D., *J. Org. Chem.* **1984**, *49*, 1917-1925; (b) Clark, J. S.; Krowiak, S. A.; Street, L. J., *Tetrahedron Letters* **1993**, *34*, 4385-4388.
40. (a) Takekuma, S.; Takekuma, H.; Matsubara, Y.; Inaba, K.; Yoshida, Z., *J. Am. Chem. Soc.* **1994**, *116*, 8849-8850; (b) Portela-Cubillo, F.; Scott, J. S.; Walton, J. C., *Chem. Comm.* **2007**, 4041.
41. (a) Abdou, W. M.; Salem, M. A. I.; Sediek, A. A., *Bull. Chem. Soc. Jpn.* **2002**, *75*, 2481-2485; (b) Xie, Z.; Li, L.; Han, M.; Xiao, M., *Synlett* **2011**, *2011*, 1727-1730; (c) Neunhoeffler, O.; Lehmann, G., *Chem. Ber.* **1961**, *94*, 2965-2967; (d) Gosteli, J., *Helv. Chim. Acta* **1977**, *60*, 1980-1983.
42. Okuma, K.; Matsunaga, N.; Nagahora, N.; Shioji, K.; Yokomori, Y., *Chem. Comm.* **2011**, *47*, 5822.
43. (a) Greci, L.; Tommasi, G.; Bruni, P.; Sgarabotto, P.; Righi, L., *Eur. J. Org. Chem.* **2001**, 3147; (b) Boyer, J.; Bernardes-Genisson, V.; Farines, V.; Souhard, J.-P.; Nepveu, F., *Free Radical Research* **2009**, *38*, 459-471.
44. Astolfi, P.; Panagiotaki, M.; Rizzoli, C.; Greci, L., *Org. Biomol. Chem.* **2006**, *4*, 3282.

45. (a) Yuan, Y.; Li, X.; Ding, K., *Org. Lett.* **2002**, *4*, 3309-3311; (b) Alaimo, P. J.; O'Brien, R.; Johnson, A. W.; Slauson, S. R.; O'Brien, J. M.; Tyson, E. L.; Marshall, A.-L.; Ottinger, C. E.; Chacon, J. G.; Wallace, L.; Paulino, C. Y.; Connell, S., *Org. Lett.* **2008**, *10*, 5111-5114; (c) Vaccaro, L.; Pizzo, F.; Lanari, D.; Piermatti, O., *Synthesis* **2012**, *44*, 2181-2184.
46. Johansen, M. B.; Kerr, M. A., *Org. Lett.* **2010**, *12*, 4956-4959.
47. (a) Lian, Y.; Davies, H. M. L., *Org. Lett.* **2012**, *14*, 1934-1937; (b) Lian, Y.; Davies, H. M. L., *Org. Lett.* **2010**, *12*, 924-927.
48. Gibe, R.; Kerr, M. A., *J. Org. Chem.* **2002**, *67*, 6247-6249.
49. (a) Tucker, A. M.; Grundt, P., *Arkivoc* **2012**, *2012*, 546; (b) Jahng, Y., *Archives of Pharmacal Research* **2013**, *36*, 517-535.
50. (a) Mitscher, L. A.; Baker, W., *Med. Res. Rev.* **1998**, *18*, 363-374; (b) Takei, Y.; Kunikata, T.; Aga, M.; Inoue, S.-i.; Ushio, S.; Iwaki, K.; Ikeda, M.; Kurimoto, M., *Biol. Pharm. Bull.* **2003**, *26*, 365-367; (c) Recio, M.-C.; Cerdá-Nicolás, M.; Potterat, O.; Hamburger, M.; Ríos, J.-L., *Planta Med* **2006**, *72*, 539-546; (d) Yang, S.; Li, X.; Hu, F.; Li, Y.; Yang, Y.; Yan, J.; Kuang, C.; Yang, Q., *J. Med. Chem.* **2013**, *56*, 8321-8331.
51. Zhu, S.; Dong, J.; Fu, S.; Jiang, H.; Zeng, W., *Org. Lett.* **2011**, *13*, 4914-4917.
52. Salomon, R. G.; Kochi, J. K., *J. Am. Chem. Soc.* **1973**, *95*, 3300-3310.

Chapter Three

Trapping of Reactive *C*-Acylimines with Electron-rich Arenes as Nucleophiles *via* Dual Catalysis: Part I, Mechanism and Scope of the Reaction, and Part II, Asymmetric Versions.

3.1 Introduction

As we have seen in Chapter Two, considerable efforts have been directed at the introduction of a variety of nucleophiles to the intermediate *C*-acylimines derived from the trapping of acceptor metallocarbenes and acceptor/acceptor metallocarbenes with azides. Despite considerable progress, we still encountered limitations when we were attempting to extend the generality of this domino functionalization using electron-rich arenes. This hampered the gram-scale preparation of the desired indole adduct, which was necessary to test the key reactions for the proposed forward synthesis to isatisine A (Chapter One) and more importantly, to probe the function of the western fragment against Respiratory Syncytial Virus (RSV). For instance, the conditions used to functionalize dicarbonyl stabilized diazo compounds (Compounds **29a-d** in Chapter Two) necessitates temperatures as high as 110 °C, conditions which are not ideal for chemo-, and regioselective addition of ambident nucleophiles, such as indole derivatives. In an effort to trouble-shoot this process, we attempted to approach the synthesis through the eyes of a transition metal chemist, and in the end, this approach paid off.

Mild and selective carbon-hydrogen bond functionalization using transition metal complexes embodies an important present-day challenge in the field of organic chemistry.¹ Although this field is currently in its early stages, such organic transformations can fundamentally change retrosynthetic approaches to complex molecule synthesis and rapidly expand the organic chemist's synthetic toolbox. In addition, they can serve as powerful

transformations for the rapid and direct accessibility of diverse functionalized products for structure–activity relationship (SAR) studies in medicinal and materials chemistry. Numerous mechanisms have been studied and proposed for the cleavage of C-H bonds, for example, oxidative addition (equation 1, Figure 3.1) and σ -bond metathesis (equation 2, Figure 3.1).² Additionally, stepwise electrophilic metalation/deprotonation (equation 3, Figure 3.1)³ and 1,2-addition across a metallocarbene (equation 4, Figure 3.1)^{4,5} mechanisms have also been suggested.

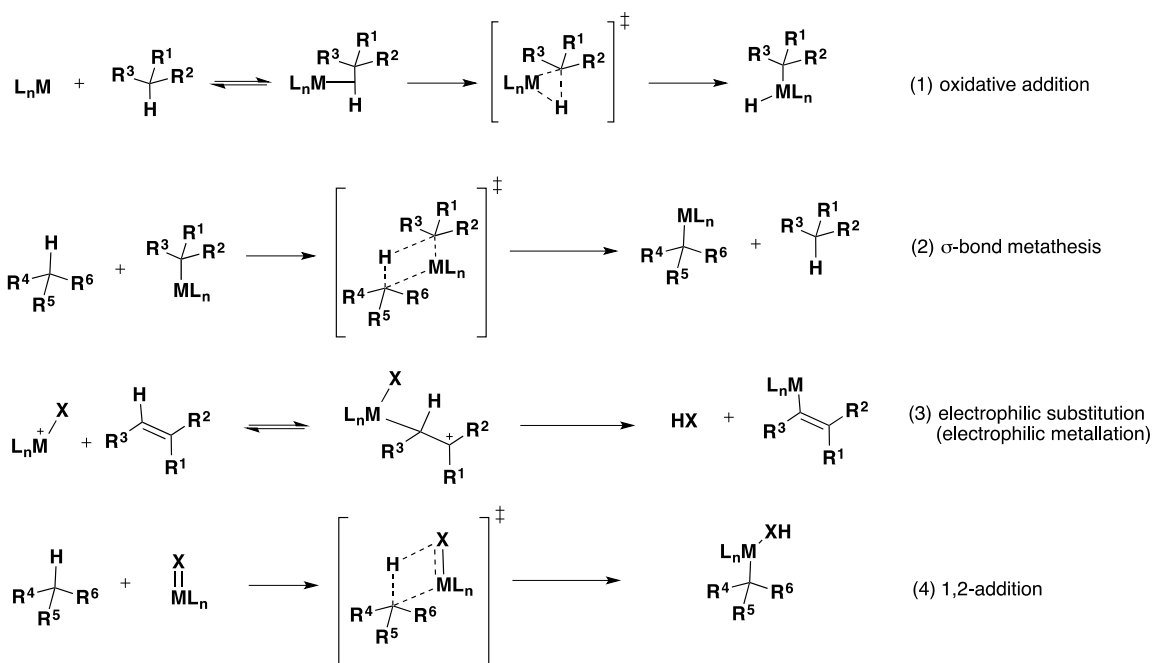


Figure 3.1: Schematic representation of the different mechanisms for C-H activation.

As highlighted in equation 3 of Figure 3.1, electrophilic metalation is a particularly attractive elementary step. Oftentimes, electrophilic metalation is much more commonly implicated in the direct and catalytic arylation of electron rich arenes, such as pyrroles and indoles. Common transition metal complexes that are employed in the catalytic arylation of electron rich arenes are primarily palladium-based and copper-based.

Recently, the coordination behavior of indoles towards transition metal centers, such as copper and palladium, has drawn considerable attention. Through low-hapticity modes, these indole complexes have been implicated in certain metal-catalyzed transformations,⁶ e.g., arylation of indoles⁷ and some were described in the next section. This conundrum has been difficult address, mainly owing to the labile nature of the hetero-arene metal complexes.⁶ This lability of heteroarene metal complexes indicates that after homolysis of the implicated weak σ -type complexes (described in the section), another oxidation state of the transition metal is hypothetically accessible. This could conceivably be done by matching the reactivity of the transition metal, such as copper, with indole.

This chapter documents the first application of electrophilic metalation of indoles to develop a mild regio- and chemoselective addition of electron rich arenes to intermediate C-acylimines generated from the trapping of acceptor/acceptor metallocarbenes with azides. In order to develop an appreciation for this reaction, known precedents on the relative kinetics of metallocarbene formation, including the generation of the pertinent oxidation state of copper, is imparted first. A brief survey of precedents of electrophilic metalation of indole, as a hypothetical solution to the current problem in Chapter Two, is then conveyed last. The intention of the last survey is, however, not to discuss all of the known reaction transformations supporting this mechanism, but to educate the reader that while there is a considerable certainty, multiple assumptions in the electrophilic metalation mechanism must still be made, e.g., the analogy of findings in palladium to copper chemistry as is discussed in the next sections.

3.2.1 Pertinent precedents in metallocarbene chemistry

Doyle, McKervery and Ye⁸ have established that diazoacetates (dicarbonyl-stabilized diazo compounds) normally require higher temperatures for reactions with transition metal

catalysts than do diazoacetates, which could undergo catalytic nitrogen loss at or below room temperature (Figure 3.2).

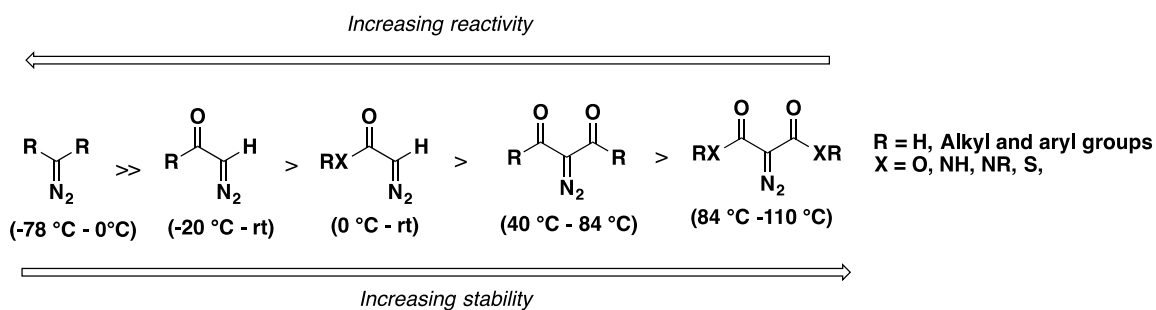
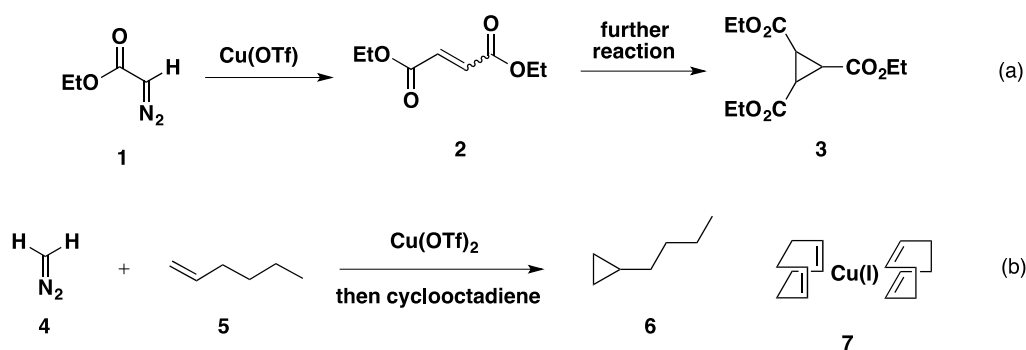


Figure 3.2: Reactivity of the diazo with varying number of flanking carbonyl groups and approximated temperature range to initiate the decomposition.

Salomon and Kochi⁹ showed that the kinetically active copper species in copper carbene formation from diazocarbonyl compound **1** was copper(I). This could then afford **2** *via* dimerization, followed by formation of cyclopropane **3** *via* cyclopropanation of **2** with the copper carbene of **1** (Scheme 3.1a). It was further accepted that any copper(II) precatalyst would need to be reduced using a sacrificial amount of diazoketone before it could mediate the formation of the desired metallocarbene. For instance, the reaction of diazomethane **4** with hexene **5** to make cyclopropane **6** in the presence of copper(II) triflate, is assumed to occur after the initial reduction of copper(II) triflate. The cyclooctadiene copper(I) complex $\text{Cu}(\text{COD})_2(\text{OTf})$ **7** (with triflate counterion) was also isolated and characterized from the reaction involving copper(II) precatalyst, reinforcing the previous idea (Scheme 3.1b). However, to the best of our knowledge, the exact mechanism of the reduction is unknown and has not been thoroughly studied. The same authors also observed that the interaction of monocarbonyl stabilized diazo compounds is inherently slower compared to the non-stabilized diazomethane.



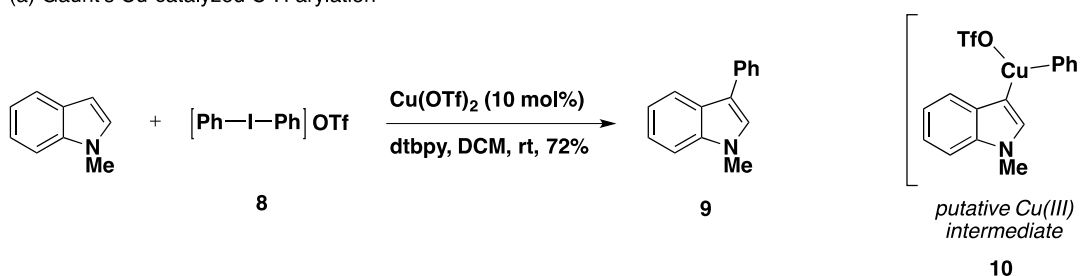
Scheme 3.1: Kochi's cyclopropanation experiment and isolation of Cu(I) complex.

Additionally, Nakamura,¹⁰ Davies and Singleton¹¹ have shown, computationally using density functional theory that the rate-determining elementary step in analogous rhodium (II) carbene formation was the extrusion of the nitrogen. Kinetic studies conducted by Teysie,¹² Pirrung,¹³ and Alonso,¹⁴ have also supported the conclusion that the rate-determining elementary step in metallocarbene formation was the extrusion of nitrogen molecule. These previous precedents were, in a way, consistent with the lesser reactivity of dicarbonyl-stabilized diazo compounds for the copper-catalyzed decomposition observed in Chapter Two; presumably these dicarbonyl stabilized diazo compounds were inherently resistant to oxidation, and/or to diazo decomposition, requiring high temperatures to initiate the reduction of copper(II) precatalyst. It is, however, unclear in copper catalytic systems whether the actual rate-determining step resulting in the requirement for high temperatures is caused by a slow reduction of copper(II) precatalyst and/or a slow nitrogen extrusion. To the best of our knowledge, calculations using density functional theory in copper catalytic systems have not been thoroughly studied. Regardless, we focus our attention on alternate source of copper(I), preferably *in-situ* generation, to avoid the difficulty imposed by weighing air sensitive copper(I) salts, as most of them are prone to oxidation.

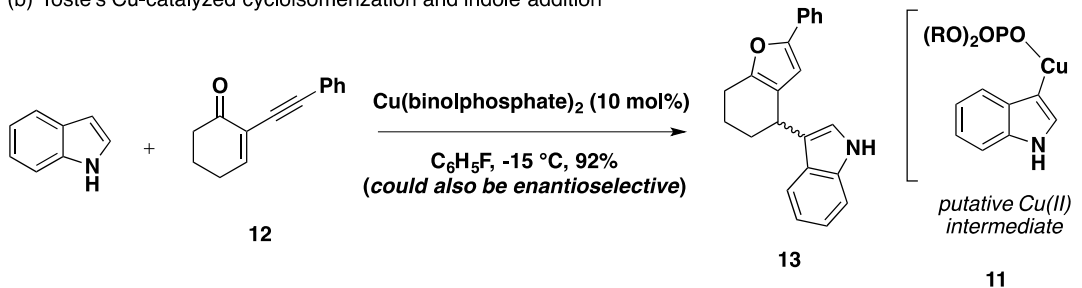
3.2.2 Known representative precedents on electrophilic metalation

Gaunt and Phipps have proposed that coupling of indole with hypervalent iodine compound **8** to make aryl indole **9** at room temperature, using an appropriate copper(II) precatalyst, proceeds through the formation of elusive C-3 copper(III) indole intermediate **10**.^{7a, 15b} The copper(I) was presumably formed from the facile homolysis of the C-3 copper(II) indole intermediate first formed from the precatalyst, followed by oxidative addition of hypervalent iodine species and subsequent electrophilic metalation on the copper(III) species (Scheme 3.2a). Toste and co-workers have implicated that this C-3 copper(II) indole intermediate **11** could catalyze the cycloisomerization and further indole addition to their 2-alkynyl enone **12** starting material to make furan **13** at -15 °C (Scheme 3.2b).¹⁶ The same authors have also shown that a copper(I) catalyst was equally effective in the same transformation. This allowed us to hypothesize that the copper(I) might also be operative in Toste's case, even in instances where they directly used copper(II) as the pre-catalyst, presumably via the homolysis of indole **11**.

(a) Gaunt's Cu-catalyzed C-H arylation

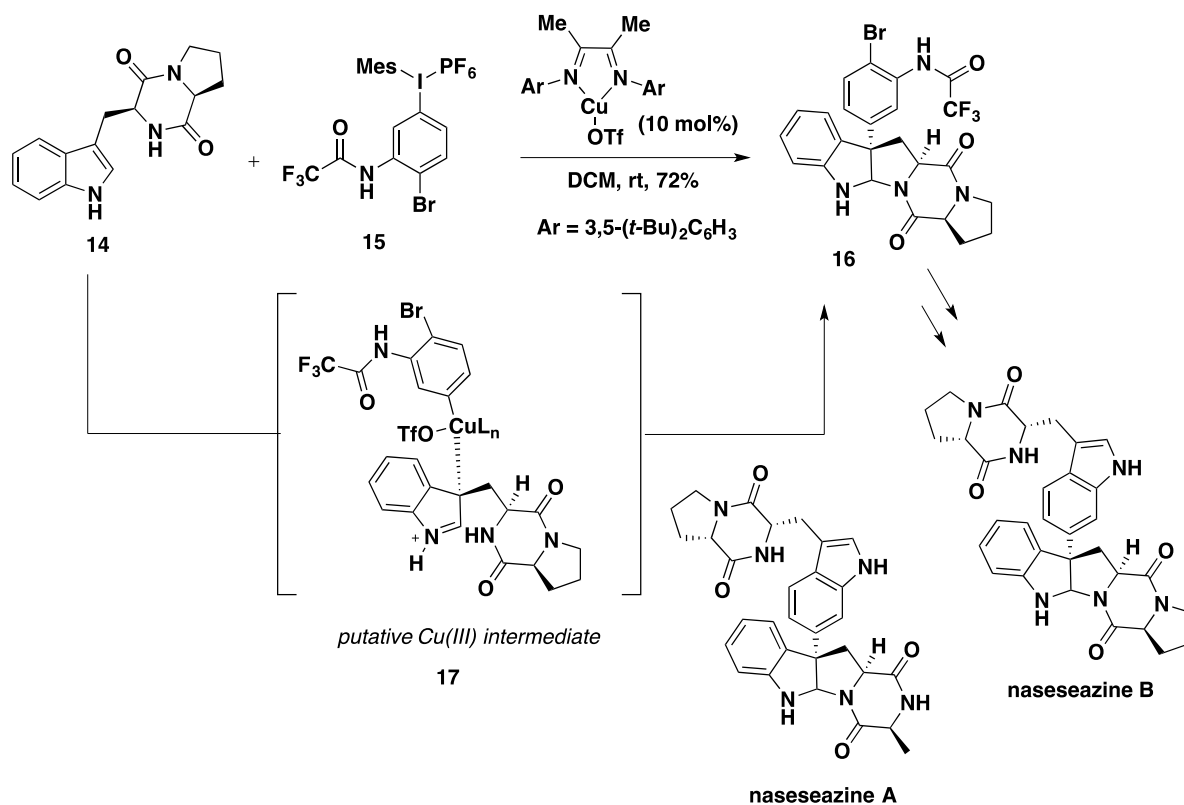


(b) Toste's Cu-catalyzed cycloisomerization and indole addition



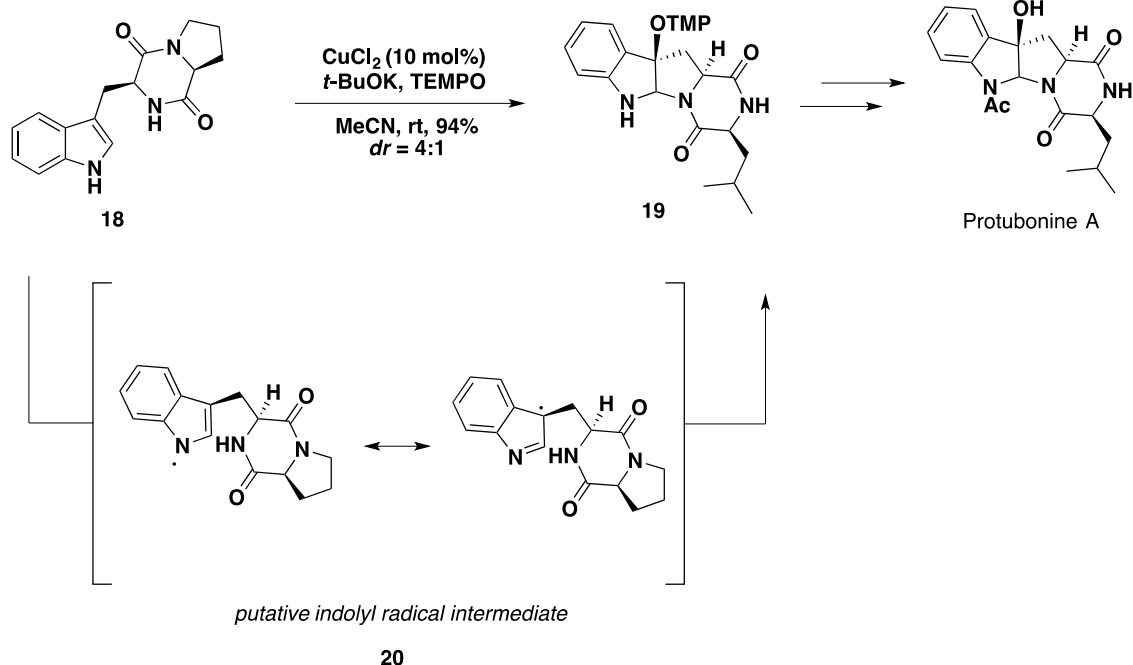
Scheme 3.2: Catalytic electrophilic metalation experiments.

The Reisman group^{7c} and the Xia group¹⁷ have also demonstrated the usefulness of tryptamine-derivative radical cyclization on the biomimetic synthesis of the indole alkaloids nasesesazine A and B (Scheme 3.3), and protubonine A (Scheme 3.4), respectively. Reisman showed that indole **14** and iodonium salt **15**, when mixed together in the presence of copper catalyst, could cyclize to form arylated diketopiperazine **16**. Diketopiperazine **16** was proposed to form from oxidative addition of **15** with copper(I) catalyst, followed by electrophilic metalation of **14** on a more electronegative Cu(III) intermediate to form intermediate **17**, which then undergoes reductive elimination en route to **16**. This reaction was used by Reisman and co-workers to make nasesesazine B. An analogous transformation (not shown) was also used to make a related natural product nasesesazine A. Related to this transformation; MacMillan and co-workers have also explored a similar approach using simple chiral enamine instead of an indole.¹⁸ Notably, they implicated similar carbon-based cupration of enamine as opposed to nitrogen-based.



Scheme 3.3: Reisman's concise total synthesis of nasesezine A and B.

Xia and co-workers, on the other hand, synthesized protubonine A by cyclization of indole **18** to diketopiperazine **19**, via a single electron transfer from CuCl_2 and subsequent trapping by TEMPO. Xia, however, proposed that the reduction of Cu(II) precatalyst to make radical intermediate **20** occurred at the nitrogen.



Scheme 3.4: Xia's concise total synthesis of protubonine A.

Despite the advances made in this area, none of these authors have unambiguously identified these elusive intermediates, warranting a great deal of speculation. Recently, analogous palladated indole complexes were characterized using X-ray crystallography by the groups of Yamamoto and Murahashi at the Tokyo Institute of Technology,⁶ shedding some light on metal catalysis involving indole activation and putting more weight on the concept of C3-metallated indole (or C2-C3 π -complexes with transition metals), as opposed to N1-metallated indole. Regardless of the provenance, the consistent observation in all of these precedents was that copper(I) could be accessed from a copper(II) precatalyst under mild conditions in the presence of indole and electrophilic metalation was kinetically sensitive to oxidation state, with a Cu(III) intermediate being the fastest, and Cu(I) species being the slowest.

3.2.3 Hypothetical solution to the current problem

To tackle the current limitation on the methodology discussed in Chapter Two, a simple approach would be to increase the temperature and let a sufficient amount of the diazoketone do the reduction or directly use a copper(I) salt as the catalyst. None of these approaches, however, are suitable for ambident nucleophiles like indole and pyrrole, where regio- and chemoselective functionalization is a frequent issue (Chapter 2). Additionally, copper(I) complexes, as stated earlier, are generally prone to oxidation, making their handling and weighing less simple and generally not efficient compared to copper(II) pre-catalyst, as is discussed in the next sections. Moreover, the possibility of controlling the stereoselectivity of nucleophilic addition onto the C-acylimine intermediate was anticipated to be less efficient at high temperatures.

Electrophilic metalation of indole, as discussed earlier, presented an opportunity as a solution to the current problem: the accessibility of copper(I) *in situ* under mild conditions from copper(II) pre-catalyst to make the necessary metallocarbene. We thought that if we could harness the same elementary step in our system, this would be a novel application of electrophilic metalation/reduction in metallocarbene chemistry. Given these precedents, our hope was that a re-examination of the reaction parameters, such as catalyst, solvent, temperature, concentration and/or addition of additives, could allow us to prepare the desired bis(indole) adducts, thereby extending the generality of the domino functionalization.

3.3 Results and discussion

3.3.1 Survey of reaction conditions

The West group, as previously stated from the review introduction in Chapter Two, has a long history of research pertaining to ammonium ylide rearrangements. The West group also had the inclination to start the optimization of any metallocarbene chemistry project with typical copper salts like Cu(acac)₂, Cu(tfacac)₂ or Cu(hfacac)₂. The Clark group in Glasgow University, a respected research group in the area of analogous oxonium ylide rearrangements, seemingly had the same penchant with these salts.¹⁹ While this looked purely coincidental, these salts were known to be well soluble in variety of organic solvents and were seemingly well behaved with metallocarbene formation and subsequent ylide chemistry.²⁰ Therefore, it is not surprising that the pioneering alumna of West group who tackled this project, Dr. Bott, started her initial foray in this chemistry using Cu(acac)₂, and later found that Cu(hfacac)₂ was an excellent catalyst for the desired transformation described in Chapter Two. However, treatment of **21a** with indole instead of the silyl enol ether, along with Cu(hfacac)₂ in refluxing toluene, led to rapid consumption of **21a** (Table 1, entry 1) and formation of several yellow spots. Separation of this mixture using silica gel resulted in purification of a modest amount (42%) of known **22**,²¹ along with approximately 10% impurity from the regioisomer **23**, apparently where the attachment occurred at the C2 position of the indole.²² This isolated yield, however enticing, would impose a significant drawback in the total synthesis if used in further transformations. Also, to avoid structural ambiguity between the regioisomers assigned initially based on NMR, appropriate crystals necessary for X-ray diffraction were prepared by slowly evaporating a saturated solution of **22** in a 1:1:1 mixture of EtOAc:DCM:Hexanes (three attempts). In Figure 3.3, the indole C-3

connection of the desired regioisomer, corresponding to the connectivity needed for the synthesis of isatisine A, is shown.

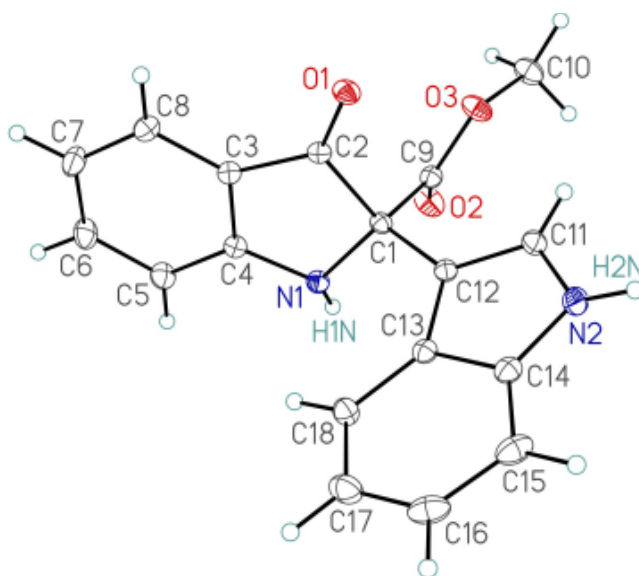


Figure 3.3: ORTEP diagram, derived from X-ray diffraction data of the desired regioisomer **22.**

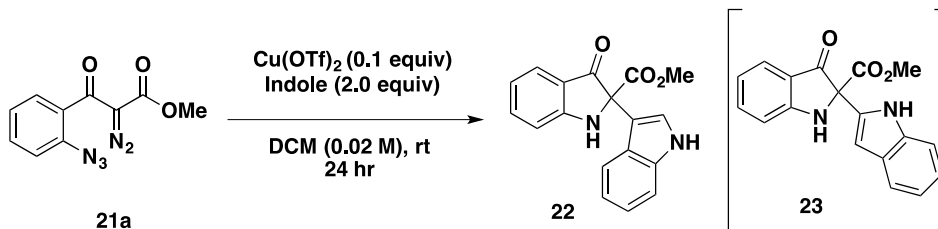
Accordingly, the temperature was adjusted to room temperature (22 °C) to attempt to improve the regioselectivity (entry 2), but no substantial consumption of the starting material was observed after the reagents were mixed for 24 hours. Gaunt^{7a} and Toste¹⁶ have used copper(II) triflate and copper(II) binol phosphate salts as effective pre-catalysts in the previously mentioned transformations. However, mixing **21a**, indole, and copper(II) triflate as the catalyst, and stirring for 24 hours resulted in incomplete consumption of **21a**. The reaction mixture after purification, however, afforded a promising 26% yield of **22** (entry 3). Notably, no formation of undesired isomer **23** was observed in the crude reaction mixture, indicating the desired kinetic control on the nucleophilic addition of indole onto the *C*-acylimine intermediate. To improve the reaction conversion, prolonging the mixing of reagents and/or increasing the solubility of the starting material, catalyst and putative intermediates was necessary. To this end, a set of solvents was next inspected; ethereal solvents like THF (entry not shown) and diethyl ether (entry 4) did

not result in the formation of the desired adduct or decomposition of the starting material. Presumably, the coordination of THF²³ deactivated the copper(II) triflate in the necessary reduction steps. Using chlorinated solvents showed a good conversion to the desired adduct. Approximately 68% of **22** was isolated when the reaction was done in CHCl₃. Although a substantial amount of **22** was isolated, this reaction generated multiple colored compounds observed in TLC apart from the desired adduct. Switching to DCM as the solvent was a welcomed choice; the starting material was fully converted after 18-24 hours and 92% of **22** was isolated with no contamination from **23** (entry 6).

Upon increasing the reaction to gram scale (1 to 5 g of starting material), a slight drop in isolated yield (83%) was noticed. Additionally, the purification of product **22** in gram scale was switched to direct recrystallization from the crude reaction mixture using methanol solvent or hexane/ethyl acetate/dichloromethane (1:1:1) solvent mixtures, instead of conventional column chromatography; a good 74% yield of the desired indolinone **22** was isolated. In order to compare the efficiency of this catalysis with directly using copper(I) as the catalyst, a fresh toluene complex of copper(I) triflate was used (entry 7). Surprisingly, although full conversion of the starting material was observed; this catalyst was not comparably effective to entry 6 as only 12 % of the desired adduct **22** was isolated, providing some useful mechanistic information on the mechanism of the reaction, *vide infra*. Using copper(0) powder as the catalyst (entry 8) or even lowering the reaction temperature to 0 °C (entry 9) did not result in further improvement of yield, but the reactions, as expected, suffered from sluggish conversion of the starting material. Other Lewis acids in catalytic amount (10 mol% of AgOTf, FeCl₃, Fe₂(SO₄)₃, Zn(OTf)₂, Rh₂(OAc)₄) (not shown) were also screened but all gave inferior results when compared with Cu(OTf)₂ and using entry 6 conditions.

As previously stressed in Chapter One, the western fragment of Isatisine A is chiral. Chiral bisoxazoline ligands are known to coordinate well with copper transition metals and lead to enantioenriched adducts.²⁴ Thus, it was decided to screen chiral bisoxaline ligands to test whether enantioenrichment of **22** would be possible. Unfortunately, these chiral ligands (only one entry is shown in the table, see experimental details for further information), upon performing a complex with copper(II), did not induce substantial conversion of the starting material **21a** to the desired adduct. The issue of an asymmetric transformation, at that time, was temporarily set aside. Although a good reaction protocol for electron rich arenes had been developed and examination of the reaction scope was the next attractive step to do, an exciting opportunity came up and it needed careful consideration. One noteworthy observation during the optimization process captured our attention, more specifically the seemingly anomalous result between Cu(II) (Entry 6) and Cu(I) (Entry 7) triflate salts, considering that Cu(I) was generally accepted as the active catalyst for the diazoketone decomposition. In order to explain the anomalous results, some mechanistic control experiments had to be done.

Table 3.1: Survey of reaction conditions



Entry	Change from the optimized condition	Isolated Yield of 22
1	Cu(hfacac) ₂ instead of Cu(OTf) ₂ PhMe instead of DCM Reflux instead of room temperature	42% ^a
2	Cu(hfacac) ₂ instead of Cu(OTf) ₂ PhMe instead of DCM	trace
3	PhMe instead of DCM	26%
4	Diethyl ether instead of DCM	trace
5	Chloroform instead of DCM	68% ^b
6	no change	92% (83%)^c (74%)^d
7	Cu(OTf)(PhMe) instead of Cu(OTf) ₂	12% ^e
8	Cu(0) instead of Cu(OTf) ₂	N. R.
9	0 °C instead of room temperature	trace
10	Cu(OTf) ₂ (L*) ^f	trace

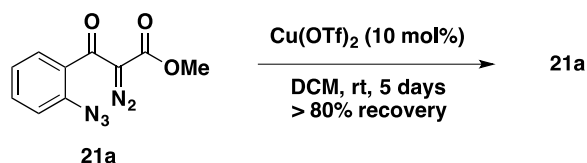
a. Mixture of regioisomers. b. Multiple colored products were observed. c. Gram-scale reaction d. Gram-scale reaction and direct crude recrystallization. e. Complete consumption of starting material and formation of multiple colored products. f. With chiral bisoxazoline ligand (see supporting information)

3.3.2 Mechanistic considerations

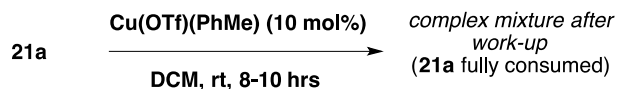
3.3.2.1 What is the copper oxidation state in the catalytic cycle?

The outcome of the optimization experiments in entries 6 and 7 did not explicitly differentiate between copper(I) and copper(II) in the elementary steps associated with the diazoketone-azide metallocarbene coupling, as both were conceivably effective. To discriminate between the two oxidation states, separate exposure of fresh copper(I) and copper(II) catalysts with the starting diazo-azide without the presence of a heteroaromatic trap was necessary (Scheme 3.5). The distinct diazoketone/azide functional groups present in the starting material could be used to monitor the progress of the decomposition using IR spectroscopy. Notably, these functional groups overlap as broad strong peaks at *ca.* 2100 cm^{-1} , thus, it was not possible to differentiate the relative decomposition kinetics between the two functional groups using IR alone. Doyle and co-workers, however, showed previously that diazoketone decomposition was kinetically faster than that of azide in the presence of a copper catalyst.²⁵ In fact, they also showed that only rhodium salts were effective in coupling an azide with a diazoketone, through an initial metallocarbene formation as opposed to a metallonitrene formation.

(a) $\text{Cu}(\text{OTf})_2$ - catalyzed decomposition



(b) $\text{Cu}(\text{OTf})(\text{PhMe})$ - catalyzed decomposition.



Scheme 3.5: Diazo azide decomposition in the presence of different copper catalyst.

Thus, deliberate exposure of 10 mol% of copper(II) triflate with diazoketone **21a** starting material resulted in kinetically slow (> 80% recovered starting material after 5 d) decomposition of diazoketone and azide functional groups (Figure 3.4a). Broadening of the carbonyl peaks after 24 h was, however, prominent in IR spectroscopy. This suggests a possible dative interaction occurring between copper(II) and the carbonyl or the diazo, but it is not an indication of decomposition of the diazo/azide functional groups. Comparatively, exposure of 10 mol% of copper(I) triflate as a toluene complex completely decomposed the starting diazo-azide after 8-10 h. The complete absence of a broad peak at 2137 cm^{-1} indicated complete decomposition of the diazoketone and the azide functional groups. Note that the IR spectra depicted herein showed that after the 24 h period the IR spectra did not have any peak corresponding to the diazo/azide functional groups well within the observed optimized reaction time (16-36 h) (Figure 3.4b). Clearly, this pair of control experiments indicated that the elementary steps in the C-acylimine formation were facilitated by copper(I) and very slowly by copper(II). Identical conclusion was observed when NMR spectroscopy was used instead of IR spectroscopy.

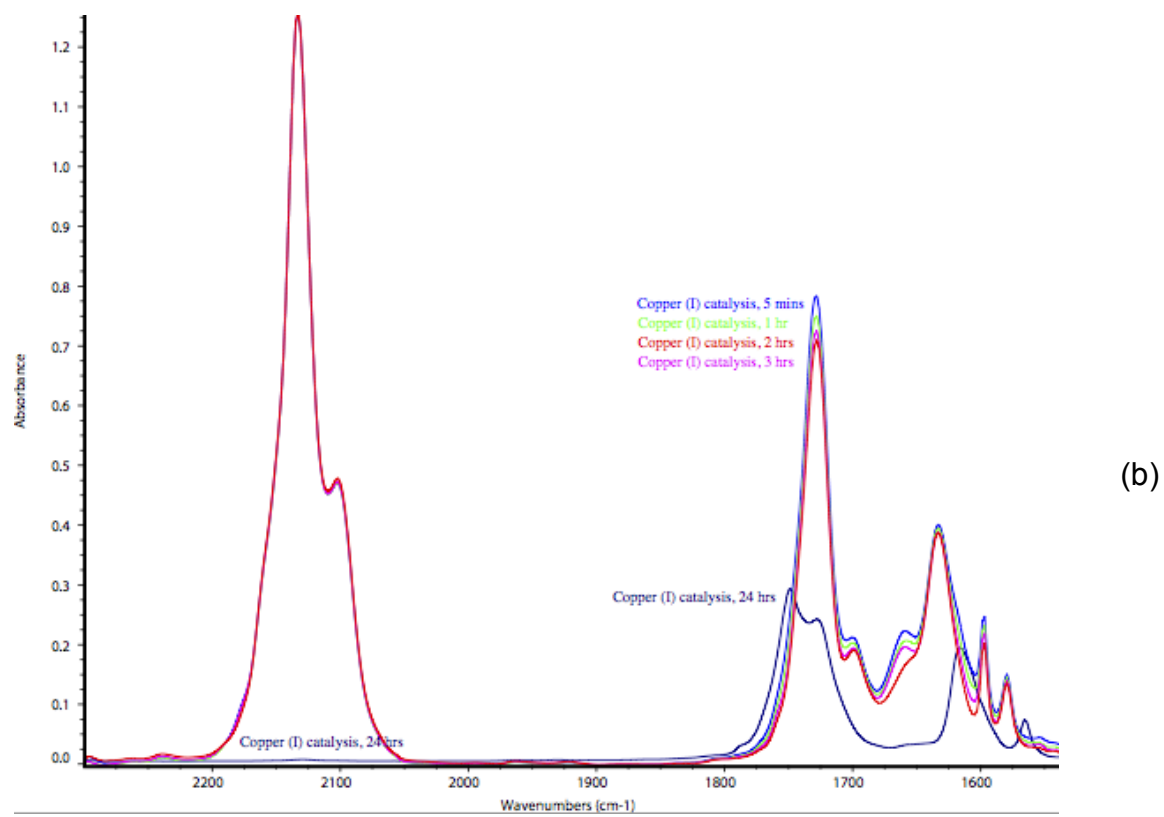
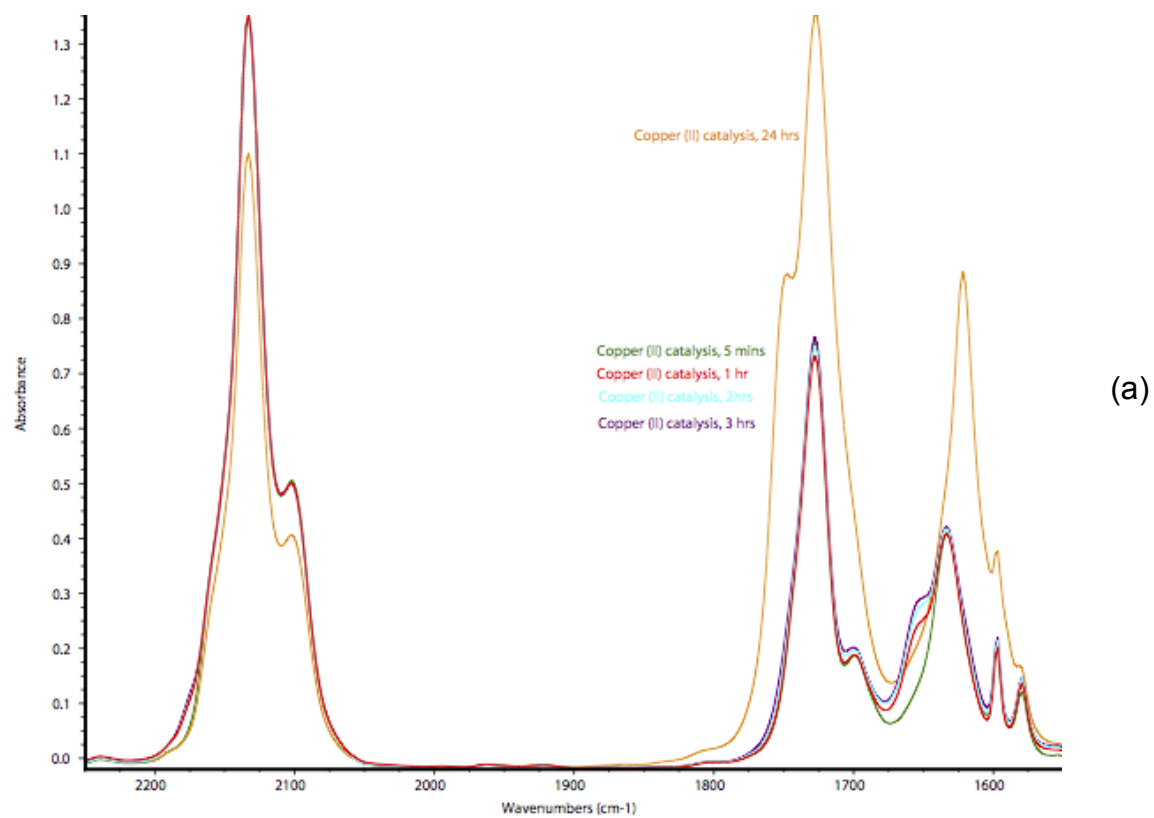


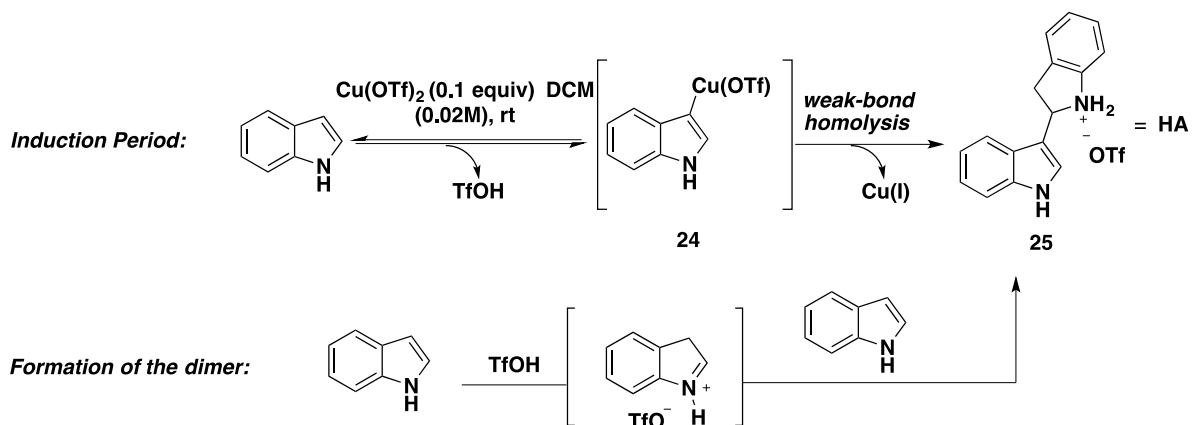
Figure 3.4: Reaction monitoring using IR spectroscopy.

Additionally, consistent with Kochi's conclusion on the first order dependence of diazo decomposition with varying concentration of copper(I) catalyst,⁹ upon addition of 20 mol% of copper(I) complex to **21a** at 0.02 M concentration in DCM, acceleration of decomposition time of **21a** to approximately 3-4 hours was noticed. However, the copper(I) reaction, no matter how much was present in the solution, did not result in substantial formation of the desired adduct **22** when indole was added, but rather resulted in a mixture of compounds, suggesting that an additional reaction component was necessary to turn over the Friedel-Crafts catalytic cycle.

3.3.2.2 How does the copper (I) form in solution from a copper (II) pre-catalyst?

In the competition experiments between copper(I) triflate and copper(II) triflate, it was clear that copper(I) was the viable oxidation state during the elementary steps associated with the metallocarbene formation and very likely the C-acylimine formation as well.

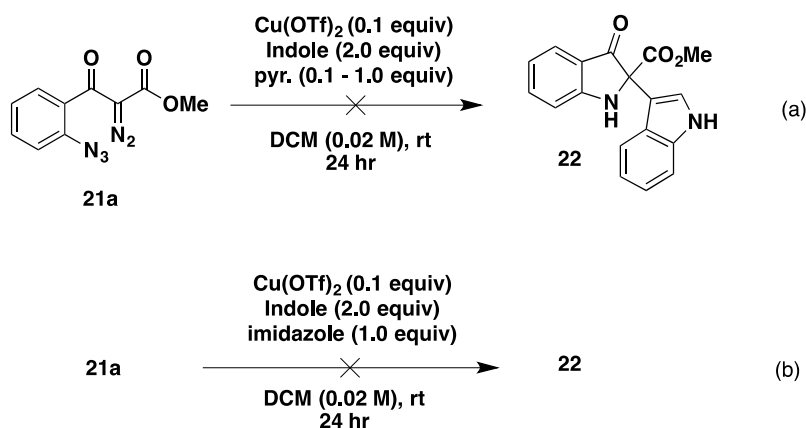
Attention was then paid to indole as the reductant *in-situ*. As previously described by Gaunt and others and highlighted in the introductory part of this chapter, mixing copper(II) triflate and indole generates Cu(I) and triflic acid as by-products.^{4a} In this instance, also analogous to the observation of Noland, oligomerization (dimerization) of indole, catalyzed by triflic acid, was expected to happen.¹¹ Indeed, when an aliquot of a stirred solution of indole and a catalytic amount of Cu(OTf)₂ was subjected to UV-VIS spectroscopy, a build up of new peaks at 390 nm was observed, indicating formation of a new complex, presumably **24**.⁶ When the same aliquot was subjected to electrospray ionization-mass spectrometry analysis, evidence for the presence of **24** and oligomerization product **25** was also seen. This indicated that the triflic acid was generated upon mixing indole and Cu(OTf)₂ in solution. The dimer structure was assigned as **25**, based on the precedent from Noland's isolated product.



Scheme 3.6: Proposed mechanism for the reduction of Cu(II) precatalyst.

As seen in the survey of reaction conditions, attachment of the electron donating chiral bisoxazoline ligand to Cu(OTf)₂ did not result to substantial formation of the desired adduct. The formation of a tight chelate with Cu(II), which disfavored the initiation of diazo-azide decomposition (Table 1, Entry 10), presumably inhibited the electrophilic metalation step and, therefore, the reduction.¹² Related to this reasoning, other known ligands of copper(II) catalysts in metallocarbene chemistry were also mixed with copper(II) triflate, indole, and diazoazide **21a** in DCM solvent, to further analyze the sensitivity of copper to other heteroarene-based ligands in solution. Nozaki has shown that pyridine binds tightly with copper(I), rendering it catalytically inactive for the metallocarbene formation.²⁶ Thus, addition of 0.1 equiv. and 1.0 equiv. of pyridine to separate reaction mixtures both resulted in dramatic diminution in the formation of the desired indolinone **22** (Scheme 3.7a). Notably, 1.0 equiv. of pyridine completely suppressed the consumption of **21a** indicating a thorough interruption of the catalytic cycle. In this outcome, however, it was not clear whether the reduction of copper(II) precatalyst or copper(I) carbenoid formation was inhibited, as pyridine may theoretically coordinate with copper(II).

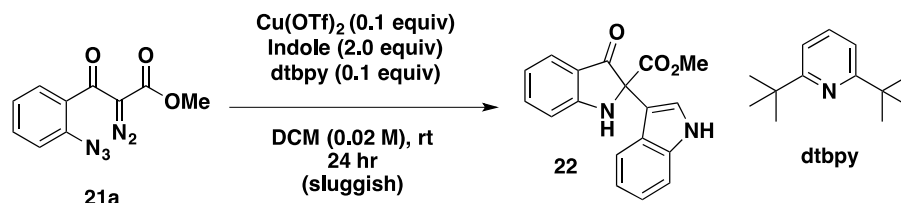
Other ligands, such as imidazole, were also added in separate reactions. Imidazole is known to complex well with copper(II) salts in DCM. Similar results were obtained upon addition of 1.0 equiv. of imidazole (Scheme 3.7b), although this reaction initially formed an intensely green colored solution within a minute after addition of the imidazole, suggesting pre-complexation.



Scheme 3.7: Addition of pyridine and imidazole as catalyst poison.

Gaunt has shown that the presence of 2,6-di-*tert*-butyl pyridine (dtbpy) and copper(II) precatalyst could still catalyze the previously mentioned reaction at the slight expense of temperature (40 °C).^{7a} Presumably, this additive selectively consumed the Brønsted acid by-product after electrophilic metalation and was unable to form a tight complex with bulky copper(II) pre-catalyst because of steric encumbrance imposed by the bulky *tert*-butyl groups. Thus, copper(II), in theory, should still convert **21a** *via* the anticipated electrophilic metalation mechanism. Consistent with this notion, sluggish formation of the desired adduct upon addition of 0.1 equiv. of di *tert*-butyl pyridine in the reaction was observed. A faster decomposition of the starting material was noticeable compared to when pyridine was added. This series of

experiments pointed to the conclusion that non-coordinated copper was necessary for the successful decomposition of the starting material.



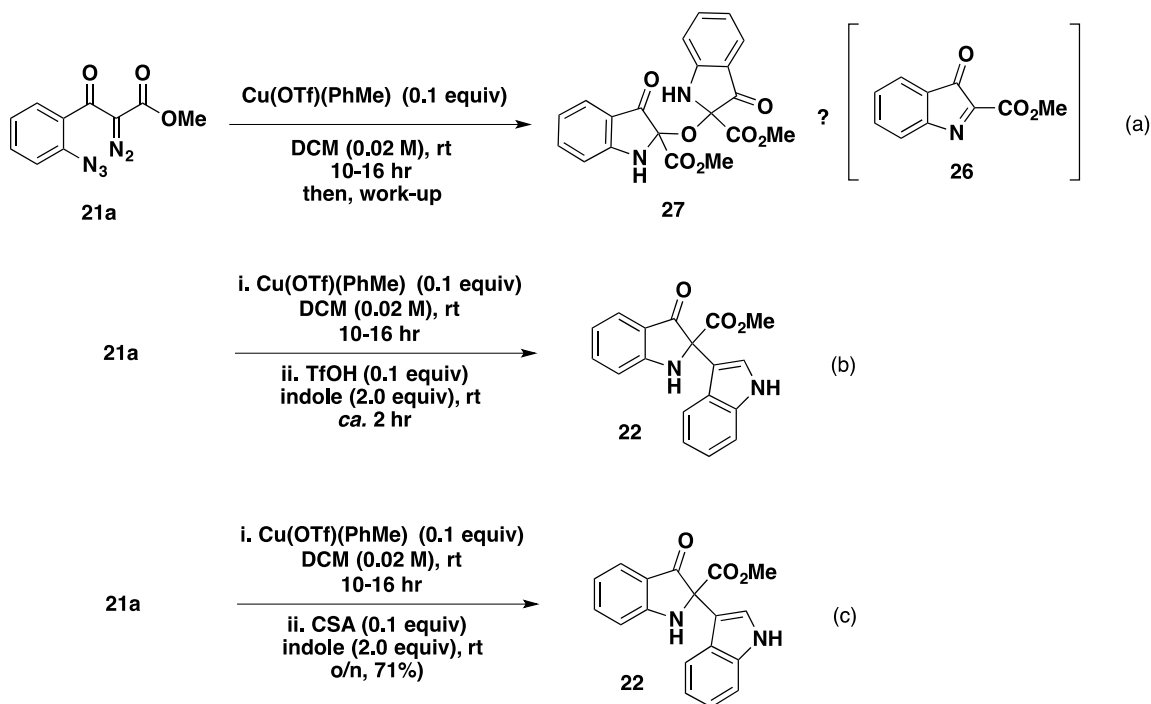
Scheme 3.8: Addition of di *tert*-butylpyridine poison.

3.3.2.3 Which species catalyzes the Friedel- Crafts alkylation?

In the first and second phase of the mechanistic studies, it became clear that the reduction of copper(II) precatalyst to copper(I) was mediated by indole as the reducing agent. The copper(I) was necessary for the decomposition of **21a** and another reaction component was necessary for the efficient formation of **22**. We hypothesized that the production of Brønsted acid, the potential key component to the efficient formation of **22**, was likely very slow in copper(I) compared to copper(II) during the optimization studies. Sanford has shown that the relative kinetics of analogous electrophilic metalation of indole, followed by arylation using a palladium catalyst, was dependent on the electronics of the palladium complexes.^{7d} Highly oxidized palladium salts containing weak ligands (e.g., OAc) tend to undergo much faster electrophilic metalation than electron-rich palladium bearing pyridine-based ligands, presumably because of the difference in electronics of the metal centres. They also noted, however, that the sterics associated with the ligand surrounding the palladium complex might also be involved.

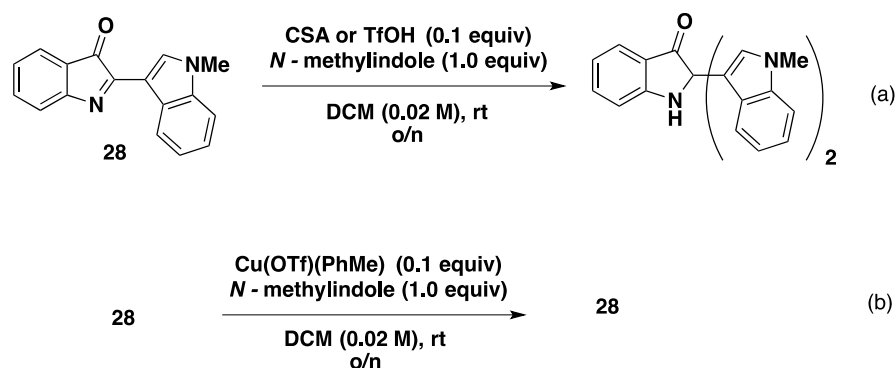
Related to this paradigm, we reasoned therefore that the copper(I) complex experiment, in the optimization studies, did not substantially produce the desired product **22** because the

copper(I) reaction was devoid of Brønsted acid coming from electrophilic metalation. To experimentally understand this, attempts to isolate the putative *C*-acylimine **26** intermediate and investigations on the *C*-acylimine reactivity were made. However, upon exposure of the diazo azide with copper(I) catalyst in a solution of DCM over 8-12 h, followed by a work-up with water to remove copper salt, the imine intermediate suffered from hydrolysis and further oxidation. This was indicated by the presence of a 2:1 mixture of adduct **27**, formed from imine **26** and water, with *m/z* equal to 419.0847 as its $[M + Na]^+$ ion observed in high resolution ESI-MS, along with oxidation by-products also observed by high resolution ESI-MS (Scheme 3.9a). In an attempt to circumvent the hydrolysis and further oxidation problems, a sequential addition technique (without intermediate work-up), coupled with rigorous air-free reaction conditions was done. Exposure of the starting material with a fresh copper(I) complex in DCM solution over 12 hours, followed by immediate introduction 0.1 equiv. of triflic acid and 2.0 equiv. of indole nucleophile resulted in the formation of the desired adduct **22** as observed by TLC and crude NMR analysis. The yield for this reaction, however, could not be accurately determined, as separation from impurities later became problematic. Using camphor sulfonic acid (CSA) in place of triflic acid resulted in 71% yield of adduct **22** along with other yellow spots in TLC, more or less comparable to results obtained with copper(II) catalysis (Scheme 3.9b).



Scheme 3.9: Attempts to isolate the C-acylimine 26 and sequential addition reaction.

In order to further probe the reactivity of the imine towards copper(I) and Brønsted acid catalysis, an isolable and more easily handled model C-acylimine **28**, generated from the reaction described in Chapter Two, was mixed with triflic acid and indole. Complete consumption of imine **28** in 30 minutes (overnight, with CSA as the Brønsted acid) was observed (Scheme 3.10, equation A). In contrast, exposure of indole and imine **28** with Cu(OTf)(PhMe) (Scheme 3.10, equation b) complex resulted in incomplete consumption of starting material (<10% conversion), even after prolonged exposure, suggesting that the Brønsted acid was the likely catalyst in the Friedel-Crafts cycle.



Scheme 3.10: Comparison of the reactivity of the stable C-acylimine with Cu(I) or Brønsted acid catalyst.

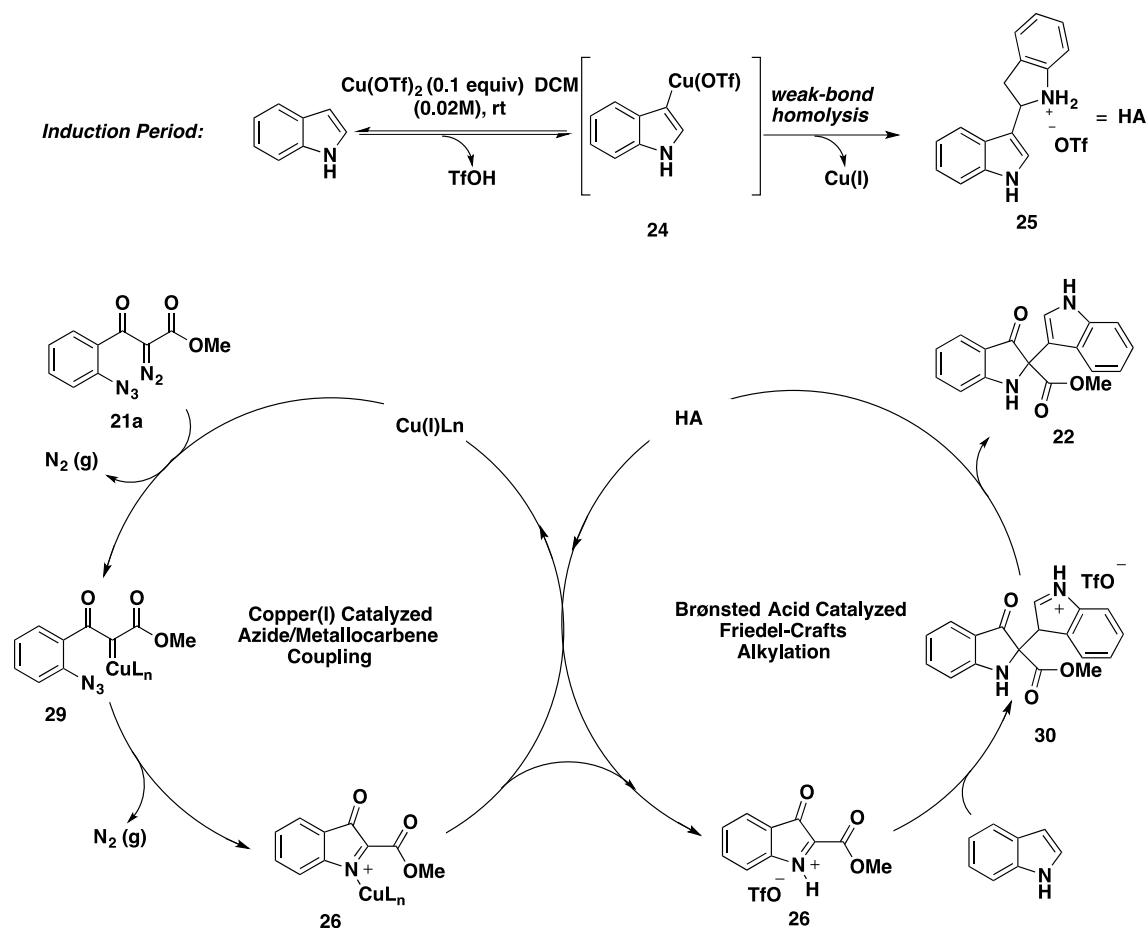
At this point, we were already convinced that the reduction process happened in the induction period, through electrophilic metalation, and both copper(I) and the ensuing Brønsted acid were necessary. Thus, an experiment was performed where 0.2 equiv. of indole was pre-stirred with 10 mol% copper(II) triflate precatalyst for one to two hours, followed by slow addition of diazoketone azide **21a** and 1.8 equiv of indole to mimic the proposed reaction sequence, *vide infra* (Scheme 3.11). Indeed, the isolated yield of the desired product after purification was identical to that of the original reaction conditions described in entry 6 of Table 3.1.

Noland has shown that strongly ionizing hydrochloric acid mediates the dimerization of indole within a couple of minutes and typically under cold temperatures,²⁷ suggesting that this reaction is quite fast. The form of the acid after this reaction now becomes phenyl ammonium chloride (**25** with a chloride counterion instead of triflate). Hence, the acid catalyzing the addition of electron rich indole on the C-acylimine might well be the phenyl ammonium triflate **25**, and not triflic acid per se. Literature data has approximated the pKa of a similar salt to be around 4.6, close to benzoic acid which has a pKa of 4.2.²⁸ Notably, additional evidence to

support the notion that phenyl ammonium triflate **25** rather than the strong triflic acid was the active Brønsted acid catalyst was gained from the signal around -78.5 ppm in the ^{19}F -NMR spectrum of the crude reaction mixture with and without the presence of diazo starting material. This signal was attributed to free triflate (or weakly H-bonded), as it was comparatively more shielded than triflic acid itself, which displays a signal at around -76.40 ppm in the ^{19}F -NMR spectrum. Lastly, significant levels of decomposition were not observed when **21a** was added to TfOH or AcOH with no indole or $\text{Cu}(\text{OTf})_2$ present, indicating that the Brønsted alone is not a competent catalyst for the *C*-acylimine formation.

3.3.2.4 Combining all the information: the proposed catalytic cycles.

Taking all the experimental mechanistic analysis into consideration and the previous precedents in electrophilic metalation chemistry, a mechanism involving a fast and reversible copper(II) catalyzed electrophilic metalation, followed by a slow reduction of copper(II), presumably through the homolysis of the putative C-3 cuprated indole **24**, to release the active copper(I) catalyst was proposed. The copper(I) could then undergo a slow formation of metallocarbene **29**. We were not sure whether the actual rate-determining step in the catalytic cycle was the extrusion of nitrogen from the diazo precursor, following precedents from Nakamura and others^{10, 11, 13} on analogous rhodium carbene chemistry, or the reduction of copper(II) through homolysis. In either case, the reaction produces imine **26** after irreversible extrusion of two molecules of dinitrogen from the diazo and the azide. The *C*-acylimine is then activated by ammonium triflate **25** for further electron rich arene addition and rearomatization of **30** to close the catalytic cycle and afford **22**. Notably, there are two intersecting catalytic cycles at play, and that the different catalysts for each cycle are both produced in the initiation step (Scheme 3.11).



Scheme 3.11: Proposed mechanism of the reaction.

3.3.3 Scope of the reaction

Having the ideal conditions in hand and armed with a sound mechanistic postulate, attention was then steered towards the scope of this reaction. Table 2 displays some of the adducts that were prepared using the methodology described above (entry 6, Table 1). With the necessary diazo azide starting material **21a-g** prepared from the reactions described in Chapter Two in hand, other indole derivatives with varying steric and electronic properties were subjected to the reaction conditions. Initially, examination of the scope of the reaction was dedicated to electron rich arenes, thus parent diazo **21a** was used for this sequence. Having a

simple *N*-methyl or *N*-benzyl protected indole as a trap did not significantly affect the reaction rate in comparison with the parent indole, and as expected, adducts **31** and **32** were produced in excellent yields. Surprisingly, an indole bearing a C-2 phenyl substituent also underwent the reaction in very good yield and in a comparable amount of time to unsubstituted indole, affording adduct **33**. This was in contrast to the effect found by Toste and others in their catalysis, where the methyl group at the C-2 position adversely affected the rate of the reaction and the yield of their desired product, presumably because of steric encumbrance during the electrophilic metalation.¹⁶ However, their catalyst contained a bulky binol phosphate, suggesting that the nature of the ligands on copper could also affect the electrophilic metalation step. Consistent with the proposed electrophilic metalation induction mechanism, the bromo indole derivative tolerated the reaction and produced **34** in reasonable yield, with a prolonged reaction time (36 h), while the electron rich methoxy indole derivative produced **35** in moderate yield and in a shorter amount of time (<16 h). The successful formation of adduct **34** was notable, as the bromide should enable further functionalization using known cross-coupling methodologies. Unfortunately, use of the electron poor 1-acetyl indole did not result in formation of the desired **36** at room temperature or even at higher temperature (40 °C).

To further examine the generality of this methodology, other types of heteroaromatics, such as pyrrole, thiophene, furan and benzofuran, were also examined and gave moderate yields of adducts **37-40** after chromatographic purification. Notably, no substantial induction period was observed for pyrrole, and the reaction could be done at room temperature; whereas all others required a slightly higher temperature (40 °C) to obtain a decent yield in a reasonable amount of time (8-16 hr). This amenability of other heteroaromatics, apart from indole and its derivatives, to this type of catalysis suggests a nice extension to copper(II) catalyzed (or mediated) reactions

proceeding via the electrophilic metalation mechanism described by Gaunt and others. For thiophene, furan and benzofuran cases, it was likely that direct triflic acid catalysis occurred during the addition of arenes to the *C*-acylimine, as opposed to the ammonium triflate, since no ammonium salt analogous to **25** could be formed in these cases.

Substitutions on the diazo-azide partner were likewise examined; starting material containing an electron donating methyl (**21b**) or methoxy (**21c**) group gave better yields than the diazo with an electron-withdrawing nitro group **21d**, affording adducts **41-43** (84-87%) and **47** (14%), and 68-76% recovery of starting material **21d** after 24 hours of stirring. This effect was attributed to the reduced nucleophilicity of the electron-poor diazoketone in the decomposition reaction, despite the production of active copper(I) catalyst. Notably, these results pointed to a conclusion that the elementary steps associated with the reduction of copper(II) to copper(I), be it from diazocarbonyl or more nucleophilic indole, and the extrusion nitrogen from diazocarbonyl are close in relative energy. Attachment of a halogen *meta* to the azide, **21e**, was also tolerated, producing adducts **44-46** in 89-92% yield. Extending the ring from the anthranilic acid derivative to the corresponding 2-amino naphthoic acid derivative **21f** also gave adduct **48** in nearly quantitative yield.

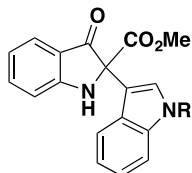
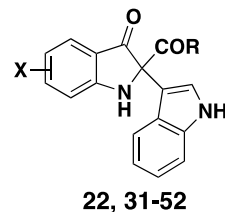
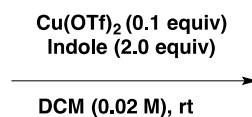
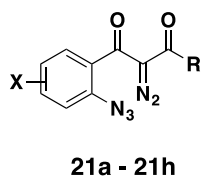
The reaction is also not limited to methyl esters, as other groups, such as allyl in **21g** and vinyl in **21h**, which are good handles for further functionalization, have all been tolerated, producing adducts **49-51** in 71-83% yield. Experimentally, cyclopropanation from the reaction of the ensuing metalcarbene with the allylic or vinylic double bonds was not observed; this was presumably because of the conformational requirement (entropic bias) in the ester moiety during the cyclopropanation event, as well as the inclination towards the formation of a five-membered ring versus a strained three-membered ring, suggesting a kinetic preference for the indolone

formation.²² Finally, using diketo derived diazo **21i** instead of a β -keto ester furnished adduct **52** in moderate 37% yield. This compound showed messy streaking on normal silica gel flash column chromatography, suggesting that the compound was unstable in acidic silica. Thus, the 37% isolated yield for **52** may not represent the true yield for this reaction. Noticeable formation of several colored spots was observed during the separation process. Upon pre-treatment of the silica gel with 2 drops of triethylamine in 100 mL of hexanes and eluting the basic hexanes solution several times before the loading of crude reaction mixture of **21i** mildly improves the separation process. A yield as high as 60-75% was isolated upon using unconventional VLC (vacuum liquid chromatography) on a short pad of silica layered with activated charcoal.

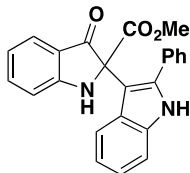
After the successful construction of these compounds (**22**, **31-52**), a representative number of adducts from this library were then tested against Respiratory Syncytial Virus (RSV). The results of these assays were used to prioritize the next synthesis efforts. A total of 25 other compounds, not mentioned here, were then tested. These compounds are subject for a provisional patent application. Thus, the identity of these adducts could not be revealed.

Table 3.2: Scope of the reaction.

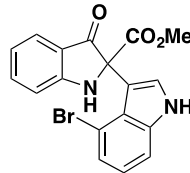
21a R = OMe, X = H
 21b R = OMe, X = 3-Me
 21c R = OMe, X = 4,5-OMe
 21d R = OMe, X = 4-Cl
 21e R = OMe, X = 3-NO₂
 21f (naphthalene derivative)
 21g R = Allyl, X = H
 21h R = Ovinyl, X = H
 21i R = Ph, X = H



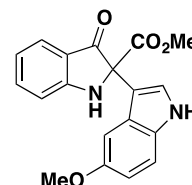
22, R = H, 92%
 31, R = Me, 89%
 32, R = Bn, 93%



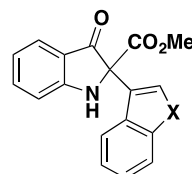
33, 93%



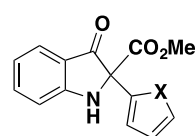
34, 71%



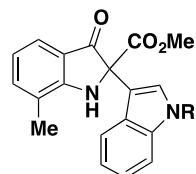
35, 78%



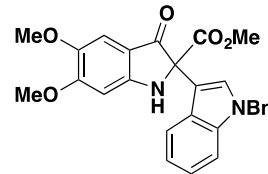
36, X = NAc, 0%
 37, X = O, 46%



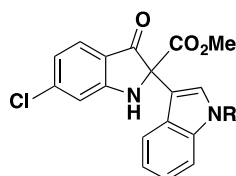
38, X = NH, 68%
 39, X = O, 48%
 40, X = S, 41%



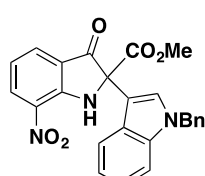
41, R = H, 86%
 42, R = Me, 84%



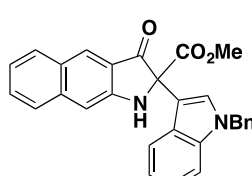
43, 94%



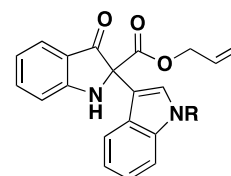
44, R = H, 89%
 45, R = Me, 92%
 46, R = Bn, 90%



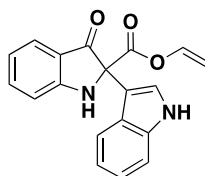
47, 14%



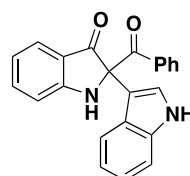
48, 96%



49, R = H, 81%
 50, R = Me, 83%



51, 73%



52, 37%

3.4. Part II: asymmetric preparation of indol-3-one adducts

As we have seen in Part I of this chapter, considerable efforts have been directed towards finding mild conditions for chemo- and regioselective addition of ambident electron rich arenes to the intermediate *C*-acylimines, derived from trapping of acceptor/acceptor metallocarbenes with azides. This progress revealed yet another potentially insurmountable obstacle, the stereoselective (diastereoselective and/or enantioselective) addition of electron rich arenes on the prochiral faces of the intermediate *C*-acylimines in the presence of a Brønsted acid. Since examples of asymmetric preparation of indol-3-ones, bearing quaternary centre at the 2-position, are rare in the literature,^{30,41} this also presented a good opportunity for us to explore this area.

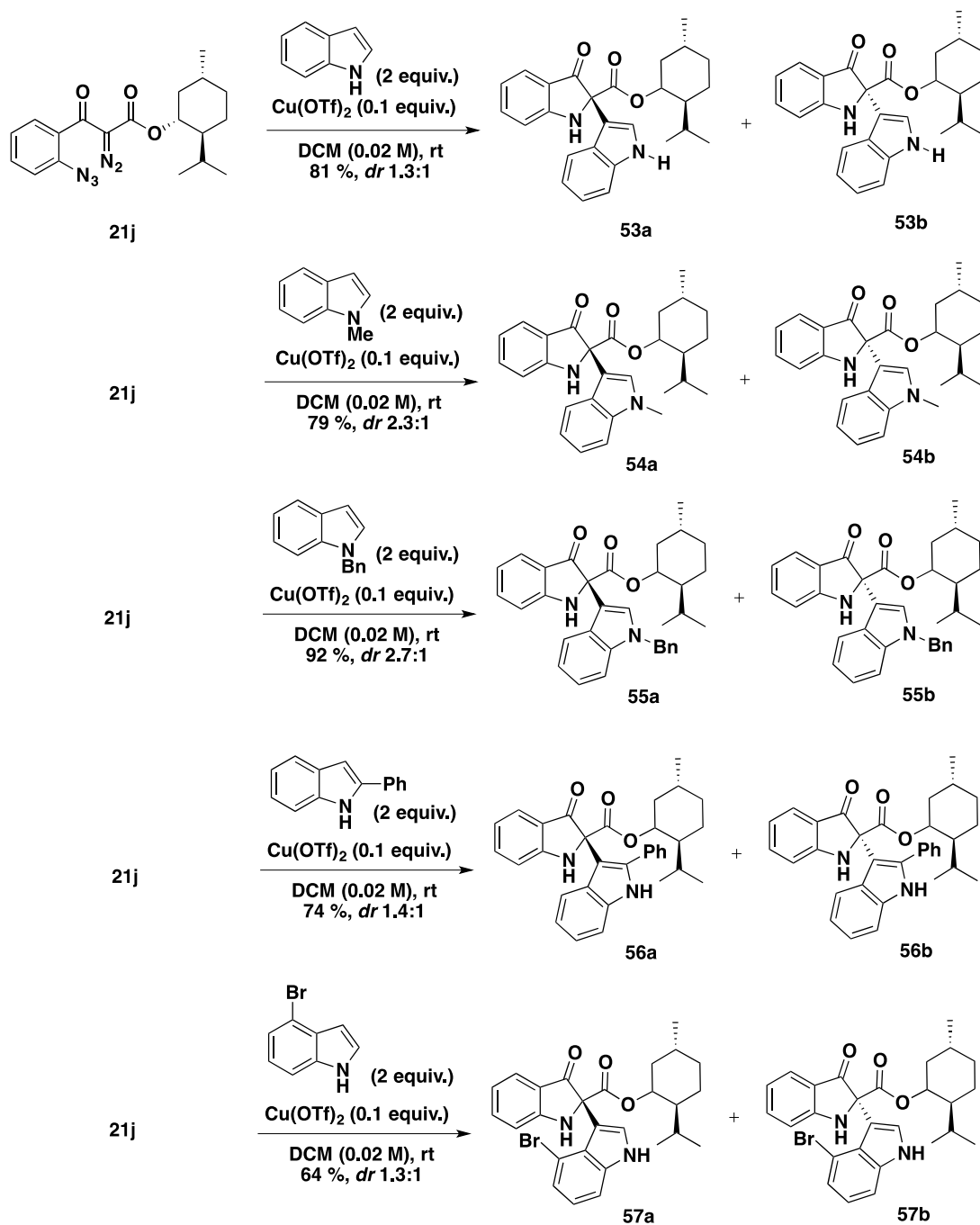
We hypothesized that two approaches might be possible to overcome this obstacle: (1) classic attachment of a chiral auxiliary, which requires an extra removal step of the auxiliary, and (2) addition of a kinetically competitive chiral Brønsted acid. The latter approach seemed more sensible, as the mechanistic studies from Part I told us the copper transition metal is weakly involved during the stereoselectivity determining step. Since the preparation of racemic adducts has been successfully established using the knowledge learned from the key electrophilic metalation concept imparted in Part I of this chapter, Part II will document the development of two complementary strategies to access the desired stereo-enriched bis-indole adducts. For purposes of brevity, related literature precedents pertaining to the discussion of the next sections will only be included as a citation.

3.4.1 Asymmetric preparation of indol-3-one adducts using chiral auxiliary.

With the successful methodology for the racemic preparation of indol-3-one in hand, the goal was eventually stretched to the preparation of the chiral adducts. At this point, we were limited in options, as attachment of chiral ligands on copper (II) precatalyst did not work in our favor. Attachment of chiral auxiliary through an ester starting material seemed to be a simple and attractive starting point. To do this, (-)-menthyl acetate¹⁶ as the corresponding stabilizing ester, instead of a methyl acetate, was subjected to the Tanabe cross Claisen reaction²⁹ to afford the desired chiral keto ester.

The corresponding chiral keto ester was directly subjected to the next step: the Regitz diazo transfer. The chiral diazo azide **21j** was easily purified by column chromatography and subjected to the next reaction using indole as the coupling partner, affording the two corresponding diastereomers of **53** (**53a/53b**) in a combined 81% yield (Scheme 3.12). However, these diastereomers were not separable using isocratic or gradient elution techniques in silica gel flash column chromatography, and so the crude NMR was used to estimate the diastereomeric ratio. Using the methyl groups in the menthyl moiety, the ratio of the corresponding diastereomers was approximated to be 1.3:1. A chiral HPLC separation technique, using previously described conditions,³⁰ was also used to quantitate the amount of each of the diastereomer, and the results agreed well with the NMR ratio. When methyl indole was used as the coupling partner for **21j**, the isolated yield for the corresponding mixture of diastereomers was 79%, along with a moderately improved diastereomeric ratio of 2.3:1 (HPLC ratio). Using bulkier benzyl indole, the diastereomeric ratio began to increase even further to 2.7:1 (HPLC ratio). Fortunately, the mixture of diastereomers from the benzyl indole reaction could be partially separated using gradient elution techniques. Other substituted indole derivatives were

likewise examined as coupling partners for **21j**. Using 2-phenyl indole as a nucleophilic trap gave **56a/56b** in a combined 92% yield, *albeit* with a poor diastereomeric ratio (1.4:1). Bromo indole gave **57a/57b** in a combined 64% yield and a *ca.* 1.3:1 diastereomeric ratio.



Scheme 3.12: Diastereoselective preparation of bis(indole) adducts using menthol chiral auxiliary.

The crystals of **55a**, the partially separable major diastereomer coming from the benzyl indole reaction, could be prepared by slowly diffusing saturated ethyl acetate solution in hexane solvent, allowing for unambiguous determination of the absolute stereochemistry of the major diastereomer using X-ray crystallography (Figure 3.5). Using spectral analogy to **55a**, this also allowed for the assignment of the stereochemistry for the major diastereomers of the other indole coupling reactions (**53a-57a**).

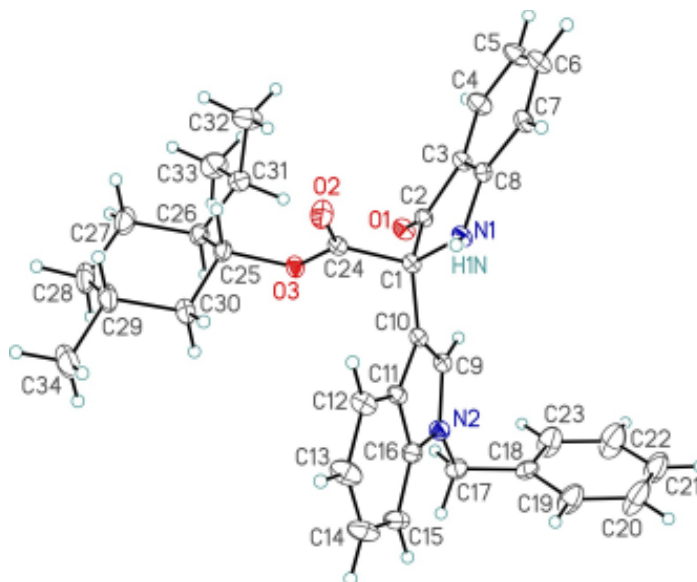
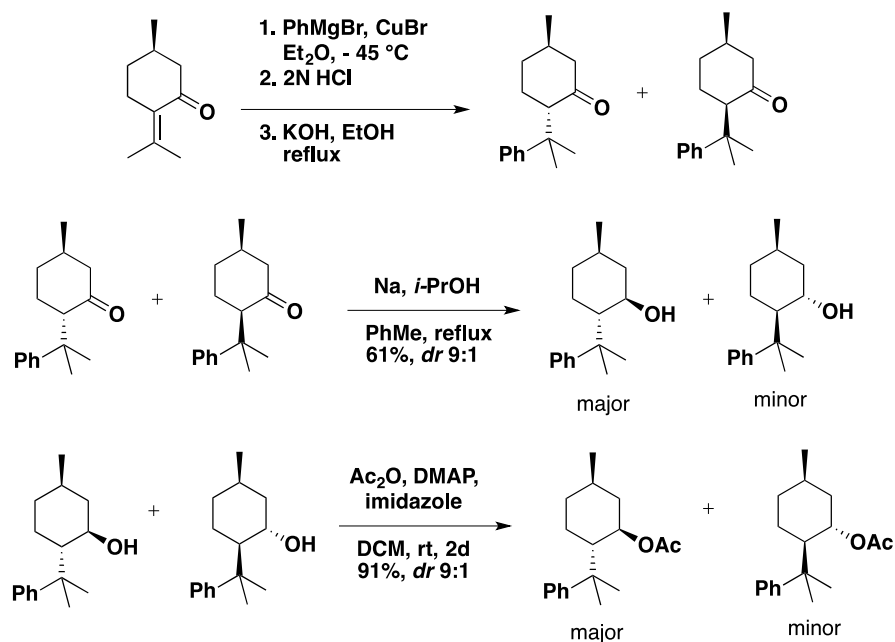


Figure 3.5: ORTEP derived from X-ray diffraction data of the major diastereomer of 55 (55a).

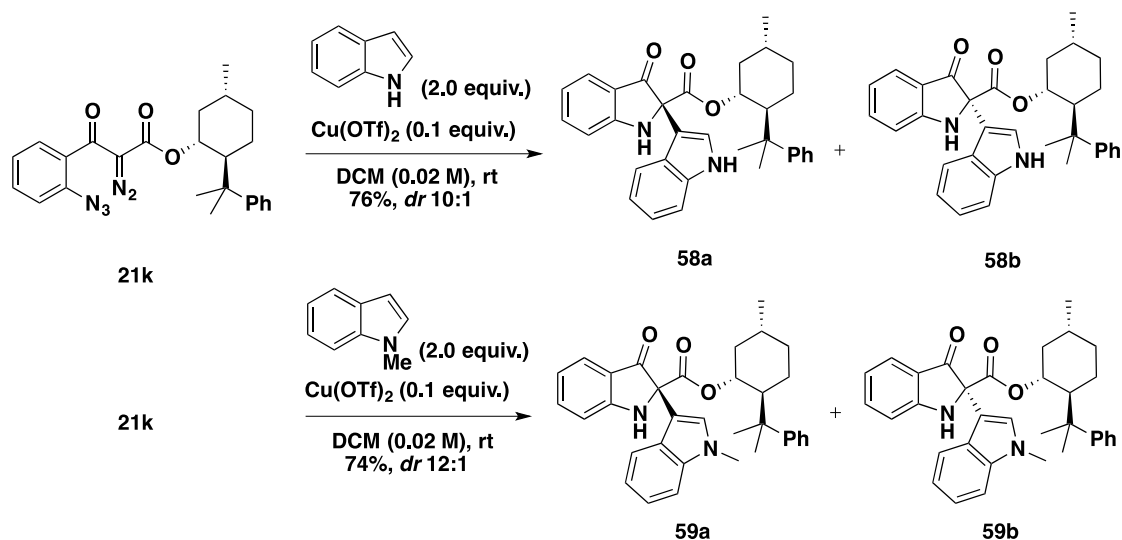
Corey has demonstrated that (*R*)-8-phenyl menthol was a much better chiral auxiliary than the parent menthol.³¹ Both menthol and 8-phenyl menthol as chiral auxiliary are thought to operate on the same idea of steric encumbrance on one face of the carbonyl or its derivative once the major conformer (assuming, this would have the lower transition state towards the major product) is substantially stabilized. Thus, the synthesis of the chiral (*R*)-8-phenyl menthol auxiliary from (*R*)-pulegone was accomplished following a known literature procedure depicted Scheme 3.12.³¹⁻³² The major diastereomer (labeled in Scheme 3.13) of (*R*)-8-phenyl menthol, after the five-step synthesis, could be partially purified from the minor diastereomer by an

acetylation reaction and using the gradient elution technique in column chromatography. The major diastereomer was then subjected to a Tanabe cross Claisen and Regitz diazo transfer to afford the desired chiral diazo azide **21k**.



Scheme 3.13: Preparation of (*R*)-8-phenylmenthol.

The diazo azide **21k**, bearing the major (*R*)-8-phenyl menthol chiral auxiliary, upon reaction with an indole partner to afford indolinones **58a/58b**, displayed a much better diastereomeric ratio (*ca.* 10:1) at the slight expense of reaction yield. Using methyl indole in place of indole also provided an excellent ratio (*ca.* 12:1) of indolinones **59a/59b** (Scheme 3.13).



Scheme 3.14: Diastereoselective preparation of the bis(indole) adducts 58 and 59 using (*R*)-8-phenylmenthol chiral auxiliary.

The absolute stereochemistry of the major diastereomer for the *N*-methyl indole (**59a**) reaction was likewise assigned unambiguously using X-ray crystallography (see appendix). Consistent with the major conformer idea, the major diastereomer presumably arose from the major conformer, because of intramolecular H-bonding between the iminium proton and the ester carbonyl. Using the computational molecular modeling software Merck Molecular Force Field (MMFF94), carried out by my colleague Dr. Christine Dunbar, an optimized structure of the major conformer was acquired (Figure 3.6).³³ Notably, H-bonding stabilization was seen and the major conformer had about 3 kcal/mol more stability than the next stable conformer (the one for minor product). The conclusion drawn from these data was, however, based on the assumption that the relative energy of transition states from the conformers to the corresponding diastereomers was not reversibly altered (Curtin-Hammett principle).³⁴ Further computational work is needed to validate these hypotheses.

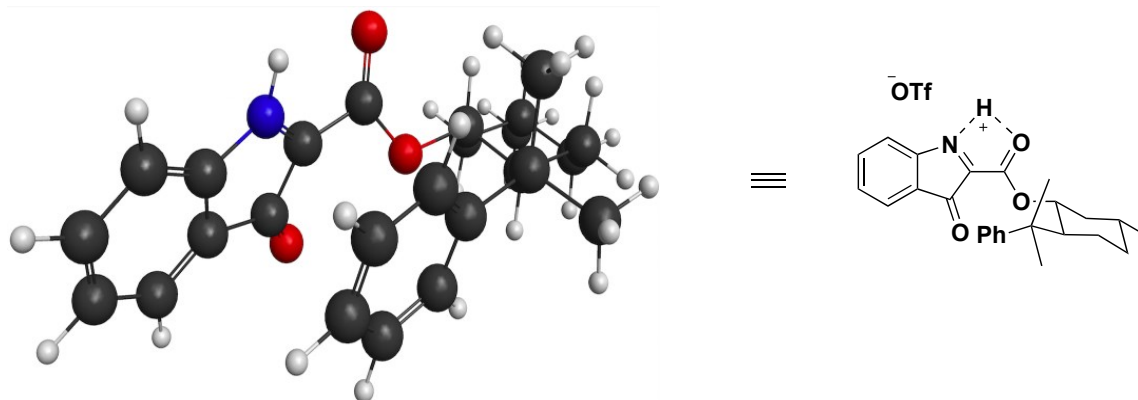


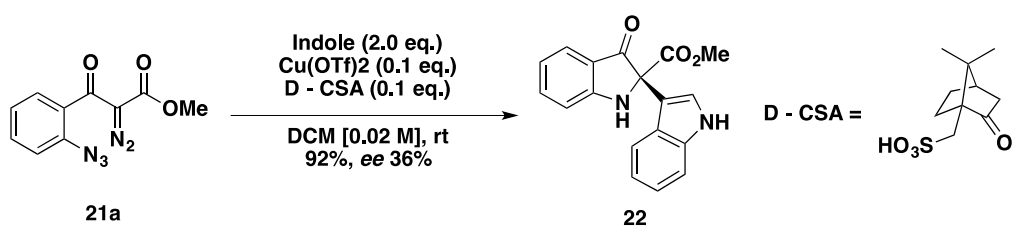
Figure 3.6: Structure of the major conformer of the intermediate C-acyliminium ion.

3.4.2 Asymmetric preparation of adducts using chiral phosphoric acid co-catalyst: attempts to correlate pKa with the enantioselectivity.

Another option to induce asymmetry was to use a kinetically competitive chiral catalyst. Notice that in the mechanistic considerations shown previously, one conclusion that was drawn was the limited involvement of copper(I) during the indole addition onto the C-acylimine intermediate. Thus, incorporation of chiral ligand on copper was not an option.

Sharpless and others have demonstrated that addition of a chiral cinchona alkaloid ligand on OsO₄ could increase the reaction rate of an already existing classic catalytic dihydroxylation.³⁵ The chiral cinchona ligand on OsO₄ could also result in enantioenriched dihydroxyl products coming from a prochiral alkene, in competition with a racemic background reaction. This type of catalysis is referred to as “ligand-accelerated catalysis”.³⁵ Enthralled by the possibility of stereoselectively controlling the addition of indole through addition of a chiral co-catalyst,³⁶ we hypothesized that a chiral acid with sufficient pKa could kinetically outcompete (or help)³⁷ the phenyl ammonium triflate inherent in the catalytic cycle. Without kinetic experiments to accurately predict the effect of additives on the kinetics of the reaction, or *in-*

silico calculations to predict the energetics of the reaction, we preliminarily used thermodynamic pKa data to guide us on the selection of chiral co-catalysts in the next step. Literature data has approximated the pKa of CSA **60** to be 1.2 pKa units. Additionally, CSA is a well-known chiral Brønsted acid catalyst.³⁸ Thus, the original reaction, in the presence of 10 mol% (+)-camphorsulfonic acid (D-CSA) co-catalyst, was done to test whether any detectable enantioenrichment of the product could be achieved (Scheme 3.14).



Scheme 3.15: Enantioselective preparation of **22 using D-CSA chiral co-catalyst.**

Indeed, indolinone **22** was obtained with a modest 36% enantiomeric excess and with no substantial decline in isolated yield. Similarly, as a control experiment to the working hypothesis, a variety of chiral carboxylic acids (e.g. L-proline **61**, (*S*)-ketopinic acid **62**, L-tartaric acid **63**) whose pKa lie around the region of phenyl ammonium triflate were also tested (Figure 3.7). These acids exhibit near to nil enantioselectivity and in some instances (for example, **61**, **63**) eroded the yield significantly (*ca.* 20 - 46% isolated yield).

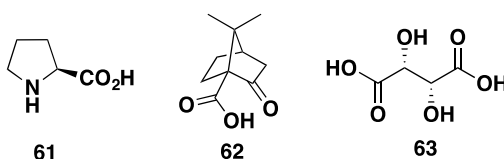
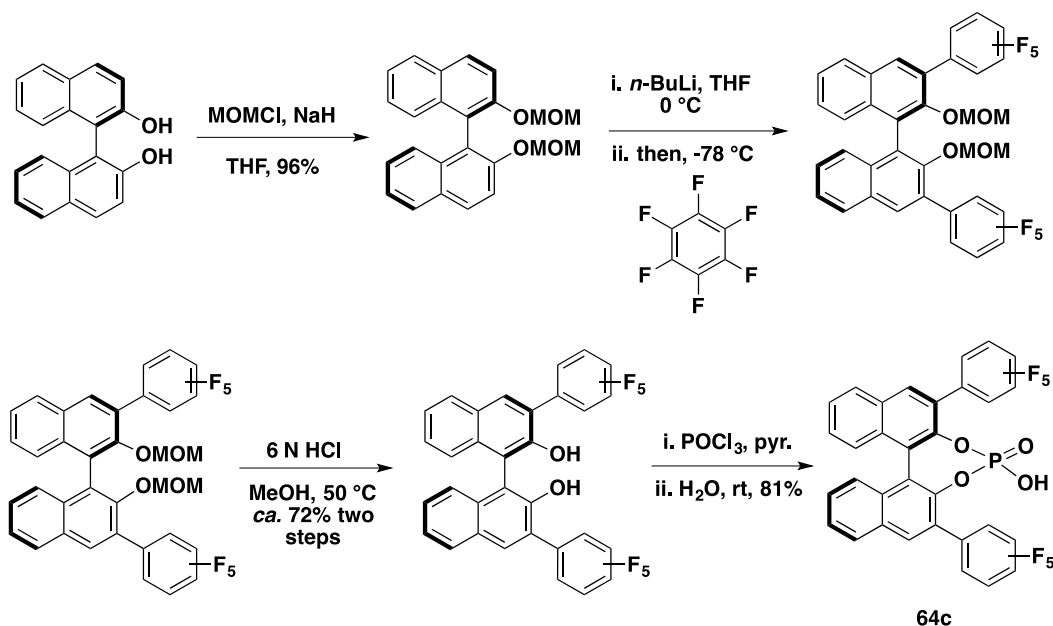


Figure 3.7: Other chiral Brønsted acids tested.

Our campaign to prepare the desired chiral adduct using the addition of chiral co-catalyst continued and was further fueled by the surge of reports using chiral phosphoric acid (CPA) catalysts,³⁹ e.g., **64a-d**. This family of catalyst is known to induce high enantioselectivity upon intra- or intermolecular addition of nucleophiles in prochiral functional groups like imines. Their pKa, depending on the group attached at the 3 and 3' positions of the BINOL scaffold, was estimated to lie around -2 to 4 pKa units.⁴⁰ You³⁰ and Rueping⁴¹ have shown nice precedents related to the enantioselective addition of a variety of nucleophiles, for example, electron rich arenes and cyclopentadienes, on *C*-acylimines using chiral phosphoric acids. As such, the HPLC conditions developed by You's group³⁰ were nicely adapted for our purposes.

At the time this idea was initiated, our research group was not originally stocked with chiral BINOL and Hall's (Prof. Dennis Hall) research group was kind enough to lend us some starting material (*ca.* 200 mg of BINOL). Driven by the desire to prove the conceptual approach, it was deemed appropriate to start the campaign with perfluorophenyl CPA **64c**. Upon completing the synthesis of the desired chiral phosphoric acid using the original method described by Terada,⁴² this catalyst (10 mol%) was similarly subjected to the original reaction conditions. Indeed, this catalyst substantially improved the enantiomeric excess to 58 % and it also furnished a comparable yield of the desired adduct **22** (entry 2, Table 3). This motivated us to screen other chiral phosphoric acids and reaction conditions; thus, the preparation of Terada's catalyst in gram scale was initiated. Other chiral phosphoric acids were also made using the sequence depicted in scheme 3.16. For example, triphenyl silyl substituted⁴³ (CPA **64a**) and perfluorobiphenyl⁴⁴ (CPA **64d**) were used in place of perfluorophenyl (CPA **64c**) to afford the corresponding chiral phosphoric acids.

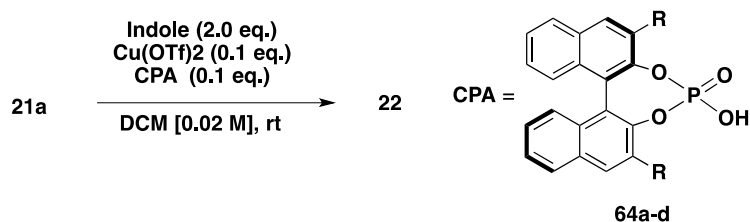


Scheme 3.16: Synthesis of chiral phosphoric acid (CPA) co-catalyst.

Using CPA **64c** and screening for a variety of solvents, we were unable to improve the enantioselectivity even further. Use of toluene, despite the prolonged reaction time (120 hours) did furnish the desired product in 51% yield, but with disappointingly low enantiomeric excess. Anisole, chlorobenzene and nitrobenzene were also screened as solvents. While chlorobenzene and anisole exhibited comparable reaction rates with toluene, nitrobenzene enhanced the conversion of the starting material (74%, 24 hours) to the desired product. Unfortunately, these solvents, like toluene, did not further improve the enantioselectivity. The effect of substitution around the BINOL scaffold was the next screen. Several research groups have demonstrated that bulky triphenylsilyl (TiPSY) and (1,3,5-triisopropyl)-phenyl (TRIP) groups around the 3 and 3' positions of BINOL phosphoric acid could dramatically increase the enantioselectivity. In fact, they are known as privileged catalysts among the family of chiral phosphoric acids. The inherent bulkiness of the groups made them efficient for many enantioselective CPA catalyzed reactions.

After the preparation and use of chiral phosphoric acid catalyst bearing triphenylsilyl groups, the observed enantioselectivity was close to nil and the isolated yield of the desired product plummeted considerably (entry 1, Table 3.3), suggesting that the silyl groups are not compatible with the reaction conditions. In our hands, the preparation of TRIP in a small scale was difficult and oftentimes impure; hence, we were not able to use this for comparison. Use of the parent unsubstituted chiral binol phosphoric acid, as expected, resulted in no discrimination in the indole addition between faces of the imine (entry 2, Table 3.3). When we investigated the regime of bulkier, perfluorinated aromatics, considerable improvement in enantioselectivity was observed. For instance, using the CPA substituted nonafluorobiphenyl version, the enantioselectivity increased to 88% (entry 4, Table 3.3), at the slight expense of yield. Further improvement of the enantiomeric purity of the adducts could be realized using recrystallization.

Table 3.3: Survey of chiral phosphoric acid (CPA) co-catalyst.



Entry	R in CPA additive	Isolated yield of 22 (%)	Enantiomeric excess of 22 (%)
1	SiPh ₃ (64a)	ca. 62	0
2	H (64b)	93	0
3	Pentafluorobiphenyl (64c)	90	58
4	Nonafluorobiphenyl (64d)	87	88

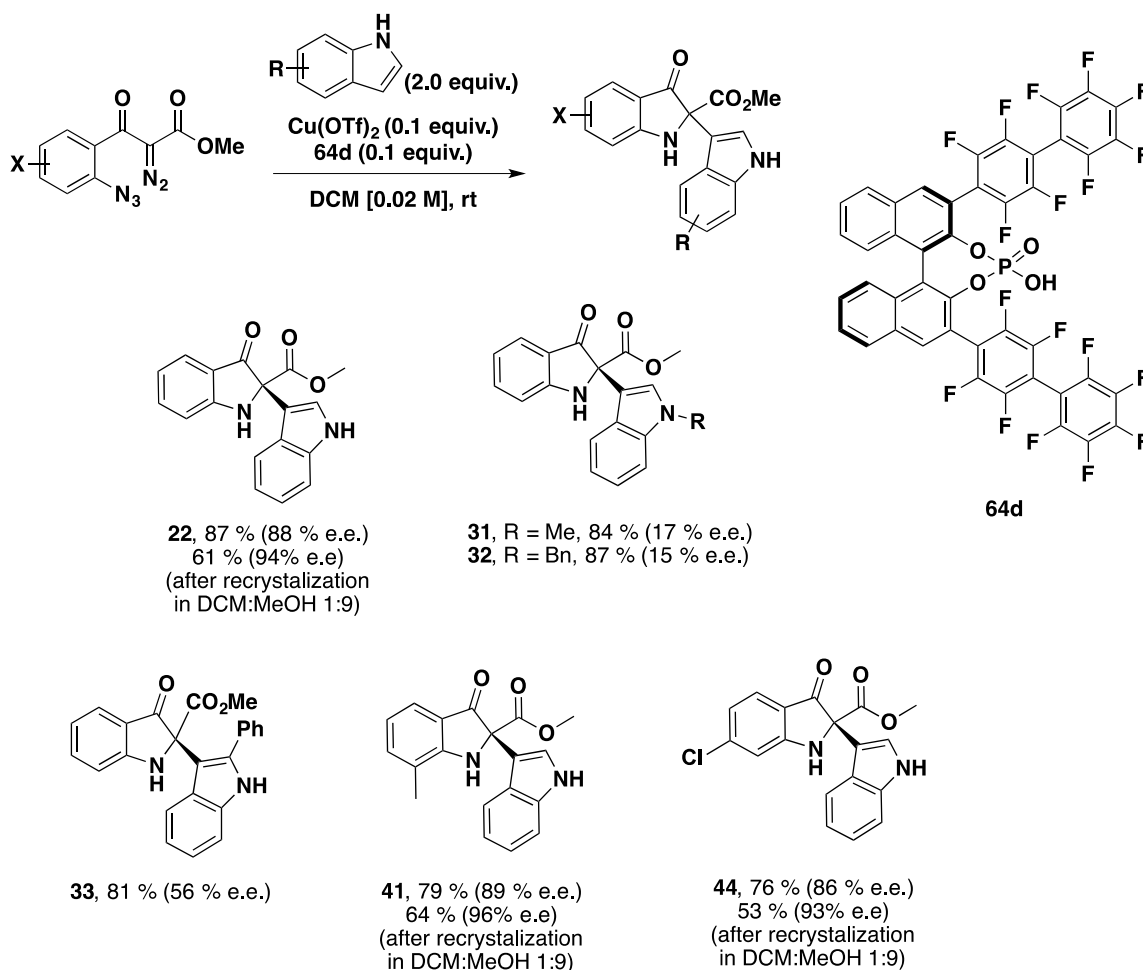
*a. Reaction conditions: a solution of **21a** (0.02 M) in DCM was added dropwise 10 minutes by syringe pump or manual addition to a solution of Cu(OTf)₂ (0.1 equiv), appropriate CPA (0.1 equiv) and indole (2 equiv.) in DCM*

Indolinone **22**, however, was notable. The ethyl acetate solution of enantioenriched **22**, despite being saturated with one enantiomer (94:6), preferred to crystallize initially with minute fractions of less enriched crystals (76:24). Upon filtration of the crystals using a Hirsch funnel, the enantioselectivity of the mother liquor improved over several cycles. This enantioenriched mother liquor stayed as an oil after concentration for some time (days), before slowly transforming into a fine yellow solid, but not crystalline enough for X-ray crystallography. However, You and co-workers have reported a methodology similar to ours.³⁰ Using comparison of the optical rotation of a structurally similar compound reported by You and co-workers, of which the absolute configuration was secured using X-ray crystallography,³⁰ we were able to propose the absolute configuration for our compounds, which are depicted in Table 4. Attempts to convert **53a** to optically pure **22** using various acid- or base-catalyzed transesterification reactions were met with failure. In the presence of a base (e.g. catalytic NaOH, KOH), indolinone **53a** decomposed, and while in the presence of a Brønsted acid (e.g. catalytic H₂SO₄, HCl in methanol or ethanol and toluene), only recovery of the corresponding **53a** was observed most of the time.

When attention was turned to the tolerance of substitution around the parent diazo azide and indole partner; it became apparent that the reaction in the presence of the optimized chiral phosphoric acid (**64d**) was not sensitive to the substitution around the parent diazo azide. Consistent excellent yield and enantioselectivity were seen, for example, both chloro (**21d**) and methyl (**21b**) substituents gave the desired adducts **41** and **44** in 86-88 % *ee*, similar to the parent **21a**. However, the reaction suffered from dramatic loss of enantioselectivity when *N*-substituted indole derivatives were used; for example, *N*-benzyl indole and *N*-methyl indole delivered adducts **31** and **32** in 15-17% *ee*, suggesting that the N-H bond in indole (or derivatives) was

necessary to achieve high enantioselectivity. The presence of a bulky 2-phenyl on the indole also delivered the desired adduct, **33**, in high yield but a modest 56% *ee*.

Table 3.4: Scope of the chiral phosphoric acid (CPA) co-catalyzed reaction.

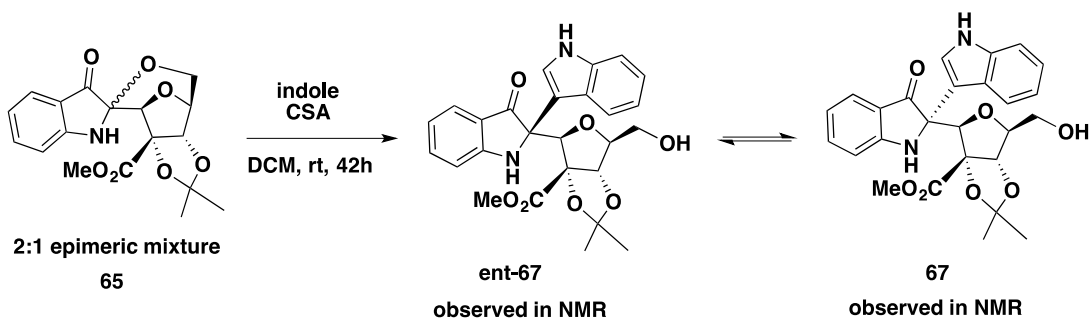


3.4.3 Product isomerization experiment

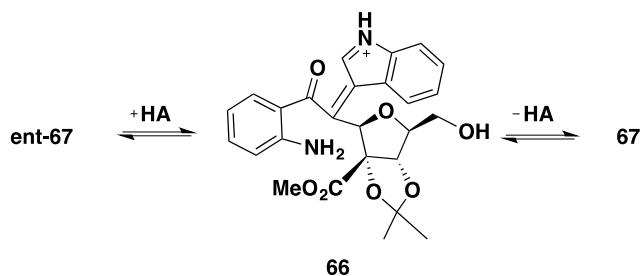
During the course of our study, we were aware of slightly conflicting arguments between Kerr's preparation of indolinone **67**⁴⁵ (equation a and b, Scheme 3.17) and You's enantioselective preparation of **70**³⁰ (equation c, Scheme 3.16). Notably, Kerr implied that indolinone **67** resulted from the thermodynamic equilibration of intermediate **66**, which is

derived from indole **65** via a Hofmann-type elimination mechanism and a re-addition of the amine to the vinylogous iminium ion, mediated by Brønsted acid CSA. In You's case, however, the enantioenrichment of indolinone **70**, which is derived from the ring opening of spiro **68**, followed by enantioselective addition of indole on C-acylimine **69**, originates due to kinetic control.

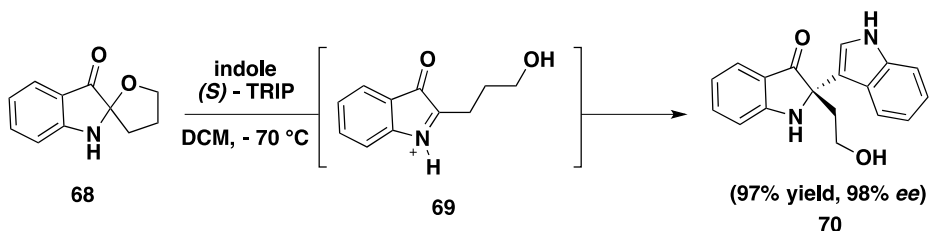
(a) Kerr's thermodynamic equilibration



(b) Proposed mechanism of equilibration



(c) You's enantioselective synthesis



Scheme 3.17: Kerr and You's indol-3-one synthesis.

Thus, crystalline indolinone **55a** was subjected to the original reaction conditions to test whether a racemization would be observed. However, purification of the product after the attempted racemization lead to the re-isolation of **55a**. The crude NMR also revealed that only

55a was formed, indicating that the diastereomeric ratio was purely kinetic. Notably, this result implied that two (essentially one) factors governed the thermodynamic isomerization of these types of indolinones: (1) temperature and (2) the nature of the groups stabilizing the developing carbocation during the Hofmann elimination, ultimately leading to temperature sensitivity. We proposed that the ester increases the energetic barrier to isomerization *via* the destabilization of developing vinylogous iminium carbocation during the Hofmann elimination step. However, further experiments are needed, preferably *in silico* studies, to validate this hypothesis.

3.5 Conclusions

In summary, a novel dual catalysis between a transition metal catalyzed azide trapping of electronically derailed metallocarbenes and a Brønsted acid catalyzed addition of electron rich arenes to the resulting *C*-acylimine has been achieved, forming the desired synthon for the synthesis of isatisine A. After elucidation of the mechanism, the accumulation of two orthogonal catalysts was attributed to a fast and a favorable electrophilic metalation, followed by a one-electron reduction of copper(II) precatalyst. A variety of functional groups around the electron-rich arenes and the parent diazocarbonyl compounds was tolerated. Other electron-rich arenes, apart from indole, also showed good reactivity, opening a nice new extension to the current repertoire of transformations involving the electrophilic metalation concept. The reaction was robust and was highly scalable to multi gram scale preparation of the desired adduct. The purification of the desired adducts were also, in most cases, simple and used direct recrystallization. Preparation of chiral derivatives was likewise achieved using two approaches: (1) attachment of a chiral ester, in the form of menthol or 8-phenyl menthol, to selectively control the addition of electron rich arenes on one face of the *C*-acylimine. (2) selected chiral

phosphoric acids also worked as kinetically competitive catalysts in the presence of an already active ammonium triflate, inducing high enantioselectivity.

3.6 Experimental

3.6.1 General Information

Reactions were carried out in an oven (130 °C) or flame-dried glassware under a positive argon atmosphere unless otherwise stated. Transfer of anhydrous reagents was accomplished with oven-dried syringes or cannulae. Solvents were distilled before use: acetonitrile (CH₃CN), dichloromethane (DCM) and dichloroethane (DCE) from calcium hydride, toluene (PhMe) from sodium metal, diethyl ether (Et₂O) and tetrahydrofuran (THF) from sodium metal/benzophenone ketyl. Thin layer chromatography was performed on glass plates pre-coated with 0.25 mm silica gel with fluorescent indicator UV₂₅₄ (Rose Scientific). Flash chromatography columns were packed with 230-400 mesh silica gel (Silacycle). Proton nuclear magnetic resonance spectra (¹H NMR) were recorded at 400 MHz, or 500 MHz and coupling constants (*J*) are reported in Hertz (Hz). Carbon nuclear magnetic resonance spectra (¹³C NMR) were recorded at 125 MHz. The chemical shifts are reported on the δ scale (ppm) and referenced to the residual solvent peaks: CDCl₃ (7.26 ppm, ¹H; 77.06 ppm, ¹³C), *d*₆-DMSO (2.49 ppm, ¹H; 39.5 ppm, ¹³C), and *d*₂-DCM (5.32 ppm, ¹H; 53.5 ppm, ¹³C). The preparations for compounds **21a**, **21b**, **21d**, **21g** **28** and the corresponding keto ester were all reported in Chapter Two. Please refer to Chapter Two for relevant syntheses and characterizations. The known chiral phosphoric acids (CPA), **64a**⁴⁴, **64b**⁴³, **64c**⁴⁴, **64d**⁴⁴ were prepared using literature procedures.

Control Experiments:

What is the copper oxidation state in the catalytic cycle?

Decomposition studies (% Recovery analysis)

Copper (II) oxidation state

A solution of diazo-azide **21a** (50 mg, 0.20 mmol) in DCM (5 mL) was added to a solution of Cu(OTf)₂ (7.3 mg, 0.02 mmol) in DCM (5 mL) at room temperature *via* syringe pump over 1 h. Once the addition was complete, the reaction was monitored by TLC for consumption of the diazo-azide starting material. After 24 h, the solution was extracted with water (10 mL, 3x) to remove the copper salt, the DCM solution was dried with MgSO₄, filtered and concentrated under reduced pressure. The crude oil was purified using silica gel flash column chromatography eluting with 20% EtOAc/Hexanes. This procedure resulted in the recovery of **21a**, in 81-93% (three repeats). Using identical conditions but allowing the mixture to stir for 5 d instead of 24 h resulted to the recovery of 73-84% (three repeats) starting material **21a**. Analysis of the TLC and NMR spectra of the crude mixture revealed the presence of starting material and a faint spot on the baseline using 20% EtOAc/Hexanes eluent.

Copper (I) oxidation state

A solution of diazo-azide **21a** (50 mg, 0.20 mmol) in DCM (5 mL) was added to a solution of Cu(OTf)(PhMe) (10.1 mg, 0.02 mmol) in DCM (5 mL) at room temperature *via* syringe pump over 1 h. Once the addition was complete, the reaction was monitored by TLC for consumption of the diazo-azide starting material. After 24 h, the solution was extracted with water (10 mL, 3x) to remove the copper salt, the DCM solution was dried with MgSO₄, filtered and concentrated under reduced pressure. The crude oil was purified using silica gel flash column

chromatography eluting with 20% EtOAc/Hexanes. Only traces of **21a** were recovered. Analysis of the TLC and NMR spectra of the crude mixture revealed the presence of multiple colored (mostly yellow) spots.

Decomposition studies (*in-situ* IR analysis and ¹H-NMR spectroscopy)

Copper (II) oxidation state

A solution of diazo-azide **21a** (50 mg, 0.20 mmol) in DCM (5 mL) was added to a solution of Cu(OTf)₂ (7.6 mg, 0.02 mmol) in DCM (5 mL) at room temperature *via* syringe pump over 1 h. Once the addition was complete, the reaction was monitored by TLC for consumption of the diazo-azide starting material. An aliquot of the stirred solution (0.5 mL), was taken after *ca.* 5 min, 1 h, 2 h, 3 h, and 24 h of stirring, each aliquots were diluted with DCM (1 mL). The diluted solution was analyzed using IR spectroscopy and plotted as overlaid spectra (Figure 3.4).

Copper (I) oxidation state

Using IR spectroscopy

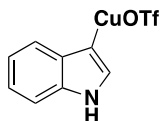
A solution of diazo-azide **21a** (50 mg, 0.20 mmol) in DCM (5 mL) was added to a solution of Cu(OTf)(PhMe) (10.3 mg, 0.02 mmol) in DCM (5 mL) at room temperature *via* syringe pump over 1 h. Once the addition was complete, the reaction was monitored by TLC for consumption of the diazo-azide starting material. An aliquot of the stirred solution (0.5 mL), was taken after *ca.* 5 min, 1 h, 2 h, 3 h and 24 h of stirring, each aliquots were diluted with DCM (1 mL). The diluted solution was analyzed using IR spectroscopy and plotted as overlaid spectra (Figure 3.4).

Using $^1\text{H-NMR}$ spectroscopy.

In a 2.0 mL vial, a solution of diazo-azide **21a** (10 mg, 0.04 mmol) in deuterated DCM (0.5 mL) at room temperature was added to $\text{Cu}(\text{OTf})(\text{PhMe})$ (*ca.* 2 mg, 0.0039 mmol) as a solid. The solution was quickly transferred in an NMR tube, purged with argon, and capped immediately. NMR spectra (400 MHz) were acquired once per hour over a 10 h period. The array of spectra was plotted and is included in the appendix. It was clear that after 8-10 h, the starting material **21a** was completely consumed.

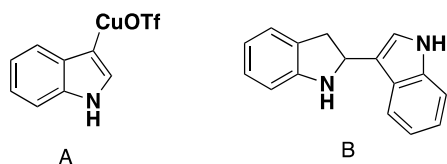
How does the copper (I) form in solution from a copper (II) pre-catalyst?

Using UV spectroscopy, formation of new charge transfer complex.



Solution A: A solution of indole (55 mg, 0.2 mmol) was added with $\text{Cu}(\text{OTf})_2$ (7.3 mg, 0.02 mmol) in DCM (5 mL) at room temperature. Once the addition was done, noticeable formation of light green solution occurred after 1 h. An aliquot of this solution (1 mL) was diluted with 5 mL of DCM solvent and was subjected to UV spectroscopy. **Solution B:** An aliquot (1 mL) of a solution of indole dissolved in DCM (0.02 M, 10 mL) at room temperature was also subjected to UV spectroscopy. **Solution C:** An aliquot (1 mL) of a solution of $\text{Cu}(\text{OTf})_2$ dissolved in DCM (0.02 M, 10 mL) at room temperature was also subjected to UV spectroscopy. Note: see the appendix for spectra pertaining to these experiments. After analysis of the three spectra, formation a broad new peak at 395 nm was seen from **Solution A**, indicating the formation of a new colored complex.

Using ESI-MS, detection of the mass fragments corresponding to the dimer and the charge transfer complex.



A solution of indole (55 mg, 0.2 mmol) was added to $\text{Cu}(\text{OTf})_2$ (7.3 mg, 0.02 mmol) in DCM (5 mL) at room temperature. Once the addition was done, noticeable formation of light green solution occurred after one hour. An aliquot of this solution (1 mL) was diluted with acetonitrile and directly subjected to ESI-MS analysis. After analysis of the ESI-MS, the following fragments were detected and partially ascribed to the formation: **A** HRMS calc'd for $\text{C}_9\text{H}_6\text{CuF}_3\text{NO}_3\text{S}$ $[\text{M}]^+$ 327.9316, found 327.9645, for **B** HRMS calc'd for $\text{C}_{16}\text{H}_{14}\text{N}_2\text{O}$ $[\text{M}+\text{H}]^+$ 235.1230, found 235.1230.

Which species catalyzes the Friedel-Crafts alkylation?

Using C-acylimine **28 in the presence of $\text{Cu}(\text{OTf})(\text{PhMe})$**

A solution of C-acylimine **28** (50 mg, 0.19 mmol) and indole (50 mg, 0.20 mmol) was added to $\text{Cu}(\text{OTf})(\text{PhMe})$ (9.7 mg, *ca* 0.02 mmol) in DCM (5 mL) at room temperature. Once the addition was complete, the solution was allowed to stir overnight. After stirring for 16 h, the solution was extracted with water (5 mL, 2x), the organic layer was dried with MgSO_4 , filtered and concentrated under reduced pressure. Analysis of crude reaction mixture suggests that substantial quantities of **28** was present. Upon purification on a short pad of silica (20% EtOAc/Hexanes), *ca.* 91% of **28** was recovered.

Using *C*-acylimine **28** in the presence of TfOH.

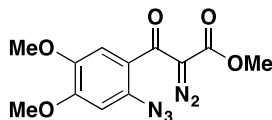
A solution of *C*-acylimine **28** (50 mg, 0.19 mmol) and indole (50 mg, 0.20 mmol) was added to TfOH (1 drop) in DCM (5 mL) at room temperature. Once the addition was complete, within 5 minutes a change in color was noticed, the color of the solution changed from deep purple to light orange. The solution was diluted with water (5 mL) and extracted with DCM (5 mL, 3x). The organic layer was dried using MgSO₄ concentrated under reduced pressure. Analysis of the crude mixture indicated that **28** was completely consumed.

Using *C*-acylimine **28** in the presence of CSA.

A solution of *C*-acylimine **28** (50 mg, 0.19 mmol) and indole (50 mg, 0.20 mmol) was added to camphorsulfonic acid CSA (4 mg, *ca.* 0.02 mmol) in DCM (5 mL) at room temperature. Once the addition was complete, the solution gradually (overnight) changed color from deep purple to a yellow suspension. Analysis of the TLC indicated that **28** was completely consumed. The suspension was filtered. The filtered solid was dissolved in deuterated DMSO and was analyzed using NMR spectroscopy. Analysis of the spectra revealed that the 2:1 adduct (indole:indol-3-one) was present in solution. Please refer to Chapter Two for the characterization of the 2:1 adduct.

Additional starting materials:

Compound 21c:

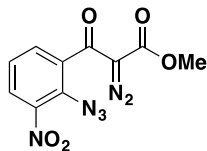


Dichloromethane (*ca.* 30-40 ml) was added to a conical flask containing 4,5-dimethoxy-2-azido benzoic acid (1.0 g, 4.5 mmol) and the suspension was cooled to 0 °C before addition of methyl

acetate (1.0 equiv) and trichloroacetyl chloride (1.2 equiv). This solution was slowly transferred via cannula to a suspension of NaH (1.2 equiv) in DCM (10-20 mL) at 0 °C. After stirring at 0 °C for 15 min, the solution was cooled to -45 °C before the addition of 1-methylimidazole (1.2 equiv). The solution was then stirred for an additional 10 min at -45 °C before slowly adding TiCl₄ (3.4 equiv) followed by NEt₃ (4.0 equiv). The dark red/brown solution was kept at -78 °C for 30 min before being warmed to 0 °C and kept for 1 h and subsequently quenched with water (30 mL). The organic layer was separated and the aqueous layer was washed 3x with equal portions of DCM. The combined organic layers were washed with an equivalent volume of water and brine, dried over MgSO₄, filtered, and concentrated under reduced pressure. The crude product was partially purified by flash chromatography to afford an orange oil whose R_f was about 0.3 (7:3 hexanes:EtOAc). The orange oil was concentrated and added to a stirred solution of triethylamine (1.2 equiv) in CH₃CN (20 mL). Tosyl azide (1.0 equiv) in CH₃CN (10 mL) was transferred via cannula into the flask and the reaction was left to stir overnight. Concentration under reduced pressure followed by purification via flash chromatography (silica gel, 8:2 hexanes:EtOAc→7:3 hexanes:EtOAc slowly added in gradient) furnished **21c** as a yellow oil in 40-55 % yield (from starting 4,5-dimethoxy-2-azidobenzoic acid).

21c: R_f = 0.25 (7:3 hexanes:EtOAc); IR (cast film) 2978, 2134, 1711, 1695, 1565, 1292 cm⁻¹; ¹H NMR (500 MHz, CDCl₃) δ 6.87 (s, 1H), 6.62 (s, 1H), 3.94 (s, 3H), 3.86 (s, 3H), 3.78 (s, 3H); ¹³C NMR (125 MHz, CDCl₃) δ 184.5, 161.2, 152.4, 146.4, 131.4, 121.9, 111.6, 101.5, 56.3, 56.2, 52.3; HRMS calc'd for C₁₂H₁₁N₅O₅Na [M+Na]⁺ 328.0652, found 328.0651. (Note: the ¹³C signal for the diazo carbon was not detected)

Compound 21e:

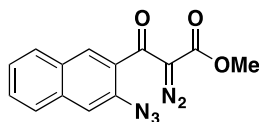


Compound **21c** was prepared analogously to **21e** using 3-nitro-2-azido benzoic acid in place of 2-azido-4,5-dimethoxybenzoic acid.

Isolated as a brown oil in 23% yield (from 3-nitro-2-azido benzoic acid and methyl acetate starting materials): $R_f = 0.19$ (7:3 hexanes:EtOAc); IR (cast film) 3022, 2141, 1732, 1694, 1637, 1567, 1293 cm^{-1} ; ^1H NMR (500 MHz, CDCl_3) δ 8.14 (dd, $J = 8.2, 1.6$ Hz, 1H), 7.51 (dd, $J = 7.6, 1.6$ Hz, 1H), 7.38 (ddd, $J = 8.2, 7.6$ Hz, 1H), 3.76 (s, 3H); ^{13}C NMR (125 MHz, CDCl_3) δ 184.2, 160.5, 135.8, 132.7, 132.5, 132.4, 127.8, 125.8, 52.6; LC-MS calc'd for $\text{C}_{10}\text{H}_7\text{N}_6\text{O}_5$ $[\text{M}+\text{H}]^+$ 291.1, found 291.1.

(Notes: (1) the preparation for this starting material was limited to 70-100 mg. (2) the ^{13}C signal for the diazo carbon was not detected).

Compound 21f:

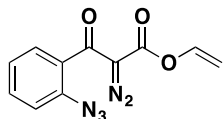


Compound **21f** was prepared analogously to **21c** using 3-azido-2-naphthoic acid in place of 2-azido-4,5-dimethoxybenzoic acid.

Isolated as a brown oil in 51% yield (from 3-azido-2-naphthoic acid and methyl acetate starting materials): $R_f = 0.68$ (7:3 hexanes:EtOAc); IR (cast film) 2971, 2136, 1724, 1693, 1633, 1567, 1290 cm^{-1} ; ^1H NMR (500 MHz, CDCl_3) δ 7.83-7.76 (m, 3H), 7.53 (br s, 1H), 7.54 (ddd, $J = 8.2, 6.9, 1.2$ Hz, 1H), 7.28-7.21 (ddd, $J = 8.2, 7.0, 1.2$ Hz, 1H), 3.74 (s, 3H); ^{13}C NMR (125 MHz,

CDCl₃) δ 185.6, 160.9, 135.2, 134.7, 130.3 (2x), 129.5, 128.9, 128.7, 128.4, 126.7, 126.2, 115.6, 52.3; HRMS calc'd for C₁₄H₉N₅O₃Na [M+Na]⁺ 318.0597, found 318.0594. (Note: the ¹³C signal for the diazo carbon was not detected)

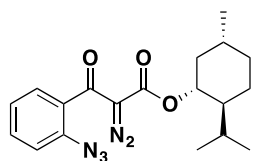
Compound 21h:



Compound **21h** was prepared analogously to **21c** using vinyl acetate in place of methyl acetate, and using 2-azido-benzoic acid in place of 2-azido-4,5-dimethoxybenzoic acid.

Isolated as a yellow oil in 46% yield (from 2-azido-benzoic acid and vinyl acetate starting materials): $R_f = 0.51$ (7:3 hexanes:EtOAc); IR (cast film) 2924, 2931, 2136, 1724, 1684 cm⁻¹; ¹H NMR (400 MHz, CDCl₃) δ 7.47 (ddd, $J = 8.1, 7.5, 1.6$ Hz, 1H), 7.28-7.25 (m, 1H), 7.17-7.12 (m, 3H), 4.70 (dd, $J = 13.9, 2.0$ Hz, 1H), 4.54 (dd, $J = 6.2, 2.0$ Hz, 1H); ¹³C NMR (125 MHz, CDCl₃) δ 185.3, 157.7, 140.1, 137.9, 132.2, 130.2, 128.6, 124.8, 118.3, 98.5; HRMS calc'd for C₁₁H₇N₅O₃Na [M+Na]⁺ 280.0441, found 280.0439. (Note: the ¹³C signal for the diazo carbon was not detected.)

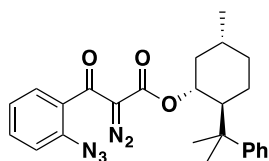
Compound 21j:



Compound **21j** was prepared analogously to **21c** using (-)-menthyl acetate in place of methyl acetate, and using 2-azido-benzoic acid in place of 2-azido-4,5-dimethoxybenzoic acid. Isolated as a yellow oil in 48% yield (from 2-azido-benzoic acid and (-)-menthyl acetate starting

materials): $R_f = 0.64$ (7:3 hexanes:EtOAc); $[\alpha]_D^{20} : -67.76$ ($c = 0.52$, DCM) IR (cast film) 2956, 2928, 2870, 2130, 1719, 1691, 1302, 958 cm^{-1} ; ^1H NMR (500 MHz, CDCl_3) δ 7.45 (ddd, $J = 8.1, 7.4, 1.7$ Hz, 1H), 7.30-7.28 (m, 1H), 7.19-7.14 (m, 2H), 4.70 (ddd, $J = 10.9, 10.9, 4.4$, 1H), 2.00-1.96 (m, 1H), 1.71-1.58 (m, 3H), 1.44-1.36 (m, 1H), 1.15-0.93 (m, 2H), 0.87 (d, $J = 6.5$ Hz, 3H), 0.83 (d, $J = 7.0$ Hz, 3H), 0.87-0.83 (m, 2H), 0.72 (d, $J = 7.0$ Hz, 3H); ^{13}C NMR (125 MHz, CDCl_3) δ 185.9, 160.3, 137.6, 131.7, 130.8, 128.3, 124.7, 118.1, 75.9, 46.9, 40.9, 34.0, 31.3, 26.4, 23.4, 21.9, 20.7, 16.3; HRMS calc'd for $\text{C}_{19}\text{H}_{23}\text{N}_5\text{O}_3\text{Na}$ $[\text{M}+\text{Na}]^+$ 392.1693, found 392.1692. (Note: the ^{13}C signal for the diazo carbon was not detected.)

Compound 21k:



Compound **21k** was prepared analogously to **21c** using (*R*)-8-phenylmenthyl acetate in place of methyl acetate, and using 2-azido-benzoic acid in place of 2-azido-4,5-dimethoxybenzoic acid. Isolated as a yellow oil in 41% yield (from 2-azido-benzoic acid and (*R*)-8-phenylmenthyl acetate starting materials):

$R_f = 0.74$ (7:3 hexanes:EtOAc); IR (cast film) 2954, 2911, 2874, 2138, 1727, 1698, 1305, 948 cm^{-1} ; ^1H NMR (500 MHz, CDCl_3) δ 7.53-7.51 (m, 1H), 7.50-7.42 (m, 3H), 7.41-7.20 (m, 5H), 4.96 (ddd, $J = 10.8, 10.8, 4.5$, 1H), 2.00-1.96 (m, 1H), 1.71-1.58 (m, 3H), 1.44-1.36 (m, 1H), 1.15-0.93 (m, 3H), 1.21 (s, 3H), 1.38 (s, 3H), 0.76 (d, $J = 7.0$ Hz, 3H); ^{13}C NMR (125 MHz, CDCl_3) δ 185.6, 159.3, 151.5, 151.2, 131.7, 128.4, 128.3, 127.9, 127.5, 125.7, 125.3, 125.1, 124.6, 118.2, 75.2, 72.9, 50.7, 39.5, 34.6, 30.5, 27.8, 27.8, 24.5, 22.2; LC-MS calc'd for $\text{C}_{25}\text{H}_{28}\text{N}_5\text{O}_3$ $[\text{M}+\text{H}]^+$ 446.5, found 446.5.

Representative procedures for reactions of **21a-j** with electron-rich arene nucleophiles:

Racemic, Method A:

For ≤ 0.250 g (1.02 mmol): A solution of diazo-azide **21a** (0.250 g, 1.02 mmol) in DCM (25 mL) was added to a solution of indole (0.239 g, 2.04 mmol) and Cu(OTf)₂ (37 mg, 0.102 mmol) in DCM (25 mL) at room temperature *via* syringe pump over 1h. The reaction mixture turned light green over 2 h and slowly turning dark brown over 24 h. Once the addition was complete, the reaction was monitored by TLC for consumption of the diazo-azide starting material. Upon consumption of **21a**, the reaction mixture was poured in a conical flask, thoroughly dissolved in ethyl acetate (*ca.* 10 mL), dried over MgSO₄, filtered, concentrated under reduced pressure and purified by flash chromatography (Note: the crude mixture after concentration, at times, was noticeably insoluble in DCM. In this case, ethyl acetate was used as a solvent to load the sample) (silica gel, 7:3 hexanes:EtOAc), all pure fractions of **22** were concentrated together to afford a yellow oil. The oil was dissolved with generous amount of DCM (*ca.* 10 mL) and concentrated under reduced pressure. Dissolution using DCM solvent and reconcentration were repeated once more to reduce the amount of EtOAc onto the yellow oil. Then, the minimum amount of hexanes (*ca.* 1-3 mL, dropwise) was added to induce crystallization of the product (*ca.* 30-60 min), the mother liquor containing crystals of **22** was stored at -4 °C overnight to secure more crystals.

(Note: this method was also adapted for substrates bearing menthyl and 8-phenyl menthyl chiral auxiliaries. Oftentimes, the diastereomers were inseparable but for *N*-benzylindole reaction, noted in the text, partial separation of **55a** was achieved using equal volumes of 10%

EtOAc/Hexanes → 20% EtOAc/Hexanes → 30% EtOAc/Hexanes slowly added in gradient, using silica gel flash column chromatography.)

Racemic, Method B:

For scale more than 0.250 g (1.02 mmol): A solution of diazo-azide **21a** (5.00 g, 20.4 mmol) in DCM (100 mL) was added to a solution of indole (4.80 g, 40.8 mmol) and Cu(OTf)₂ (740 mg, 2.04 mmol) in DCM (100 mL) at room temperature *via* syringe pump over 1 h or manual addition over 10 min. The reaction mixture turned light green over 2 h and slowly turned darkened to afford a green solid suspended in a dark brown solution, over 24 hours. Once the addition was complete, the reaction was monitored by TLC for consumption of the diazo-azide starting material. Upon consumption of **21a**, the solid was filtered directly from the reaction mixture to afford light green needles of **22** (78-83%). Minimal amount of hot ethyl acetate was then added dropwise until the crystals were fully dissolved. The oil was allowed to cool down to room temperature before dropwise addition of cold hexanes. In some cases, after two hours, light yellow crystals of **22** began to emerge but storage at -4 °C overnight was the ideal conditions to acquire more crystals of **22**.

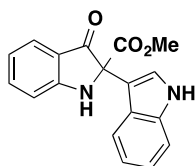
(Note: For reactions using protected indole, for example, *N*-benzyl indole and *N*-methyl indole, the crude reaction mixtures did not yield direct crystals. In these instances, the crude reaction mixture was poured in a conical flask, dried with MgSO₄, filtered and concentrated. The damp solid was added to generous amount of methanol and was brought to reflux for 5 min (solid extraction). The suspension was then cooled down to room temperature before suction filtration to afford a yellow powder. In many cases, this yellow powder was pure enough for further transformation but if the purpose of the next step was for bioactivity assay an extra

recrystallization step, to ensure high purity, was necessary. This can be done using the step described in Method A, using combination of ethyl acetate and methanol as the solvent. This procedure was also found highly scalable, using for example, 15 grams of starting material.

Asymmetric method using chiral phosphoric co-catalyst:

A solution of diazo-azide **21a** (50 mg, 0.20 mmol) in DCM (5 mL) was added to a solution of indole (46 mg, 0.40 mmol), Cu(OTf)₂ (7.3 mg, 0.02 mmol), and the chiral phosphoric acid **64d** (0.02 mmol) in DCM (5 mL) at room temperature *via* syringe pump over 1 h. The reaction mixture turned light green over 2 h and slowly turning dark brown over 24 h. Once the addition was complete, the reaction was monitored by TLC for consumption of the diazo-azide starting material. Similar to Method A, upon consumption of **21a**, the reaction mixture was poured in a conical flask, thoroughly dissolved in ethyl acetate (*ca.* 10 mL), dried over MgSO₄, filtered, concentrated under reduced pressure and purified by flash chromatography (Note: the crude mixture after concentration, at times, was noticeably insoluble in DCM. In this case, and certainly necessary, ethyl acetate was used as a solvent to load the sample onto the silica gel (silica gel, 7:3 hexanes:EtOAc). All pure fractions of **22** were concentrated together to afford a yellow oil. Upon standing for at least 24 hours, this oil slowly forms a yellow solid.

Compound 22:

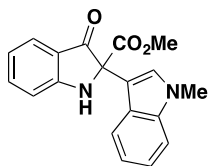


Following the Method A for the synthesis of **22**, a 0.231 g (74%) of yellow crystalline **22** was isolated after recrystallization. Concentration of mother liquor afforded another 0.056 g (21%) of

yellow/brown amorphous powder. The combined total of **22** was 0.287 g (92%) as a mixture of yellow/brown amorphous powder and crystals, m.p. = 110-111 °C (powder), m.p. = 215-216 °C (crystals) (Using (*R*)-**64d**, $[\alpha]_D^{20}$ -128.5, $c = 0.92$, acetone, 88% *ee*) $R_f = 0.15$ (yellow spot, 7:3 hexanes:EtOAc); IR (cast film) 3392, 3059, 2953, 1726, 1697, 1491, 1434, 1214, 748 cm^{-1} ; ^1H NMR (500 MHz, CDCl_3) δ 8.22 (br s, 1H), 7.70 (d, $J = 7.7$ Hz, 1H), 7.59 (d, $J = 8.3$ Hz, 1H), 7.53 (app td, $J = 8.3, 1.3$ Hz, 1H), 7.40 (d, $J = 2.4$ Hz, 1H), 7.37 (d, $J = 8.1$ Hz, 1H), 7.20 (app t, $J = 7.2$ Hz, 1H), 7.11 (app t, $J = 7.9$ Hz, 1H), 7.01 (d, $J = 8.3$ Hz, 1H), 6.93 (app t, $J = 7.7$ Hz, 1H), 5.73 (brs, 1H), 3.80 (s, 3H); ^{13}C NMR (125 MHz, CDCl_3) 193.3, 168.5, 159.5, 140.4, 136.5, 127.8, 125.3, 123.5, 122.8, 121.4, 120.5, 119.4, 115.1, 112.6, 111.7, 111.2, 73.0, 53.9; HRMS calc'd for $\text{C}_{18}\text{H}_{15}\text{N}_2\text{O}_3$ $[\text{M}+\text{H}]^+$ 307.1077, found 307.1078; HPLC: Chiralpak AD-H, 80:20, Hexanes:*i*-PrOH, rt, using (*R*)-**64d** retention time = 33.77 min (major), 37.71 min (minor).

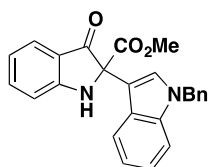
Notes: (1) The ^1H -NMR spectral characterizations were in good agreement with Jessing and Baran's previous report. The ^{13}C -NMR spectral characterizations were, however, off by 0.6 ppm in some ^{13}C NMR resonances. There were also additional three carbon resonances reported here but not with Baran's case (missing three ^{13}C signals). Similar to ^1H -NMR spectral characterizations, IR wavenumbers and melting point (powder) were likewise in good agreement. (2) The optimization table for chiral phosphoric acid catalyzed reaction was accomplished using *S*-BINOL starting material generously provided by the Hall group (200 mg), but the scope of the reaction was done using the *R* enantiomer purchased commercially from AK scientific. An *S* enantiomer was likewise purchased for comparison purposes.

Compound 31:



Isolated as yellow cubic crystals in 89% yield (using methanol as the solvent, instead of the hexanes): m.p. = 80-81 °C (powder) (reported 82 °C), m.p. = 215-216 (crystals); R_f = 0.31 (yellow spot, 7:3 hexanes:EtOAc); IR (cast film) 3366, 3051, 1744, 1702, 1616, 1485, 1293, 742 cm^{-1} ; ^1H NMR (500 MHz, CDCl_3): δ 7.73 (d, J = 7.0 Hz, 1H), 7.62 (d, J = 7.5 Hz, 1H), 7.54 (app t, J = 6.5 Hz, 1H), 7.34 (d, J = 8.0 Hz, 1H), 7.30 (d, J = 5.5 Hz, 1H), 7.27 (app t, J = 7.0 Hz, 1H), 7.14 (app t, J = 7.0 Hz, 1H), 7.00 (d, J = 8.0 Hz, 1H), 6.96 (app t, J = 6.8 Hz, 1H), 5.34 (br s, 1H), 3.84 (s, 3H), 3.77(s, 3H); ^{13}C NMR (125MHz, CDCl_3): δ 195.2, 169.1, 161.0, 137.9, 137.4, 128.0 126.0, 125.4, 122.3, 120.4, 120.0, 119.9, 119.5, 113.6, 109.8, 109.8, 72.4, 53.8, 32.9; HRMS calc'd for $\text{C}_{19}\text{H}_{17}\text{N}_2\text{O}_3$ $[\text{M}+\text{H}]^+$ 321.1234, found 321.1233; HPLC: Chiralpak AD-H, 80:20, Hexanes:*i*-PrOH, rt, using (*R*)-**64d** retention time = 26.23 min (major), 34.33 min (minor).

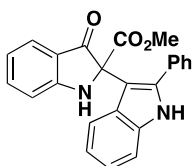
Compound 32:



Isolated as a yellow crystalline solid in 93% combined yield (77-83% yield if direct recrystallization from crude reaction mixture and using methanol as the solvent was used as a purification method): m.p. = 181-183 °C; R_f = 0.40 (yellow spot, 7:3 hexanes:EtOAc); IR (cast film) cm^{-1} ; ^1H NMR (500 MHz, CDCl_3): δ 7.72 (d, J = 7.7 Hz, 1H), 7.64 (d, J = 7.9 Hz, 1H),

7.55 (ddd, $J = 8.3, 7.2, 1.3$ Hz, 1H), 7.42 (s, 1H), 7.32 - 7.25 (m, 4H), 7.20 (app td, $J = 8.3, 1.0$ Hz, 1H), 7.15 - 7.11 (m, 3H), 7.02 (d, $J = 8.3$ Hz, 1H), 6.95 (app t, $J = 7.9$ Hz, 1H), 5.79 (br s, 1H), 5.30 (s, 2H), 3.83 (s, 3H); ^{13}C NMR (125MHz, CDCl_3): δ 194.7, 169.0, 161.0, 137.9, 137.0, 136.9, 128.8, 127.7, 127.6, 126.9, 126.3, 125.4, 122.4, 120.4, 120.2, 119.9, 119.8, 113.6, 110.5, 110.3, 72.4, 53.8, 50.4; HRMS calc'd for $\text{C}_{25}\text{H}_{20}\text{N}_2\text{O}_3\text{Na}$ $[\text{M}+\text{Na}]^+$ 419.1366, found: 419.1363. HPLC: Chiralpak AD-H, 80:20, Hexanes:*i*-PrOH, rt, using (*R*)-**64d** retention time = 26.97 min (major), 40.79 min (minor).

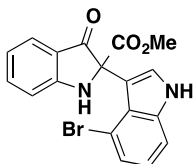
Compound 33:



Isolated as a bright yellow solid in 88% yield: $[\alpha]_{\text{D}}^{20} +75.32$ ($c = 0.51$, acetone, 56% *ee* coming from an (*S*)-**64d**); m.p. = 127 °C (decomp.); $R_f = 0.28$ (yellow spot, 7:3 hexanes:EtOAc); IR (cast film) 3360, 3062, 2950, 1710, 1617, 1487, 1239, 748 cm^{-1} ; ^1H NMR (500 MHz, CDCl_3): δ 8.29 (br s, 1H), 7.66 (br d, $J = 8.1$ Hz, 1H), 7.57 (ddd, $J = 8.4, 7.2, 1.5$ Hz, 1H), 7.48 - 7.46 (m, 2H), 7.42 - 7.37 (m, 3H), 7.35 (d, $J = 8.1$ Hz, 1H), 7.23 (d, $J = 8.3$ Hz, 1H), 7.20 (ddd, $J = 8.3, 7.2, 1.1$ Hz, 1H), 7.05 (ddd, $J = 8.3, 7.2, 1.1$ Hz, 1H), 7.00 (d, $J = 8.3$ Hz, 1H), 6.97 (app t, $J = 7.9$ Hz, 1H), 5.62 (br s, 1H), 3.24 (s, 3H); ^{13}C NMR (125MHz, CDCl_3): δ 195.1, 168.8, 160.8, 138.0, 137.9, 135.5, 132.5, 129.6, 128.8, 128.4, 126.8, 125.2, 122.7, 120.6, 120.4, 120.2, 119.7, 113.4, 111.2, 108.2, 73.3, 53.2; HRMS calc'd for $\text{C}_{24}\text{H}_{19}\text{N}_2\text{O}_3$ $[\text{M}+\text{H}]^+$ 383.1390, found 383.1385; HPLC: Chiralpak AD-H, 80:20, Hexanes:*i*-PrOH, rt, Using (*R*)-**64d**, retention time =

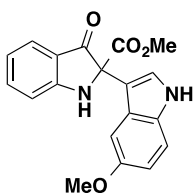
30.81 min (major), 39.72 min (minor). Using (*S*)-**64d**, retention time = 30.64 min (min), 39.84 (major).

Compound 34:



Isolated as a light green crystalline solid in 71% yield: m.p. = 241-243 °C; R_f = 0.23 (yellow spot, 7:3 hexanes:EtOAc); IR (microscope) 3365, 3006, 2953, 1726, 1706, 1610, 1488, 1219, 792 cm^{-1} ; ^1H NMR (500 MHz, d^6 - DMSO): δ 7.60 (br s, 1H), 7.55 (d, J = 7.9 Hz, 1H), 7.51 (app t, J = 8.3 Hz, 1H), 7.45 (d, J = 7.9 Hz, 1H), 7.27 (d, J = 7.5 Hz, 1H), 7.10 (d, J = 2.8 Hz, 1H), 7.06 (app t, J = 7.9 Hz, 1H), 7.04 (d, J = 8.3 Hz, 1H), 6.81 (app t, J = 7.5 Hz, 1H), 3.61 (s, 3H); ^{13}C NMR (125 MHz, d^6 - DMSO): δ 195.9, 169.9, 162.2, 138.6 (2x), 126.4, 125.1, 125.0, 124.0, 123.3, 118.9, 118.0, 114.0, 113.0, 112.1, 111.4, 72.4, 53.5; HRMS calc'd for $\text{C}_{18}\text{H}_{14}^{79}\text{BrN}_2\text{O}_3$ $[\text{M}+\text{H}]^+$ 385.0182, found 385.0182.

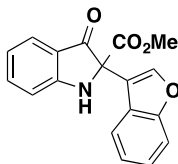
Compound 35:



Isolated as a bright yellow crystals in 78% yield: m.p. = 186-188 °C; R_f = 0.11 (yellow spot, 7:3 hexanes:EtOAc); IR (cast film) 3301, 3060, 2947, 1742, 1685, 1487, 1232, 1218, 756 cm^{-1} ; ^1H NMR (500 MHz, CDCl_3): δ 8.19 (br s, 1H), 7.74 (dd, J = 7.9, 0.6 Hz, 1H), 7.56 (app td, J = 8.3, 1.3 Hz, 1H), 7.38 (d, J = 2.6 Hz, 1H), 7.30 – 7.26 (m, 2H), 7.06 - 7.04 (m, 2H), 6.98 (app t, J = 7.2 Hz, 1H), 6.89 (dd, J = 8.8, 2.4 Hz, 1H), 5.71 (br s, 1H), 3.81 (s, 3H), 3.77 (s, 3H); ^{13}C NMR

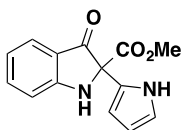
(125MHz, CDCl₃): δ 194.9, 169.0, 161.0, 154.4, 137.9, 131.7, 125.8, 125.4, 124.3, 120.4, 120.0, 113.5, 112.7, 112.3, 111.2, 101.5, 72.4, 55.8, 53.7; HRMS calc'd for C₁₉H₁₇N₂O₄ [M+H]⁺ 337.1183, found 337.1185.

Compound 37:



Isolated as a yellow oil in 46% yield: R_f = 0.40 (yellow spot, 7:3 hexanes:EtOAc); IR (cast film) 3363, 3065, 2954, 1748, 1711, 1617, 1488, 1242, 751 cm⁻¹; ¹H NMR (500 MHz, CDCl₃): δ 7.69 (d, J = 7.9 Hz, 1H), 7.55 (dd, J = 7.7, 0.6 Hz, 1H), 7.54 (ddd, J = 8.3, 7.2, 1.3 Hz, 1H), 7.45 (dd, J = 8.1, 0.6 Hz, 1H), 7.28 (app td, J = 7.2, 1.3 Hz, 1H), 7.21 (app td, J = 7.9, 1.1 Hz, 1H), 7.03 (d, J = 8.3 Hz, 1H), 6.95 (overlapped app td, J = 7.7, 0.6 Hz, 1H), 6.94 (overlapped s, 1H), 5.74 (br s, 1H), 3.85 (s, 3H); ¹³C NMR (125MHz, CDCl₃): δ 191.3, 166.6, 161.2, 155.0, 150.9, 138.2, 127.7, 125.7, 124.9, 123.1, 121.6, 120.8, 119.3, 113.7, 111.3, 105.6, 71.9, 54.2; HRMS calc'd for C₁₈H₁₃NO₄Na [M+Na]⁺ 330.0737, found 330.0739.

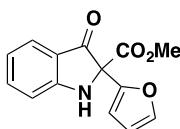
Compound 38:



Isolated as a yellow oil in 68% yield: R_f = 0.34 (yellow spot, 7:3 hexanes:EtOAc); IR (cast film) 3426, 3390, 3056, 2954, 1726, 1697, 1488, 1233, 751 cm⁻¹; ¹H NMR (500 MHz, CDCl₃): δ 9.43

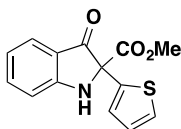
(br s, 1H), 7.63 (d, $J = 7.9$ Hz, 1H), 7.56 (app td, $J = 7.5, 1.5$ Hz, 1H), 7.09 (d, $J = 7.5$ Hz, 1H), 6.94 (app td, $J = 7.2, 0.7$ Hz, 1H), 6.87 (app td, $J = 2.6, 1.7$ Hz, 1H), 6.33 (ddd, $J = 3.5, 2.7, 1.7$ Hz, 1H), 6.19 – 6.14 (m, 1H), 5.68 (br s, 1H), 3.84 (s, 3H); ^{13}C NMR (125MHz, CDCl_3): δ 193.2, 167.6, 161.6, 138.0, 125.8, 124.8, 120.7, 119.2, 118.8, 113.6, 112.3, 108.2, 106.3, 71.8, 53.9; HRMS calc'd for $\text{C}_{14}\text{H}_{13}\text{N}_2\text{O}_3$ $[\text{M}+\text{H}]^+$ 257.0921, found 257.0915.

Compound 39:



Isolated as a yellow oil in 48% yield: $R_f = 0.37$ (yellow spot, 7:3 hexanes:EtOAc); IR (cast film) 3362, 3125, 2954, 1748, 1710, 1617, 1488, 1233, 751 cm^{-1} ; ^1H NMR (500 MHz, CDCl_3): δ 7.69 (d, $J = 7.2$ Hz, 1H), 7.55 (app td, $J = 7.2, 0.9$ Hz, 1H), 7.44 (dd, $J = 1.8, 0.9$ Hz, 1H), 7.03 (d, $J = 8.3$ Hz, 1H), 6.96 (app t, $J = 7.7$ Hz, 1H), 6.56 (d, $J = 3.3$ Hz, 1H), 6.42 (dd, $J = 3.3, 1.9$ Hz, 1H), 5.66 (br s, 1H), 3.86 (s, 3H); ^{13}C NMR (125MHz, CDCl_3): δ 191.8, 166.9, 161.1, 148.4, 143.3, 138.1, 125.7, 120.7, 119.3, 113.6, 110.7, 108.8, 106.3, 71.7, 54.1; HRMS calc'd for $\text{C}_{14}\text{H}_{12}\text{NO}_4$ $[\text{M}+\text{H}]^+$ 258.0761, found 258.0764.

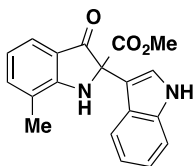
Compound 40:



Isolated as a yellow oil in 41% yield: $R_f = 0.42$ (7:3 hexanes:EtOAc); IR (cast film) 3360, 3071, 2952, 1747, 1709, 1616, 1486, 1231, 754 cm^{-1} ; ^1H NMR (500 MHz, CDCl_3): δ 7.62 (ddd, $J = 7.2,$

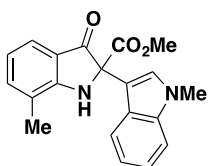
1.4, 0.7 Hz, 1H), 7.54 (ddd, $J = 8.4, 7.2, 1.4$ Hz, 1H), 7.49 (dd, $J = 3.7, 1.3$ Hz, 1H), 7.24 (dd, $J = 5.1, 1.3$ Hz, 1H), 7.07 (d, $J = 8.3$ Hz, 1H), 7.03 (dd, $J = 5.1, 3.7$ Hz, 1H), 6.95 (app td, $J = 7.9, 0.7$ Hz, 1H), 5.79 (br s, 1H), 3.85 (s, 3H); ^{13}C NMR (125MHz, CDCl_3): δ 192.2, 167.4, 160.9, 148.4, 138.8, 137.9, 127.6, 125.9, 125.7, 125.5, 121.1, 119.0, 113.7, 73.4, 54.1; HRMS calc'd for $\text{C}_{14}\text{H}_{12}\text{NSO}_3$ $[\text{M}+\text{H}]^+$ 274.0532, found 274.0536.

Compound 41:



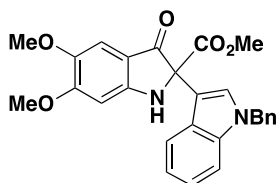
Isolated as a yellow powder in 86% yield: m.p. = 191-193 °C; $R_f = 0.16$ (yellow spot, 7:3 hexanes:EtOAc); IR(cast film) 3371, 3057, 2952, 1739, 1702, 1608, 1459, 1238, 745 cm^{-1} ; ^1H NMR (500 MHz, CDCl_3): δ 8.40 (br s, 1H), 7.58-7.55 (m, 2H), 7.37-7.31 (m, 3H), 7.18 (ddd, $J = 7.9, 7.0, 1.2$ Hz, 1H), 7.10 (ddd, $J = 8.1, 7.1, 1.0$ Hz, 1H), 6.89 (app t, $J = 7.5$ Hz, 1H), 5.53 (br s, 1H), 3.79 (s, 3H), 2.30 (s, 3H); ^{13}C NMR (125MHz, CDCl_3) δ 195.2, 169.2, 160.3, 138.0, 136.6, 125.5, 123.7, 122.8 (2x), 122.7, 120.6, 120.4, 119.5 (2x), 111.8, 111.7, 72.6, 53.8, 15.8; HRMS calc'd for $\text{C}_{19}\text{H}_{17}\text{N}_2\text{O}_3$ $[\text{M}+\text{H}]^+$ 321.1234, found: 321.1233; HPLC: Chiralpak AD-H, 80:20, Hexanes:*i*-PrOH, rt, Using (*R*)-**64d**, retention time = 11.84 min (major), 22.80 min (minor).

Compound 42:

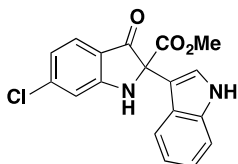


Isolated as yellow crystals in 84% yield (using methanol as the solvent for recrystallization): m.p. = 170-171 °C; R_f = 0.35 (yellow spot, 7:3 hexanes:EtOAc); IR(cast film) 3359, 3055, 2950, 1746, 1705, 1608, 1460, 1241, 743 cm^{-1} ; ^1H NMR (500 MHz, CDCl_3) δ 7.61 (app t, J = 8.2 Hz, 2H), 7.39-7.26 (m, 4H), 7.15 (app t, J = 7.9 Hz, 1H), 6.91 (app t, J = 7.3 Hz, 1H), 5.58 (brs, 1H), 3.84 (s, 3H), 3.79 (s, 3H), 2.33 (s, 3H); ^{13}C NMR (125MHz, CDCl_3) δ 195.2, 169.2, 160.2, 137.9, 137.4, 128.1, 126.1, 122.8, 122.7, 122.2, 120.5, 119.9, 119.5, 119.5, 110.0, 109.8, 72.5, 53.8, 32.9, 15.8; HRMS calc'd for $\text{C}_{20}\text{H}_{19}\text{N}_2\text{O}_3$ $[\text{M}+\text{H}]^+$ 335.1390, found: 335.1388.

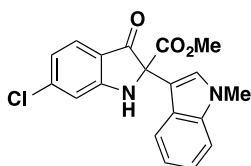
Compound 43:



Isolated as a yellow powder in 94% yield (using methanol as the solvent for recrystallization): m.p. = 184-186 °C; R_f = 0.16 (7:3 hexanes:EtOAc); IR(cast film) 3349, 3015, 2942, 1748, 1712, 1623, 1451, 1239, 731 cm^{-1} ; ^1H NMR (500 MHz, CDCl_3) δ 7.61 (d, J = 7.8 Hz, 1H), 7.60 (s, 1H), 7.28-7.09 (m, 9H), 6.48 (brs, 1H), 5.28 (s, 2H), 3.92 (s, 3H), 3.87 (s, 3H), 3.82 (s, 3H); ^{13}C NMR (125MHz, CDCl_3) δ 192.7, 169.4, 158.9 (2x), 145.2, 136.9 (2x), 128.7, 127.6, 126.8, 126.4, 122.3, 120.1, 119.5, 111.5, 110.8, 110.3, 104.5, 95.8, 73.0, 56.3, 56.2, 53.7, 50.3; HRMS calc'd for $\text{C}_{27}\text{H}_{25}\text{N}_2\text{O}_3$ $[\text{M}+\text{H}]^+$ 457.1685, found: 457.1683.

Compound 44:

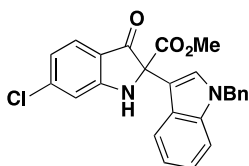
Isolated as a yellow powder in 89% yield: m.p. = 236-238 °C; Using (*R*)-**64d**, $[\alpha]_{\text{D}}^{20}$ -147.8, $c = 0.81$, acetone, 86% *ee*; $R_f = 0.19$ (yellow spot, 7:3 hexanes:EtOAc); IR (cast film) 3364, 3052, 2952, 1746, 1711, 1610, 1242, 741 cm^{-1} ; ^1H NMR (500 MHz, CDCl_3): δ 8.21 (brs, 1H), 7.61 (d, $J = 8.3$ Hz, 1H), 7.55 (d, $J = 8.1$ Hz, 1H), 7.40 – 7.37 (m, 2H), 7.22 (app t, $J = 7.7$ Hz, 1H), 7.12 (app t, $J = 8.1$ Hz, 1H), 7.00 (d, $J = 1.1$ Hz, 1H), 6.90 (dd, $J = 8.3, 1.7$ Hz, 1H), 5.77 (brs, 1H), 3.81 (s, 3H); ^{13}C NMR (125MHz, CDCl_3) δ 193.2, 168.6, 161.2, 144.5, 136.5, 126.5, 125.3, 123.5, 122.9, 121.2, 120.6, 119.4, 118.3, 113.4, 111.7, 111.3, 72.8, 53.9; HRMS calc'd for $\text{C}_{18}\text{H}_{13}^{35}\text{ClN}_2\text{O}_3\text{Na}$ $[\text{M}+\text{Na}]^+$ 363.0507, found: 363.0508. Using (*R*)-**64d** HPLC: Chiralpak AD-H, 80:20, Hexanes:*i*-PrOH, rt, retention time = 22.33 min (major), 29.20 min (minor).

Compound 45:

Isolated as bright yellow crystals in 76% yield (using methanol as the solvent for recrystallization): m.p. = 194-195°C; $R_f = 0.35$ (7:3 hexanes:EtOAc); IR (cast film) 3364, 3052, 2952, 1746, 1711, 1610, 1242, 741 cm^{-1} ; ^1H NMR (500 MHz, CDCl_3): δ 7.61 (d, $J = 8.0$ Hz, 1H), 7.52 (ddd, $J = 8.0, 1.8, 1.0$ Hz, 1H), 7.31 (ddd, $J = 8.3, 1.8, 1.1$ Hz, 1H), 7.26-7.22 (m, 2H),

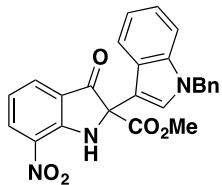
7.10 (ddd, $J = 8.1, 7.0, 1.1$ Hz, 1H), 6.99 (dd, $J = 1.7, 0.5$ Hz, 1H), 6.89 (dd, $J = 8.3, 1.7$ Hz, 1H) 5.80 (brs, 1H), 3.81 (s, 3H), 3.75 (s, 3H); ^{13}C NMR (125MHz, CDCl_3) δ 193.3, 168.6, 161.1, 144.5, 137.3, 128.0, 126.4, 125.8, 122.3, 121.1, 120.1, 119.3, 118.1, 113.3, 109.8, 109.3, 72.7, 53.9, 32.9; HRMS calc'd for $\text{C}_{19}\text{H}_{16}^{35}\text{ClN}_2\text{O}_3$ $[\text{M}+\text{H}]^+$ 355.0844, found: 355.0846.

Compound 46:



Isolated as a bright yellow crystals in 90% yield (80% yield from direct recrystallization of crude and using methanol as the solvent for recrystallization): m.p. = 174-175 °C; $R_f = 0.42$ (yellow spot, 7:3 hexanes:EtOAc); IR (cast film) 3364, 3052, 2952, 1746, 1711, 1610, 1242, 741 cm^{-1} ; ^1H NMR (500 MHz, CDCl_3): δ 7.62 (app t, $J = 8.3$ Hz, 2H), 7.40 (s, 1H), 7.31-7.26 (m, 4H), 7.20 (app td, $J = 7.0, 0.9$ Hz, 1H), 7.14-7.11 (m, 3H), 6.97 (d, $J = 1.7$ Hz, 1H), 6.89 (dd, $J = 8.3, 1.7$ Hz, 1H) 5.96 (brs, 1H), 5.26 (s, 2H), 3.81 (s, 3H); ^{13}C NMR (125MHz, CDCl_3) δ 193.3, 168.6, 161.1, 144.4, 136.9, 136.8, 128.8, 127.7, 127.6, 126.8, 126.4, 126.1, 122.5, 120.9, 120.2, 119.7, 118.0, 113.2, 110.4, 110.0, 72.8, 53.8, 50.3; HRMS calc'd for $\text{C}_{25}\text{H}_{19}^{35}\text{ClN}_2\text{NaO}_3$ $[\text{M}+\text{Na}]^+$ 453.0976, found: 453.0984.

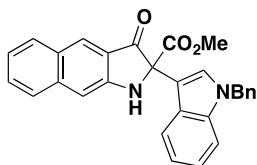
Compound 47:



Partial characterization:

Isolated as a light yellow solid in *ca.* 14% yield (with trace impurity from EtOAc and water): $R_f = 0.24$ (yellow spot, 7:3 hexanes:EtOAc); IR (cast film) 3324, 3048, 2956, 1738, 1714, 1610, 1251, 731 cm^{-1} ; ^1H NMR (500 MHz, CDCl_3): δ 8.38 (dd, $J = 8.2, 1.2$ Hz, 1H), 8.01 (s, 1H), 8.00-7.98 (m, 2H), 7.56 (dd, $J = 8.1, 1.0$ Hz, 1H), 7.38 (brs, 1H), 7.29-7.12 (m, 5H), 6.95 (dd, $J = 8.2, 7.3$ Hz, 1H), 5.30 (s, 2H), 5.26 (s, 2H), 3.83 (s, 3H); LC-MS calc'd for $\text{C}_{25}\text{H}_{19}\text{N}_3\text{O}_5$ $[\text{M}+\text{H}]^+$ 442.1, found: 442.1.

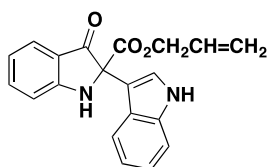
Compound 48:



Isolated as an orange oil in 96% yield: $R_f = 0.47$ (orange spot, 7:3 hexanes:EtOAc); IR (cast film) 3359, 3055, 2950, 1746, 1705, 1608, 1460, 1241, 743 cm^{-1} ; ^1H NMR (500 MHz, CDCl_3) δ 8.29 (s, 1H), 7.84 (d, $J = 8.3$ Hz, 1H), 7.67 (d, $J = 8.4$ Hz, 1H), 7.64 (d, $J = 8.1$ Hz, 1H), 7.48 (ddd, $J = 8.1, 6.8, 1.1$ Hz, 1H), 7.42 (s, 1H), 7.29-7.23 (m, 6H), 7.17 (app t, $J = 8.1$ Hz, 1H), 7.11 (dd, $J = 8.0, 1.5$ Hz, 2H), 7.08 (app td, $J = 8.1, 7.2$ Hz, 1H), 5.76 (br s, 1H), 5.27 (s, 2H), 3.81 (s, 3H); ^{13}C NMR (125MHz, CDCl_3) δ 195.7, 169.3, 153.7, 139.9, 137.1, 136.9, 130.8, 129.6, 128.8,

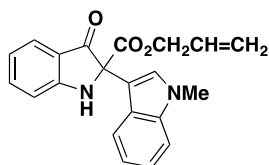
128.6, 127.7, 127.6, 127.2, 126.9, 126.7, 126.2, 123.7, 122.4, 121.8, 120.2, 120.1, 110.8, 110.3, 107.0, 72.7, 53.7, 50.4; HRMS calc'd for C₂₉H₂₂N₂O₃Na [M+Na]⁺ 469.1523, found: 447.1530.

Compound 49:



Isolated as a yellow powder in 81% yield: m.p. = 158-159 °C; *R_f* = 0.19 (yellow spot, 7:3 hexanes:EtOAc); IR (cast film) 3368, 3055, 2919, 1732, 1711, 1635, 1491, 1225, 757 cm⁻¹; ¹H NMR (500 MHz, CDCl₃): δ 8.36 (br s, 1H), 7.69 (ddd, *J* = 7.8, 1.3, 0.7 Hz, 1H), 7.57 (d, *J* = 8.1 Hz, 1H), 7.52 (ddd, *J* = 8.4, 7.1, 1.4 Hz, 1H), 7.32 (d, *J* = 1.3 Hz, 1H), 7.30 (app t, *J* = 1.0 Hz, 1H), 7.17 (ddd, *J* = 8.3, 7.1, 1.3 Hz, 1H), 7.08 (ddd, *J* = 8.2, 7.1, 1.2 Hz, 1H), 6.98 (dt, *J* = 8.3, 0.7 Hz, 1H), 6.93 (ddd, *J* = 7.9, 7.1, 0.9 Hz, 1H), 5.84 (tdd, *J* = 5.6, 10.5, 17.2 Hz, 1H), 5.83 (brs, 1H), 5.23 (tdd, *J* = 1.5, 1.5, 17.2 Hz, 1H), 5.16 (tdd, *J* = 1.3, 1.3, 10.5 Hz, 1H), 4.69 (tdd, *J* = 1.3, 5.6, 13.2 Hz, 2H); ¹³C NMR (125MHz, CDCl₃): δ 194.8, 168.2, 161.1, 137.9, 136.5, 131.1, 125.4 (2x), 123.8, 122.6, 120.3 (2x), 119.8, 119.6, 119.2, 113.5, 111.7, 111.3, 72.6, 67.2; HRMS calc'd for C₂₀H₁₇N₂O₃ [M+H]⁺ 333.1234, found: 333.1232.

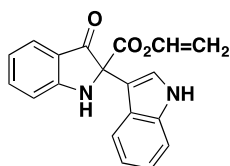
Compound 50:



Isolated as a yellow crystals in 83% yield (using methanol as the solvent for recrystallization): m.p. = 148-150 °C; *R_f* = 0.36 (yellow spot, 7:3 hexanes:EtOAc); IR (cast film) 3371, 3051, 2919,

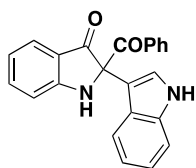
1742, 1703, 1615, 1485, 1225, 743 cm^{-1} ; ^1H NMR (500 MHz, CDCl_3): δ 7.72 (d, $J = 7.8$ Hz, 1H), 7.63 (d, $J = 8.1$ Hz, 1H), 7.52 (ddd, $J = 8.3, 7.1, 1.3$ Hz, 1H), 7.32-7.30 (m, 2H), 7.26 (ddd, $J = 8.2, 7.0, 1.1$ Hz, 1H), 7.12 (ddd, $J = 8.0, 7.0, 1.1$ Hz, 1H), 6.99 (d, $J = 8.2$ Hz, 1H), 6.94 (app t, $J = 7.8$ Hz, 1H), 5.88 (ddt, $J = 17.2, 10.5, 5.6$ Hz, 1H), 5.83 (brs, 1H), 5.29 (ddt, $J = 17.2, 1.5, 1.5$ Hz, 1H), 5.22 (ddt, $J = 10.4, 1.2, 1.2$ Hz, 1H), 4.73 (ddt, $J = 13.2, 5.6, 1.3$ Hz, 2H), 3.73 (s, 3H); ^{13}C NMR (125MHz, CDCl_3): δ 194.7, 168.3, 161.0, 137.8, 137.4, 131.2, 128.1, 126.0, 125.4, 122.2, 120.2, 119.9(2x), 119.8, 119.1, 113.5, 109.8, 109.7, 72.5, 67.1, 32.9; HRMS calc'd for $\text{C}_{21}\text{H}_{19}\text{N}_2\text{O}_3$ $[\text{M}+\text{H}]^+$ 347.1390, found: 347.1393.

Compound 51:



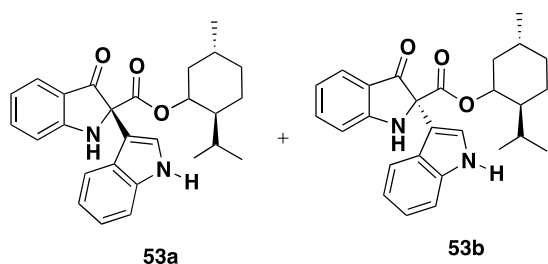
Isolated as a yellow powder in 73% yield: m.p. = 193-195 $^{\circ}\text{C}$; $R_f = 0.21$ (yellow spot, 7:3 hexanes:EtOAc); IR (cast film) 3351, 3011, 2915, 1738, 1712, 1635, 1465, 1233, 758 cm^{-1} ; ^1H NMR (500 MHz, CDCl_3): δ 8.25 (br s, 1H), 7.70 (d, $J = 8.0$ Hz, 1H), 7.60 (dd, $J = 8.1, 0.9$ Hz, 1H), 7.54 (ddd, $J = 8.3, 7.2, 1.4$ Hz, 1H), 7.43 (d, $J = 2.7$ Hz, 1H), 7.37 (app dt, $J = 8.2, 0.8$ Hz, 1H), 7.25 (dd, $J = 13.9, 6.2$ Hz, 1H), 7.20 (ddd, $J = 8.2, 7.2, 1.1$ Hz, 1H), 7.10 (ddd, $J = 8.2, 7.2, 1.0$ Hz, 1H), 7.01 (d, $J = 8.3$ Hz, 1H), 6.94 (app t, $J = 7.8$ Hz, 1H), 5.68 (brs, 1H), 4.99 (dd, $J = 13.9, 2.0$ Hz, 1H), 4.66 (dd, $J = 6.1, 2.0$ Hz, 1H); ^{13}C NMR (125MHz, CDCl_3): δ 194.0, 165.8, 160.9, 141.3 (2x), 138.0, 136.5, 125.5, 125.3, 123.7, 122.8, 120.5 (2x), 119.7, 119.6, 113.5, 111.6, 111.0, 100.0, 72.1; HRMS calc'd for $\text{C}_{19}\text{H}_{14}\text{N}_2\text{O}_3\text{Na}$ $[\text{M}+\text{Na}]^+$ 318.1004, found: 318.1007.

Compound 52:



Isolated as bright yellow crystals in 37% yield: m.p. = 215-216 °C; R_f = 0.20 (yellow spot, 7:3 hexanes:EtOAc); IR (cast film) 3364, 3052, 2952, 1711, 1610, 1242, 741 cm^{-1} ; ^1H NMR (500 MHz, CDCl_3): δ 8.43 (brs, 1H), 8.15 (d, J = 7.3 Hz, 2H), 7.66 (d, J = 7.7 Hz, 1H), 7.52 (app t, J = 8.3 Hz, 1H), 7.43 (app t, J = 7.4 Hz, 1H), 7.39 (d, J = 8.0 Hz, 1H), 7.34 (d, J = 8.1 Hz, 1H), 7.30-7.27 (m, 3H), 7.17 (app t, J = 7.2 Hz, 1H), 7.06 (app t, J = 7.2 Hz, 1H), 7.03 (d, J = 8.2 Hz, 1H), 6.92 (app t, J = 7.2 Hz, 1H), 6.25 (brs, 1H); ^{13}C NMR (125MHz, CDCl_3) δ 195.2, 193.5, 161.2, 137.9, 136.5, 134.2, 133.3, 131.4, 127.9, 125.6, 125.3, 123.2, 122.9, 120.7, 120.6, 120.4, 119.3, 114.0, 113.9, 111.6, 79.1; HRMS calc'd for $\text{C}_{23}\text{H}_{16}\text{N}_2\text{O}_2\text{Na}$ $[\text{M}+\text{Na}]^+$ 375.1104, found: 375.1109.

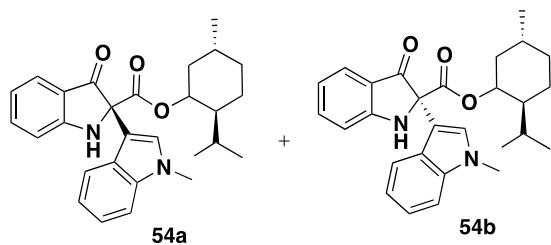
Compound 53:



Isolated as bright yellow powder in 81% yield (*ca.* 1.3:1 of **53a**:**53b**, characterized as mixture of diastereomers): R_f = 0.21 (yellow spot, 7:3 hexanes:EtOAc); IR (cast film) 3362, 3051, 2955, 1705, 1618, 1242, 739 cm^{-1} ; ^1H NMR (500 MHz, CDCl_3): δ 8.26 (br s, 1H, major), 8.24 (br s, 1H, minor), 7.70 (dddd, J = 7.8, 1.4, 0.6, 0.6 Hz, 1H, minor), 7.69 (dddd, J = 7.8, 1.4, 0.7, 0.7 Hz, 1H, major), 7.61 – 7.60 (m, 1H, minor), 7.59 – 7.58 (m, 1H, major), 7.51 (ddd, J = 8.3, 7.2, 1.4,

1H), 7.50 (ddd, $J = 8.3, 7.2, 1.4$, 1H), 7.38 (d, $J = 2.7$ Hz, 1H, minor), 7.37 (d, $J = 2.7$ Hz, 1H, major), 7.34 (ddd, $J = 8.2, 0.9, 0.9$ Hz, 1H), 7.33 (ddd, $J = 8.1, 0.9, 0.9$ Hz, 1H), 7.19 – 7.15 (overlapping peaks, 2H), 7.09 (ddd, $J = 8.1, 7.1, 1.1$ Hz, 1H), 7.06 (ddd, $J = 8.1, 7.1, 1.0$ Hz, 1H), 7.00 (dd, $J = 0.7, 0.7$ Hz, 1H), 6.99 (dd, $J = 0.8, 0.8$ Hz, 1H), 6.93 (ddd, $J = 7.1, 0.9, 0.9$ Hz, 1H), 6.92 (ddd, $J = 7.1, 0.9, 0.9$ Hz, 1H), 5.76 (br s, 1H, minor), 5.65 (br s, 1H, major) 4.77 (ddd, $J = 10.9, 10.9, 4.3$ Hz, 1H, major), 4.72 (ddd, $J = 11.0, 11.0, 4.4$ Hz, 1H, minor), 1.96 – 1.92 (overlapping peaks, 2H), 0.86 (d, $J = 6.5$ Hz, 3H, minor), 0.84 (d, $J = 6.5$ Hz, 3H, major), 0.82 (d, $J = 7.0$ Hz, 3H, major), 0.64 (d, $J = 6.9$ Hz, 3H, major), 0.51 (d, $J = 7.1$ Hz, 3H, minor), 0.43 (d, $J = 6.9$ Hz, 3H, minor) (Note: some aliphatic protons could not be properly assigned due to extensive overlap); ^{13}C NMR (125MHz, CDCl_3) δ 194.8, 194.6, 168.0 (2x), 161.2, 161.0, 137.7, 137.6, 136.6, 136.5, 125.7, 125.6, 125.4, 125.3, 123.7, 123.4, 122.6 (2x), 120.3, 120.2 (2x), 120.1 (3x), 120.0, 119.6, 113.7, 113.5, 111.9, 111.8, 111.5 (2x), 77.5, 77.4, 72.8, 72.7, 46.8, 46.7, 40.3, 40.2, 34.1 (2x), 31.5, 25.8, 25.5, 23.2, 23.0, 22.0, 20.8, 20.4, 15.9, 15.7; HRMS calc'd for $\text{C}_{27}\text{H}_{31}\text{N}_2\text{O}_3$ $[\text{M}+\text{H}]^+$ 431.2329, found: 431.2332; HPLC: Chiralpak AD-H, 80:20, Hexanes:*i*-PrOH, rt, retention time = 10.17 min (minor), 25.95 min (major).

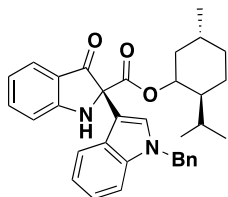
Compound 54:



Isolated as bright yellow powder in 79% yield (*ca.* 2.3:1 of **54a**:**54b**, characterized as mixture of diastereomers): $R_f = 0.33$ (yellow spot, 7:3 hexanes:EtOAc); IR (cast film) 3362, 3051, 2955, 1704, 1618, 1242, 740 cm^{-1} ; ^1H NMR (500 MHz, CDCl_3): δ 7.70 – 7.67 (overlapping peaks, 2H),

7.59 (ddd, $J = 8.0, 0.9, 0.9$ Hz, 1H, minor), 7.58 (ddd, $J = 8.0, 1.0, 1.0$ Hz, 1H, major), 7.51 (ddd, $J = 8.3, 7.1, 1.3$ Hz, 1H), 7.50 (ddd, $J = 8.4, 7.2, 1.4$, 1H), 7.29 – 7.26 (overlapping peaks, 4H), 7.23 – 7.19 (overlapping peaks, 2H), 7.09 (ddd, $J = 8.1, 7.1, 1.0$ Hz, 1H, minor), 7.06 (ddd, $J = 8.1, 7.1, 1.1$ Hz, major), 7.00 – 6.98 (overlapping peaks, 2H), 6.93 – 6.90 (overlapping peaks, 2H), 5.76 (brs, 1H, minor), 5.65 (brs, 1H, major), 4.77 (ddd, $J = 10.8, 10.8, 4.3$ Hz, 1H, major), 4.73 (ddd, $J = 10.9, 10.9, 4.4$ Hz, 1H, minor), 3.75 (s, 3H), 3.74 (s, 3H), 1.96 – 1.91 (overlapping peaks, 2H), 1.85 (sepd, $J = 7.1, 2.9$ Hz, 1H, major), 1.19 (sepd, $J = 7.0, 2.9$ Hz, minor), 0.87 (d, $J = 6.6$ Hz, 3H), 0.86 (d, $J = 6.6$ Hz, 3H), 0.83 (d, $J = 7.0$ Hz, 3H), 0.64 (d, $J = 7.0$ Hz, 3H), 0.52 (d, $J = 7.0$ Hz, 3H), 0.44 (d, $J = 6.9$ Hz, 3H) (Note: some aliphatic protons could not be properly assigned due to extensive overlap); ^{13}C NMR (125MHz, CDCl_3) δ 194.9, 194.7, 168.1, 168.0, 161.2, 160.9, 137.7, 137.6, 137.3 (2x), 128.1, 127.9, 126.2, 126.0, 125.4, 125.3, 122.1 (2x), 120.2 (2x), 120.0 (3x), 119.7 (3x), 113.7, 113.5, 110.1, 110.0, 109.6, 109.5, 77.4, 77.3, 72.8, 72.7, 46.7, 46.6, 40.3, 40.2, 34.1 (2x), 32.9 (2x), 31.4, 25.7, 25.4, 23.1, 23.0, 21.9, 20.8, 20.4, 15.9, 15.7; HRMS calc'd for $\text{C}_{28}\text{H}_{32}\text{N}_2\text{O}_3$ $[\text{M}+\text{H}]^+$ 445.2486, found: 445.2492; HPLC: Chiralpak AD-H, 80:20, Hexanes:i-PrOH, rt, retention time = 25.67 min (major), 31.44 min (minor).

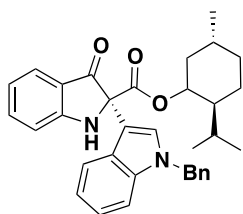
Compound 55a:



Major diastereomer **55a** (partially isolated as green needles): $R_f = 0.42$ (yellow spot, 7:3 hexanes:EtOAc); $[\alpha]_D^{20} : +23.76$ ($c = 1.01$, DCM); IR (cast film) cm^{-1} ; ^1H NMR (500 MHz, CDCl_3): δ 7.68 (d, $J = 7.8$ Hz, 1H), 7.62 (d, $J = 8.8$ Hz, 1H), 7.52 (ddd, $J = 8.3, 7.2, 1.3$, 1H),

7.39 (s, 1H), 7.30-7.22 (m, 4H), 7.14 (ddd, $J = 8.2, 7.1, 1.1$, 1H), 7.13-7.11 (m, 2H), 7.06 (ddd, $J = 8.1, 7.1, 1.0$, 1H), 7.01 (d, $J = 8.2$ Hz, 1H), 6.92 (app t, $J = 7.8$ Hz, 1H), 5.66 (br s, 1H), 5.28 (app br s, 2H), 4.75 (ddd, $J = 11.0, 11.0, 4.4$ Hz, 1H), 1.91-1.88 (m, 1H), 1.81 (sepd, $J = 7.0, 2.9$ Hz, 1H), 1.66-1.61 (m, 2H), 1.45-1.39 (m, 2H), 1.03-0.96 (m, 1H), 0.88 (app td, $J = 12.2, 11.0$ Hz, 1H) 0.87-0.70 (m, 1H), 0.84 (d, $J = 6.6$ Hz, 3H), 0.81 (d, $J = 7.0$ Hz, 3H), 0.62 (d, $J = 7.0$ Hz, 3H); ^{13}C NMR (125MHz, CDCl_3) δ 194.8, 167.9, 161.0, 137.6, 137.1, 137.0, 128.8, 127.7, 127.6, 127.0, 126.3, 125.4, 122.3, 120.3, 120.2, 120.1, 120.0, 113.5, 110.7, 110.1, 77.4, 72.8, 50.3, 46.8, 40.2, 34.1, 31.4, 25.8, 23.2, 22.0, 20.7, 15.9; HRMS calc'd for $\text{C}_{34}\text{H}_{37}\text{N}_2\text{O}_3$ $[\text{M}+\text{H}]^+$ 521.2799, found: 521.2810.

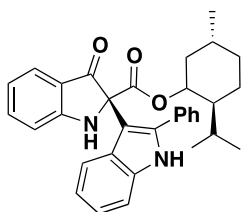
Compound 55b



Minor diastereomer (partial assignment was made based on deduction, using the spectra of the mixture of diastereomers and the spectra of the major diastereomer, multiplicity of some peaks could not be properly assigned due to substantial overlap): H NMR (500 MHz, CDCl_3): δ 7.68 (d, $J = 7.8$ Hz, 1H), 7.65 (d, $J = 7.6$ Hz, 1H), 7.51 (ddd, $J = 8.4, 7.2, 1.3$ Hz, 1H), 7.41 (s, 1H), 7.30 – 7.22 (m, 4H), 7.15 (app t, $J = 7.2$ Hz, 1H), 7.12 – 7.11 (m, 3H), 7.02 (d, $J = 8.16$ Hz, 1H, 1H), 6.92 (app t, $J = 7.8$ Hz, 1H), 5.80 (br s, 1H), 5.28 (app br s, 2H), 4.72 (ddd, $J = 11.0, 10.9, 4.4$ Hz, 1H), 1.95 – 1.92 (m, 1H), 1.66 – 1.55 (m, 2H), 1.47 – 1.33 (m, 2H), 1.15 (sepd, $J = 6.9, 2.9$ Hz, 1H), 0.87 (d, $J = 6.6$ Hz, 3H), 0.48 (d, $J = 7.0$ Hz, 3H), 0.40 (d, $J = 6.9$ Hz, 3H) (Note: three other protons on the aliphatic region could not be properly assigned due to extensive overlap); ^{13}C NMR (125MHz, CDCl_3) δ 194.5, 168.1, 161.2, 137.7, 137.2, 136.9, 128.8, 127.7, 127.4,

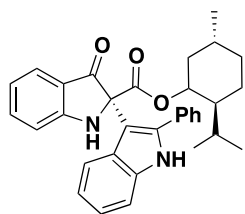
126.7, 126.5, 125.4, 122.3, 120.3, 120.2, 120.0, 113.7, 110.9, 110.1, 77.4, 72.7, 50.3, 46.7, 40.3, 34.1, 31.4, 25.5, 23.0, 22.0, 20.4, 15.7 (Note: one resonance ^{13}C was missing and could not be properly assigned due to extensive overlap).

Compound 56a:



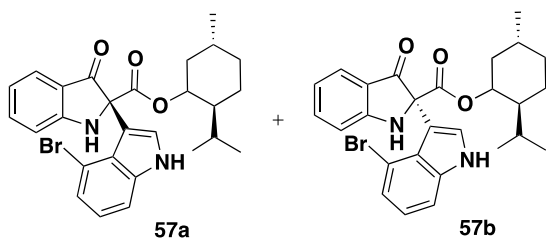
Major diastereomer **55a** (yellow solid, partially enriched 93:7 *dr*): $R_f = 0.30$ (yellow spot, 7:3 hexanes:EtOAc); IR (cast film) cm^{-1} ; ^1H NMR (500 MHz, CDCl_3): δ 8.16 (brs, 1H), 7.58 (d, $J = 7.8$ Hz, 1H), 7.50-7.47 (m, 2H), 7.44-7.42 (m, 2H), 7.36-7.29 (m, 4H), 7.16 (ddd, $J = 8.2, 7.1, 1.1$ Hz, 1H), 7.04 (ddd, $J = 8.2, 7.1, 1.1$ Hz, 1H), 6.89 (ddd, $J = 8.2, 7.1, 1.1$ Hz, 1H), 6.85 (app td, $J = 8.2, 0.8$ Hz, 1H), 5.43 (brs, 1H), 4.48 (ddd, $J = 10.9, 10.9, 4.4$ Hz, 1H), 1.56-1.51 (m, 4H), 1.42-1.32 (m, 1H), 1.30-1.22 (m, 2H), 0.93-0.86 (m, 1H), 0.75-0.67 (m, 1H), 0.80 (d, $J = 6.5$ Hz, 3H), 0.66 (d, $J = 7.1$ Hz, 3H), 0.43 (d, $J = 7.0$ Hz, 3H); ^{13}C NMR (125MHz, CDCl_3) δ 195.3, 168.4, 160.2, 137.4 (2x), 135.6, 133.2, 129.5, 128.7, 128.5, 127.2, 125.0, 122.6, 120.7, 120.5, 120.3, 120.1, 113.0, 110.9, 107.6, 77.6, 73.5, 46.6, 39.5, 34.0, 31.3, 25.2, 22.8, 21.9, 20.6, 15.5; HRMS calc'd for $\text{C}_{33}\text{H}_{35}\text{N}_2\text{O}_3$ $[\text{M}+\text{H}]^+$ 507.2642, found: 507.2643; HPLC: Chiralpak AD-H, rt, retention time = 9.63 min (minor), 11.51 min (major).

Compound 56b:



Minor diastereomer **56b** (partial assignment was made based on deduction, using the spectra of the mixture and the spectra of the enriched diastereomer, multiplicity of some peaks could not be properly assigned due to extensive overlap): ^1H NMR (500 MHz, CDCl_3): δ 8.15 (br s, 1H) 7.56 (d, $J = 7.8$ Hz, 1H), 7.52-7.49 (m, 2H), 7.44-7.42 (m, 2H), 7.36-7.29 (m, 4H), 7.17 (ddd, $J = 8.2$, 7.1, 1.1 Hz, 1H), 7.08 (ddd, $J = 8.2$, 7.1, 1.1, 1H), 6.87 (ddd, $J = 8.2$, 7.1, 1.1 Hz, 1H), 6.81 (app td, $J = 8.2$, 0.8 Hz, 1H), 5.38 (br s, 1H), 4.56 (ddd, $J = 10.9$, 10.9, 4.4 Hz, 1H), 0.77 (d, $J = 6.5$ Hz, 3H), 0.65 (d, $J = 7.1$ Hz, 3H), 0.53 (d, $J = 7.0$ Hz, 3H) (Note: 9 aliphatic protons are difficult to assign due to extensive overlap in the aliphatic region); ^{13}C NMR (125MHz, CDCl_3) δ 194.7, 168.1, 160.1, 137.4, 137.1 135.5, 133.2, 129.5, 128.7, 128.5, 127.2, 125.2, 122.5, 120.7, 120.5, 120.3, 119.9, 112.9, 110.9, 107.9, 77.6, 73.4, 46.5, 39.6, 34.0, 31.3, 25.4, 22.9, 22.0, 20.7, 15.8.

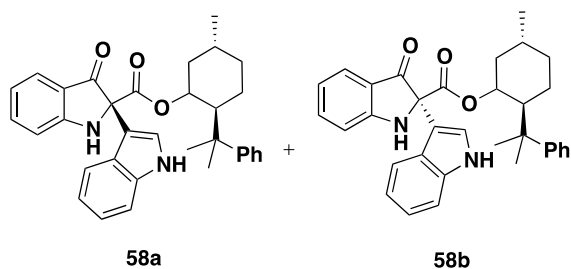
Compound 57:



Isolated as bright yellow powder in 67% yield (*ca.* 1.3:1 of **57a**:**57b**, mixture of diastereomers): $R_f = 0.27$ (yellow spot, 7:3 hexanes:EtOAc); IR (cast film) 3362, 3051, 2955, 1705, 1618, 1242, 739 cm^{-1} ; ^1H NMR (500 MHz, CDCl_3): δ 8.56 (br s, 1H, major), 8.54 (br s, 1H, minor), 7.71 (d,

$J = 7.7$ Hz, 1H), 7.70 (d, $J = 7.9$ Hz, 1H), 7.49 (ddd, $J = 8.4, 7.2, 1.4$ Hz, 1H), 7.47 (ddd, $J = 8.5, 7.1, 1.6$ Hz, 1H), 7.31-7.18 (overlapping peaks, 6H), 7.00-6.84 (overlapping peaks, 6H), 6.19 (br s, 1H, minor), 6.11 (br s, 1H, major), 4.70 (ddd, $J = 10.8, 10.8, 4.2$ Hz, 1H), 4.62 (ddd, $J = 11.0, 11.0, 4.4$ Hz, 1H), 2.17-2.06 (overlapping peaks, 4H), 1.61-0.70 (overlapping peaks, 14H), 0.87 (d, $J = 6.4$ Hz, 3H), 0.86 (d, $J = 6.4$ Hz, 3H), 0.83 (d, $J = 6.6$ Hz, 3H), 0.76 (d, $J = 7.0$ Hz, 3H), 0.58 (d, $J = 6.9$ Hz, 3H), 0.47 (d, $J = 7.0$ Hz, 3H); ^{13}C NMR (125MHz, CDCl_3) δ 195.2, 194.8, 168.9, 168.7, 161.0, 160.9, 138.3, 138.2 (2x), 138.0, 126.3, 126.2, 125.4, 125.3, 125.1, 125.0, 124.5, 124.4, 123.4 (2x), 119.6, 119.4, 119.3, 119.2, 113.2, 113.1, 112.4 (2x), 111.7, 111.6, 111.3, 111.2, 77.2, 77.3, 72.5, 72.4, 46.8 (2x), 40.0, 39.7, 34.2, 34.1, 31.4 (2x), 25.8, 25.4, 23.1, 23.0, 22.1, 22.0, 20.9, 20.5, 16.2, 16.0; HRMS calc'd for $\text{C}_{27}\text{H}_{30}^{79}\text{BrN}_2\text{O}_3$ $[\text{M}+\text{H}]^+$ 509.1434, found: 509.1447.

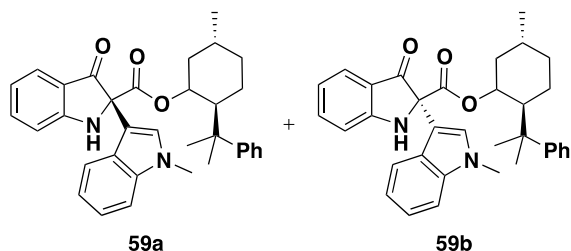
Compound 58:



Isolated as bright yellow solid in 76% combined yield (*ca.* 10:1 of **58a**:**58b**, mixture of diastereomers): $R_f = 0.33$ (yellow spot, 7:3 hexanes:EtOAc); IR (cast film) 3351, 3047, 2941, 1712, 1614, 1243, 751 cm^{-1} ; ^1H NMR (500 MHz, CDCl_3): δ 8.36 (br s, 1H), 7.71 (d, $J = 7.8$ Hz, 2H), 7.48 (ddd, $J = 8.4, 7.2, 1.3$ Hz, 1H), 7.31 (d, $J = 2.7$ Hz, 1H), 7.29-7.07 (overlapping peaks, 9H), 6.95 (d, $J = 8.1$ Hz, 1H), 5.64 (br s, 1H), 4.81 (ddd, $J = 10.6, 10.6, 4.4$ Hz, 1H), 1.97-1.86 (m, 2H), 1.63-0.71 (overlapping peaks, 6H), 1.15 (s, 3H), 0.98 (s, 3H), 0.81 (d, $J = 6.4$ Hz, 3H);

^{13}C NMR (125MHz, CDCl_3) δ 194.6, 167.1, 160.8, 150.2, 137.5, 137.6, 129.4, 128.3, 128.1, 127.9, 126.5, 125.7, 125.4, 125.2, 122.4, 120.2, 120.6, 119.7, 113.4, 109.5, 109.5, 78.4, 72.3, 50.2, 41.3, 40.1, 34.2, 31.3, 29.4, 27.5, 23.4, 21.9; HRMS calc'd for $\text{C}_{33}\text{H}_{34}\text{N}_2\text{O}_3\text{Na}$ $[\text{M}+\text{Na}]^+$ 529.2461, found: 529.2457. (Note: since the minor diastereomer is present in a small amount, only the characterization for the major diastereomer was included here.)

Compound 59:



Isolated as bright yellow solid in 74% combined yield (*ca.* 12:1 of **59a**:**59b**, mixture of diastereomers): R_f 0.40 (yellow spot, 7:3 hexanes:EtOAc); IR (cast film) 3362, 3051, 2955, 1705, 1618, 1242, 739 cm^{-1} ; ^1H NMR (500 MHz, CDCl_3): δ 7.71 (dd, $J = 7.7, 0.9$ Hz, 2H), 7.52 (ddd, $J = 8.4, 7.2, 1.3$ Hz, 1H), 7.36 (s, 1H), 7.29-7.07 (overlapping peaks, 9H), 7.02 (d, $J = 8.3$ Hz, 1H), 5.66 (br s, 1H), 4.81 (ddd, $J = 10.6, 10.6, 4.4$ Hz, 1H), 3.75 (s, 3H), 1.96-1.86 (m, 2H), 1.61-0.70 (overlapping peaks, 6H), 0.96 (s, 3H), 0.83 (d, $J = 6.6$ Hz, 3H), 0.78 (s, 3H); ^{13}C NMR (125MHz, CDCl_3) δ 194.4, 167.4, 160.9, 150.0, 137.6, 137.5, 129.5, 128.4, 128.1, 127.9, 126.3, 125.8, 125.4, 125.3, 122.2, 120.1, 120.0, 119.8, 113.6, 109.7, 109.5, 78.5, 72.5, 50.2, 41.2, 40.1, 34.4, 32.9, 31.4, 29.5, 27.4, 23.5, 21.7; HRMS calc'd for $\text{C}_{34}\text{H}_{36}\text{N}_2\text{O}_3\text{Na}$ $[\text{M}+\text{Na}]^+$ 543.2618, found: 543.2616. (Note: since the minor diastereomer is present in a small amount, only the characterization for the major diastereomer was included here.)

3.7 References:

1. Dick, A. R.; Sanford, M. S., *Tetrahedron* **2006**, *62*, 2439-2463.
2. (a) Lin, Z., *Coord. Chem. Rev.* **2007**, *251* (17-20), 2280-2291; (b) Boutadla, Y.; Davies, D. L.; Macgregor, S. A.; Poblador-Bahamonde, A. I., *Dalton Trans.* **2009**, (30), 5820; (c) Balcells, D.; Clot, E.; Eisenstein, O., *Chem. Rev.* **2010**, *110*, 749-823.
3. (a) Grimster, N. P.; Gauntlett, C.; Godfrey, C. R. A.; Gaunt, M. J., *Angew. Chem. Int. Ed.* **2005**, *44*, 3125-3129; (b) Beck, E. M.; Grimster, N. P.; Hatley, R.; Gaunt, M. J., *J. Am. Chem. Soc.* **2006**, *128*, 2528-2529.
4. Lapointe, D.; Fagnou, K., *Chem. Lett.* **2010**, *39*, 1118-1126.
5. (a) Lane, B. S.; Brown, M. A.; Sames, D., *J. Am. Chem. Soc.* **2005**, *127*, 8050-8057; (b) Park, C.-H.; Ryabova, V.; Seregin, I. V.; Sromek, A. W.; Gevorgyan, V., *Org. Lett.* **2004**, *6*, 1159-1162.
6. Yamamoto, K.; Kimura, S.; Murahashi, T., *Angew. Chem. Int. Ed.* **2016**, *55*, 5322-5326.
7. (a) Phipps, R. J.; Grimster, N. P.; Gaunt, M. J., *J. Am. Chem. Soc.* **2008**, *130*, 8172-8174; (b) Kieffer, M. E.; Chuang, K. V.; Reisman, S. E., *Chem. Sci.* **2012**, *3*, 3170-3174; (c) Kieffer, M. E.; Chuang, K. V.; Reisman, S. E., *J. Am. Chem. Soc.* **2013**, *135*, 5557-5560; (d) Deprez, N. R.; Kalyani, D.; Krause, A.; Sanford, M. S., *J. Am. Chem. Soc.* **2006**, *128*, 4972-4973.
8. Doyle, M. P.; McKervey, M. A.; Ye, T., *Modern catalytic methods for organic synthesis with diazo compounds: from cyclopropanes to ylides*. Wiley: New York, 1998.
9. Salomon, R. G.; Kochi, J. K., *J. Am. Chem. Soc.* **1973**, *95*, 3300-3310.
10. Nakamura, E.; Yoshikai, N.; Yamanaka, M., *J. Am. Chem. Soc.* **2002**, *124*, 7181-7192.

11. Nowlan, D. T.; Gregg, T. M.; Davies, H. M. L.; Singleton, D. A., *J. Am. Chem. Soc.* **2003**, *125*, 15902-15911.
12. Anciaux, A. J.; Hubert, A. J.; Noels, A. F.; Petiniot, N.; Teyssie, P., *J. Org. Chem.* **1980**, *45*, 695-702.
13. (a) Pirrung, M. C.; Morehead, A. T., *J. Am. Chem. Soc.* **1996**, *118*, 8162-8163; (b) Pirrung, M. C.; Liu, H.; Morehead, A. T., *J. Am. Chem. Soc.* **2002**, *124*, 1014-1023.
14. Alonso, M. E.; del Carmen García, M., *Tetrahedron* **1989**, *45*, 69-76.
15. (a) Phipps, R. J.; Gaunt, M. J., *Science* **2009**, *323*, 1593-7; (b) Bigot, A.; Williamson, A. E.; Gaunt, M. J., *J. Am. Chem. Soc.* **2011**, *133*, 13778-13781.
16. Rauniyar, V.; Wang, Z. J.; Burks, H. E.; Toste, F. D., *J. Am. Chem. Soc.* **2011**, *133*, 8486-8489.
17. Deng, X.; Liang, K.; Tong, X.; Ding, M.; Li, D.; Xia, C., *Org. Lett.* **2014**, *16*, 3276-3279.
18. Allen, A. E.; MacMillan, D. W., *J. Am. Chem. Soc.* **2011**, *133*, 4260-4263.
19. (a) Clark, J. S.; Hansen, K. E., *Chem. Eur. J.* **2014**, *20*, 5454-5459; (b) Clark, J. S.; Berger, R.; Hayes, S. T.; Senn, H. M.; Farrugia, L. J.; Thomas, L. H.; Morrison, A. J.; Gobbi, L., *J. Org. Chem.* **2013**, *78*, 673-696; (c) Clark, J. S.; Vignard, D.; Parkin, A., *Org. Lett.* **2011**, *13*, 3980-3983; (d) Clark, J. S.; Labre, F.; Thomas, L. H., *Org. Biomol. Chem.* **2011**, *9*, 4823; (e) Clark, J. S.; Walls, S. B.; Wilson, C.; East, S. P.; Drysdale, M. J., *Eur. J. Org. Chem.* **2006**, *2006*, 323-327.
20. Marmsäter, F. P.; Vanecko, J. A.; West, F. G., *Org. Lett.* **2004**, *6*, 1657-1660.
21. S. Baran, P.; Jessing, M., *Heterocycles* **2010**, *82*, 1739.
22. Bott, T. M.; Atienza, B. J.; West, F. G., *RSC Adv.* **2014**, *4*, 31955-31959.
23. Fier, P. S.; Luo, J.; Hartwig, J. F., *J. Am. Chem. Soc.* **2013**, *135*, 2552-2559.

24. Desimoni, G.; Faita, G.; Jørgensen, K. A., *Chem. Rev.* **2006**, *106*, 3561-3651.
25. Mandler, M. D.; Truong, P. M.; Zavalij, P. Y.; Doyle, M. P., *Org. Lett.* **2014**, *16*, 740-743.
26. Nozaki, H.; Takaya, H.; Moriuti, S.; Noyori, R., *Tetrahedron* **1968**, *24*, 3655-3669.
27. Noland, W. E.; Vijay Kumar, H.; Lu, C.; Brown, C. D.; Wiley-Schaber, E.; Johansson, A.; LaBelle, E. V.; O'Brian, N. C.; Jensen, R. C.; Tritch, K. J., *Tetrahedron Lett.* **2016**, *57* (20), 2158-2160.
28. Crampton, M. R.; Robotham, I. A., *J. Chem. Res.* **1997**, 22-23.
29. Misaki, T.; Nagase, R.; Matsumoto, K.; Tanabe, Y., *J. Am. Chem. Soc.* **2005**, *127*, 2854-2855.
30. Yin, Q.; You, S.-L., *Chem. Sci.* **2011**, *2*, 1344.
31. Corey, E. J.; Ensley, H. E., *J. Am. Chem. Soc.* **1975**, *97*, 6908-6909.
32. Ort, O., *Organic Syntheses* **1987**, *65*, 203.
33. Halgren, T. A., *J. Comput. Chem.* **1996**, *17*, 490-519.
34. Seeman, J. I., *J. Chem. Ed.* **1986**, *63*, 42.
35. Berrisford, D. J.; Bolm, C.; Sharpless, K. B., *Angew. Chem. Int. Ed.* **1995**, *34*, 1059-1070.
36. Hong, L.; Sun, W.; Yang, D.; Li, G.; Wang, R., *Chem. Rev.* **2016**, *116*, 4006-4123.
37. Zhang, X.; Mu, T.; Zhan, F.; Ma, L.; Liang, G., *Angew. Chem. Int. Ed.* **2011**, *50*, 6164-6166.
38. Liu, C.; Zhu, Q.; Huang, K.-W.; Lu, Y., *Org. Lett.* **2011**, *13*, 2638-2641.
39. Parmar, D.; Sugiono, E.; Raja, S.; Rueping, M., *Chem. Rev.* **2014**, *114*, 9047-9153.
40. Christ, P.; Lindsay, A. G.; Vormittag, S. S.; Neudörfl, J.-M.; Berkessel, A.; O'Donoghue, A. C., *Chem. Eur. J.* **2011**, *17*, 8524-8528.

41. Rueping, M.; Raja, S., *Beilstein J. Org. Chem.* **2012**, *8*, 1819-1824.
42. Momiyama, N.; Nishimoto, H.; Terada, M., *Org. Lett.* **2011**, *13*, 2126-2129.
43. Storer, R. I.; Carrera, D. E.; Ni, Y.; MacMillan, D. W. C., *J. Am. Chem. Soc.* **2006**, *128*, 84-86.
44. Momiyama, N.; Okamoto, H.; Kikuchi, J.; Korenaga, T.; Terada, M., *ACS Catal.* **2016**, *6*, 1198-1204.
45. (a) Karadeolian, A.; Kerr, M. A., *J. Org. Chem.* **2010**, *75*, 6830-6841; (b) Karadeolian, A.; Kerr, M. A., *Angew. Chem. Int. Ed.* **2010**, *49*, 1133-1135.

Chapter Four

Towards the Total Synthesis of Isatisine A, and the Total Synthesis of Halichrome A from Common Intermediate.

4.1 Introduction

As we have seen in Chapter Three, considerable efforts have been made towards the preparation of the western fragment of isatisine A, derived from the trapping of acceptor/acceptor metallocarbenes with an azide and subsequent nucleophilic addition of indole *via* dual catalysis. A library of truncated analogs of isatisine A has also been made using the procedure described in Chapter Three. Additionally, two complementary strategies were developed to access the diastereo- and enantioenriched truncated analogs of isatisine A. With the necessary western fragment in hand, we began to examine the possibility of elaborating one of the truncated analogs to the total synthesis of isatisine A (early stage installation of indole). Initially, we also explored the feasibility of applying the procedure developed in Chapter Three as a late stage reaction in the proposed total synthesis.

This chapter documents the evolutionary improvement of our strategies towards the total synthesis of isatisine A. Although, we have already intercepted a compound known as an intermediate to isatisine A (formal synthesis), as is discussed towards the last sections, our methods allow for better modularity than the previously reported synthesis.¹ Given that the reactions described in Chapter Three are amenable to gram-scale preparations, we wanted to explore alternative routes to isatisine A, ideally a synthetic route that would allow access to gram-scale production of this natural product which would be essential for a more thorough exploration of its antiviral activity. We also wanted to explore the diversification of ambident C-

acylimines for further construction of chemical libraries. During our exploration of possible umpolung reactivity of ambident *C*-acylimines, a promising regiodivergent functionalization using a variety of σ -type nucleophiles was observed, resulting in the first short synthesis of a natural alkaloid, halichrome A. Towards the end of this chapter, we will disclose these findings.

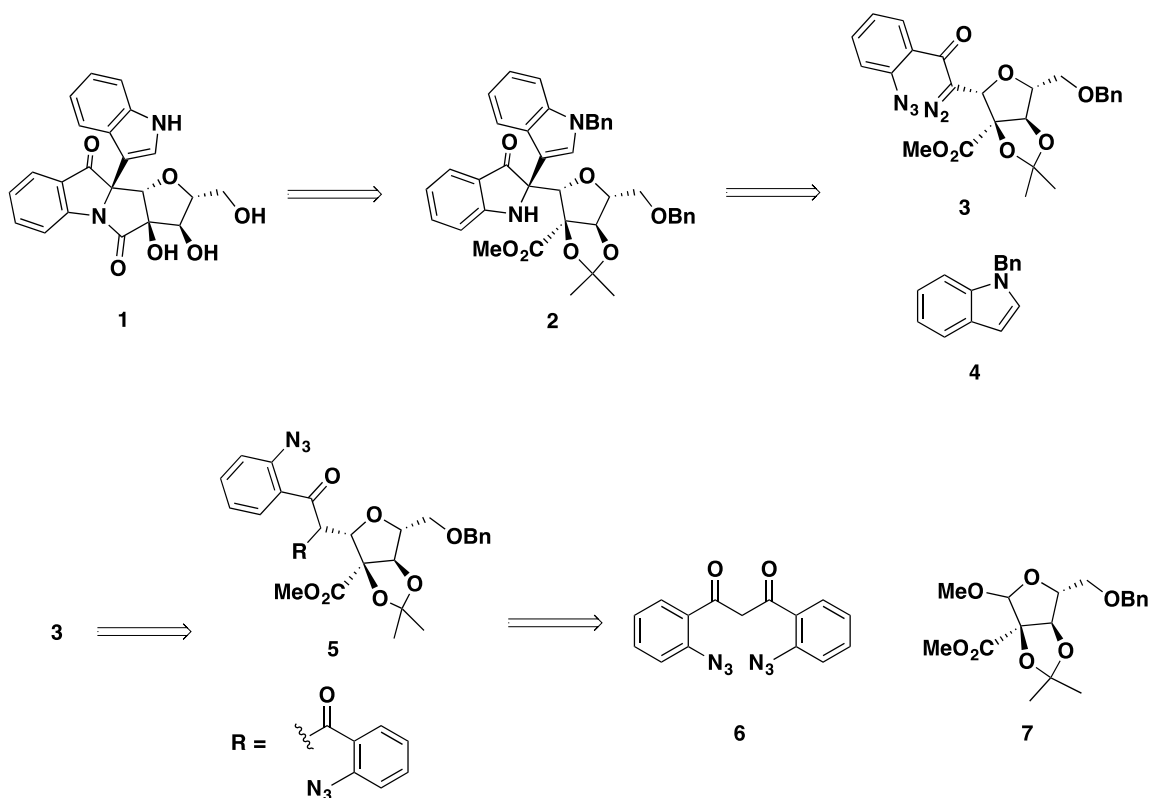
4.2 Results and discussion

When we started to tackle the challenge of the synthesis posed by the complex architecture of isatisine A (Chapter One), it was my personal conviction that a strong and firm synthetic foundation would lead to a well-founded total synthesis. Perhaps, I was influenced by the other members of the group to approach the natural product at different angles and to be “Edisonian” – a person willing to try a number of experiments with some leap of faith, hoping that one day it will yield an encouraging result. It was for these reasons that our strategies commenced with exploring disparate retrosyntheses until a promising route was eventually recognized, with the caveat that this unique route must involve the reactions developed in Chapters Two and Three and should be highly scalable for future SAR studies.

4.2.1 Strategy using a late stage azide metallocarbene coupling/indole addition

Thus, we first began to explore the possibility of a late stage installation of indole in our retrosynthesis. Outlined in Scheme 4.1 is the retrosynthesis first considered. It was first envisioned that isatisine A **1** could come from ester **2**, through a lactamization and deprotection. Ester **2** was proposed to come from diazo/azide **3**, bearing the necessary sugar linkage, and a protected indole **4** through a domino azide metallocarbene coupling reaction, followed by indole addition. The diazo/azide **3** was envisioned to originate from a deacylative diazo transfer² reaction of diketo/azide **5**. The diketo/azide **5** could then arise from *C*-glycosylation of diketone

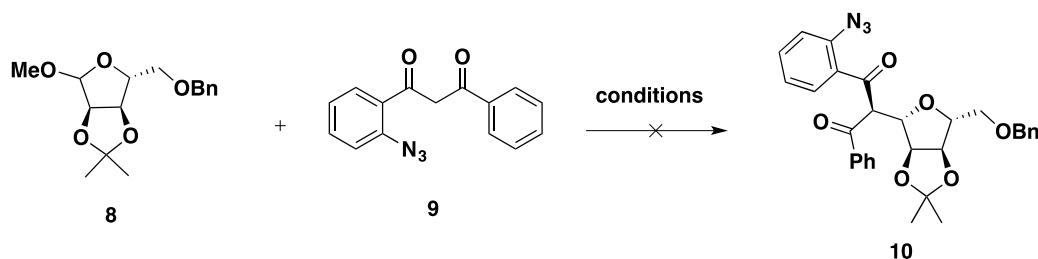
6 with protected sugar **7**. The diketone **6** having the two azide, on both aryl ring, would avoid the formation of the undesired diazo.



Scheme 4.1: Proposed late stage Friedel-Crafts alkylation.

With the two seemingly simple starting materials necessary for this retrosynthesis, we started testing the *C*-glycosylation to install the necessary diazo functional group on the next step. Our initial idea was to use an easily accessible material, which was also stable enough to be prepared in a large scale. During the preliminary testing of this retrosynthesis, we were worried that the oxocarbenium ion intermediate derived from **7** would have too much steric hindrance imposed by the ester, preventing nucleophilic attack from the bulky enolate. This, however, can perhaps be mitigated later by using a protected hydroxymethyl instead of an ester.³ Thus, to test

the feasibility of this hypothetical reaction, we used the known model tetrahydrofuran **8**,⁴ lacking the ester at the C-2 position and diketo **9**, previously made in Chapters Two and Three (Scheme 4.3). Notably, tetrahydrofuran **8** and diketo **9** were both amenable to large-scale preparation.

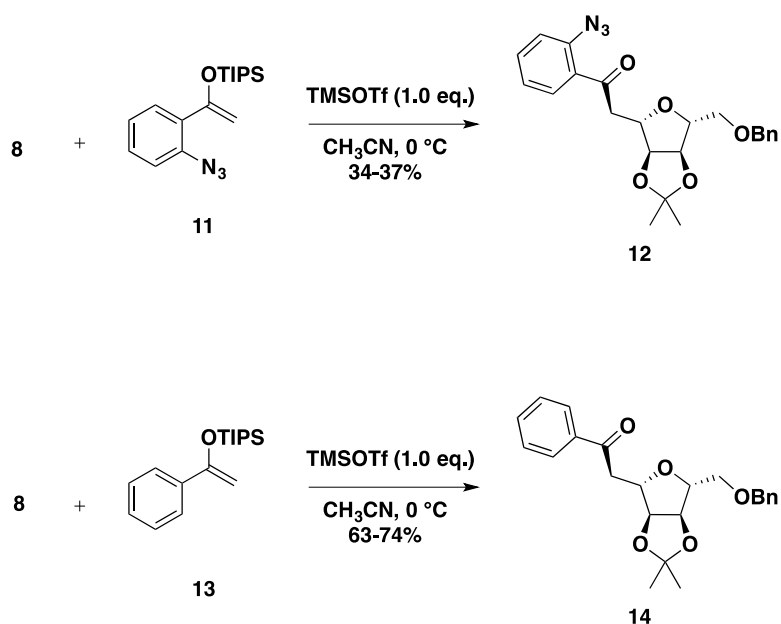


Scheme 4.2: Attempts on initial C-glycosylation.

Tetrahydrofuran **8** and the diketone **9** were mixed together under various conditions to attempt to induce a transformation depicted in Scheme 4.2, such as testing some permutations of Lewis acids (TMSOTf, TESOTf, TIPSOTf, $\text{BF}_3 \cdot \text{Et}_2\text{O}$, $\text{Sc}(\text{OTf})_3$, $\text{Zn}(\text{OTf})_2$, $\text{Cu}(\text{OTf})_2$), Brønsted acids (*p*-TsOH, dilute TfOH, dilute H_2SO_4 , dilute HCl), solvents (CH_3CN , DCM, PhMe, THF), temperatures ($-78\text{ }^\circ\text{C}$, $0\text{ }^\circ\text{C}$, rt, $40\text{ }^\circ\text{C}$) and known additives (MS 4 \AA and MS 3 \AA); however, all attempts were met with failure. Attempts to use a more nucleophilic sodium enolate salt of **9** were also unsuccessful. Only decomposition of tetrahydrofuran **8** and recovery of diketone **9** were observed in most conditions.

The susceptibility of tetrahydrofuran **8** to decomposition indicated that this starting material was sufficiently reactive to permit anomeric functionalization. Thus, we believe the failure of this transformation hinges on the sterically hindered enol form of **9**, caused by the ortho azide and the additional aryl group, preventing it from successfully attacking as a nucleophile to the ensuing oxocarbenium ion from **8**. To validate this, we stirred the less hindered (TIPS or TMS) silyl enol ether **11** and tetrahydrofuran **8** in the presence of a

stoichiometric amount of TMSOTf with acetonitrile as the solvent, depicted in Scheme 4.3. Indeed, the reaction proceeded to afford azide **12** in modest 34-37% yield. Upon using silyl enol ether **13**, lacking the azide on the ortho position, the reaction proceeded more efficiently to furnish **14** in 63-74% yield. However attractive the utility of this methodology for some other applications, with these results, it was clear that the retrosynthesis depicted in Scheme 4.1 would be difficult to realize, especially given the need for a sterically demanding quaternary center next to the anomeric position. Moreover, the presence of an ortho azido group on the nucleophile was essential in order to carry out the subsequent domino *C*-acylimine formation/Friedel-Crafts trapping. In light of these concerns, another retrosynthesis was considered.

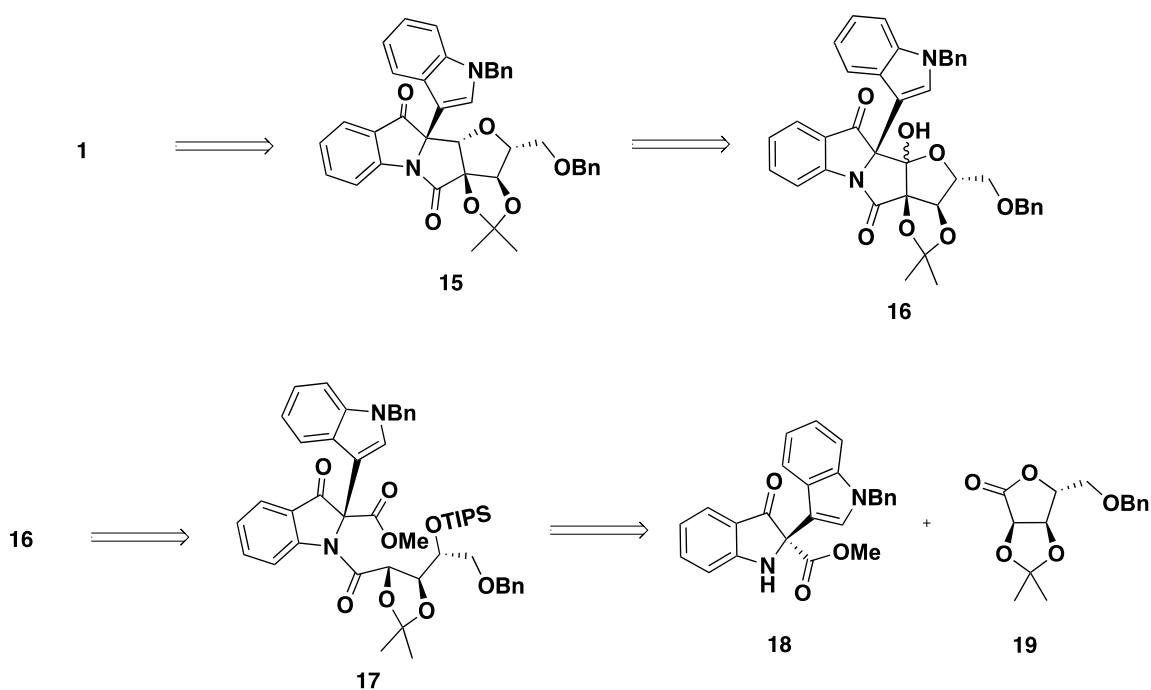


Scheme 4.3: Successful attempts to induce *C*-glycosylation.

4.2.2 Strategy using early stage azide metallocarbene coupling/indole addition

The second strategy that we explored commenced with using the transformations depicted in Scheme 4.4. Using the adduct accessible in Chapter Three, our second retrosynthesis

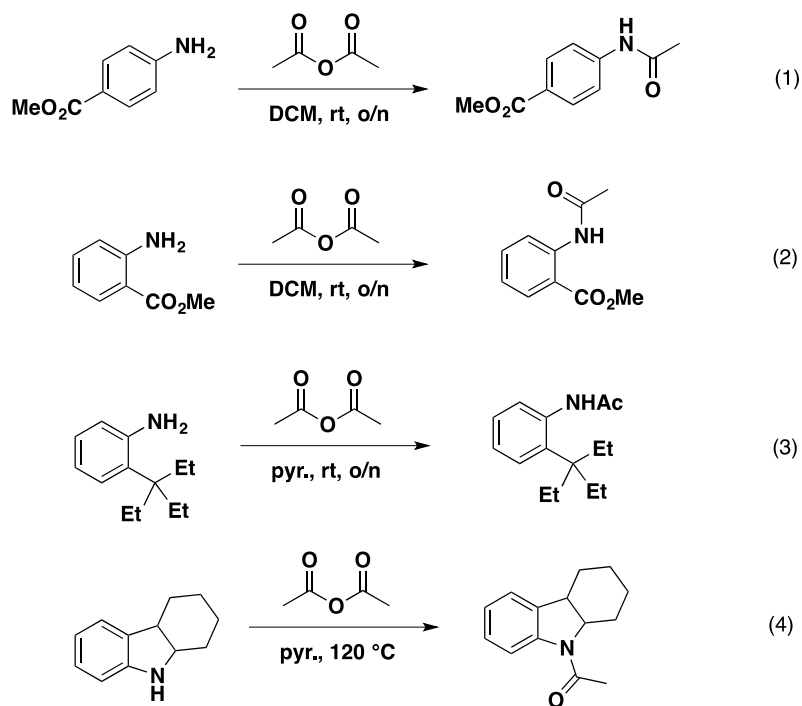
was devised as the following: we assumed **1** could be accessible from **15** *via* a debenzoylation and hydrolysis of the benzyl and acetonide protecting groups, respectively. Synthetic intermediate **15** could then be formed from **16** *via* a deoxygenation reaction, possibly effected by triethyl silane in the presence of boron trifluoride, shown in the previous synthesis of isatisine A by the Ramana group.³ Synthetic intermediate **16** could then be envisioned to come from a cyclization of intermediate **17**. We then hoped to make **17** *via* exploration of a seemingly difficult amidation of **18** and the known furanone **19**⁵ (or its derivative). Indole **18** could be prepared stereoselectively using a chiral auxiliary. Thus, in essence, we could also use a compound similar to **18** bearing either menthyl or 8-phenyl menthyl ester instead of methyl ester, as depicted in Scheme 4.5. To this end, we initially used adduct **18** to validate the next step.



Scheme 4.4: Proposed second retrosynthesis.

Although prejudged as a seemingly difficult transformation, amidation of compounds with structural similarity to **18** are known in the literature. Briefly shown in Scheme 4.5 are some

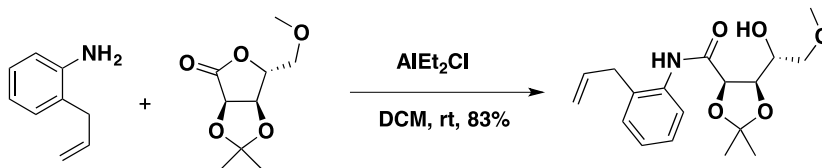
examples of amidation of simple anilines bearing an electron withdrawing-group in the para (equation 1, Scheme 4.5)⁶ and ortho (equation 2)⁷ positions, sterically encumbering alkyl groups in the ortho position of anilines (equation 3)⁸ and alkyl groups next to indolines (equation 4).⁹ These examples range from reaction conditions requiring stirring with acetic anhydride at 0 °C or addition of DMAP or pyridine (pyr.) to hasten the reaction rate. Using alternative heating with toluene or pyridine solvents or microwave conditions can also initiate the reaction. However, the dearth of literature attempting to effect coupling of a carboxylic acid derivative and a compound bearing an electron-withdrawing group ortho to the aniline, while also containing a sterically demanding alkyl group next to the aniline, prompted us to do more extensive experimentation.



Scheme 4.5: Representative examples of amide formation.

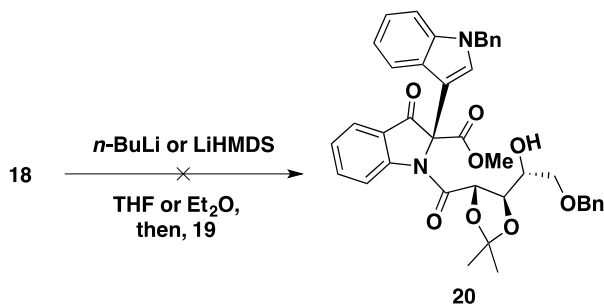
Sticking to the same tenets of our synthetic approach, we decided to employ readily accessible starting material that would be highly amenable to large-scale preparation. We

initially used the known furanone **19**, a compound that can be prepared in large scale from a known member of the carbohydrate pool, D-ribose.⁵ Amidation of a compound similar to **19** with an ortho-allylaniline was known in the literature, using aluminum based reagents to effect this transformation (Scheme 4.6).¹⁰ Thus, we deemed it worth trying.



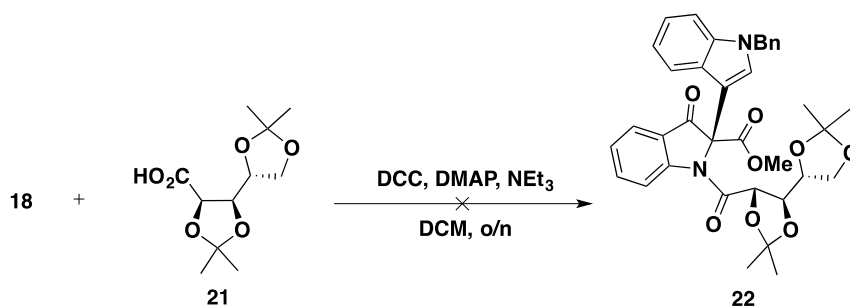
Scheme 4.6: Amidation of *o*-allylaniline with protected ribonolactone.

However, upon mixing indole **18** with furanone **19** in the presence of aluminum reagents, such as AlEt₃, AlCl₃ or AlMe₃, using similar conditions to those in Scheme 4.6 with a slight adjustment of temperature (40 °C), only recovery of indole **18** and decomposition of **19** was observed. Upon subjecting a mixture of **18** and **19** with benzene derivatives like toluene, mesitylene or pyridine under reflux or microwave conditions (for toluene), only the partial (trace) hydrolysis of acetonide in **19** was observed. To rationalize this result, we hypothesized that the failure of this transformation was partially due to the weak nucleophilic character of the aniline. In an attempt to solve this problem, we decided to deprotonate indole adduct **18** using two variants of strong base (for example, LiHMDS or *n*-BuLi) in THF or diethyl ether, followed by the addition of **19** (Scheme 4.7). The change in color of a solution of **18** in THF or diethyl ether from a yellow solution to deep brown after about an hour of stirring with *n*-BuLi or LiHMDS was a good indication that the desired deprotonation of indole **18** N-H occurred in solution. However, the attempts to effect addition of lithium amide of **18** to furanone **19** were also met with failure.



Scheme 4.7: Deprotonation of indole 18.

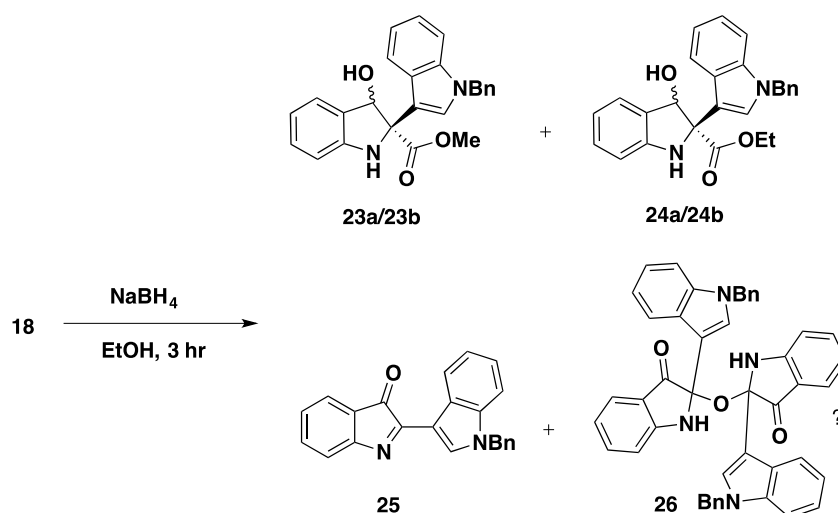
We then began to look at a more electrophilic version of **20**, using known carboxylic acid **21**¹¹ as a precursor. Our idea was to examine the possibility of amidation of **18** with **21** using variations of Steglich coupling¹² to make **22**. However, upon mixing **18** and **21**, in the presence of DIPEA (diisopropyl ethyl amine) and DCC (dicyclohexyl carbodiimide) to activate carboxylic acid **21** and stirring the mixture in DCM overnight, no noticeable amide formation was observed (Scheme 4.8). Addition of HOBT (*N*-hydroxybenzotriazole) to attempt to promote amidation was also unsuccessful.



Scheme 4.8: Attempts to induce Steglich amidation.

We realized that another possible reason for the failure of these series of experiments was the weak nucleophilicity of indole **18**, presumably because of the effective conjugation with the ortho-carbonyl, giving it the stability of some sort of vinylogous amide. We decided to reduce the ortho-ketone using various equivalents of NaBH_4 in ethanol. In what seemed like a simple,

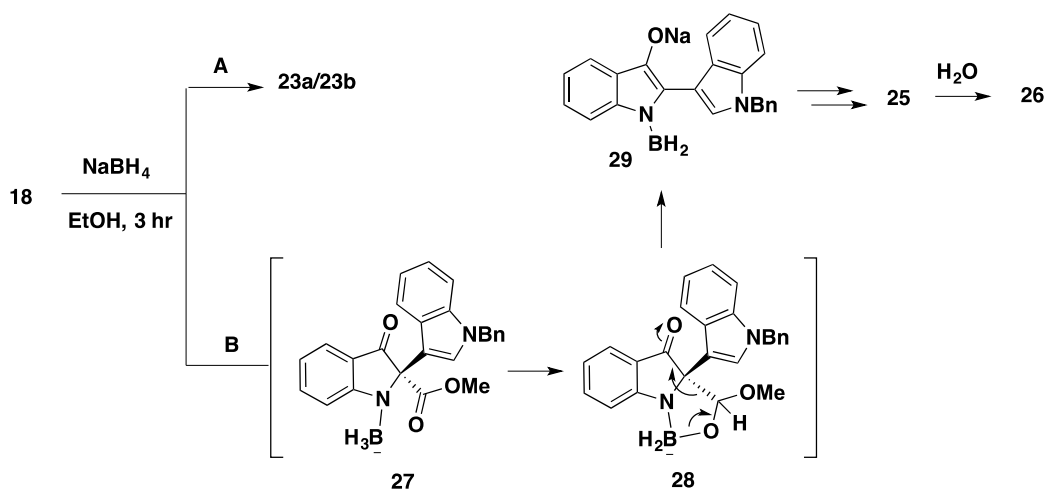
foolproof reaction, came another myriad of problems. To summarize, while we were able to obtain both diastereomers of alcohol **23** (**23a/23b**) in low yield (*ca.* 18%, combined) on small scales, the reaction suffered from undesired reductive deacylation of the methyl ester to furnish *C*-acylimine **25**. There was also formation of isolable diastereomers (only one characterized) of ethyl ester **24** (**24a/24b**) and a possible 2:1 dimer of **25** and water, which was detected by LC-MS, assigned as **26** and a mixture of other uncharacterized colored compounds (Scheme 4.9).



Scheme 4.9: Partial reduction of 18.

The formation of **23a/23b**, **25**, and **26** can be rationalized based on the proposed mechanism depicted in Scheme 4.10. We believe that **18** could have two possible pathways upon mixing with NaBH₄. In pathway A, the borohydride could directly attack the ketone forming the desired alcohol **23a/23b** after a nonselective addition. Alternatively, in pathway B, the borohydride could deprotonate the somewhat acidic vinylogous amide forming trihydroamidoborate **27**. The borate in compound **27** can then internally deliver one or two equivalents of hydride to the ester to form **28** (only one delivery of hydride was shown) followed by a retro-aldol to furnish enol **29**. Enol **29** could then be protonated to afford indolinone (not

shown), which can then dehydrogenate¹³ to form *C*-acylimine **25**. The *C*-acylimine **25** can then be slowly attacked by water during workup to afford **26**, which was detected in the crude mixture by LC-MS. It is likely that the ester **24a/24b** arose from transesterification from the borane activated ester.



Scheme 4.10: Proposed mechanism for the formation of **23, **25**, and **26**.**

The formation of ester **24a/24b** can be fully suppressed by using a *t*-BuOH/THF (9:1) mixture instead of ethanol as the solvent at the expense of reaction rate (two days). Notably, this solvent system, on small scales, also allowed for the diastereoselective formation of **23** (*ca.* 8:1), albeit in somewhat irreproducible yields (27-63%). The relative stereochemistry of **23** (assigned as **23a**) was tentatively assigned using ROESY. A through space correlation between the singlet (C2-H) in the indole portion of the molecule and the O-H was observed in the 2D spectra, suggesting that the alcohol is located *syn* to the indole (Figure 4.1).

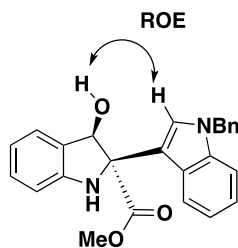


Figure 4.1: rOe correlation of the alcohol with the C-H on the indole moiety (23a).

Other mild reducing agents such as DIBAL-H and LiBH₄ in toluene solvent gave a much inferior results. For example, using more than 1.0 equiv of DIBAL-H did not result in a traceable formation of **23**. However, upon scaling up the reaction to at least 500 mg of starting material, using NaBH₄, the yield dramatically dropped even further (14%). Substantial formation of the *C*-acylimine **25** was the principal outcome observed. This discouraging failure thwarted our ability thoroughly investigate the retrosynthesis depicted in Scheme 4.5.

It became apparent that using **18** might not be a viable pathway to the synthesis of isatisine A. The discouraging outcomes from these series of failures led us to review the products from these reactions. With this, we noticed an accumulation of *C*-acylimine **25**. Incidentally, a compound similar to **25**, bearing a tosyl instead of benzyl protecting group, was used by the Xie group as a starting material for the synthesis isatisine A. Upon examination of the procedure to make isatisine A using a similar compound to **25**,^{1a} the authors cited an old procedure to prepare the *C*-acylimine.^{1b} This protocol uses oxidative dimerization of an indole.

However, as noted by Kerr and Karadeolian in their pioneering synthesis,¹⁴ this transformation is limited in yield, as complications from the over addition of indole often arise. Another limitation imposed by this transformation is the modularity of the starting material. For instance, subjecting two differentially substituted indole based starting materials under oxidative dimerization can theoretically yield to four different *C*-acylimines (two homodimers and two

heterodimers). This problem can limit the accessibility of the desired compound in fair amount, necessary for diversification and structure-activity relationship studies.

Staying optimistic, we were also aware that by using this *C*-acylimine intermediate **25** (or analog), a variety of simple alkaloids possessing *C*-2 alkylated indolinones, such as metagenebiindole A¹⁵ and halichrome A,¹⁶ might be accessible. Halichrome A is a weakly cytotoxic yellow pigment isolated by Abe and co-workers from *Halicondria okadai*. Metagenebiindole A is also a yellow pigment; however, it was isolated from deep-sea bacteria through metagenomics by Qiu and co-workers. (Figure 4.2) Notably, the synthesis of these simple alkaloids has never been demonstrated in the laboratory. Our interest to access these alkaloids (or at least one of them) stems from questions like “how simple are these alkaloids?” and “how can we make them?” In the following sections, we will attempt to answer these questions.

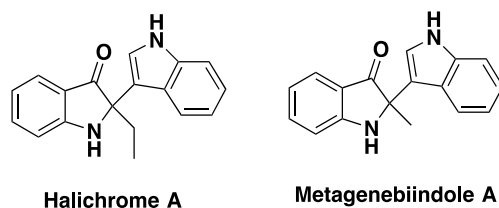


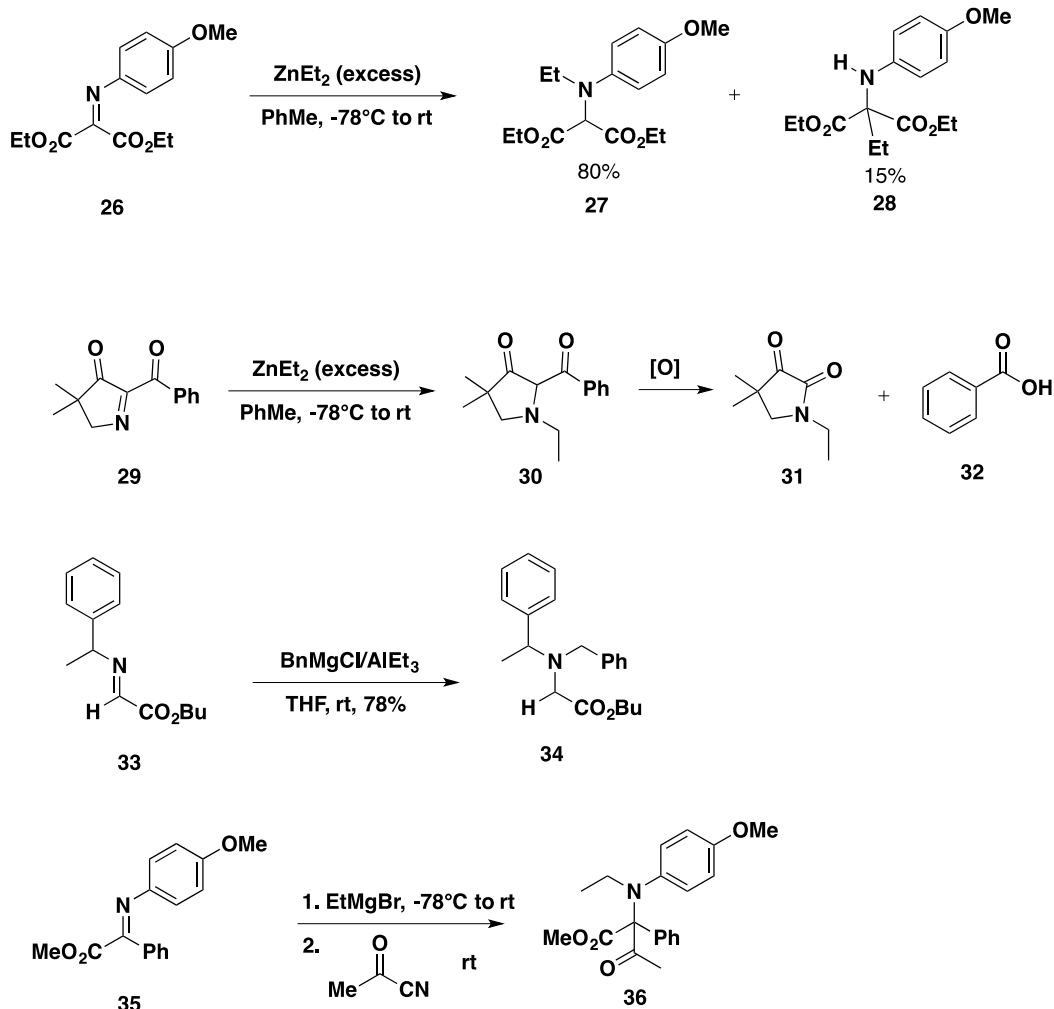
Figure 4.2: The structure of halichrome A and metagenebiindole A.

4.2.3 Functionalization using the stable *C*-acylimine

Regio- and chemoselective addition of nucleophiles on compounds that contain carbonyls and imines (keto-imines) that are strategically placed next to each other poses a significant challenge to chemists and examples of this in the literature are scarce. Perhaps, this can be ascribed to the limited number of procedures for the preparation of compounds containing both a

ketone and an imine, as the imine is typically made by mixing a ketone and an amine.

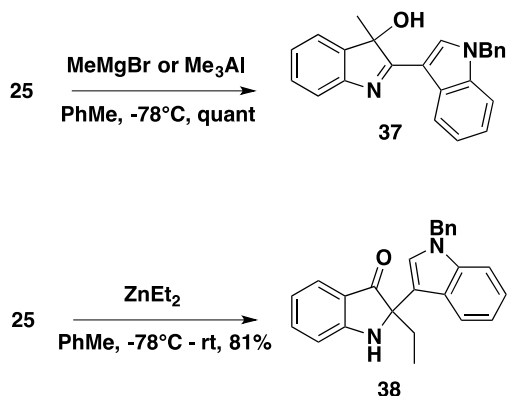
Additionally, there are notable examples in the literature, utilizing similar substrates for umpolung (reversal of polarity) functionalization. Summarized in Scheme 4.10 are some examples of imino esters utilizing umpolung functionalization. For instance, both imine **26**¹⁷ and imine **29**, when treated with diethyl zinc in toluene solution, furnished *N*-ethyl amine **27** and **30**, respectively. West and Bott (unpublished dissertation) have shown that amine **30** oxidized even further to ketolactam **31** and benzoic acid **32** through an oxidation/debenzoylation reaction. Shimizu, however, did not observe further oxidation of **27**, but rather an impurity from **28**.¹⁷ This α -iminoester functionalization is not only limited to the use of diethyl zinc. It has been shown that imine **33** can furnish **34** when treated with benzyl magnesium chloride in the presence of triethylaluminum reagent.¹⁸ Interestingly, no ethyl addition coming from the triethylaluminum reagent was observed, suggesting that Grignard reagents are kinetically faster as nucleophiles than triethyl aluminum. Another landmark functionalization using this methodology was shown by Kozlowski.¹⁹ She demonstrated that imine **35** can undergo a domino umpolung functionalization when treated with ethyl magnesium bromide, followed by the capture of the enolate with an electrophile; in this case, a pyruvitrile electrophile. In this regard, we decided to examine whether σ -type nucleophiles could be used to prepare halichrome A and other analogs or undergo umpolung functionalization, as discussed earlier.



Scheme 4.11: Literature examples of α -iminocarbonyl umpolung reactivity.

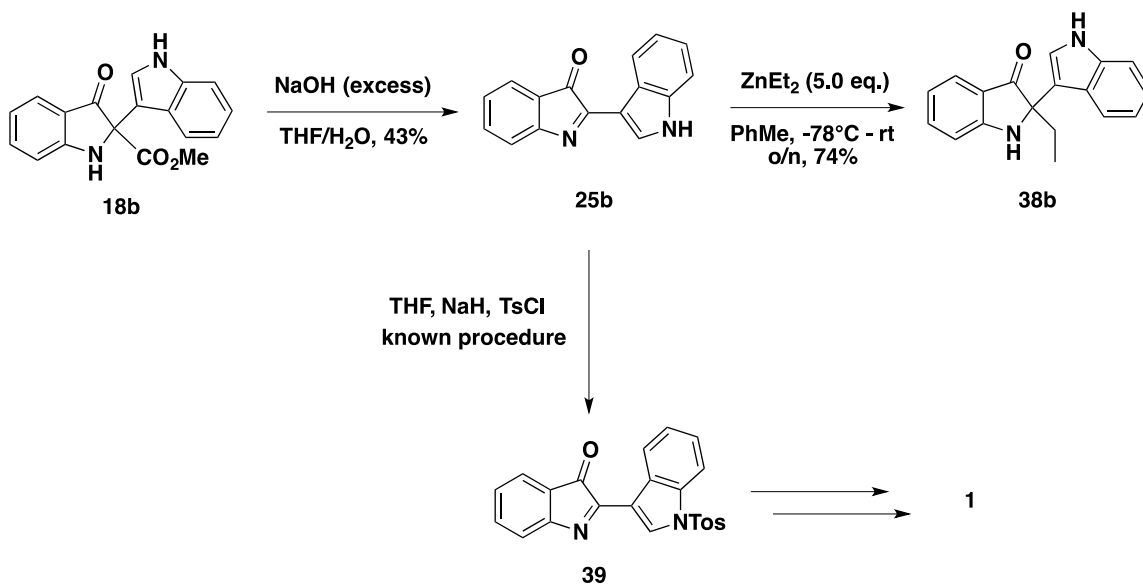
To begin the investigation into the reactivity of *C*-acylimines with σ -type nucleophiles, we decided to mix **25** with methylmagnesium bromide in toluene. The reaction afforded **37** in quantitative yield after work up and purification (Scheme 4.11). Addition of the Grignard reagent, as expected, happened at the carbonyl. Using trimethylaluminum in place of methyl Grignard under the same reaction conditions afforded **26** in nearly quantitative yield as well. Similar to methylmagnesium bromide, trimethylaluminum preferentially added to the carbonyl carbon. Using diethylzinc instead of methylmagnesium bromide under the same reaction conditions, but with a different reaction time, however, afforded a different adduct, though with a lower 81%

yield. In the diethyl zinc case, the addition happened preferentially at the imine to afford **38**. No umpolung functionalization was observed, presumably because of the lack of ester that could chelate with imine and subsequently direct the σ -nucleophile onto the nitrogen because of proximity and possibly the formation a stable metal enolate.¹⁹



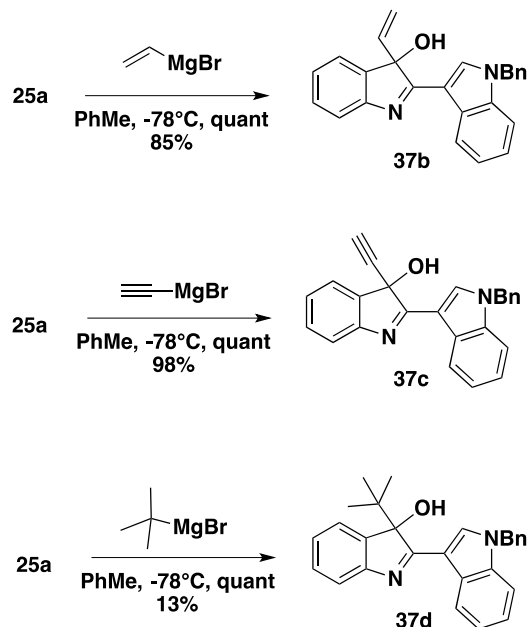
Scheme 4.12: Regiodivergent reactivity of σ -type nucleophiles.

Delighted by this result, we then subjected unprotected indole **18b** to decarboxylation to afford *C*-acylimine **25b** in 43% yield (see note in the procedure). Treatment of the *C*-acylimine **25b** with excess diethyl zinc (5 equiv) resulted in the short synthesis of the natural product halichrome A **38b** in 74% yield (Scheme 4.13). At the moment, it is currently unclear to us why diethylzinc preferentially adds to the imine. Further studies are necessary to rationalize this regiodivergency.



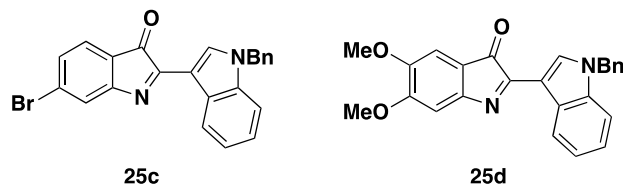
Scheme 4.13: Total synthesis of halichrome A.

Furthermore, treatment of *C*-acylimine **25b** with TsCl and NaH in THF afforded the exact starting material used by Xie in the synthesis of isatisine A, suggesting that this route, from a highly modular reaction, is a viable pathway to the synthesis of isatisine A and its highly diverse analogs.²⁰ Other Grignard reagents are likewise amenable, displaying consistent addition to the carbonyl of the *C*-acylimine **25** to afford **37b-d** (Scheme 4.13).



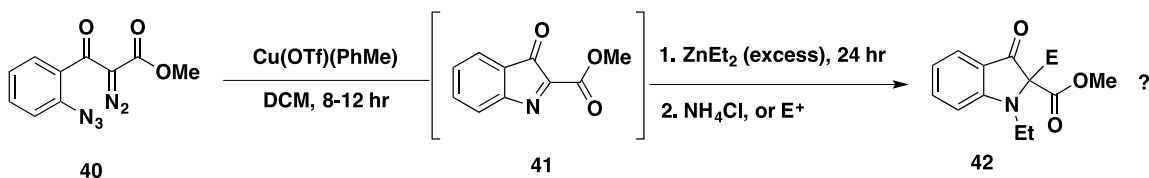
Scheme 4.14: Diversity with the Grignard reagents.

Further examinations of these reactions are currently being pursued by a talented undergraduate student, Issac Zeer-Wanklyn. For example, after reproducing the yields for some Grignard reactions and diethyl reactions depicted in Scheme 12, he has further shown that bromo *C*-acylimine **25c** could likewise engage an addition, from diethyl zinc, to the imine (Scheme 4.15). He likewise extended the scope of the trialkylaluminum additions to the carbonyl using the parent **25a**. Moreover, upon stirring 4,5-dimethoxysubstituted *C*-acylimine **25d** with the diethylzinc reagent, considerable retardation on the reaction rate was observed, presumably because of the chelation of the two methoxy groups to the diethylzinc reagent. However, for the purpose distribution of credits, these transformations will not be further discussed here. A preface outlining a possible publication disclosing all the information shown here and likewise that of Issac Zeer-Wanklyn's data will be included as one manuscript.



Scheme 4.15: Other C-acylimines amenable to regiodivergent functionalization.

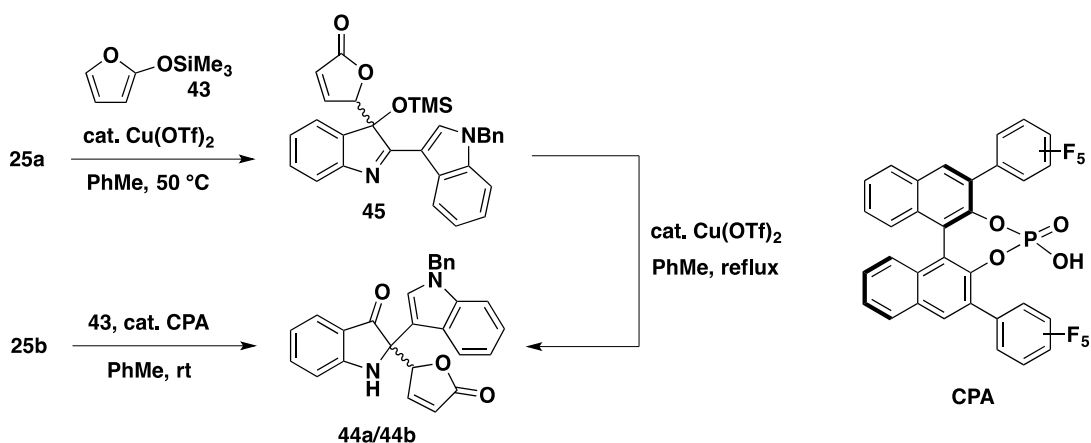
With all the data given here, it seemed that the ester in imino esters for umpolung functionalization was crucial. Thus, another possibility that is currently being investigated, guided by the mechanism outlined in Chapter Three in combination with the work described in this chapter, is the possibility of a telescoped synthesis from the diazo **40** and then treatment with copper(I) catalyst to make intermediate **41** *in-situ*, and then addition of the σ -type nucleophile, followed by capture with an electrophile to furnish compounds similar to **42**. However, with the current status of this approach, only limited success was obtained.



Scheme 4.16: Potential domino umpolung functionalization.

Finally, as various aspects of this project were being completed, I decided to briefly investigate the reactive potential of known siloxy furan **43** (Scheme 4.17), which was available in our laboratory. In looking at this chemical, I went back to the drawing board and pondered. Can C-acylimine **25a** undergo a vinylogous Mukaiyama reaction with siloxy furan **43** to conceivably afford a much closer structure to isatisine A?

Thus, treatment of *C*-acylimine **25a** with siloxyfuran **43** in the presence of a chiral BINOL phosphoric acid (CPA) afforded indolinones **44a** and **44b** in 84% yield as a combined, 3:1, mixture of diastereomers. In agreement with the reactivity seen in Chapter Three, no reaction occurred upon mixing **25a** with **43** at room temperature in the presence of Cu(OTf)₂ as the Lewis acid. However, upon slight adjustment of the temperature to 50 °C, slow conversion of **25a** to a diastereomeric mixture of **45** (*ca.* 1:1) was observed. The siloxyfuran added preferentially to the carbonyl, suggesting that copper did not activate the imine, consistent with the conclusion seen in Chapter Three (see Scheme 3.9, Chapter Three). Upon heating the mixture **45** in toluene at reflux with Cu(OTf)₂ present, a possible reformation of the imine **25a** was observed due to formation of a distinct purple solution, then formation of a yellow solution again after a few minutes. Purification of this mixture using column chromatography, yielded **44a** and **44b**, *albeit* as a 1:1 mixture of diastereomers. This result suggested that indolinones **44a** and **44b** are thermodynamically more stable than **45**. This is presumably due to the stronger bond strength of the carbonyl versus the imine.



Scheme 4.17: Kinetic and thermodynamic addition of siloxyfuran.

4.3 Conclusion

In summary, while we were not able to effect the desired transformations from the two retrosyntheses proposed earlier, formation of an interesting *C*-acylimine was found to be one of the side products. Furthermore, a novel method of regiodivergent addition of nucleophiles to ambident electrophiles like indole based *C*-acylimines has been disclosed. Grignard and trialkyl aluminum reagents preferentially added to the carbonyl, while dialkyl zinc reagents favoured addition to the imine under identical conditions. This strategy was used to synthesize a marine natural product halichrome A. For the π -type siloxyfuran nucleophiles, regiodivergency was established based on the catalysts present in solution. This, however, was found to be thermodynamically reversible and ultimately funneled to the more stable indolinone products, allowing for the construction of core structure of isatisine A in addition to the formal synthesis described earlier.

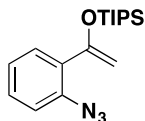
4.4 Experimental

4.4.1 General Information

Reactions were carried out in an oven-dried (130 °C) glassware or a flame-dried glassware under a positive argon atmosphere unless otherwise stated. Transfer of anhydrous reagents was accomplished with oven-dried syringes or cannulae. Solvents were distilled before use: acetonitrile (CH₃CN), dichloromethane (DCM) and dichloroethane (DCE) from calcium hydride, toluene (PhMe) from sodium metal, diethyl ether (Et₂O) and tetrahydrofuran (THF) from sodium metal/benzophenone ketyl. Thin layer chromatography was performed on glass plates pre-coated with 0.25 mm silica gel with fluorescent indicator UV₂₅₄ (Rose Scientific). Flash chromatography columns were packed with 230-400 mesh silica gel (Silacyle). Proton nuclear magnetic resonance spectra (¹H NMR) were recorded at 500 MHz, or 700 MHz and

coupling constants (J) are reported in Hertz (Hz). Carbon nuclear magnetic resonance spectra (^{13}C NMR) were recorded at 125 MHz. The chemical shifts are reported on the δ scale (ppm) and referenced to the residual solvent peaks: CDCl_3 (7.26 ppm, ^1H ; 77.06 ppm, ^{13}C).

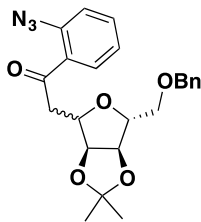
For the preparation of compound **11** used in C -glycosidation:



Hünig's ($i\text{-Pr}_2\text{NEt}$) base (560 μL , 3.10 mmol) was added to a stirred DCM solution of azidoacetophenone (500 mg, 3.10 mmol) at 0 $^\circ\text{C}$ and stirred further for 30 min. After the addition of the Hünig's base, TIPSOTf (840 μL , 3.10 mmol) was added dropwise. The mixture was stirred for another 1 h and then quenched by saturated NaHCO_3 . The solution was then extracted with generous amount of DCM, dried with MgSO_4 , and evaporated to afford a crude oil. The oil was purified by flash column chromatography using 20% EtOAc/Hexanes.

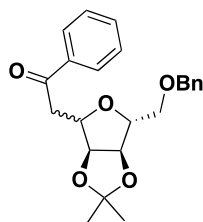
Isolated as a viscous yellow oil: $R_f = 0.81$ (10% EtOAc/Hexanes); ^1H NMR (500 MHz, CDCl_3): δ 7.56 (ddd, $J = 7.7, 1.6, 0.3$ Hz, 1H), 7.31 (ddd, $J = 8.1, 7.3, 1.6$ Hz, 1H), 7.16 (ddd, $J = 8.1, 1.2, 0.5$ Hz, 1H), 7.12 (ddd, $J = 7.7, 7.3, 1.2$ Hz, 1H), 4.82 (s, 1H), 4.67 (s, 1H), 1.22-1.28 (m, 3H), 1.10 (app. d, $J = 7.2$ Hz, 18 H); ^{13}C NMR (125 MHz, CDCl_3): δ 153.1, 136.7, 130.9, 129.6, 129.0, 124.5, 119.1, 96.1, 18.0, 12.7; LC-MS: calc'd for $\text{C}_{17}\text{H}_{28}\text{N}_3\text{OSi}$ $[\text{M}+\text{H}]^+$ 318.2, found 318.2.

For the preparation of furan **12** and furan **14**:



An acetonitrile (10 mL) solution of a known sugar **8**⁴ (294 mg, 1.00 mmol) was added with silane **11** (317 mg, 1.0 equiv) previously dissolved in acetonitrile (1 mL). Then, TMSOTf was added dropwise (180 μ L, 1.0 equiv) and stirred for the next 1 h. The solution was quenched with water (5 mL), and then extracted with DCM (10 mL, 3x). The organic layer was dried with MgSO₄, concentrated and purified using flash column chromatography (15% EtOAc/Hexanes).

12: isolated as a red oil in (152 mg) 36% yield; R_f = 0.32 (red spot, 7:3 hexanes:EtOAc); IR (cast film): 2933, 2863, 2127, 1683, 1484 cm^{-1} ; ¹H NMR (500 MHz, CDCl₃): δ 7.70 (dd, J = 7.8, 1.3 Hz, 1H), 7.53 (app. t, J = 7.8 Hz, 1H), 7.34-7.28 (m, 5H), 7.22-7.18 (m, 2H), 4.70 (dd, J = 6.5, 3.8 Hz, 1H), 4.56-4.58 (m, 3H), 4.50-4.52 (m, 1H), 4.17-4.18 (m, 1H), 3.61-3.59 (m, 2H), 3.40-3.38 (m, 2H), 1.57 (s, 3H), 1.38 (s, 3H); ¹³C NMR (125 MHz, CDCl₃): δ 198.8, 138.5, 137.9, 133.0, 130.9, 130.5, 128.4, 127.7, 127.6, 124.8, 119.0, 114.1, 84.9, 83.6, 82.3, 81.2, 73.5, 70.7, 47.2, 27.4, 25.6. HRMS calc'd for C₂₃H₂₅N₃NaO₅ [M+Na]⁺ 446.1686, found 446.1687.

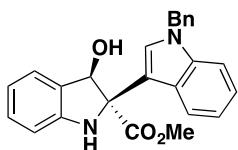


Compound **14** was prepared analogously to **12** but using a commercially available 1-trimethylsiloxystyrene (or the TIPS version²¹) instead of compound **13**.

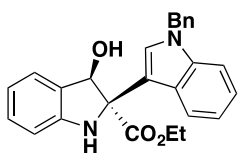
14: isolated as a light yellow oil in 63-74% (three trials) yield; $R_f = 0.38$ (faint red spot, 7:3 hexanes:EtOAc); IR (cast film): 3085, 3062, 2857, 1686, 1484 cm^{-1} ; ^1H NMR (500 MHz, CDCl_3): δ 7.92 (app. dd, $J = 8.4, 1.3$ Hz, 2H), 7.57 (tt, $J = 7.4, 1.3$ Hz, 1H), 7.43-7.46 (m, 2H), 7.28-7.36 (m, 5H), 4.71 (dd, $J = 6.0, 3.8$ Hz, 1H), 4.57-4.60 (m, 4H), 4.20 (q, $J = 3.9$ Hz, 1H), 3.62 (m, 2H), 3.39-3.43 (m, 1H), 3.24-3.28 (m, 1H), 1.38 (s, 3H), 1.58 (s, 3H); ^{13}C NMR (125 MHz, CDCl_3): δ 197.5, 137.9, 136.9, 133.2, 128.6, 128.4, 128.2, 127.8, 127.7, 114.1, 85.1, 83.7, 82.3, 81.3, 73.7, 70.8, 42.4, 27.4, 25.6; HRMS calc'd for $\text{C}_{23}\text{H}_{26}\text{NaO}_5$ $[\text{M}+\text{Na}]^+$ 405.1672, found 405.1666.

For the reduction of bis(indole) **18b** using NaBH_4 reducing agent:

To a solution of **18b** (57.5 mg, 0.19 mmol) in absolute ethanol (5 mL) was added to NaBH_4 (7.1 mg, 0.19 mmol) and stirred for 3 h at rt. Upon stirring, noticeable formation of red hue was observed. The solution was quenched immediately with dropwise addition of NH_4Cl and extracted with DCM (10 mL, 3x). The organic layer was dried with MgSO_4 , filtered, concentrated and purified using flash column chromatography (20%→30→40% EtOAc in hexane gradient elution).



23a: isolated as a brown oil (with trace EtOAc impurity) in varying yields; $R_f = 0.12$ (faint yellow spot, 7:3 hexanes:EtOAc); IR (cast film): 3324, 3081, 3062, 2859, 1643, 1484 cm^{-1} ^1H NMR (500 MHz, CDCl_3): δ 7.95 (d, $J = 8.6$ Hz, 1H), 7.43 (d, $J = 7.2$ Hz, 1H), 7.39 (s, 1H), 7.33-7.14 (m, 10H), 6.86 (app t, $J = 8.4$ Hz, 2H), 5.91 (d, $J = 6.2$, Hz, 1H), 5.30 (app br s, 2H), 5.18 (br s, 1H). 3.69 (s, 3H), 1.74 (d, $J = 6.1$ Hz, 1H (OH)); ^{13}C NMR (125 MHz, CDCl_3): δ 173.9, 149.4, 137.4, 136.9, 130.3, 128.9, 128.6, 127.8, 127.0, 126.4, 126.1, 122.4, 120.8, 120.3, 120.2, 110.8, 110.3, 110.2, 75.6, 74.9, 53.0, 50.4; HRMS calc'd for $\text{C}_{25}\text{H}_{23}\text{N}_2\text{O}_3$ $[\text{M}+\text{H}]^+$ 399.1703, found 399.1705.

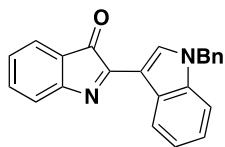


24a: isolated as a brown oil (with trace impurity from EtOAc); $R_f = 0.19$ (faint yellow spot, 7:3 hexanes:EtOAc); ^1H NMR (500 MHz, CDCl_3): δ 8.00 (d, $J = 8.1$ Hz, 1H), 7.42 (d, $J = 7.5$ Hz, 1H), 7.40 (s, 1H), 7.33-7.14 (m, 9H), 6.89-6.86 (m, 2H), 5.92 (d, $J = 6.1$, Hz, 1H), 5.30 (s, 2H), 5.22 (brs, 1H). 4.16 (q, $J = 7.2$ Hz, 1H), 1.79 (d, $J = 6.1$ Hz, 1H (OH)), 1.19 (t, $J = 7.2$ Hz, 3H); ^{13}C NMR (125 MHz, CDCl_3): δ 173.4, 149.5, 137.3, 136.9, 130.2, 128.9, 128.7, 128.6, 127.8, 127.0, 126.3, 126.2, 122.3, 121.1, 120.2, 120.1, 110.8, 110.3, 110.1, 75.6, 74.9, 62.1, 50.3, 14.0; HRMS calc'd for $\text{C}_{26}\text{H}_{25}\text{N}_2\text{O}_3$ $[\text{M}+\text{H}]^+$ 413.1860, found 413.1864.

Synthesis of the *C*-acylimine **25a**:

Indolinone **18a** (0.51 g, 1.3 mmol) was added to a round bottom flask and dissolved in THF and distilled water (13 mL, *ca.* 1:1). Powdered NaOH (0.16 g, 4.0 mmol) was added to the flask. After stirring for 2-3 d in an open flask. The product was diluted with DCM (10 mL) and extracted with water (10 mL, 3x). The organic layer was washed with brine, dried with MgSO₄, and concentrated under reduced pressure. The purple oil was purified by flash column chromatography using 20% EtOAc in hexanes to afford the *C*-acylimine **25a** in 45 - 60% yield. (The yield varies greatly, depending on the time the solution of the starting material and NaOH is left stirring in an open flask.)

(Note: This procedure was adapted by Isaac Zeer-Wanklyn to make the analogues **25c** and **25d**.)



Isolated as a purple solid: $R_f = 0.74$ (purple spot, 7:3 hexanes:EtOAc); IR (cast film): 3050, 2942, 2853, 1718, 1484 cm^{-1} ; ¹H NMR (500 MHz, CDCl₃) δ 8.62 (d, $J = 7.9$ Hz, 1H), 8.49 (s, 1H), 7.47-7.50 (m, 2H), 7.26-7.37 (m, 6H), 7.19 (d, $J = 7.5$, 2H), 7.11 (td, $J = 7.7$ Hz, 0.7 Hz, 1H), 5.40 (s, 2H); ¹³C NMR (125 MHz, CDCl₃) $\delta = 195.9, 163.6, 158.3, 137.2, 137.0, 135.9, 135.6, 129.0, 128.2, 127.4, 127.0, 126.2, 124.5, 123.9, 123.7, 123.0, 122.6, 121.2, 110.5, 107.4, 51.0$; HRMS calc'd for C₂₃H₁₇N₂O [M+H]⁺ 337.1338, found 337.1335.

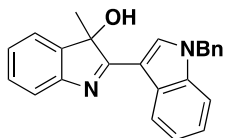
Representative procedure for using Grignard reagents as a nucleophile:

C-Acylimine **25a** (66 mg, 0.20 mmol) was added to a flame-dried round bottom flask, and dissolved in 8 mL of anhydrous toluene. The solution was then cooled in an ice-water bath. Methyl magnesium bromide (100 μL in 3.0 M ether solution, 0.30 mmol) was added to the flask

(dropwise), under a positive pressure of nitrogen and was left stirring for 30 min. At this stage, the reaction mixture changed from an initial deep purple color to a fluorescent yellow solution. The reaction was immediately quenched with a single addition of saturated NH_4Cl (ca. 6 mL). The crude reaction mixture was extracted with DCM (15 mL, 4x), dried with MgSO_4 and concentrated under reduced pressure to afford a light pink oil. The oil was purified via flash column chromatography using equal volumes of 20%, 30% and 40% EtOAc in hexanes added in gradient to afford a yellow oil, **37a**.

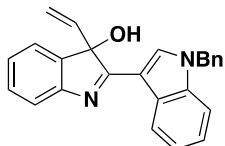
Procedure for using trimethylaluminum reagent:

C-Acylimine **25a** (82 mg, 0.24 mmol) was added to a flame-dried round bottom flask, and dissolved in 8 mL of anhydrous toluene. The solution was then cooled to $-78\text{ }^\circ\text{C}$. Trimethylaluminum (150 μL , 1.2 equiv, 2.0 M in hexanes or toluene solution) was added to the flask (dropwise), under a positive pressure of nitrogen and was left stirring for 30 min. At this stage, the reaction mixture changed from an initial deep purple color to a fluorescent yellow solution. The reaction was immediately quenched with a single addition of saturated NH_4Cl (ca. 6 mL). The crude reaction mixture was extracted with DCM (15 mL, 4x), dried with MgSO_4 and concentrated under reduced pressure to afford a light pink oil. The oil was purified via flash column chromatography using equal volumes of 20%, 30% and 40% EtOAc in hexanes added in gradient to afford 85.1 mg of a yellow oil, **37a**.



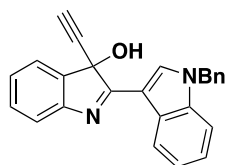
37a: isolated as a yellow oil in quantitative yield: $R_f = 0.33$ (yellow spot, 7:3 hexanes:EtOAc); IR (cast film): 3340, 3053, 2975, 1697, 1641 cm^{-1} ; ^1H NMR (500 MHz, CDCl_3) δ 8.56 (d, $J = 7.5$ Hz, 1H); 7.85 (brs, 1H); 7.32-7.24 (m, 8H); 7.13-7.10 (m, 3H); 7.00-6.96 (m, 1H), 5.22 (d, J

= 16.0 Hz, 1H), 5.03 (d, $J = 16.0$ Hz, 1H), 3.60 (br s, 1H), 1.52 (s, 3H); ^{13}C NMR (125 MHz, CDCl_3) δ 178.3, 153.6, 141.1, 136.7, 136.4, 133.9, 129.4, 129.0, 128.0, 127.0, 126.8, 124.6, 123.5, 123.2, 122.0, 121.5, 120.0, 109.8, 108.5, 84.0, 50.6, 27.1; HRMS calc'd for $\text{C}_{24}\text{H}_{21}\text{N}_2\text{O}$ $[\text{M}+\text{H}]^+$ 353.1646, found 353.1648.



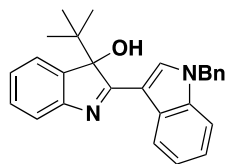
Compound **37b** was prepared by a method analogous to the procedure described for **37a**, using vinylmagnesium bromide in place of methylmagnesium bromide.

37b isolated as a yellow oil in 88% yield: $R_f = 0.35$ (yellow spot, 7:3 hexanes:EtOAc); IR (cast film) 3337, 3049, 2991, 2973, 1694, 1641 cm^{-1} ; ^1H NMR (500 MHz, CDCl_3) δ 8.51 (d, $J = 7.9$ Hz, 1H), 7.74 (s, 1H), 7.18-7.33 (m, 9H), 7.13-7.08 (m, 3H), 6.97 (td, $J = 7.3$ Hz, 0.9 Hz, 1H), 5.75 (dd, $J = 17.2$ Hz, 10.6 Hz, 1H), 5.50 (dd, $J = 17.1$ Hz, 1.5 Hz, 1H), 5.15 (d, $J = 15.8$ Hz, 1H), 5.12 (dd, $J = 10.6$ Hz, 1.5 Hz, 1H), 4.97 (d, $J = 15.8$ Hz, 1H), 3.96 (br s, 1H); ^{13}C NMR (125 MHz, CDCl_3) δ 176.3, 154.5, 139.3, 138.8, 136.5, 136.2, 135.2, 129.6, 128.9, 128.0, 126.9, 124.7, 123.4, 123.0, 122.7, 121.9, 119.9, 113.6, 109.7, 108.6, 86.9, 50.6; HRMS calc'd for $\text{C}_{25}\text{H}_{20}\text{N}_2\text{O}$ $[\text{M}+\text{H}]^+$ 365.1645, found 365.1648. (Note: one ^{13}C resonance was not detected due to overlap.)



Compound **37c** was prepared by a method analogous to the procedure described for **37a**, using alkynylmagnesium bromide in place of methylmagnesium bromide.

37c isolated as a yellow oil in 98% yield: $R_f = 0.31$ (yellow spot, 7:3 hexanes:EtOAc); IR (cast film): 3307, 3054, 2925, 1614 cm^{-1} ; ^1H NMR (500 MHz, CDCl_3) δ 8.35 (d, $J = 7.7$ Hz, 1H), 7.89 (s, 1H), 7.44 (d, $J = 7.3$ Hz, 1H), 7.33-7.24 (m, 5H), 7.19 (d, $J = 7.9$ Hz, 1H), 7.08 (d, $J = 7.25$ Hz, 2H), 6.99-6.93 (m, 3H), 5.06 (br s, 1H) 5.06 (d, $J = 16.0$ Hz, H), 4.82 (d, $J = 16.0$ Hz, 1H), 2.42 (s, 1H); ^{13}C NMR (125 MHz, CDCl_3) δ 173.5, 153.9, 138.0, 136.6, 136.1, 136.0, 130.3, 128.9, 128.0, 126.9, 126.7, 125.0, 123.3, 123.1, 122.6, 122.1, 119.7, 109.7, 107.4, 83.1, 78.1, 74.6, 50.6; HRMS calc'd for $\text{C}_{25}\text{H}_{19}\text{N}_2\text{O}$ $[\text{M}+\text{H}]^+$ 363.1498, found 363.1492.

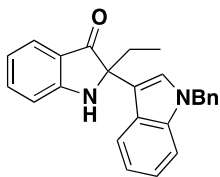


Compound **37d** was prepared analogous to the procedure described for **37a**, using *tert*-butyl Grignard reagent in place of methyl Grignard.

37d; isolated as a yellow oil in *ca.* 13% yield. Partial characterization: $R_f = 0.39$ (yellow spot, 7:3 hexanes:EtOAc); ^1H NMR (500 MHz, CDCl_3) δ 8.60 (d, $J = 7.9$ Hz, 1H), 8.00 (s, 1H), 7.53 (d, $J = 7.3$ Hz, 1H), 7.35-7.26 (m, 6H), 7.24 (t, $J = 8.5$ Hz, 2H), 7.15 (d, $J = 7.3$ Hz, 2H), 7.04 (t, $J = 7.5$ Hz, 1H), 5.27 (s, 2H), 2.40 (br s, 1H), 1.00 (s, 9H); HRMS calc'd for $\text{C}_{27}\text{H}_{27}\text{N}_2\text{O}$ $[\text{M}+\text{H}]^+$ 395.2121, found 395.2118.

Procedure for using diethylzinc as a nucleophile for *C*-acylimine:

C-acylimine **25a** (36 mg, 0.1 mmol) was added to a flame-dried round bottom flask, and dissolved in 3 mL of anhydrous toluene. The solution was then cooled to -78 °C. Diethyl zinc (0.5 mL, 5 equiv, 1.0 M in hexanes solution) was added to the flask (dropwise), under a positive pressure of nitrogen and was left stirring for overnight. At this stage, the solution changed from initial deep purple color to a yellow solution. The reaction was quenched with a single addition of saturated NH₄Cl (ca. 6 mL). The crude reaction mixture was extracted with DCM (15 mL, 4x), dried with MgSO₄ and concentrated under reduced pressure to afford a pink oil. The oil was purified via flash column chromatography using equal volumes of 20%→30→40% EtOAc in hexanes added in gradient to afford an 32 mg of a yellow oil, **38a**. (Note: this reaction is sensitive to oxygen atmosphere, and care must be taken to assure that the flask is tightly sealed prior to addition of organozinc reagent.)

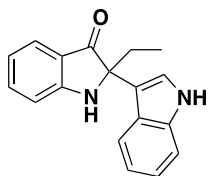


Isolated as a yellow solid in 81% yield: m.p. = 165 °C (decomp.); R_f = 0.41 (yellow spot, 7:3 hexanes:EtOAc); IR (cast film): 3337, 3061, 2964, 1697, 1607 cm^{-1} ; ^1H NMR (500 MHz, CDCl_3) δ 7.66 (d, J = 7.5 Hz, 1H), 7.54 (d, J = 8.0 Hz, 1H), 7.49 (ddd, J = 8.4, 7.2, 1.5 Hz, 1H), 7.22-7.30 (m, 5H), 7.20 (s, 1H), 7.13 (td, J = 7.7, 1.1 Hz, 1H), 7.09-7.11 (m, 2H), 7.02 (ddd, J = 8.1, 7.0, 0.9 Hz, 1H), 6.92 (d, J = 8.3 Hz, 1H), 6.85 (td, J = 7.7, 0.7 Hz, 1H), 5.26 (s, 2H), 2.28-2.33 (m, 2H), 0.910 (t, J = 7.3 Hz, 3H); ^{13}C NMR (125 MHz, CDCl_3) δ 203.1, 160.8, 137.4, 137.3, 137.2, 128.8, 127.7, 126.8, 126.6, 126.0, 125.0, 122.1, 121.1, 120.3, 119.7, 119.0, 114.1,

112.4, 110.2, 69.7, 50.2, 30.6, 8.1; HRMS calc'd for C₂₅H₂₂N₂NaO [M+Na]⁺ 389.1628, found 389.1624.

For the synthesis of halichrome A:

Indolinone **18b** (0.151 g, 0.49 mmol) was added to a round bottom flask and dissolved in THF and distilled water (10 mL, *ca.* 1:1). Powdered NaOH (0.10 g, 2.5 mmol) was added to the flask. After stirring for 2-3 d in an open flask. The product was diluted with DCM (10 mL) and extracted with water (10 mL, 3x). The organic layer was pre-dried with brine, dried with MgSO₄, and concentrated under reduced pressure. The purple oil was purified by flash column chromatography using 20% EtOAc in Hexanes to afford the *C*-acylimine **25b** in 43% yield (52 mg). The purple oil was dissolved in PhMe (7 mL) and treated with diethylzinc (1.0 mL, *ca.* 5 equiv) added dropwise (see note for diethyl zinc reaction) and allowed to stir overnight. At this stage, the solution changed from initial deep purple color to a yellow solution. The reaction was quenched with a single addition of saturated NH₄Cl (15 mL). The crude reaction mixture was extracted with DCM (20 mL, 4x), dried with MgSO₄ and concentrated under reduced pressure to afford a pink oil. The oil was purified via flash column chromatography using equal volumes of 20%→30→40% EtOAc in hexanes in gradient to furnish 43 mg of a yellow solid, **38a**.



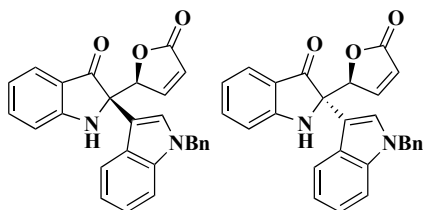
38a: Isolated as a yellow solid in 74% yield (32% over two steps): m.p. = 183 °C (decomp.); R_f = 0.37 (yellow spot, 7:3 hexanes:EtOAc); IR (cast film): 3360, 3276, 3062, 2964, 1667, 1616, 1581 cm⁻¹; ¹H NMR (500 MHz, CDCl₃) δ 8.15 (br s, 1H), 7.66 (d, *J* = 7.7 Hz, 1H), 7.48-7.52 (m,

2H), 7.34 (d, $J = 8.1$ Hz, 1H), 7.26 (s, 1H), 7.20 (d, $J = 2.7$ Hz, 1H), 7.16 (td, $J = 8.1, 0.9$ Hz, 1H), 7.03 (td, $J = 8.1, 0.9$ Hz, 1H), 6.93 (d, $J = 8.3$ Hz, 1H), 6.85 (td, $J = 7.7, 0.6$ Hz, 1H), 5.03 (br s, 1H), 2.28-2.33 (m, 2H), 0.92 (t, $J = 7.3$ Hz, 3H); ^{13}C NMR (125 MHz, CDCl_3) δ 203.2, 160.9, 137.4, 136.9, 125.2, 125.0, 122.5, 122.4, 121.1, 120.0 (2 \times), 119.0, 115.1, 112.4, 111.6, 69.7, 30.4, 8.1; HRMS calc'd for $\text{C}_{18}\text{H}_{16}\text{N}_2\text{NaO}$ $[\text{M}+\text{Na}]^+$ 299.1156, found 299.1155. (Note: the spectral data match the data provided by Abe et al.)^{16b}

For the Brønsted acid catalyzed reaction *C*-acylimine with siloxyfuran:

The *C*-acylimine (34 mg, 0.10 mmol) was dissolved in 1 mL of toluene. Trimethylsiloxyfuran **43** (31 mg, 0.20 mmol, dissolved in 1 mL toluene) was added to the flask, and stirred for 5 min. Chiral phosphoric acid (CPA) (6.8 mg, 0.01 mmol) was added to the flask, and the reaction was stirred for another hour. The reaction was quenched with a single addition of saturated NH_4Cl (ca. 2 mL). The crude reaction mixture was extracted with DCM (5 mL, 4x), dried with MgSO_4 and concentrated under reduced pressure to afford a pink oil. The oil was purified via flash column chromatography using equal volumes of 20%, 30% and 40% EtOAc in hexanes added in gradient to afford separable diastereomers **44a** and **44b**.

Compound **44b**



Minor diastereomer, isolated as a red oil in 21% yield: $R_f = 0.22$ (3:7 EtOAc:hexanes); IR (cast film): 3348, 3063, 2924, 1755, 1694, 1617, 1560 cm^{-1} ; ^1H NMR (500 MHz, CDCl_3) δ 7.75 (d, J

= 7.5 Hz, 1H), 7.67 (d, $J = 8.0$ Hz, 1H), 7.52 (dd, $J = 5.5, 1.5$ Hz, 1H), 7.48 (td, $J = 8.0$ Hz, 1.0 Hz, 1H), 7.36 (s, 1H), 7.26-7.29 (m, 4H), 7.20 (app. t, $J = 6.7$ Hz, 1H), 7.16 (app. t., $J = 7.2$ Hz, 1H), 7.12 (d, $J = 7.3$ Hz, 2H), 6.92 (d, $J = 8.0$ Hz, 1H), 6.89 (d, $J = 7.5$ Hz, 1H), 6.18 (dd, $J = 6.0, 2.0$ Hz, 1H), 5.69 (app. t, $J = 1.5$ Hz, 1H), 5.27 (s, 2H), 5.10 (br s, 1H); ^{13}C NMR (125 MHz, CDCl_3) δ 198.7, 172.1, 160.8, 152.9, 137.9, 137.4, 136.7, 128.9, 127.9, 127.3, 126.8, 125.8, 125.5, 123.8, 122.7, 120.6, 120.4, 120.3, 120.0, 113.1, 110.7, 108.1, 85.8, 69.7, 50.4; HRMS calc'd for $\text{C}_{27}\text{H}_{20}\text{N}_2\text{NaO}_3$ $[\text{M}+\text{Na}]^+$ 443.1371, found 443.1365.

Major diastereomer, isolated as a red oil in 63% yield: $R_f = 0.15$ (3:7 EtOAc:hexanes); IR (cast film): 3348, 3063, 2924, 1755, 1694, 1617, 1560 cm^{-1} , ^1H NMR (500 MHz, CDCl_3) δ 7.69 (d, $J = 7.5$ Hz, 1H), 7.53 (ddd, $J = 8.5, 7.0, 1.0$ Hz, 1H), 7.47 (s, 1H), 7.35 (d, $J = 8.0$ Hz, 1H), 7.25-7.32 (m, 4H), 7.21 (dd, $J = 5.5, 1.5$ Hz, 1H), 7.12-7.17 (m, 3H), 7.02 (td, $J = 8.0, 1.0$ Hz, 1H), 6.93 (t, $J = 7.0$ Hz, 1H), 6.88 (d, $J = 8.5$ Hz, 1H), 6.16 (dd, $J = 5.5, 2.0$ Hz, 1H), 5.85 (app. t, $J = 1.5$ Hz, 1H), 5.30 (s, 2H), 5.13 (br s, 1H); ^{13}C NMR (125 MHz, CDCl_3) δ 199.1, 172.8, 160.9, 151.4, 138.4, 137.1, 136.8, 128.9, 128.4, 127.8, 126.8, 125.6, 125.3, 124.1, 122.5, 120.3, 120.1, 119.9, 119.8, 112.9, 110.5, 110.1, 86.2, 70.1, 50.4 (2 \times); HRMS calc'd for $\text{C}_{27}\text{H}_{20}\text{N}_2\text{NaO}_3$ $[\text{M}+\text{Na}]^+$ 443.1371, found 443.1366.

(Note: due to the freedom of rotation on the bond connecting the furanone to the indolinone, unambiguous assignment was not possible using a through-space correlation.)

4.5 References:

1. (a) Wu, W.; Xiao, M.; Wang, J.; Li, Y.; Xie, Z., *Org. Lett.* **2012**, *14*, 1624-1627; (b) Astolfi, P.; Panagiotaki, M.; Rizzoli, C.; Greci, L., *Org. Biomol. Chem.* **2006**, *4*, 3282.
2. (a) DeAngelis, A.; Dmitrenko, O.; Fox, J. M., *J. Am. Chem. Soc.* **2012**, *134*, 11035-11043; (b) Doyle, M. P.; McKervey, M. A.; Ye, T., *Modern catalytic methods for organic synthesis with diazo compounds: from cyclopropanes to ylides*. Wiley: New York, 1998.
3. Patel, P.; Ramana, C. V., *J. Org. Chem.* **2012**, *77*, 10509-10515.
4. Hirai, Y.; Miyazawa, M.; Awasaguchi, K.-i.; Inoue, K.; Nakamura, K.; Yokoyama, H.; Uoya, I., *Heterocycles* **2010**, *81*, 2105.
5. Boto, A.; Hernández, D.; Hernández, R.; Montoya, A.; Suárez, E., *Eur. J. Org. Chem.* **2007**, 325-334.
6. (a) Tóth, B. L.; Kovács, S.; Sályi, G.; Novák, Z., *Angew. Chem. Int. Ed.* **2016**, *55*, 1988-1992; (b) Stuart, D. R.; Bertrand-Laperle, M. g.; Burgess, K. M. N.; Fagnou, K., *J. Am. Chem. Soc.* **2008**, *130* (49), 16474-16475.
7. (a) Englert, L.; Silber, K.; Steuber, H.; Brass, S.; Over, B.; Gerber, H.-D.; Heine, A.; Diederich, W. E.; Klebe, G., *ChemMedChem* **2010**, *5*, 930-940; (b) Kuroda, N.; Hird, N.; Cork, D. G., *J. Comb. Chem.* **2006**, *8*, 505-512.
8. (a) Pan, F.; Wu, B.; Shi, Z.-J., *Chem. Eur. J.* **2016**, *22*, 6487-6490; (b) Pan, C.; Abdukader, A.; Han, J.; Cheng, Y.; Zhu, C., *Chem. Eur. J.* **2014**, *20*, 3606-3609.
9. Jiao, L.-Y.; Oestreich, M., *Chem. Eur. J.* **2013**, *19*, 10845-10848.
10. Barrett, A. G. M.; Bezuidenhout, B. C. B.; Dhanak, D.; Gasiacki, A. F.; Howell, A. R.; Lee, A. C.; Russell, M. A., *J. Org. Chem.* **1989**, *54*, 3321-3324.

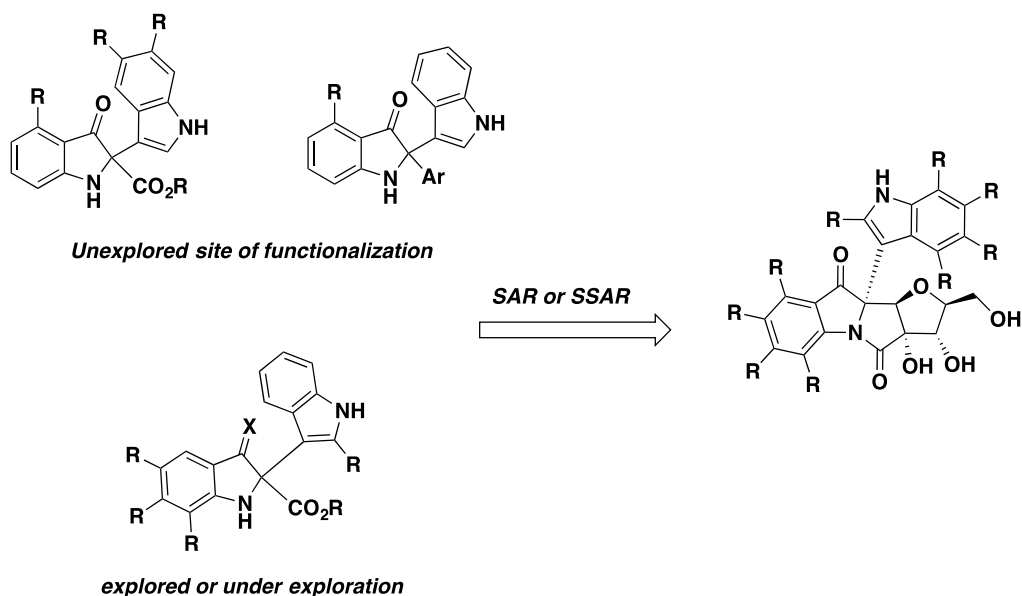
11. (a) Barton, D. H. R.; Camara, J.; Cheng, X.; Géro, S. D.; Jaszberenyi, J. C.; Quiclet-Sire, B., *Tetrahedron* **1992**, *48*, 9261-9276; (b) Barton, D. H. R.; Liu, W., *Tetrahedron* **1997**, *53*, 12067-12088.
12. Neises, B.; Steglich, W., *Angew. Chem. Int. Ed.* **1978**, *17*, 522-524.
13. Bott, T. M.; Atienza, B. J.; West, F. G., *RSC Adv.* **2014**, *4*, 31955-31959.
14. Karadeolian, A.; Kerr, M. A., *J. Org. Chem.* **2010**, *75*, 6830-6841.
15. Yan, X.; Tang, X.-X.; Chen, L.; Yi, Z.-W.; Fang, M.-J.; Wu, Z.; Qiu, Y.-K., *Mar. Drugs* **2014**, *12*, 2156-2163.
16. (a) Netz, N.; Opatz, T., Marine Indole Alkaloids. *Mar. Drugs* **2015**, *13*, 4814-4915; (b) Abe, T.; Kukita, A.; Akiyama, K.; Naito, T.; Uemura, D., *Chem Lett.* **2012**, *41*, 728-729.
17. Niwa, Y.; Takayama, K.; Shimizu, M., *Tetrahedron Lett.* **2001**, *42*, 5473-5476.
18. Yamamoto, Y.; Ito, W., *Tetrahedron* **1988**, *44*, 5415-5423.
19. Dickstein, J. S.; Fennie, M. W.; Norman, A. L.; Paulose, B. J.; Kozlowski, M. C., *J. Am. Chem. Soc.* **2008**, *130*, 15794-15795.
20. Ottoni, O.; Cruz, R.; Alves, R., *Tetrahedron* **1998**, *54*, 13915-13928.
21. Zhao, J.-F.; Tan, B.-H.; Loh, T.-P., *Chem. Sci.* **2011**, *2*, 349-352.

Chapter Five

Summary and Future Directions

In Chapter One, we showed that isatisine A is a natural product with promising antiviral activity and has been synthesized by several research groups. Despite this, the feasibility of truncated analogs of the natural product as antiviral leads has never been described.

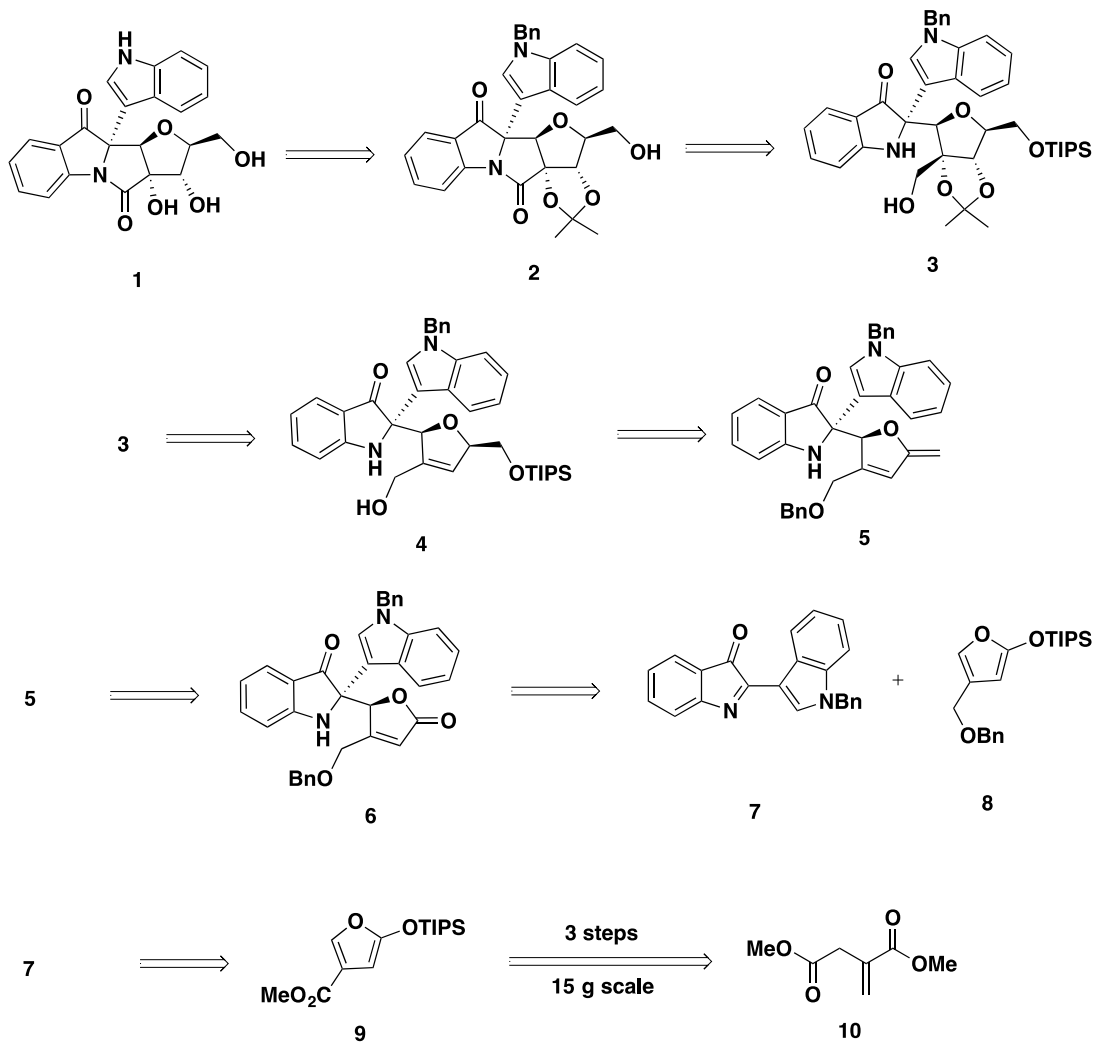
In Chapter Two, we demonstrated that a novel domino/azide metallocarbene coupling which can deliver one third of the carbon skeleton of isatisine A. Through a mechanistic study, we were able to show that this methodology can be used to access the diastereo-, and enantioenriched western fragment of isatisine A (Chapter Three). This allowed us to construct a library of compounds that could be used to probe the antiviral property. With this, several avenues can be considered for future studies (1) extensive analysis of the effect of substituents on the bis(indole) scaffold (Scheme 5.1) and (2) incorporation of relevant substituents to perform a structure activity relationship study (SAR) in which stereochemistry could also be examined through a stereostructure activity relationship study (SSAR) comparing the new compounds to the actual natural product, isatisine A.



Scheme 5.1: More comprehensive SAR and SSAR analysis.

Finally, we showed in Chapter Four that a promising regiodivergent strategy can easily expand the library of compounds to be screened for antiviral properties. This is another avenue that can be considered for future studies. The umpolung reactivity briefly described in Chapter Four can also be considered for future opportunities of research. Furthermore, the efficient addition of siloxyfuran to the C-acylimine opened a new possible route that can be potentially explored. For example, isatisine A can be imagined to come from **2** via benzyl and acetonide deprotection. The synthetic intermediate **2** can be pictured to come from lactamization of primary alcohol **3**. This alcohol can conceivably come from stereoselective allylic dihydroxylation of furanone **4**. Furanone **4** can be envisioned to come from **5** through a regio-, and stereoselective hydroboration oxidation, followed by protection by protection of primary alcohol and selective removal of the benzyl protecting group. This synthetic intermediate can then be envisioned to come the selective olefination of furanone **6**. This furanone could perhaps be accessible using the procedure described in Chapter Four. The siloxyfuran **8** can be made

from ester **9** via reduction and protection with a benzyl protecting group. The ester **9** can be made from dimethyl itaconate **10** via a three step procedure.



Scheme 5.2: Another potential retrosynthesis.

Bibliography

Chapter One:

1. Liu, J. F.; Jiang, Z. Y.; Wang, R. R.; Zheng, Y. T.; Chen, J. J.; Zhang, X. M.; Ma, Y. B., *Org. Lett.* **2007**, *9*, 4127-4129.
2. (a) Karadeolian, A.; Kerr, M. A., *J. Org. Chem.* **2010**, *75*, 6830-6841 (and citations therein); (b) Karadeolian, A.; Kerr, M. A., *Angew. Chem. Int. Ed.* **2010**, *49*, 1133-1135 (and citations therein).
3. (a) Lee, J.; Panek, J. S., *Org. Lett.* **2011**, *13*, 502-505 (and citations therein); (b) Lee, J.; Panek, J. S., *J. Org. Chem.* **2015**, *80*, 2959-2971 (and citations therein).
4. Zhang, X.; Mu, T.; Zhan, F.; Ma, L.; Liang, G., *Angew. Chem. Int. Ed.* **2011**, *50*, 6164-6166 (and citations therein).
5. Wu, W.; Xiao, M.; Wang, J.; Li, Y.; Xie, Z., *Org. Lett.* **2012**, *14*, 1624-1627 (and citations therein).
6. Patel, P.; Ramana, C. V., *J. Org. Chem.* **2012**, *77*, 10509-10515 (and citations therein).
7. Pohlhaus, P. D.; Sanders, S. D.; Parsons, A. T.; Li, W.; Johnson, J. S., *J. Am. Chem. Soc.* **2008**, *130*, 8642-8650.
8. Carson, C. A.; Kerr, M. A., *Angew. Chem. Int. Ed.* **2006**, *45*, 6560-6563.
9. (a) Huang, H.; Panek, J. S., *J. Am. Chem. Soc.* **2000**, *122*, 9836-9837; (b) Lowe, J. T.; Panek, J. S., *Org. Lett.* **2005**, *7*, 3231-3234.
10. Lowe, J. T.; Youngsaye, W.; Panek, J. S., *J. Org. Chem.* **2006**, *71*, 3639-3642.
11. Ager, D. J.; Fleming, I.; Patel, S. K., *J. Chem. Soc., Perkin Trans. 1* **1981**, 2520-2526.
12. Corey, E. J.; Gilman, N. W.; Ganem, B. E., *J. Am. Chem. Soc.* **1968**, *90*, 5616-5617.
13. Li, N. S.; Lu, J.; Piccirilli, J. A., *Org. Lett.* **2007**, *9*, 3009-3012.

14. (a) Kokubun, T.; Edmonds, J.; John, P., *Phytochemistry* **1998**, *49*, 79-87; (b) Maugard, T.; Enaud, E.; Choisy, P.; Legoy, M. D., *Phytochemistry* **2001**, *58*, 897-904.
15. Dötz, K. H.; Otto, F.; Nieger, M., *J. Organomet. Chem.* **2001**, *621*, 77-88.
16. Astolfi, P.; Panagiotaki, M.; Rizzoli, C.; Greci, L., *Org. Biomol. Chem.* **2006**, *4*, 3282.
17. Lewis, M. D.; Cha, J. K.; Kishi, Y., *J. Am. Chem. Soc.* **1982**, *104*, 4976-4978.
18. Ilias, M.; Barman, D. C.; Prajapati, D.; Sandhu, J. S., *Tetrahedron Lett.* **2002**, *43*, 1877-1879.
19. Gunanathan, C.; Ben-David, Y.; Milstein, D., *Science* **2007**, *317*, 790-792.
20. Bott, T. M.; Atienza, B. J.; West, F. G., *RSC Adv.* **2014**, *4*, 31955-31959.

Chapter Two:

1. Fleming, I., *Pericyclic reactions*. Second edition. ed.; Oxford University Press: Oxford, 2015.
2. (a) Singh, M. S., *Reactive intermediates in organic chemistry : structure and mechanism*. (online resource); (b) Olah, G. A.; Prakash, G. K. S., *Carbocation chemistry*. Wiley-Interscience: Hoboken, N.J., 2004. (c) Parsons, A. F., *An introduction to free-radical chemistry*. Blackwell Science: Oxford; Malden, MA, 2000. (d) Perkins, M. J., *Radical chemistry: the fundamentals*. Oxford University Press: Oxford ; New York, 2000. (e) Buncl, E.; Dust, J. M., *Carbanion chemistry: structures and mechanisms*. American Chemical Society ; Oxford University Press: Washington, DC Oxford, 2003.
3. Bott, T. M.; Vanecko, J. A.; West, F. G., *J. Org. Chem.* **2009**, *74*, 2832-2836.
4. (a) Kwon, Y.; Schatz, D. J.; West, F. G., *Angew. Chem. Int. Ed.* **2015**, *54*, 9940-9943; (b) Wu, Y.-K.; McDonald, R.; West, F. G., *Org. Lett.* **2011**, *13*, 3584-3587.

5. Barber, J. S.; Styduhar, E. D.; Pham, H. V.; McMahon, T. C.; Houk, K. N.; Garg, N. K., *J. Am. Chem. Soc.* **2016**, *138*, 2512-2515.
6. Tietze, L.-F.; Brasche, G.; Gericke, K. M., *Domino reactions in organic synthesis*. Wiley-VCH: Weinheim, 2006.
7. Regitz, M.; Maas, G., *Diazo compounds properties and synthesis*. Academic Press: Orlando, 1986 (online resource).
8. (a) Davies, H. M.; Morton, D., *Chem. Soc. Rev.* **2011**, *40*, 1857-1869; (b) Davies, H. M.; Beckwith, R. E., *Chem. Rev.* **2003**, *103*, 2861-2904; (c) Padwa, A.; Weingarten, M. D., *Chem. Rev.* **1996**, *96*, 223-270; (d) Doyle, M. P.; Forbes, D. C., *Chem. Rev.* **1998**, *98*, 911-936.
9. Doyle, M. P.; McKervey, M. A.; Ye, T., *Modern catalytic methods for organic synthesis with diazo compounds : from cyclopropanes to ylides*. Wiley: New York, 1998.
10. Davies, H. M.; Du Bois, J.; Yu, J. Q., *Chem. Soc. Rev.* **2011**, *40*, 1855-1856.
11. Carey, F. A.; Sundberg, R. J., *Advanced organic chemistry. Part B, Reaction and synthesis*. 5th ed.; Springer: New York, 2007.
12. Nakamura, E.; Yoshikai, N.; Yamanaka, M., *J. Am. Chem. Soc.* **2002**, *124*, 7181-7192.
13. Ford, A.; Miel, H.; Ring, A.; Slattery, C. N.; Maguire, A. R.; McKervey, M. A., *Chem. Rev.* **2015**, *115*, 9981-10080.
14. von E. Doering, W.; Knox, L. H., *J. Am. Chem. Soc.* **1956**, *78*, 4947-4950.
15. Chen, B.; Rogachev, A. Y.; Hrovat, D. A.; Hoffmann, R.; Borden, W. T., *J. Am. Chem. Soc.* **2013**, *135*, 13954-13964.
16. Frenking, G.; Solà, M.; Vyboishchikov, S. F., *J Organomet. Chem.* **2005**, *690*, 6178-6204.

17. Davies, H. M. L.; Panaro, S. A., *Tetrahedron* **2000**, *56*, 4871-4880.
18. (a) Werlé, C.; Goddard, R.; Fürstner, A., *Angew. Chemie Int. Ed.* **2015**, *54*, 15452-15456;
(b) Werlé, C.; Goddard, R.; Philipps, P.; Farès, C.; Fürstner, A., *J. Am. Chem. Soc.* **2016**, *138*, 3797-3805.
19. Kornecki, K. P.; Briones, J. F.; Boyarskikh, V.; Fullilove, F.; Autschbach, J.; Schrote, K. E.; Lancaster, K. M.; Davies, H. M. L.; Berry, J. F., *Science* **2013**, *342*, 351-354.
20. Vanecko, J. A.; Wan, H.; West, F. G., *Tetrahedron* **2006**, *62*, 1043-1062.
21. Padwa, A.; Hornbuckle, S. F., *Chem. Rev.* **1991**, *91*, 263-309.
22. Ford, A.; Miel, H.; Ring, A.; Slattery, C. N.; Maguire, A. R.; McKervey, M. A., *Chem. Rev.* **2015**, *115*, 9981-10080.
23. Biswas, B.; Singleton, D. A., *J. Am. Chem. Soc.* **2015**, *137*, 14244-14247.
24. (a) Ollis, W. D.; Rey, M.; Sutherland, I. O., *J. Chem. Soc. Perkin Trans I* **1983**, 1009-1027; (b) Eberlein, T. H.; West, F. G.; Tester, R. W., *J. Org. Chem.* **1992**, *57*, 3479-3482.
25. Vanecko, J. A.; West, F. G., *Org. Lett.* **2005**, *7*, 2949-2952.
26. (a) West, F. G.; Naidu, B. N., *J. Am. Chem. Soc.* **1993**, *115*, 1177-1178; (b) West, F. G.; Naidu, B. N., *J. Org. Chem.* **1994**, *59*, 6051-6056; (c) Bott, T. M.; Vanecko, J. A.; West, F. G., *J. Org. Chem.* **2009**, *74*, 2832-2836.
27. West, F. G.; Glaeske, K. W.; Naidu, B. N., *Synthesis* **1993**, 977-980.
28. Padwa, A.; Snyder, J. P.; Curtis, E. A.; Sheehan, S. M.; Worsencroft, K. J.; Kappe, C. O., *J. Am. Chem. Soc.* **2000**, *122*, 8155-8167.
29. Seeman, J. I., *J. Chem. Ed.* **1986**, *63*, 42.

30. (a) Bräse, S.; Gil, C.; Knepper, K.; Zimmermann, V., *Angew. Chemie Int. Ed.* **2005**, *44*, 5188-5240; (b) Rostami, A.; Wang, Y.; Arif, A. M.; McDonald, R.; West, F. G., *Org. Lett.* **2007**, *9*, 703-706.
31. Hong, K. B.; Donahue, M. G.; Johnston, J. N., *J. Am. Chem. Soc.* **2008**, *130*, 2323-8.
32. Wee, A. G. H.; Slobodian, J., *J. Org. Chem.* **1996**, *61*, 9072.
33. Blond, A.; Moumne, R.; Begis, G.; Pasco, M.; Lecourt, T.; Micouin, L., *Tetrahedron Letters* **2011**, *52*, 3201-3203.
34. Bott, T. M.; Atienza, B. J.; West, F. G., *RSC Adv.* **2014**, *4*, 31955-31959.
35. Mandler, M. D.; Truong, P. M.; Zavalij, P. Y.; Doyle, M. P., *Org. Lett.* **2014**, *16*, 740-743.
36. (a) Wu, X. P.; Su, Y.; Gu, P. M., *Org. Lett.* **2016**, *18*, 1498; (b) Qiao, J.-B.; Zhao, Y.-M.; Gu, P., *Org. Lett.* **2016**, *18*, 1984-1987; (c) Wu, X. P.; Su, Y.; Gu, P. M., *Org. Lett.* **2014**, *16*, 5339-5341.
37. Misaki, T.; Nagase, R.; Matsumoto, K.; Tanabe, Y., *J. Am. Chem. Soc.* **2005**, *127*, 2854-2855.
38. Göbel, M.; Klapötke, T. M., *Adv. Funct. Mater.* **2009**, *19*, 347-365.
39. (a) Doyle, M. P.; Griffin, J. H.; Chinn, M. S.; Vanleusen, D., *J. Org. Chem.* **1984**, *49*, 1917-1925; (b) Clark, J. S.; Krowiak, S. A.; Street, L. J., *Tetrahedron Letters* **1993**, *34*, 4385-4388.
40. (a) Takekuma, S.; Takekuma, H.; Matsubara, Y.; Inaba, K.; Yoshida, Z., *J. Am. Chem. Soc.* **1994**, *116*, 8849-8850; (b) Portela-Cubillo, F.; Scott, J. S.; Walton, J. C., *Chem. Comm.* **2007**, 4041.

41. (a) Abdou, W. M.; Salem, M. A. I.; Sediek, A. A., *Bull. Chem. Soc. Jpn.* **2002**, *75*, 2481-2485; (b) Xie, Z.; Li, L.; Han, M.; Xiao, M., *Synlett* **2011**, *2011*, 1727-1730; (c) Neunhoeffer, O.; Lehmann, G., *Chem. Ber.* **1961**, *94*, 2965-2967; (d) Gosteli, J., *Helv. Chim. Acta* **1977**, *60*, 1980-1983.
42. Okuma, K.; Matsunaga, N.; Nagahora, N.; Shioji, K.; Yokomori, Y., *Chem. Comm.* **2011**, *47*, 5822.
43. (a) Greci, L.; Tommasi, G.; Bruni, P.; Sgarabotto, P.; Righi, L., *Eur. J. Org. Chem.* **2001**, 3147; (b) Boyer, J.; Bernardes-Genisson, V.; Farines, V.; Souchard, J.-P.; Nepveu, F., *Free Radical Research* **2009**, *38*, 459-471.
44. Astolfi, P.; Panagiotaki, M.; Rizzoli, C.; Greci, L., *Org. Biomol. Chem.* **2006**, *4*, 3282.
45. (a) Yuan, Y.; Li, X.; Ding, K., *Org. Lett.* **2002**, *4*, 3309-3311; (b) Alaimo, P. J.; O'Brien, R.; Johnson, A. W.; Slauson, S. R.; O'Brien, J. M.; Tyson, E. L.; Marshall, A.-L.; Ottinger, C. E.; Chacon, J. G.; Wallace, L.; Paulino, C. Y.; Connell, S., *Org. Lett.* **2008**, *10*, 5111-5114; (c) Vaccaro, L.; Pizzo, F.; Lanari, D.; Piermatti, O., *Synthesis* **2012**, *44*, 2181-2184.
46. Johansen, M. B.; Kerr, M. A., *Org. Lett.* **2010**, *12*, 4956-4959.
47. (a) Lian, Y.; Davies, H. M. L., *Org. Lett.* **2012**, *14*, 1934-1937; (b) Lian, Y.; Davies, H. M. L., *Org. Lett.* **2010**, *12*, 924-927.
48. Gibe, R.; Kerr, M. A., *J. Org. Chem.* **2002**, *67*, 6247-6249.
49. (a) Tucker, A. M.; Grundt, P., *Arkivoc* **2012**, *2012*, 546; (b) Jahng, Y., *Archives of Pharmacal Research* **2013**, *36*, 517-535.
50. (a) Mitscher, L. A.; Baker, W., *Med. Res. Rev.* **1998**, *18*, 363-374; (b) Takei, Y.; Kunikata, T.; Aga, M.; Inoue, S.-i.; Ushio, S.; Iwaki, K.; Ikeda, M.; Kurimoto, M., *Biol.*

- Pharm. Bull.* **2003**, *26*, 365-367; (c) Recio, M.-C.; Cerdá-Nicolás, M.; Potterat, O.; Hamburger, M.; Ríos, J.-L., *Planta Med* **2006**, *72*, 539-546; (d) Yang, S.; Li, X.; Hu, F.; Li, Y.; Yang, Y.; Yan, J.; Kuang, C.; Yang, Q., *J. Med. Chem.* **2013**, *56*, 8321-8331.
51. Zhu, S.; Dong, J.; Fu, S.; Jiang, H.; Zeng, W., *Org. Lett.* **2011**, *13*, 4914-4917.
52. Salomon, R. G.; Kochi, J. K., *J. Am. Chem. Soc.* **1973**, *95*, 3300-3310.

Chapter Three:

1. Dick, A. R.; Sanford, M. S., *Tetrahedron* **2006**, *62*, 2439-2463.
2. (a) Lin, Z., *Coord. Chem. Rev.* **2007**, *251* (17-20), 2280-2291; (b) Boutadla, Y.; Davies, D. L.; Macgregor, S. A.; Poblador-Bahamonde, A. I., *Dalton Trans.* **2009**, (30), 5820; (c) Balcells, D.; Clot, E.; Eisenstein, O., *Chem. Rev.* **2010**, *110*, 749-823.
3. (a) Grimster, N. P.; Gauntlett, C.; Godfrey, C. R. A.; Gaunt, M. J., *Angew. Chem. Int. Ed.* **2005**, *44*, 3125-3129; (b) Beck, E. M.; Grimster, N. P.; Hatley, R.; Gaunt, M. J., *J. Am. Chem. Soc.* **2006**, *128*, 2528-2529.
4. Lapointe, D.; Fagnou, K., *Chem. Lett.* **2010**, *39*, 1118-1126.
5. (a) Lane, B. S.; Brown, M. A.; Sames, D., *J. Am. Chem. Soc.* **2005**, *127*, 8050-8057; (b) Park, C.-H.; Ryabova, V.; Seregin, I. V.; Sromek, A. W.; Gevorgyan, V., *Org. Lett.* **2004**, *6*, 1159-1162.
6. Yamamoto, K.; Kimura, S.; Murahashi, T., *Angew. Chem. Int. Ed.* **2016**, *55*, 5322-5326.
7. (a) Phipps, R. J.; Grimster, N. P.; Gaunt, M. J., *J. Am. Chem. Soc.* **2008**, *130*, 8172-8174; (b) Kieffer, M. E.; Chuang, K. V.; Reisman, S. E., *Chem. Sci.* **2012**, *3*, 3170-3174; (c) Kieffer, M. E.; Chuang, K. V.; Reisman, S. E., *J. Am. Chem. Soc.* **2013**, *135*, 5557-5560; (d) Deprez, N. R.; Kalyani, D.; Krause, A.; Sanford, M. S., *J. Am. Chem. Soc.* **2006**, *128*, 4972-4973.

8. Doyle, M. P.; McKervey, M. A.; Ye, T., *Modern catalytic methods for organic synthesis with diazo compounds: from cyclopropanes to ylides*. Wiley: New York, 1998.
9. Salomon, R. G.; Kochi, J. K., *J. Am. Chem. Soc.* **1973**, *95*, 3300-3310.
10. Nakamura, E.; Yoshikai, N.; Yamanaka, M., *J. Am. Chem. Soc.* **2002**, *124*, 7181-7192.
11. Nowlan, D. T.; Gregg, T. M.; Davies, H. M. L.; Singleton, D. A., *J. Am. Chem. Soc.* **2003**, *125*, 15902-15911.
12. Anciaux, A. J.; Hubert, A. J.; Noels, A. F.; Petiniot, N.; Teyssie, P., *J. Org. Chem.* **1980**, *45*, 695-702.
13. (a) Pirrung, M. C.; Morehead, A. T., *J. Am. Chem. Soc.* **1996**, *118*, 8162-8163; (b) Pirrung, M. C.; Liu, H.; Morehead, A. T., *J. Am. Chem. Soc.* **2002**, *124*, 1014-1023.
14. Alonso, M. E.; del Carmen García, M., *Tetrahedron* **1989**, *45*, 69-76.
15. (a) Phipps, R. J.; Gaunt, M. J., *Science* **2009**, *323*, 1593-7; (b) Bigot, A.; Williamson, A. E.; Gaunt, M. J., *J. Am. Chem. Soc.* **2011**, *133*, 13778-13781.
16. Rauniyar, V.; Wang, Z. J.; Burks, H. E.; Toste, F. D., *J. Am. Chem. Soc.* **2011**, *133*, 8486-8489.
17. Deng, X.; Liang, K.; Tong, X.; Ding, M.; Li, D.; Xia, C., *Org. Lett.* **2014**, *16*, 3276-3279.
18. Allen, A. E.; MacMillan, D. W., *J. Am. Chem. Soc.* **2011**, *133*, 4260-4263.
19. (a) Clark, J. S.; Hansen, K. E., *Chem. Eur. J.* **2014**, *20*, 5454-5459; (b) Clark, J. S.; Berger, R.; Hayes, S. T.; Senn, H. M.; Farrugia, L. J.; Thomas, L. H.; Morrison, A. J.; Gobbi, L., *J. Org. Chem.* **2013**, *78*, 673-696; (c) Clark, J. S.; Vignard, D.; Parkin, A., *Org. Lett.* **2011**, *13*, 3980-3983; (d) Clark, J. S.; Labre, F.; Thomas, L. H., *Org. Biomol. Chem.* **2011**, *9*, 4823; (e) Clark, J. S.; Walls, S. B.; Wilson, C.; East, S. P.; Drysdale, M. J., *Eur. J. Org. Chem.* **2006**, *2006*, 323-327.

20. Marmsäter, F. P.; Vanecko, J. A.; West, F. G., *Org. Lett.* **2004**, *6*, 1657-1660.
21. S. Baran, P.; Jessing, M., *Heterocycles* **2010**, *82*, 1739.
22. Bott, T. M.; Atienza, B. J.; West, F. G., *RSC Adv.* **2014**, *4*, 31955-31959.
23. Fier, P. S.; Luo, J.; Hartwig, J. F., *J. Am. Chem. Soc.* **2013**, *135*, 2552-2559.
24. Desimoni, G.; Faita, G.; Jørgensen, K. A., *Chem. Rev.* **2006**, *106*, 3561-3651.
25. Mandler, M. D.; Truong, P. M.; Zavalij, P. Y.; Doyle, M. P., *Org. Lett.* **2014**, *16*, 740-743.
26. Nozaki, H.; Takaya, H.; Moriuti, S.; Noyori, R., *Tetrahedron* **1968**, *24*, 3655-3669.
27. Noland, W. E.; Vijay Kumar, H.; Lu, C.; Brown, C. D.; Wiley-Schaber, E.; Johansson, A.; LaBelle, E. V.; O'Brian, N. C.; Jensen, R. C.; Tritch, K. J., *Tetrahedron Lett.* **2016**, *57* (20), 2158-2160.
28. Crampton, M. R.; Robotham, I. A., *J. Chem. Res.* **1997**, 22-23.
29. Misaki, T.; Nagase, R.; Matsumoto, K.; Tanabe, Y., *J. Am. Chem. Soc.* **2005**, *127*, 2854-2855.
30. Yin, Q.; You, S.-L., *Chem. Sci.* **2011**, *2*, 1344.
31. Corey, E. J.; Ensley, H. E., *J. Am. Chem. Soc.* **1975**, *97*, 6908-6909.
32. Ort, O., *Organic Syntheses* **1987**, *65*, 203.
33. Halgren, T. A., *J. Comput. Chem.* **1996**, *17*, 490-519.
34. Seeman, J. I., *J. Chem. Ed.* **1986**, *63*, 42.
35. Berrisford, D. J.; Bolm, C.; Sharpless, K. B., *Angew. Chem. Int. Ed.* **1995**, *34*, 1059-1070.
36. Hong, L.; Sun, W.; Yang, D.; Li, G.; Wang, R., *Chem. Rev.* **2016**, *116*, 4006-4123.
37. Zhang, X.; Mu, T.; Zhan, F.; Ma, L.; Liang, G., *Angew. Chem. Int. Ed.* **2011**, *50*, 6164-6166.

38. Liu, C.; Zhu, Q.; Huang, K.-W.; Lu, Y., *Org. Lett.* **2011**, *13*, 2638-2641.
39. Parmar, D.; Sugiono, E.; Raja, S.; Rueping, M., *Chem. Rev.* **2014**, *114*, 9047-9153.
40. Christ, P.; Lindsay, A. G.; Vormittag, S. S.; Neudörfl, J.-M.; Berkessel, A.; O'Donoghue, A. C., *Chem. Eur. J.* **2011**, *17*, 8524-8528.
41. Rueping, M.; Raja, S., *Beilstein J. Org. Chem.* **2012**, *8*, 1819-1824.
42. Momiyama, N.; Nishimoto, H.; Terada, M., *Org. Lett.* **2011**, *13*, 2126-2129.
43. Storer, R. I.; Carrera, D. E.; Ni, Y.; MacMillan, D. W. C., *J. Am. Chem. Soc.* **2006**, *128*, 84-86.
44. Momiyama, N.; Okamoto, H.; Kikuchi, J.; Korenaga, T.; Terada, M., *ACS Catal.* **2016**, *6*, 1198-1204.
45. (a) Karadeolian, A.; Kerr, M. A., *J. Org. Chem.* **2010**, *75*, 6830-6841; (b) Karadeolian, A.; Kerr, M. A., *Angew. Chem. Int. Ed.* **2010**, *49*, 1133-1135.

Chapter Four:

1. (a) Wu, W.; Xiao, M.; Wang, J.; Li, Y.; Xie, Z., *Org. Lett.* **2012**, *14*, 1624-1627; (b) Astolfi, P.; Panagiotaki, M.; Rizzoli, C.; Greci, L., *Org. Biomol. Chem.* **2006**, *4*, 3282.
2. (a) DeAngelis, A.; Dmitrenko, O.; Fox, J. M., *J. Am. Chem. Soc.* **2012**, *134*, 11035-11043; (b) Doyle, M. P.; McKervey, M. A.; Ye, T., *Modern catalytic methods for organic synthesis with diazo compounds: from cyclopropanes to ylides*. Wiley: New York, 1998.
3. Patel, P.; Ramana, C. V., *J. Org. Chem.* **2012**, *77*, 10509-10515.
4. Hirai, Y.; Miyazawa, M.; Awasaguchi, K.-i.; Inoue, K.; Nakamura, K.; Yokoyama, H.; Uoya, I., *Heterocycles* **2010**, *81*, 2105.
5. Boto, A.; Hernández, D.; Hernández, R.; Montoya, A.; Suárez, E., *Eur. J. Org. Chem.* **2007**, 325-334.

6. (a) Tóth, B. L.; Kovács, S.; Sályi, G.; Novák, Z., *Angew. Chem. Int. Ed.* **2016**, *55*, 1988-1992; (b) Stuart, D. R.; Bertrand-Laperle, M. g.; Burgess, K. M. N.; Fagnou, K., *J. Am. Chem. Soc.* **2008**, *130* (49), 16474-16475.
7. (a) Englert, L.; Silber, K.; Steuber, H.; Brass, S.; Over, B.; Gerber, H.-D.; Heine, A.; Diederich, W. E.; Klebe, G., *ChemMedChem* **2010**, *5*, 930-940; (b) Kuroda, N.; Hird, N.; Cork, D. G., *J. Comb. Chem.* **2006**, *8*, 505-512.
8. (a) Pan, F.; Wu, B.; Shi, Z.-J., *Chem. Eur. J.* **2016**, *22*, 6487-6490; (b) Pan, C.; Abdukader, A.; Han, J.; Cheng, Y.; Zhu, C., *Chem. Eur. J.* **2014**, *20*, 3606-3609.
9. Jiao, L.-Y.; Oestreich, M., *Chem. Eur. J.* **2013**, *19*, 10845-10848.
10. Barrett, A. G. M.; Bezuidenhout, B. C. B.; Dhanak, D.; Gasielki, A. F.; Howell, A. R.; Lee, A. C.; Russell, M. A., *J. Org. Chem.* **1989**, *54*, 3321-3324.
11. (a) Barton, D. H. R.; Camara, J.; Cheng, X.; Géro, S. D.; Jaszberenyi, J. C.; Quiclet-Sire, B., *Tetrahedron* **1992**, *48*, 9261-9276; (b) Barton, D. H. R.; Liu, W., *Tetrahedron* **1997**, *53*, 12067-12088.
12. Neises, B.; Steglich, W., *Angew. Chem. Int. Ed.* **1978**, *17*, 522-524.
13. Bott, T. M.; Atienza, B. J.; West, F. G., *RSC Adv.* **2014**, *4*, 31955-31959.
14. Karadeolian, A.; Kerr, M. A., *J. Org. Chem.* **2010**, *75*, 6830-6841.
15. Yan, X.; Tang, X.-X.; Chen, L.; Yi, Z.-W.; Fang, M.-J.; Wu, Z.; Qiu, Y.-K., *Mar. Drugs* **2014**, *12*, 2156-2163.
16. (a) Netz, N.; Opatz, T., Marine Indole Alkaloids. *Mar. Drugs* **2015**, *13*, 4814-4915; (b) Abe, T.; Kukita, A.; Akiyama, K.; Naito, T.; Uemura, D., *Chem Lett.* **2012**, *41*, 728-729.
17. Niwa, Y.; Takayama, K.; Shimizu, M., *Tetrahedron Lett.* **2001**, *42*, 5473-5476.
18. Yamamoto, Y.; Ito, W., *Tetrahedron* **1988**, *44*, 5415-5423.

19. Dickstein, J. S.; Fennie, M. W.; Norman, A. L.; Paulose, B. J.; Kozlowski, M. C., *J. Am. Chem. Soc.* **2008**, *130*, 15794-15795.
20. Ottoni, O.; Cruz, R.; Alves, R., *Tetrahedron* **1998**, *54*, 13915-13928.
21. Zhao, J.-F.; Tan, B.-H.; Loh, T.-P., *Chem. Sci.* **2011**, *2*, 349-352.

Appendix I: X-ray Crystallographic Data for compound 29d. (Chapter Two)

STRUCTURE REPORT

XCL Code: FGW1501

Date: 23 February 2015

Compound: Methyl 2-diazo-3-(2-azido-3-methylphenyl)-3-oxopropanoate

Formula: C₁₁H₉N₅O₃

Supervisor: F. G. West

Crystallographer: R. McDonald

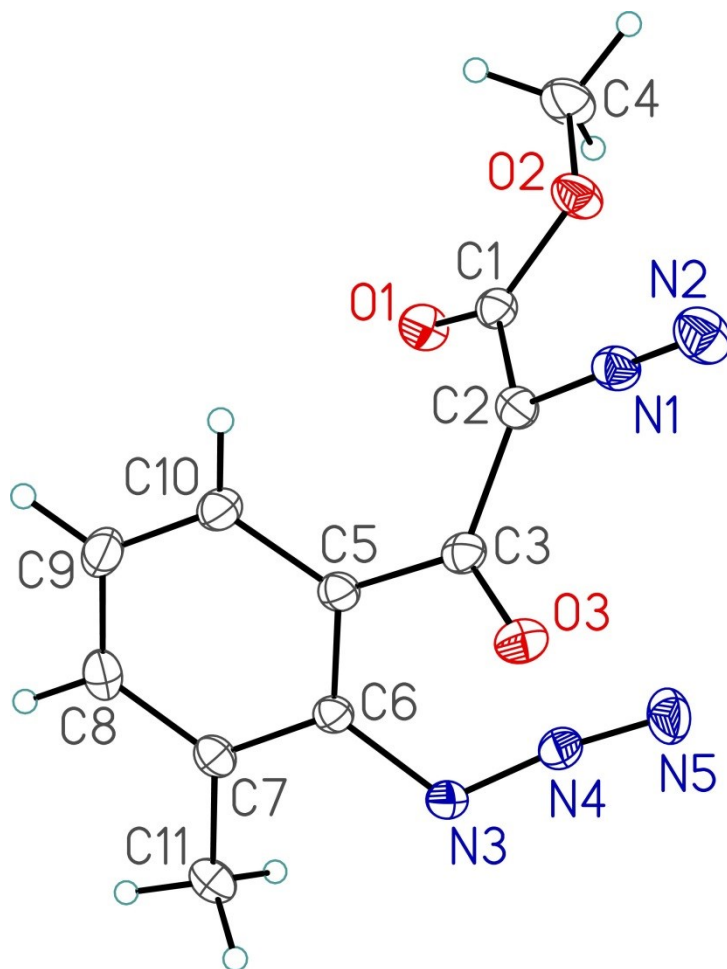
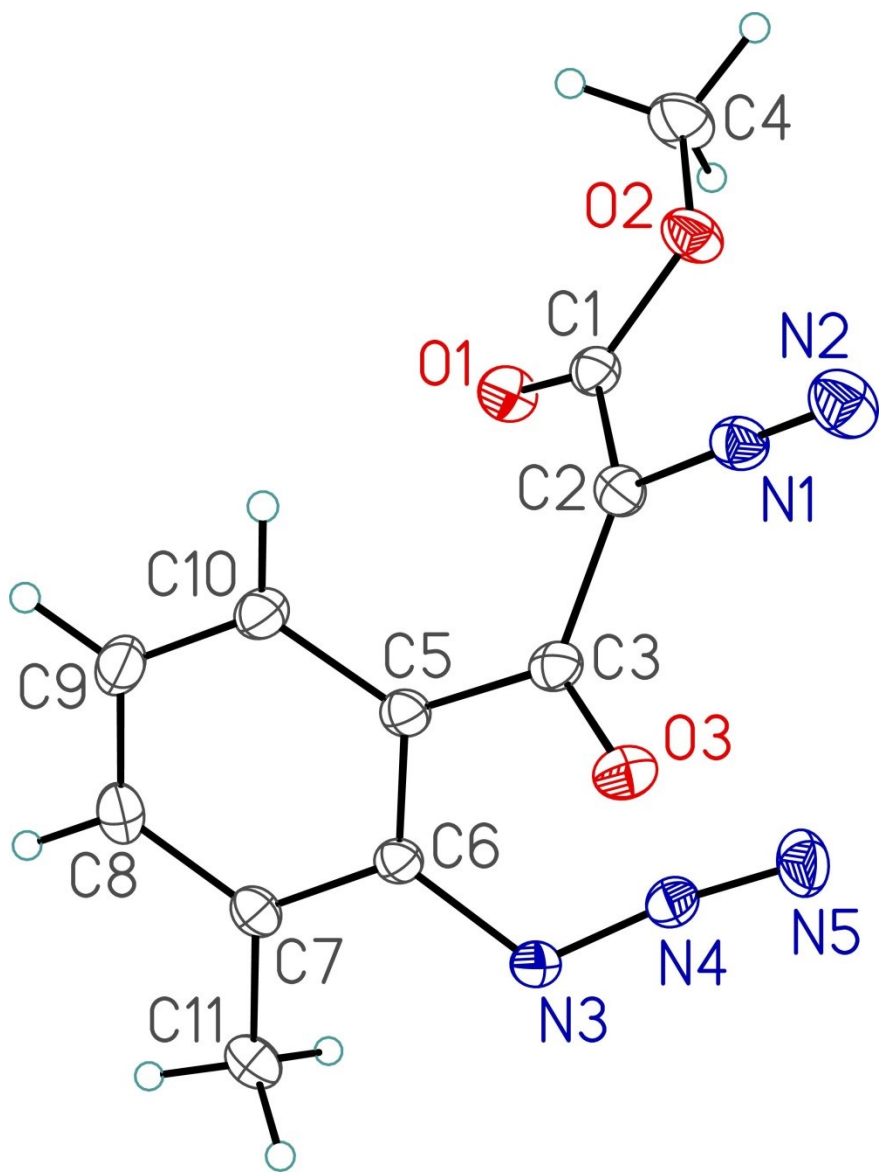
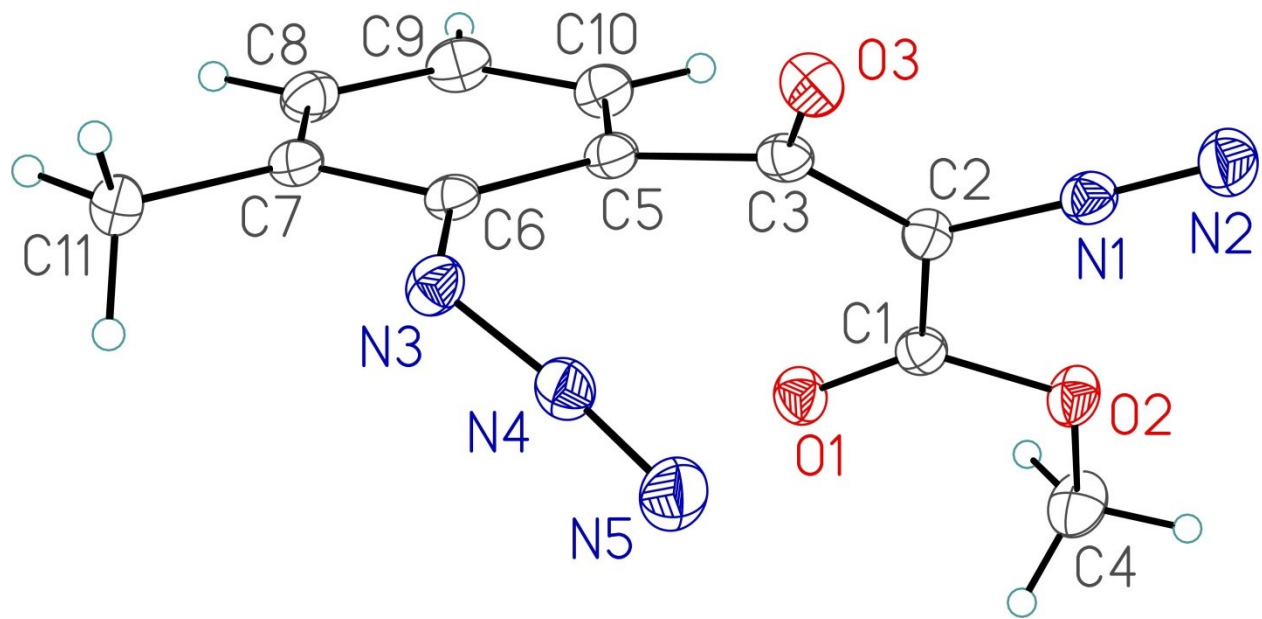


Figure Legends

- Figure 1.** Perspective view of the methyl 2-diazo-3-(2-azido-3-methylphenyl)-3-oxopropanoate molecule showing the atom labelling scheme. Non-hydrogen atoms are represented by Gaussian ellipsoids at the 30% probability level. Hydrogen atoms are shown with arbitrarily small thermal parameters.
- Figure 2.** Alternate view of the molecule.





List of Tables

- Table 1.** Crystallographic Experimental Details
- Table 2.** Atomic Coordinates and Equivalent Isotropic Displacement Parameters
- Table 3.** Selected Interatomic Distances
- Table 4.** Selected Interatomic Angles
- Table 5.** Torsional Angles
- Table 6.** Anisotropic Displacement Parameters
- Table 7.** Derived Atomic Coordinates and Displacement Parameters for Hydrogen Atoms

Table 1. Crystallographic Experimental Details*A. Crystal Data*

formula	C ₁₁ H ₉ N ₅ O ₃
formula weight	259.23
crystal dimensions (mm)	0.26 × 0.18 × 0.06
crystal system	triclinic
space group	$P\bar{1}$ (No. 2)
unit cell parameters ^a	
<i>a</i> (Å)	7.3874 (3)
<i>b</i> (Å)	8.0591 (4)
<i>c</i> (Å)	10.8556 (5)
α (deg)	96.711 (2)
β (deg)	104.962 (2)
γ (deg)	105.019 (2)
<i>V</i> (Å ³)	591.25 (5)
<i>Z</i>	2
ρ _{calcd} (g cm ⁻³)	1.456
μ (mm ⁻¹)	0.938

B. Data Collection and Refinement Conditions

diffractometer	Bruker D8/APEX II CCD ^b
radiation (λ [Å])	Cu Kα (1.54178) (microfocus source)
temperature (°C)	-100
scan type	ω and φ scans (1.0°) (5 s exposures)
data collection 2θ limit (deg)	148.11
total data collected	4241 (-9 ≤ <i>h</i> ≤ 9, -10 ≤ <i>k</i> ≤ 10, -12 ≤ <i>l</i> ≤ 10)
independent reflections	2302 (<i>R</i> _{int} = 0.0177)
number of observed reflections (<i>NO</i>)	2041 [<i>F</i> _o ² ≥ 2σ(<i>F</i> _o ²)]
structure solution method	direct methods/dual space (<i>SHELXD</i> ^c)
refinement method	full-matrix least-squares on <i>F</i> ² (<i>SHELXL-2014</i> ^d)
absorption correction method	Gaussian integration (face-indexed)
range of transmission factors	1.0000–0.7941
data/restraints/parameters	2302 / 0 / 173
goodness-of-fit (<i>S</i>) ^e [all data]	1.056
final <i>R</i> indices ^f	
<i>R</i> ₁ [<i>F</i> _o ² ≥ 2σ(<i>F</i> _o ²)]	0.0328
<i>wR</i> ₂ [all data]	0.0919
largest difference peak and hole	0.205 and -0.202 e Å ⁻³

^aObtained from least-squares refinement of 8057 reflections with 8.60° < 2θ < 147.26°.

(continued)

Table 1. Crystallographic Experimental Details (continued)

^bPrograms for diffractometer operation, data collection, data reduction and absorption correction were those supplied by Bruker.

^cSchneider, T. R.; Sheldrick, G. M. *Acta Crystallogr.* **2002**, *D58*, 1772-1779.

^dSheldrick, G. M. *Acta Crystallogr.* **2015**, *C71*, 3–8.

^e $S = [\sum w(F_o^2 - F_c^2)^2 / (n - p)]^{1/2}$ (n = number of data; p = number of parameters varied; $w = [\sum^2(F_o^2) + (0.0478P)^2 + 0.1063P]^{-1}$ where $P = [\text{Max}(F_o^2, 0) + 2F_c^2]/3$).

^f $R_1 = \sum ||F_o| - |F_c|| / \sum |F_o|$; $wR_2 = [\sum w(F_o^2 - F_c^2)^2 / \sum w(F_o^4)]^{1/2}$.

Table 2. Atomic Coordinates and Equivalent Isotropic Displacement Parameters

Atom	<i>x</i>	<i>y</i>	<i>z</i>	$U_{\text{eq}}, \text{\AA}^2$
O1	-0.07602(14)	0.15849(12)	0.28047(9)	0.0373(2)*
O2	-0.25483(14)	-0.02104(11)	0.08773(9)	0.0375(2)*
O3	0.20502(12)	0.45497(12)	0.04030(9)	0.0339(2)*
N1	-0.10557(15)	0.17607(13)	-0.04501(11)	0.0307(2)*
N2	-0.16065(18)	0.12711(15)	-0.15233(12)	0.0423(3)*
N3	0.53984(15)	0.54061(13)	0.29694(11)	0.0311(2)*
N4	0.50845(14)	0.39319(14)	0.23327(10)	0.0323(2)*
N5	0.50398(18)	0.26352(17)	0.17828(13)	0.0472(3)*
C1	-0.12195(17)	0.12608(15)	0.16376(12)	0.0284(3)*
C2	-0.03805(17)	0.23957(15)	0.08344(12)	0.0279(3)*
C3	0.12419(16)	0.40244(15)	0.12011(12)	0.0277(3)*
C4	-0.3431(2)	-0.14712(18)	0.15611(15)	0.0458(4)*
C5	0.18178(17)	0.50743(14)	0.25427(12)	0.0268(3)*
C6	0.37961(16)	0.58351(14)	0.32923(12)	0.0257(2)*
C7	0.43267(18)	0.70758(15)	0.44360(12)	0.0298(3)*
C8	0.2830(2)	0.74842(17)	0.48445(13)	0.0354(3)*
C9	0.0863(2)	0.67049(18)	0.41412(14)	0.0385(3)*
C10	0.03663(18)	0.55175(16)	0.29976(13)	0.0340(3)*
C11	0.64570(19)	0.79096(17)	0.52118(13)	0.0371(3)*

Anisotropically-refined atoms are marked with an asterisk (*). The form of the anisotropic displacement parameter is: $\exp[-2\pi^2(h^2a^*{}^2U_{11} + k^2b^*{}^2U_{22} + l^2c^*{}^2U_{33} + 2klb^*c^*U_{23} + 2hla^*c^*U_{13} + 2hka^*b^*U_{12})]$.

Table 3. Selected Interatomic Distances (Å)

Atom1	Atom2	Distance	Atom1	Atom2	Distance
O1	C1	1.2014(15)	C2	C3	1.4608(16)
O2	C1	1.3417(15)	C3	C5	1.4912(17)
O2	C4	1.4464(15)	C5	C6	1.4067(16)
O3	C3	1.2281(15)	C5	C10	1.3971(16)
N1	N2	1.1150(15)	C6	C7	1.3966(17)
N1	C2	1.3405(16)	C7	C8	1.3912(18)
N3	N4	1.2351(14)	C7	C11	1.5075(17)
N3	C6	1.4288(14)	C8	C9	1.3893(19)
N4	N5	1.1294(15)	C9	C10	1.3771(19)
C1	C2	1.4671(17)			

Table 4. Selected Interatomic Angles (deg)

Atom1	Atom2	Atom3	Angle	Atom1	Atom2	Atom3	Angle
C1	O2	C4	115.24(10)	C3	C5	C6	122.07(10)
N2	N1	C2	178.39(12)	C3	C5	C10	118.69(11)
N4	N3	C6	118.27(10)	C6	C5	C10	118.63(11)
N3	N4	N5	171.57(12)	N3	C6	C5	123.77(11)
O1	C1	O2	124.96(12)	N3	C6	C7	114.94(10)
O1	C1	C2	125.08(11)	C5	C6	C7	121.29(11)
O2	C1	C2	109.95(10)	C6	C7	C8	117.91(11)
N1	C2	C1	115.50(10)	C6	C7	C11	120.63(11)
N1	C2	C3	113.33(11)	C8	C7	C11	121.45(12)
C1	C2	C3	130.74(11)	C7	C8	C9	121.69(12)
O3	C3	C2	120.55(11)	C8	C9	C10	119.69(11)
O3	C3	C5	120.99(11)	C5	C10	C9	120.72(12)
C2	C3	C5	118.38(10)				

Table 5. Torsional Angles (deg)

Atom1	Atom2	Atom3	Atom4	Angle	Atom1	Atom2	Atom3	Atom4	Angle
C4	O2	C1	O1	-0.96(18)	C2	C3	C5	C10	-52.14(15)
C4	O2	C1	C2	177.80(11)	C3	C5	C6	N3	-12.93(17)
N4	N3	C6	C5	-27.50(17)	C3	C5	C6	C7	167.79(11)
N4	N3	C6	C7	151.82(11)	C10	C5	C6	N3	176.11(11)
O1	C1	C2	N1	177.94(11)	C10	C5	C6	C7	-3.18(17)
O1	C1	C2	C3	6.0(2)	C3	C5	C10	C9	-169.81(12)
O2	C1	C2	N1	-0.82(14)	C6	C5	C10	C9	1.46(18)
O2	C1	C2	C3	-172.71(11)	N3	C6	C7	C8	-176.62(10)
N1	C2	C3	O3	-10.64(16)	N3	C6	C7	C11	2.08(16)
N1	C2	C3	C5	166.22(10)	C5	C6	C7	C8	2.72(17)
C1	C2	C3	O3	161.39(12)	C5	C6	C7	C11	-178.58(11)
C1	C2	C3	C5	-21.75(18)	C6	C7	C8	C9	-0.56(19)
O3	C3	C5	C6	-46.25(16)	C11	C7	C8	C9	-179.26(12)
O3	C3	C5	C10	124.71(12)	C7	C8	C9	C10	-1.1(2)
C2	C3	C5	C6	136.91(11)	C8	C9	C10	C5	0.6(2)

Table 6. Anisotropic Displacement Parameters (U_{ij} , Å²)

Atom	U_{11}	U_{22}	U_{33}	U_{23}	U_{13}	U_{12}
O1	0.0398(5)	0.0381(5)	0.0312(5)	0.0080(4)	0.0098(4)	0.0073(4)
O2	0.0426(5)	0.0289(5)	0.0343(5)	0.0057(4)	0.0129(4)	-0.0013(4)
O3	0.0292(4)	0.0388(5)	0.0341(5)	0.0111(4)	0.0113(4)	0.0075(4)
N1	0.0300(5)	0.0267(5)	0.0347(6)	0.0080(4)	0.0093(4)	0.0069(4)
N2	0.0492(7)	0.0384(6)	0.0336(7)	0.0062(5)	0.0102(5)	0.0062(5)
N3	0.0256(5)	0.0272(5)	0.0390(6)	0.0038(4)	0.0107(4)	0.0058(4)
N4	0.0241(5)	0.0358(6)	0.0364(6)	0.0048(4)	0.0074(4)	0.0108(4)
N5	0.0403(6)	0.0446(7)	0.0530(8)	-0.0060(6)	0.0068(5)	0.0206(5)
C1	0.0257(5)	0.0276(6)	0.0329(7)	0.0064(5)	0.0090(5)	0.0092(4)
C2	0.0276(6)	0.0266(6)	0.0284(6)	0.0046(4)	0.0070(4)	0.0078(5)
C3	0.0230(5)	0.0278(6)	0.0347(7)	0.0096(5)	0.0082(4)	0.0106(4)
C4	0.0516(8)	0.0341(7)	0.0471(9)	0.0099(6)	0.0223(7)	-0.0032(6)
C5	0.0261(6)	0.0229(5)	0.0327(7)	0.0084(4)	0.0095(5)	0.0077(4)
C6	0.0260(6)	0.0219(5)	0.0317(6)	0.0097(4)	0.0108(4)	0.0074(4)
C7	0.0347(6)	0.0237(5)	0.0312(7)	0.0089(4)	0.0091(5)	0.0085(5)
C8	0.0473(7)	0.0291(6)	0.0336(7)	0.0055(5)	0.0149(5)	0.0153(5)
C9	0.0404(7)	0.0382(7)	0.0472(8)	0.0105(6)	0.0223(6)	0.0190(6)
C10	0.0279(6)	0.0331(6)	0.0439(8)	0.0092(5)	0.0135(5)	0.0109(5)
C11	0.0378(7)	0.0304(6)	0.0349(7)	0.0032(5)	0.0038(5)	0.0051(5)

The form of the anisotropic displacement parameter is:

$$\exp[-2\pi^2(h^2a^*2U_{11} + k^2b^*2U_{22} + l^2c^*2U_{33} + 2klb^*c^*U_{23} + 2hla^*c^*U_{13} + 2hka^*b^*U_{12})]$$

Table 7. Derived Atomic Coordinates and Displacement Parameters for Hydrogen Atoms

Atom	x	y	z	U_{eq} , Å ²
H4A	-0.4376	-0.2496	0.0931	0.055
H4B	-0.2405	-0.1835	0.2133	0.055
H4C	-0.4111	-0.0937	0.2083	0.055
H8	0.3161	0.8317	0.5624	0.042
H9	-0.0134	0.6990	0.4448	0.046
H10	-0.0978	0.4994	0.2513	0.041
H11A	0.6554	0.8749	0.5974	0.045
H11B	0.7169	0.8521	0.4669	0.045
H11C	0.7033	0.7001	0.5498	0.045

Appendix II: X-ray Crystallographic Data for compound 22 (Chapter Three)

STRUCTURE REPORT

XCL Code: FGW1320

Date: 21 November 2013

Compound: Methyl 3-oxo-1,3-dihydro-1'*H*,2*H*-2,3'-biindole-2-carboxylate

Formula: C₁₈H₁₄N₂O₃

Supervisor: F. G. West

Crystallographer: R. McDonald

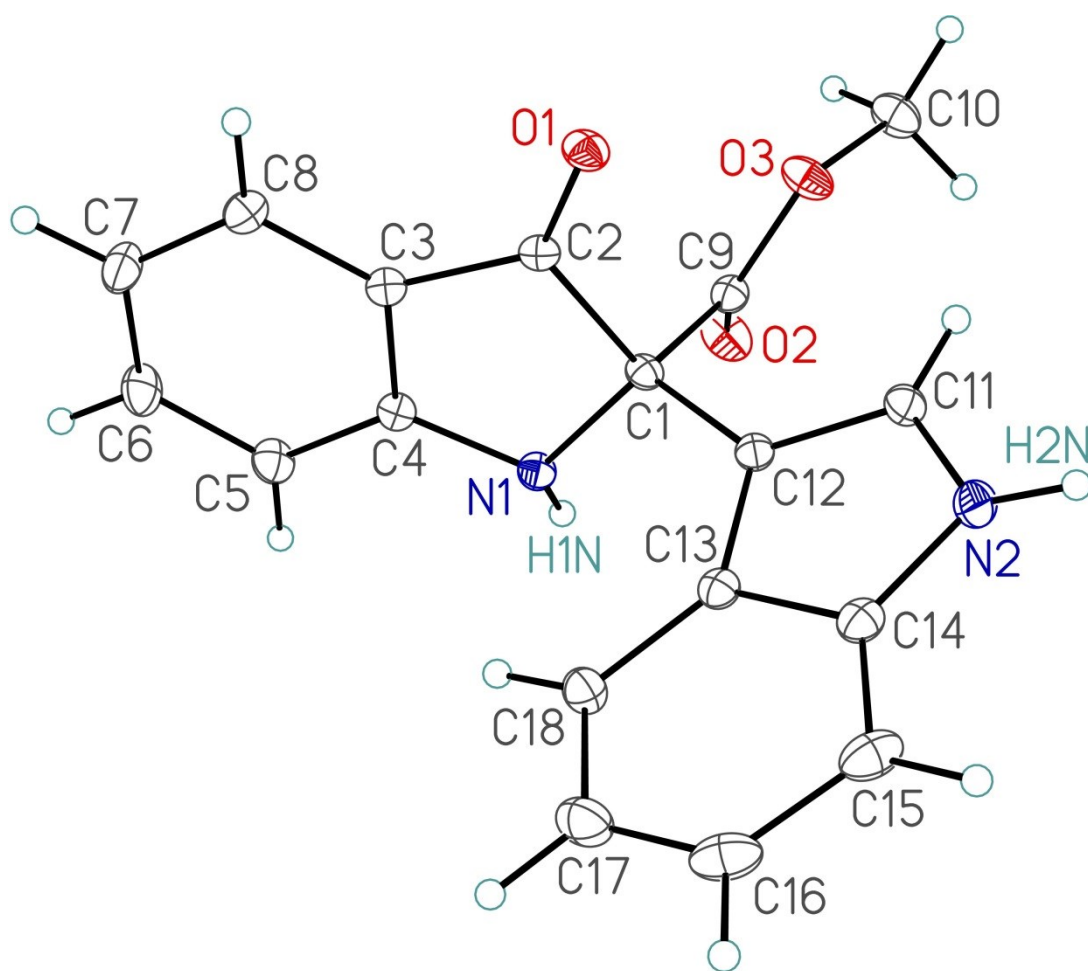
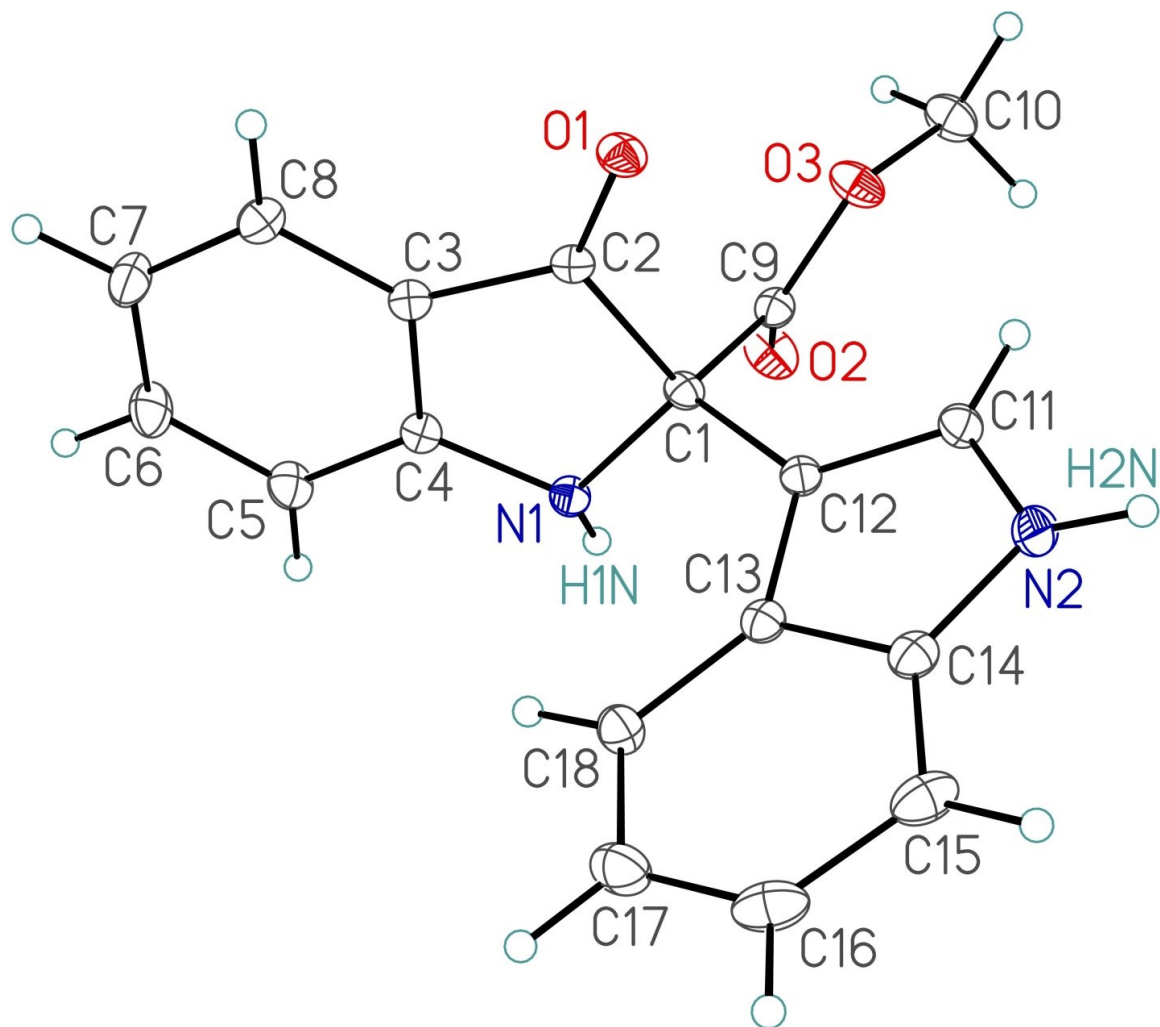
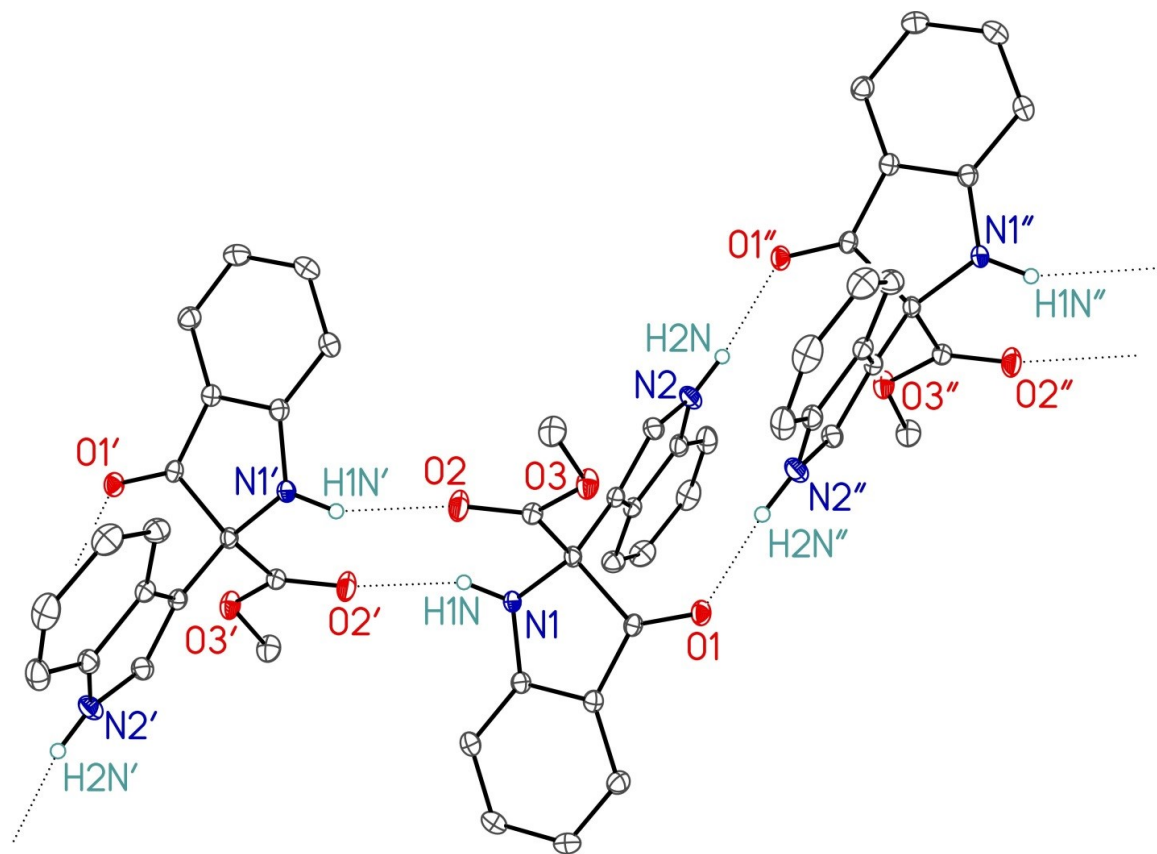


Figure Legends

- Figure 1.** Perspective view of the methyl 3-oxo-1,3-dihydro-1'*H*,2*H*-2,3'-biindole-2-carboxylate molecule showing the atom labelling scheme. Non-hydrogen atoms are represented by Gaussian ellipsoids at the 30% probability level. Hydrogen atoms are shown with arbitrarily small thermal parameters.
- Figure 2.** Illustration of hydrogen-bonded interactions (shown with dotted lines) between adjacent molecules in the crystal lattice. Primed atoms are related to unprimed ones via the crystallographic inversion center ($1/2, 0, 1/2$). Double-primed atoms are related to unprimed ones via the crystallographic inversion center ($0, 0, 1/2$). The chain propagates in a direction parallel to the crystal unit cell's *a* axis.





List of Tables

- Table 1.** Crystallographic Experimental Details
- Table 2.** Atomic Coordinates and Equivalent Isotropic Displacement Parameters
- Table 3.** Selected Interatomic Distances
- Table 4.** Selected Interatomic Angles
- Table 5.** Hydrogen-Bonded Interactions
- Table 6.** Torsional Angles
- Table 7.** Anisotropic Displacement Parameters
- Table 8.** Derived Atomic Coordinates and Displacement Parameters for Hydrogen Atoms

Table 1. Crystallographic Experimental Details*A. Crystal Data*

formula	C ₁₈ H ₁₄ N ₂ O ₃
formula weight	306.31
crystal dimensions (mm)	0.26 × 0.26 × 0.11
crystal system	monoclinic
space group	<i>P</i> 2 ₁ / <i>c</i> (No. 14)
unit cell parameters ^a	
<i>a</i> (Å)	11.9170 (4)
<i>b</i> (Å)	7.9729 (3)
<i>c</i> (Å)	15.3812 (5)
β (deg)	92.5421 (4)
<i>V</i> (Å ³)	1459.98 (9)
<i>Z</i>	4
ρ _{calcd} (g cm ⁻³)	1.394
μ (mm ⁻¹)	0.097

B. Data Collection and Refinement Conditions

diffractometer	Bruker PLATFORM/APEX II CCD ^b
radiation (λ [Å])	graphite-monochromated Mo Kα (0.71073)
temperature (°C)	-100
scan type	ω scans (0.3°) (15 s exposures)
data collection 2θ limit (deg)	54.96
total data collected	12628 (-15 ≤ <i>h</i> ≤ 15, -10 ≤ <i>k</i> ≤ 10, -19 ≤ <i>l</i> ≤ 19)
independent reflections	3347 (<i>R</i> _{int} = 0.0219)
number of observed reflections (<i>NO</i>)	2932 [<i>F</i> _o ² ≥ 2σ(<i>F</i> _o ²)]
structure solution method	direct methods/dual space (<i>SHELXD</i> ^c)
refinement method	full-matrix least-squares on <i>F</i> ² (<i>SHELXL-2013</i> ^d)
absorption correction method	Gaussian integration (face-indexed)
range of transmission factors	1.0000–0.9333
data/restraints/parameters	3347 / 0 / 216
goodness-of-fit (<i>S</i>) ^e [all data]	1.042
final <i>R</i> indices ^f	
<i>R</i> ₁ [<i>F</i> _o ² ≥ 2σ(<i>F</i> _o ²)]	0.0355
<i>wR</i> ₂ [all data]	0.0965
largest difference peak and hole	0.301 and -0.203 e Å ⁻³

^aObtained from least-squares refinement of 5674 reflections with 5.30° < 2θ < 54.84°.

^bPrograms for diffractometer operation, data collection, data reduction and absorption correction were those supplied by Bruker.

(continued)

Table 1. Crystallographic Experimental Details (continued)

^cSchneider, T. R.; Sheldrick, G. M. *Acta Crystallogr.* **2002**, *D58*, 1772-1779.

^dSheldrick, G. M. *Acta Crystallogr.* **2008**, *A64*, 112–122.

^e $S = [\sum w(F_o^2 - F_c^2)^2 / (n - p)]^{1/2}$ (n = number of data; p = number of parameters varied; $w = [\sum^2(F_o^2) + (0.0464P)^2 + 0.5204P]^{-1}$ where $P = [\text{Max}(F_o^2, 0) + 2F_c^2]/3$).

^f $R_1 = \sum ||F_o| - |F_c|| / \sum |F_o|$; $wR_2 = [\sum w(F_o^2 - F_c^2)^2 / \sum w(F_o^4)]^{1/2}$.

Table 2. Atomic Coordinates and Equivalent Isotropic Displacement Parameters

Atom	<i>x</i>	<i>y</i>	<i>z</i>	<i>U</i> _{eq} , Å ²
O1	0.13120(6)	0.33700(11)	0.49091(5)	0.02373(19)*
O2	0.40031(7)	0.01643(13)	0.58513(6)	0.0333(2)*
O3	0.22489(7)	0.08330(12)	0.61635(5)	0.0281(2)*
N1	0.37749(8)	0.13891(12)	0.42064(6)	0.0202(2)*
N2	0.04594(8)	-0.17830(13)	0.40988(7)	0.0266(2)*
C1	0.27554(9)	0.11935(13)	0.46908(7)	0.0180(2)*
C2	0.22449(9)	0.30137(13)	0.46726(7)	0.0180(2)*
C3	0.30920(9)	0.40827(14)	0.43146(7)	0.0199(2)*
C4	0.39947(9)	0.30729(14)	0.40884(7)	0.0198(2)*
C5	0.49529(10)	0.37998(16)	0.37488(8)	0.0269(3)*
C6	0.49524(11)	0.55203(17)	0.36397(9)	0.0320(3)*
C7	0.40373(11)	0.65337(16)	0.38449(9)	0.0314(3)*
C8	0.30979(10)	0.58202(15)	0.41855(8)	0.0257(3)*
C9	0.30865(9)	0.06773(14)	0.56330(7)	0.0205(2)*
C10	0.24741(11)	0.02042(18)	0.70447(8)	0.0308(3)*
C11	0.11275(9)	-0.09319(14)	0.46943(8)	0.0228(2)*
C12	0.19287(9)	-0.00399(13)	0.42824(7)	0.0182(2)*
C13	0.17340(9)	-0.03352(14)	0.33629(7)	0.0198(2)*
C14	0.07970(9)	-0.14221(14)	0.32777(8)	0.0234(2)*
C15	0.03379(11)	-0.19229(17)	0.24659(9)	0.0320(3)*
C16	0.08314(12)	-0.13135(18)	0.17368(9)	0.0363(3)*
C17	0.17854(12)	-0.02804(18)	0.18055(8)	0.0339(3)*
C18	0.22439(11)	0.02097(15)	0.26058(8)	0.0265(3)*
H1N	0.4347(13)	0.071(2)	0.4324(9)	0.032(4)
H2N	-0.0151(14)	-0.234(2)	0.4243(10)	0.042(4)

Anisotropically-refined atoms are marked with an asterisk (*). The form of the anisotropic displacement parameter is: $\exp[-2\pi^2(h^2a^{*2}U_{11} + k^2b^{*2}U_{22} + l^2c^{*2}U_{33} + 2klb^*c^*U_{23} + 2hla^*c^*U_{13} + 2hka^*b^*U_{12})]$.

Table 3. Selected Interatomic Distances (Å)

Atom1	Atom2	Distance	Atom1	Atom2	Distance
O1	C2	1.2185(13)	C3	C8	1.3995(16)
O2	C9	1.2003(14)	C4	C5	1.4020(16)
O3	C9	1.3227(13)	C5	C6	1.3820(18)
O3	C10	1.4589(14)	C6	C7	1.4043(18)
N1	C1	1.4614(13)	C7	C8	1.3796(17)
N1	C4	1.3813(14)	C11	C12	1.3683(15)
N2	C11	1.3669(15)	C12	C13	1.4424(15)
N2	C14	1.3729(16)	C13	C14	1.4149(16)
C1	C2	1.5733(15)	C13	C18	1.4059(16)
C1	C9	1.5410(15)	C14	C15	1.3990(17)
C1	C12	1.5091(15)	C15	C16	1.378(2)
C2	C3	1.4484(15)	C16	C17	1.404(2)
C3	C4	1.3998(15)	C17	C18	1.3809(17)

Table 4. Selected Interatomic Angles (deg)

Atom1	Atom2	Atom3	Angle	Atom1	Atom2	Atom3	Angle
C9	O3	C10	115.35(9)	C6	C7	C8	119.96(12)
C1	N1	C4	109.72(9)	C3	C8	C7	118.12(11)
C11	N2	C14	109.06(10)	O2	C9	O3	124.17(10)
N1	C1	C2	102.83(8)	O2	C9	C1	123.09(10)
N1	C1	C9	108.91(8)	O3	C9	C1	112.73(9)
N1	C1	C12	113.55(9)	N2	C11	C12	110.21(10)
C2	C1	C9	110.22(9)	C1	C12	C11	127.02(10)
C2	C1	C12	110.42(8)	C1	C12	C13	126.02(10)
C9	C1	C12	110.64(9)	C11	C12	C13	106.49(10)
O1	C2	C1	124.54(10)	C12	C13	C14	106.42(10)
O1	C2	C3	129.55(10)	C12	C13	C18	134.84(11)
C1	C2	C3	105.91(9)	C14	C13	C18	118.74(11)
C2	C3	C4	108.19(10)	N2	C14	C13	107.79(10)
C2	C3	C8	130.12(10)	N2	C14	C15	129.96(11)
C4	C3	C8	121.69(10)	C13	C14	C15	122.22(11)
N1	C4	C3	111.97(10)	C14	C15	C16	117.50(12)
N1	C4	C5	127.80(10)	C15	C16	C17	121.26(12)
C3	C4	C5	120.16(11)	C16	C17	C18	121.34(12)
C4	C5	C6	117.36(11)	C13	C18	C17	118.84(12)
C5	C6	C7	122.68(11)				

Table 5. Hydrogen-Bonded Interactions

D–H···A	D–H (Å)	H···A (Å)	D···A (Å)	∠D–H···A (deg)	Note
N1–H1N···O2 ^a	0.881(16)	2.116(15)	2.9281(13)	153.0(13)	^a At $1-x, \bar{y}, 1-z$.
N2–H2N···O1 ^b	0.888(17)	2.110(17)	2.9447(13)	156.2(14)	^b At $\bar{x}, \bar{y}, 1-z$.

Table 6. Torsional Angles (deg)

Atom1	Atom2	Atom3	Atom4	Angle	Atom1	Atom2	Atom3	Atom4	Angle
C10	O3	C9	O2	-4.79(17)	C1	C2	C3	C4	2.92(11)
C10	O3	C9	C1	174.03(10)	C1	C2	C3	C8	-177.21(11)
C4	N1	C1	C2	11.84(11)	C2	C3	C4	N1	4.73(12)
C4	N1	C1	C9	-105.08(10)	C2	C3	C4	C5	-178.01(10)
C4	N1	C1	C12	131.16(10)	C8	C3	C4	N1	-175.16(10)
C1	N1	C4	C3	-11.02(12)	C8	C3	C4	C5	2.10(17)
C1	N1	C4	C5	171.98(11)	C2	C3	C8	C7	178.58(11)
C14	N2	C11	C12	-1.63(13)	C4	C3	C8	C7	-1.56(17)
C11	N2	C14	C13	1.59(13)	N1	C4	C5	C6	175.86(12)
C11	N2	C14	C15	-176.41(12)	C3	C4	C5	C6	-0.92(17)
N1	C1	C2	O1	170.21(10)	C4	C5	C6	C7	-0.7(2)
N1	C1	C2	C3	-8.82(10)	C5	C6	C7	C8	1.3(2)
C9	C1	C2	O1	-73.81(13)	C6	C7	C8	C3	-0.09(18)
C9	C1	C2	C3	107.16(10)	N2	C11	C12	C1	173.50(10)
C12	C1	C2	O1	48.74(14)	N2	C11	C12	C13	0.98(13)
C12	C1	C2	C3	-130.29(9)	C1	C12	C13	C14	-172.62(10)
N1	C1	C9	O2	-15.24(15)	C1	C12	C13	C18	6.8(2)
N1	C1	C9	O3	165.93(9)	C11	C12	C13	C14	0.00(12)
C2	C1	C9	O2	-127.35(12)	C11	C12	C13	C18	179.45(13)
C2	C1	C9	O3	53.82(12)	C12	C13	C14	N2	-0.96(12)
C12	C1	C9	O2	110.23(12)	C12	C13	C14	C15	177.23(11)
C12	C1	C9	O3	-68.60(12)	C18	C13	C14	N2	179.48(10)
N1	C1	C12	C11	155.09(11)	C18	C13	C14	C15	-2.33(17)
N1	C1	C12	C13	-33.79(14)	C12	C13	C18	C17	-176.84(12)
C2	C1	C12	C11	-90.03(13)	C14	C13	C18	C17	2.56(17)
C2	C1	C12	C13	81.10(13)	N2	C14	C15	C16	177.59(12)
C9	C1	C12	C11	32.28(15)	C13	C14	C15	C16	-0.16(18)
C9	C1	C12	C13	-156.60(10)	C14	C15	C16	C17	2.39(19)
O1	C2	C3	C4	-176.05(11)	C15	C16	C17	C18	-2.2(2)
O1	C2	C3	C8	3.8(2)	C16	C17	C18	C13	-0.41(19)

Table 7. Anisotropic Displacement Parameters (U_{ij} , Å²)

Atom	U_{11}	U_{22}	U_{33}	U_{23}	U_{13}	U_{12}
O1	0.0183(4)	0.0271(4)	0.0260(4)	0.0003(3)	0.0045(3)	0.0050(3)
O2	0.0215(4)	0.0465(6)	0.0319(5)	0.0098(4)	-0.0001(4)	0.0107(4)
O3	0.0234(4)	0.0419(5)	0.0189(4)	0.0042(4)	0.0017(3)	0.0081(4)
N1	0.0146(4)	0.0205(5)	0.0259(5)	0.0005(4)	0.0045(4)	0.0027(4)
N2	0.0195(5)	0.0267(5)	0.0342(6)	-0.0034(4)	0.0069(4)	-0.0048(4)
C1	0.0145(5)	0.0202(5)	0.0196(5)	0.0004(4)	0.0023(4)	0.0024(4)
C2	0.0174(5)	0.0203(5)	0.0160(5)	-0.0012(4)	-0.0013(4)	0.0029(4)
C3	0.0186(5)	0.0211(5)	0.0200(5)	-0.0006(4)	-0.0005(4)	0.0012(4)
C4	0.0183(5)	0.0215(5)	0.0194(5)	-0.0001(4)	-0.0009(4)	0.0003(4)
C5	0.0184(5)	0.0295(6)	0.0330(6)	0.0020(5)	0.0043(5)	0.0004(4)
C6	0.0253(6)	0.0310(7)	0.0399(7)	0.0044(5)	0.0048(5)	-0.0079(5)
C7	0.0338(7)	0.0207(6)	0.0399(7)	0.0028(5)	0.0026(5)	-0.0033(5)
C8	0.0261(6)	0.0221(6)	0.0290(6)	-0.0013(5)	0.0005(5)	0.0023(4)
C9	0.0187(5)	0.0195(5)	0.0233(5)	0.0002(4)	0.0006(4)	0.0010(4)
C10	0.0328(7)	0.0410(7)	0.0185(6)	0.0038(5)	0.0008(5)	0.0039(5)
C11	0.0201(5)	0.0231(5)	0.0256(6)	-0.0002(4)	0.0052(4)	0.0008(4)
C12	0.0163(5)	0.0177(5)	0.0207(5)	0.0004(4)	0.0018(4)	0.0029(4)
C13	0.0184(5)	0.0183(5)	0.0227(5)	0.0002(4)	0.0006(4)	0.0031(4)
C14	0.0185(5)	0.0217(5)	0.0299(6)	-0.0029(5)	0.0016(4)	0.0028(4)
C15	0.0249(6)	0.0305(6)	0.0401(7)	-0.0126(5)	-0.0052(5)	0.0024(5)
C16	0.0403(8)	0.0396(8)	0.0279(6)	-0.0116(6)	-0.0098(5)	0.0091(6)
C17	0.0428(8)	0.0370(7)	0.0218(6)	0.0017(5)	0.0017(5)	0.0052(6)
C18	0.0292(6)	0.0265(6)	0.0239(6)	0.0024(5)	0.0033(5)	0.0001(5)

The form of the anisotropic displacement parameter is:

$$\exp[-2\pi^2(h^2a^*{}^2U_{11} + k^2b^*{}^2U_{22} + l^2c^*{}^2U_{33} + 2klb^*c^*U_{23} + 2hla^*c^*U_{13} + 2hka^*b^*U_{12})]$$

Table 8. Derived Atomic Coordinates and Displacement Parameters for Hydrogen Atoms

Atom	<i>x</i>	<i>y</i>	<i>z</i>	$U_{\text{eq}}, \text{\AA}^2$
H5	0.5578	0.3136	0.3600	0.032
H6	0.5597	0.6039	0.3417	0.038
H7	0.4065	0.7710	0.3749	0.038
H8	0.2473	0.6489	0.4328	0.031
H10A	0.1812	0.0380	0.7389	0.037
H10B	0.3116	0.0806	0.7315	0.037
H10C	0.2646	-0.0997	0.7022	0.037
H11	0.1047	-0.0956	0.5306	0.027
H15	-0.0290	-0.2656	0.2419	0.038
H16	0.0520	-0.1598	0.1177	0.044
H17	0.2122	0.0089	0.1291	0.041
H18	0.2893	0.0903	0.2644	0.032

Appendix III: X-ray: Crystallographic Data for compound 55a. (Chapter Three)

STRUCTURE REPORT

XCL Code: FGW1405

Date: 2 May 2014

Compound: (-)-Menthyl (2*R*)-1'-benzyl-3-oxo-1,3-dihydro-1'*H*,2*H*-2,3'-biindole-2-carboxylate

Formula: C₃₄H₃₆N₂O₃

Supervisor: F. G. West

Crystallographer: R. McDonald

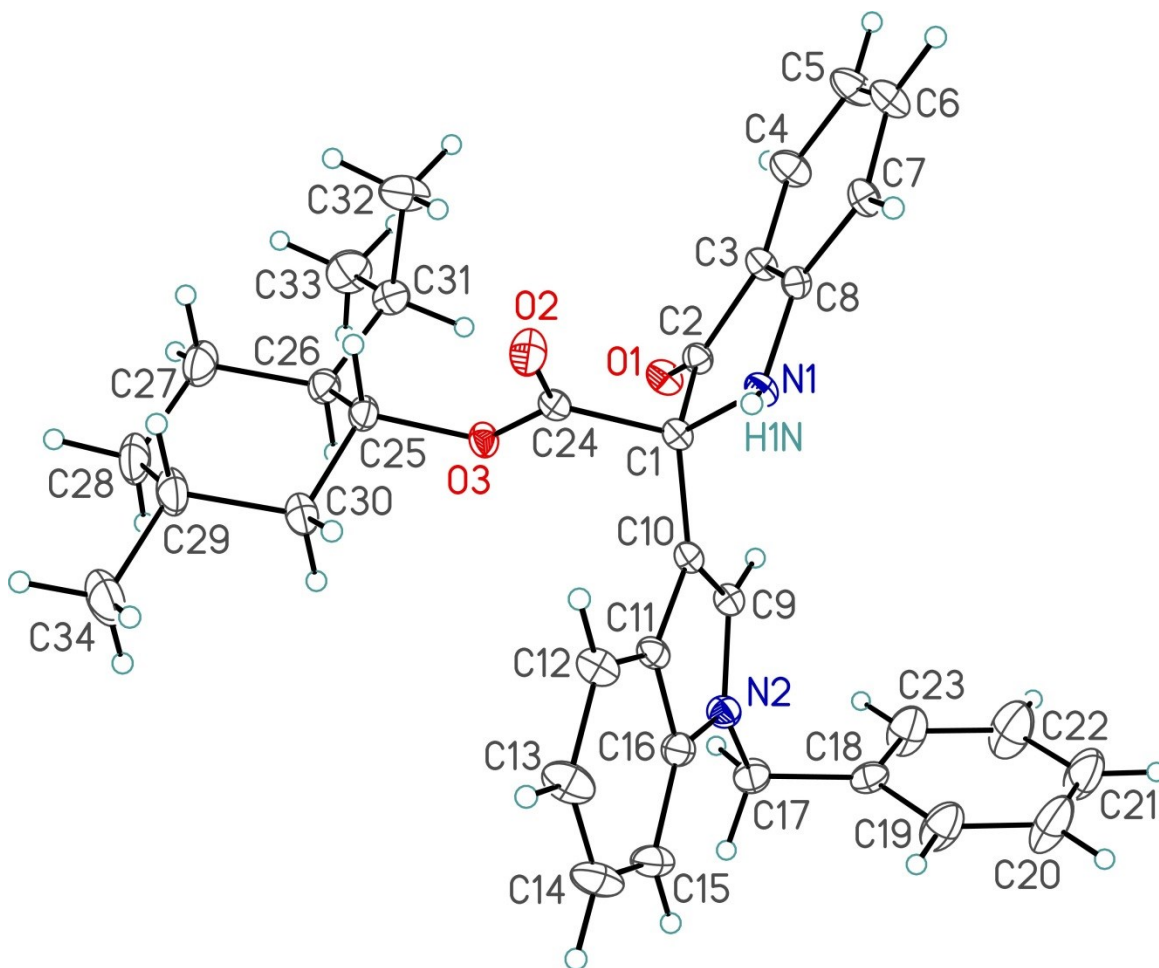
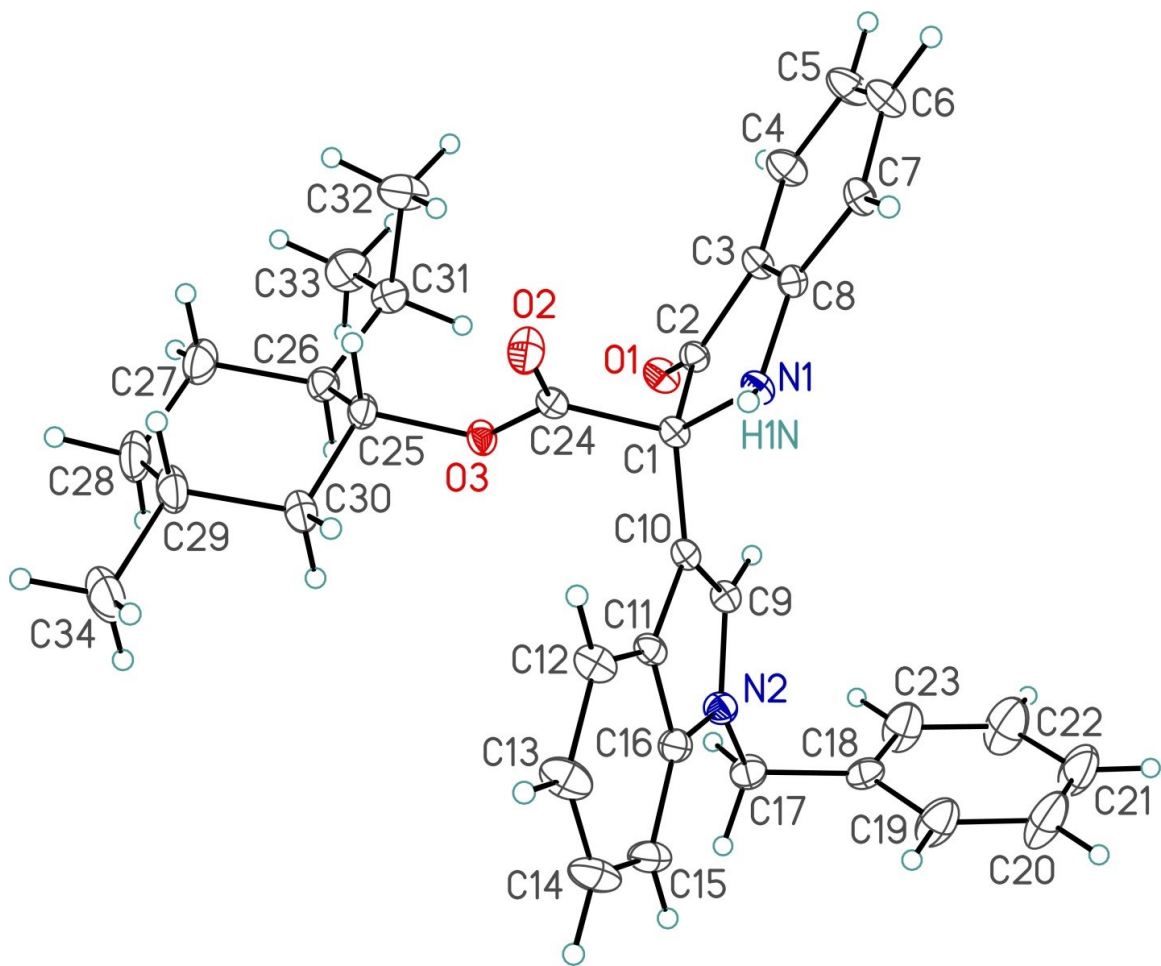
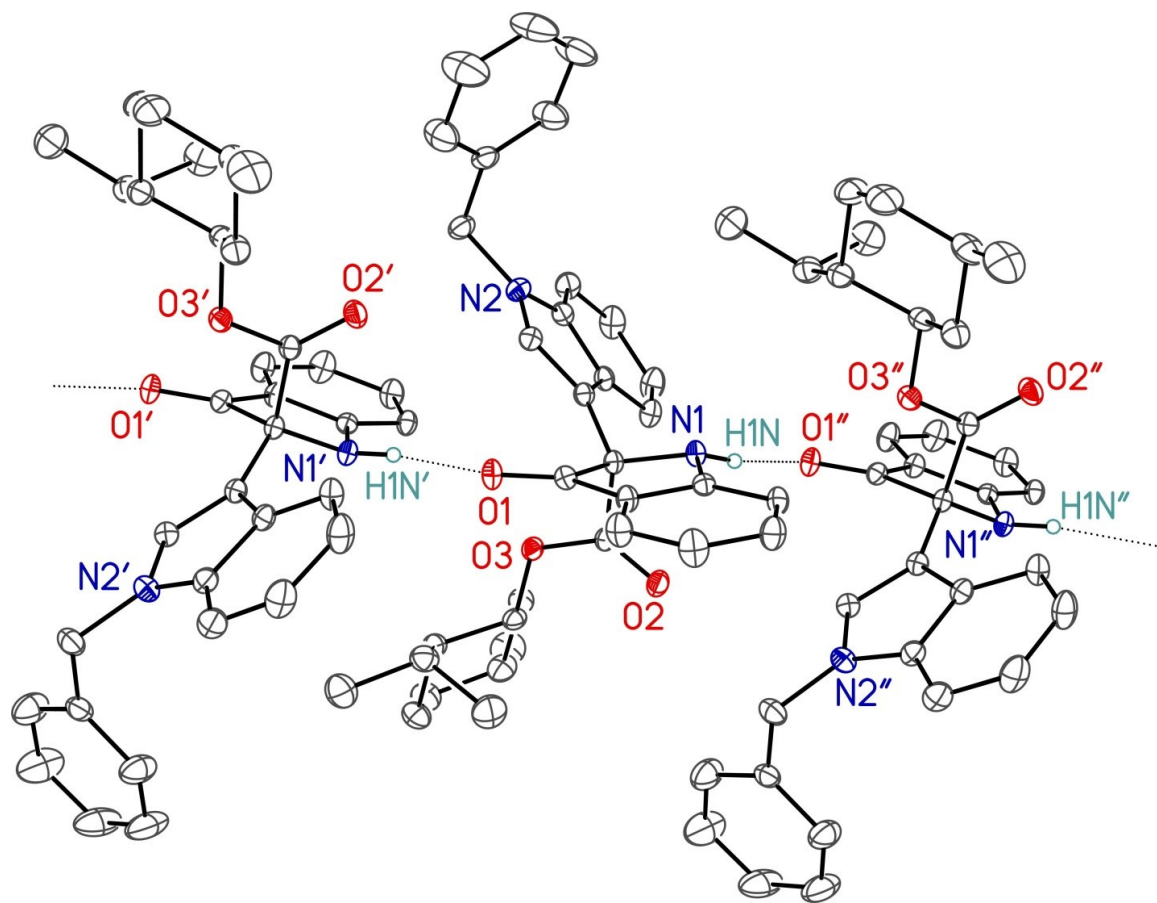


Figure Legends

- Figure 1.** Perspective view of the (-)-menthyl (2*R*)-1'-benzyl-3-oxo-1,3-dihydro-1'*H*,2*H*-2,3'-biindole-2-carboxylate molecule showing the atom labelling scheme. Non-hydrogen atoms are represented by Gaussian ellipsoids at the 30% probability level. Hydrogen atoms are shown with arbitrarily small thermal parameters. Assignment of the absolute structure for this compound is based on the known stereochemistry of the (-)-menthyl group.
- Figure 2.** Illustration of hydrogen-bonded interactions between adjacent molecules within the crystal lattice. Primed atoms are related to unprimed ones via the crystallographic rotational-translational symmetry operation $(\bar{x}, -1/2+y, 1-z)$, while double-primed atoms are related to unprimed ones via the crystallographic rotational-translational symmetry operation $(\bar{x}, 1/2+y, 1-z)$ (both of these operations represent rotation about and translation along a direction parallel to the crystal unit cell's *b* axis). The chain propagates in a direction parallel to the crystal unit cell's *b* axis.





List of Tables

- Table 1.** Crystallographic Experimental Details
- Table 2.** Atomic Coordinates and Equivalent Isotropic Displacement Parameters
- Table 3.** Selected Interatomic Distances
- Table 4.** Selected Interatomic Angles
- Table 5.** Torsional Angles
- Table 6.** Anisotropic Displacement Parameters
- Table 7.** Derived Atomic Coordinates and Displacement Parameters for Hydrogen Atoms

Table 1. Crystallographic Experimental Details*A. Crystal Data*

formula	C ₃₄ H ₃₆ N ₂ O ₃
formula weight	520.65
crystal dimensions (mm)	0.75 × 0.14 × 0.12
crystal system	monoclinic
space group	<i>P</i> 2 ₁ (No. 4)
unit cell parameters ^a	
<i>a</i> (Å)	11.0321 (5)
<i>b</i> (Å)	11.4646 (5)
<i>c</i> (Å)	11.5824 (5)
β (deg)	95.6775 (6)
<i>V</i> (Å ³)	1457.74 (11)
<i>Z</i>	2
ρ _{calcd} (g cm ⁻³)	1.186
μ (mm ⁻¹)	0.075

B. Data Collection and Refinement Conditions

diffractometer	Bruker D8/APEX II CCD ^b
radiation (λ [Å])	graphite-monochromated Mo Kα (0.71073)
temperature (°C)	-100
scan type	ω scans (0.3°) (20 s exposures)
data collection 2θ limit (deg)	56.62
total data collected	13193 (-14 ≤ <i>h</i> ≤ 14, -15 ≤ <i>k</i> ≤ 15, -14 ≤ <i>l</i> ≤ 14)
independent reflections	6914 (<i>R</i> _{int} = 0.0192)
number of observed reflections (<i>NO</i>)	6090 [<i>F</i> _o ² ≥ 2σ(<i>F</i> _o ²)]
structure solution method	direct methods/dual space (<i>SHELXD</i> ^c)
refinement method	full-matrix least-squares on <i>F</i> ² (<i>SHELXL-2013</i> ^d)
absorption correction method	Gaussian integration (face-indexed)
range of transmission factors	1.0000–0.9186
data/restraints/parameters	6914 / 0 / 356
Flack absolute structure parameter ^e	-0.1(3)
goodness-of-fit (<i>S</i>) ^f [all data]	1.033
final <i>R</i> indices ^g	
<i>R</i> ₁ [<i>F</i> _o ² ≥ 2σ(<i>F</i> _o ²)]	0.0385
<i>wR</i> ₂ [all data]	0.0952
largest difference peak and hole	0.203 and -0.207 e Å ⁻³

^aObtained from least-squares refinement of 8226 reflections with 5.02° < 2θ < 56.34°.

(continued)

Table 1. Crystallographic Experimental Details (continued)

^bPrograms for diffractometer operation, data collection, data reduction and absorption correction were those supplied by Bruker.

^cSchneider, T. R.; Sheldrick, G. M. *Acta Crystallogr.* **2002**, *D58*, 1772-1779.

^dSheldrick, G. M. *Acta Crystallogr.* **2008**, *A64*, 112–122.

^eFlack, H. D. *Acta Crystallogr.* **1983**, *A39*, 876–881; Flack, H. D.; Bernardinelli, G. *Acta Crystallogr.* **1999**, *A55*, 908–915; Flack, H. D.; Bernardinelli, G. *J. Appl. Cryst.* **2000**, *33*, 1143–1148. The Flack parameter will refine to a value near zero if the structure is in the correct configuration and will refine to a value near one for the inverted configuration. The low anomalous scattering power of the atoms in this structure (none heavier than oxygen) implies that the data alone cannot be used for absolute structure assignment, thus the Flack parameter is provided for informational purposes only. Assignment of absolute structure herein is based on the known stereochemistry of the (-)-menthyl group.

$$fS = [\sum w(F_o^2 - F_c^2)^2 / (n - p)]^{1/2} \quad (n = \text{number of data}; p = \text{number of parameters varied}; w = [\sum^2(F_o^2) + (0.0496P)^2 + 0.1498P]^{-1} \text{ where } P = [\text{Max}(F_o^2, 0) + 2F_c^2]/3).$$

$$gR_1 = \sum ||F_o| - |F_c|| / \sum |F_o|; wR_2 = [\sum w(F_o^2 - F_c^2)^2 / \sum w(F_o^4)]^{1/2}.$$

Table 2. Atomic Coordinates and Equivalent Isotropic Displacement Parameters

Atom	<i>x</i>	<i>y</i>	<i>z</i>	$U_{\text{eq}}, \text{\AA}^2$
O1	-0.05451(13)	0.09169(12)	0.59193(13)	0.0297(3)*
O2	0.17965(14)	0.37380(13)	0.58972(14)	0.0368(4)*
O3	0.18820(12)	0.18432(12)	0.54041(12)	0.0268(3)*
N1	-0.06284(15)	0.38955(14)	0.51395(14)	0.0234(3)*
N2	-0.07007(16)	0.12303(15)	0.22015(15)	0.0286(4)*
C1	-0.00234(18)	0.27766(16)	0.49969(17)	0.0216(4)*
C2	-0.06141(17)	0.19737(17)	0.58848(16)	0.0232(4)*
C3	-0.12033(18)	0.27628(17)	0.66334(17)	0.0249(4)*
C4	-0.1750(2)	0.2549(2)	0.76541(19)	0.0350(5)*
C5	-0.2224(2)	0.3482(2)	0.8206(2)	0.0402(6)*
C6	-0.2166(2)	0.4608(2)	0.7739(2)	0.0351(5)*
C7	-0.16559(18)	0.48305(17)	0.67232(18)	0.0262(4)*
C8	-0.11602(17)	0.38851(17)	0.61640(16)	0.0223(4)*
C9	-0.08505(18)	0.14082(18)	0.33538(17)	0.0256(4)*
C10	-0.01447(17)	0.23201(17)	0.37764(16)	0.0228(4)*
C11	0.05019(18)	0.27386(17)	0.28364(17)	0.0250(4)*
C12	0.1371(2)	0.36112(19)	0.27291(19)	0.0322(5)*
C13	0.1845(2)	0.3746(2)	0.1675(2)	0.0425(6)*
C14	0.1456(3)	0.3039(2)	0.0720(2)	0.0436(6)*
C15	0.0592(2)	0.2185(2)	0.07952(19)	0.0364(5)*
C16	0.01234(19)	0.20330(18)	0.18648(17)	0.0280(4)*
C17	-0.1266(2)	0.0274(2)	0.1509(2)	0.0350(5)*
C18	-0.2620(2)	0.0454(2)	0.12372(18)	0.0330(5)*
C19	-0.3061(3)	0.1368(3)	0.0552(2)	0.0546(7)*
C20	-0.4297(3)	0.1568(3)	0.0339(3)	0.0711(10)*
C21	-0.5107(3)	0.0836(4)	0.0804(3)	0.0704(10)*
C22	-0.4679(3)	-0.0089(4)	0.1466(3)	0.0775(12)*
C23	-0.3438(3)	-0.0280(3)	0.1684(3)	0.0567(8)*
C24	0.13304(18)	0.28665(17)	0.54827(17)	0.0238(4)*
C25	0.31618(18)	0.17507(18)	0.58921(18)	0.0287(4)*
C26	0.33291(19)	0.05554(19)	0.64539(19)	0.0318(5)*
C27	0.4680(2)	0.0448(2)	0.6919(2)	0.0457(6)*
C28	0.5522(2)	0.0657(3)	0.5974(3)	0.0506(7)*
C29	0.5312(2)	0.1837(2)	0.5384(2)	0.0429(6)*
C30	0.39745(19)	0.1953(2)	0.4926(2)	0.0349(5)*
C31	0.2415(2)	0.0327(2)	0.73605(19)	0.0376(5)*
C32	0.2368(3)	0.1301(3)	0.8255(2)	0.0542(7)*
C33	0.2630(3)	-0.0848(3)	0.7968(3)	0.0539(7)*

Table 2. Atomic Coordinates and Displacement Parameters (continued)

Atom	<i>x</i>	<i>y</i>	<i>z</i>	$U_{\text{eq}}, \text{\AA}^2$
C34	0.6125(3)	0.2027(3)	0.4408(3)	0.0607(8)*
H1N	-0.028(2)	0.455(2)	0.491(2)	0.028(6)

Anisotropically-refined atoms are marked with an asterisk (*). The form of the anisotropic displacement parameter is: $\exp[-2\pi^2(h^2a^*2U_{11} + k^2b^*2U_{22} + l^2c^*2U_{33} + 2klb^*c^*U_{23} + 2hla^*c^*U_{13} + 2hka^*b^*U_{12})]$.

Table 3. Selected Interatomic Distances (Å)

Atom1	Atom2	Distance	Atom1	Atom2	Distance
O1	N1 ^a	2.977(2) ^b	C11	C12	1.400(3)
O1	C2	1.214(2)	C11	C16	1.415(3)
O1	H1N ^a	2.10(3) ^b	C12	C13	1.383(3)
O2	C24	1.202(3)	C13	C14	1.404(4)
O3	C24	1.329(2)	C14	C15	1.376(4)
O3	C25	1.472(2)	C15	C16	1.399(3)
N1	C1	1.463(2)	C17	C18	1.511(3)
N1	C8	1.375(2)	C18	C19	1.375(4)
N1	H1N	0.89(3)	C18	C23	1.372(3)
N2	C9	1.376(2)	C19	C20	1.381(4)
N2	C16	1.377(3)	C20	C21	1.375(5)
N2	C17	1.461(3)	C21	C22	1.365(5)
C1	C2	1.569(3)	C22	C23	1.385(4)
C1	C10	1.501(3)	C25	C26	1.520(3)
C1	C24	1.547(3)	C25	C30	1.519(3)
C2	C3	1.451(3)	C26	C27	1.538(3)
C3	C4	1.401(3)	C26	C31	1.549(3)
C3	C8	1.399(3)	C27	C28	1.523(4)
C4	C5	1.375(3)	C28	C29	1.523(4)
C5	C6	1.404(3)	C29	C30	1.523(3)
C6	C7	1.377(3)	C29	C34	1.527(4)
C7	C8	1.401(3)	C31	C32	1.528(4)
C9	C10	1.365(3)	C31	C33	1.527(4)
C10	C11	1.442(3)			

^aAt \bar{x} , $-1/2+y$, $1-z$. ^bNonbonded distance.

Table 4. Selected Interatomic Angles (deg)

Atom1	Atom2	Atom3	Angle	Atom1	Atom2	Atom3	Angle
C24	O3	C25	117.75(15)	C13	C14	C15	121.4(2)
C1	N1	C8	109.16(15)	C14	C15	C16	117.6(2)
C9	N2	C16	108.76(17)	N2	C16	C11	107.94(17)
C9	N2	C17	123.91(18)	N2	C16	C15	130.2(2)
C16	N2	C17	127.14(18)	C11	C16	C15	121.8(2)
N1	C1	C2	102.52(15)	N2	C17	C18	111.82(18)
N1	C1	C10	114.39(16)	C17	C18	C19	120.7(2)
N1	C1	C24	109.60(15)	C17	C18	C23	120.8(2)
C2	C1	C10	114.12(16)	C19	C18	C23	118.5(2)
C2	C1	C24	104.44(15)	C18	C19	C20	121.1(3)
C10	C1	C24	111.03(15)	C19	C20	C21	119.8(3)
O1	C2	C1	125.32(17)	C20	C21	C22	119.5(3)
O1	C2	C3	129.26(18)	C21	C22	C23	120.4(3)
C1	C2	C3	105.40(16)	C18	C23	C22	120.6(3)
C2	C3	C4	130.63(19)	O2	C24	O3	125.50(19)
C2	C3	C8	107.86(16)	O2	C24	C1	124.08(17)
C4	C3	C8	121.51(18)	O3	C24	C1	110.40(16)
C3	C4	C5	118.1(2)	O3	C25	C26	107.49(16)
C4	C5	C6	120.14(19)	O3	C25	C30	108.66(17)
C5	C6	C7	122.5(2)	C26	C25	C30	113.42(17)
C6	C7	C8	117.56(19)	C25	C26	C27	107.13(19)
N1	C8	C3	112.15(16)	C25	C26	C31	112.52(17)
N1	C8	C7	127.71(18)	C27	C26	C31	115.00(19)
C3	C8	C7	120.11(17)	C26	C27	C28	112.0(2)
N2	C9	C10	110.02(17)	C27	C28	C29	112.7(2)
C1	C10	C9	126.82(17)	C28	C29	C30	109.5(2)
C1	C10	C11	126.20(17)	C28	C29	C34	112.6(2)
C9	C10	C11	106.94(17)	C30	C29	C34	110.5(2)
C10	C11	C12	134.38(19)	C25	C30	C29	110.62(19)
C10	C11	C16	106.34(17)	C26	C31	C32	113.8(2)
C12	C11	C16	119.27(18)	C26	C31	C33	112.3(2)
C11	C12	C13	118.7(2)	C32	C31	C33	110.3(2)
C12	C13	C14	121.2(2)	N1	H1N	O1 ^a	169(2) ^b

^aAt \bar{x} , $1/2+y$, $1-z$. ^bAngle includes nonbonded N–H···O interaction.

Table 5. Torsional Angles (deg)

Atom1	Atom2	Atom3	Atom4	Angle	Atom1	Atom2	Atom3	Atom4	Angle
C25	O3	C24	O2	1.8(3)	C8	C3	C4	C5	-1.5(3)
C25	O3	C24	C1	-176.42(15)	C2	C3	C8	N1	2.2(2)
C24	O3	C25	C26	141.82(17)	C2	C3	C8	C7	-179.30(18)
C24	O3	C25	C30	-95.07(19)	C4	C3	C8	N1	-177.63(19)
C8	N1	C1	C2	16.9(2)	C4	C3	C8	C7	0.8(3)
C8	N1	C1	C10	140.98(17)	C3	C4	C5	C6	0.7(4)
C8	N1	C1	C24	-93.58(18)	C4	C5	C6	C7	0.6(4)
C1	N1	C8	C3	-12.9(2)	C5	C6	C7	C8	-1.3(3)
C1	N1	C8	C7	168.8(2)	C6	C7	C8	N1	178.7(2)
C16	N2	C9	C10	0.4(2)	C6	C7	C8	C3	0.5(3)
C17	N2	C9	C10	175.88(18)	N2	C9	C10	C1	-178.50(18)
C9	N2	C16	C11	-0.1(2)	N2	C9	C10	C11	-0.6(2)
C9	N2	C16	C15	178.3(2)	C1	C10	C11	C12	0.1(4)
C17	N2	C16	C11	-175.33(19)	C1	C10	C11	C16	178.45(18)
C17	N2	C16	C15	3.0(4)	C9	C10	C11	C12	-177.8(2)
C9	N2	C17	C18	72.1(3)	C9	C10	C11	C16	0.5(2)
C16	N2	C17	C18	-113.3(2)	C10	C11	C12	C13	177.4(2)
N1	C1	C2	O1	166.2(2)	C16	C11	C12	C13	-0.8(3)
N1	C1	C2	C3	-15.2(2)	C10	C11	C16	N2	-0.3(2)
C10	C1	C2	O1	42.0(3)	C10	C11	C16	C15	-178.8(2)
C10	C1	C2	C3	-139.43(17)	C12	C11	C16	N2	178.36(19)
C24	C1	C2	O1	-79.4(2)	C12	C11	C16	C15	-0.2(3)
C24	C1	C2	C3	99.15(17)	C11	C12	C13	C14	0.9(4)
N1	C1	C10	C9	-107.1(2)	C12	C13	C14	C15	-0.1(4)
N1	C1	C10	C11	75.4(2)	C13	C14	C15	C16	-0.9(4)
C2	C1	C10	C9	10.5(3)	C14	C15	C16	N2	-177.2(2)
C2	C1	C10	C11	-166.96(18)	C14	C15	C16	C11	1.0(3)
C24	C1	C10	C9	128.2(2)	N2	C17	C18	C19	65.0(3)
C24	C1	C10	C11	-49.3(2)	N2	C17	C18	C23	-113.9(3)
N1	C1	C24	O2	-0.8(3)	C17	C18	C19	C20	-177.2(3)
N1	C1	C24	O3	177.41(15)	C23	C18	C19	C20	1.7(5)
C2	C1	C24	O2	-110.1(2)	C17	C18	C23	C22	177.8(3)
C2	C1	C24	O3	68.19(18)	C19	C18	C23	C22	-1.2(5)
C10	C1	C24	O2	126.5(2)	C18	C19	C20	C21	-0.9(6)
C10	C1	C24	O3	-55.2(2)	C19	C20	C21	C22	-0.5(6)
O1	C2	C3	C4	6.8(4)	C20	C21	C22	C23	1.1(7)
O1	C2	C3	C8	-173.1(2)	C21	C22	C23	C18	-0.2(6)
C1	C2	C3	C4	-171.7(2)	O3	C25	C26	C27	177.80(17)
C1	C2	C3	C8	8.4(2)	O3	C25	C26	C31	-54.9(2)
C2	C3	C4	C5	178.7(2)	C30	C25	C26	C27	57.7(2)

Table 5. Torsional Angles (continued)

Atom1	Atom2	Atom3	Atom4	Angle	Atom1	Atom2	Atom3	Atom4	Angle
C30	C25	C26	C31	-175.00(18)	C27	C26	C31	C32	72.3(3)
O3	C25	C30	C29	-178.61(18)	C27	C26	C31	C33	-53.9(3)
C26	C25	C30	C29	-59.1(2)	C26	C27	C28	C29	56.5(3)
C25	C26	C27	C28	-55.4(3)	C27	C28	C29	C30	-54.6(3)
C31	C26	C27	C28	178.7(2)	C27	C28	C29	C34	-177.9(2)
C25	C26	C31	C32	-50.8(3)	C28	C29	C30	C25	54.8(3)
C25	C26	C31	C33	-177.0(2)	C34	C29	C30	C25	179.4(2)

Table 6. Anisotropic Displacement Parameters (U_{ij} , Å²)

Atom	U_{11}	U_{22}	U_{33}	U_{23}	U_{13}	U_{12}
O1	0.0366(8)	0.0184(7)	0.0355(8)	0.0023(6)	0.0105(6)	0.0020(6)
O2	0.0312(8)	0.0250(8)	0.0525(10)	-0.0091(7)	-0.0050(7)	0.0015(6)
O3	0.0221(7)	0.0245(7)	0.0334(7)	-0.0063(6)	0.0014(5)	0.0035(5)
N1	0.0258(9)	0.0186(8)	0.0270(8)	0.0018(6)	0.0084(7)	0.0018(7)
N2	0.0279(9)	0.0300(9)	0.0280(9)	-0.0050(7)	0.0031(7)	-0.0023(7)
C1	0.0226(9)	0.0185(8)	0.0245(9)	0.0015(7)	0.0059(7)	0.0007(7)
C2	0.0225(9)	0.0232(9)	0.0243(9)	0.0019(7)	0.0047(7)	0.0001(7)
C3	0.0256(10)	0.0227(9)	0.0276(10)	0.0007(8)	0.0083(8)	0.0027(8)
C4	0.0428(13)	0.0299(11)	0.0348(11)	0.0057(9)	0.0166(10)	0.0013(9)
C5	0.0491(15)	0.0390(13)	0.0367(12)	0.0048(10)	0.0253(11)	0.0045(11)
C6	0.0381(12)	0.0308(11)	0.0388(12)	-0.0046(9)	0.0162(10)	0.0060(9)
C7	0.0247(10)	0.0209(9)	0.0339(11)	0.0000(8)	0.0074(8)	0.0026(8)
C8	0.0194(9)	0.0236(9)	0.0242(9)	0.0002(7)	0.0028(7)	-0.0003(7)
C9	0.0237(9)	0.0262(10)	0.0274(9)	-0.0006(8)	0.0046(8)	0.0003(8)
C10	0.0217(10)	0.0222(9)	0.0252(9)	-0.0003(7)	0.0053(8)	0.0024(7)
C11	0.0273(10)	0.0224(9)	0.0261(9)	0.0010(7)	0.0070(8)	0.0042(8)
C12	0.0387(12)	0.0246(10)	0.0348(11)	-0.0011(8)	0.0117(9)	-0.0022(9)
C13	0.0556(16)	0.0308(12)	0.0448(13)	0.0031(10)	0.0229(12)	-0.0067(11)
C14	0.0641(17)	0.0381(13)	0.0322(12)	0.0052(9)	0.0230(11)	0.0021(11)
C15	0.0490(14)	0.0362(12)	0.0249(10)	-0.0022(9)	0.0083(9)	0.0047(10)
C16	0.0306(11)	0.0265(10)	0.0269(10)	0.0016(8)	0.0031(8)	0.0037(8)
C17	0.0357(12)	0.0351(12)	0.0334(11)	-0.0099(9)	-0.0010(9)	-0.0024(10)
C18	0.0372(12)	0.0354(12)	0.0253(10)	-0.0030(8)	-0.0023(9)	-0.0068(9)
C19	0.0455(15)	0.0610(18)	0.0548(16)	0.0258(14)	-0.0073(12)	-0.0132(14)
C20	0.0517(17)	0.084(2)	0.072(2)	0.0384(18)	-0.0217(15)	-0.0069(17)
C21	0.0353(14)	0.110(3)	0.0632(19)	0.0273(19)	-0.0098(13)	-0.0070(17)
C22	0.0415(16)	0.103(3)	0.086(2)	0.044(2)	-0.0030(16)	-0.0216(18)
C23	0.0445(15)	0.0584(18)	0.0657(18)	0.0254(15)	-0.0021(13)	-0.0087(13)
C24	0.0251(10)	0.0224(9)	0.0245(9)	-0.0016(7)	0.0053(7)	0.0012(8)
C25	0.0218(10)	0.0306(11)	0.0329(10)	-0.0080(8)	-0.0017(8)	0.0017(8)
C26	0.0289(11)	0.0320(11)	0.0338(11)	-0.0063(9)	-0.0007(9)	0.0052(9)
C27	0.0357(13)	0.0474(14)	0.0518(14)	-0.0004(12)	-0.0071(11)	0.0111(11)
C28	0.0267(12)	0.0548(17)	0.0687(18)	-0.0078(13)	-0.0036(11)	0.0121(11)
C29	0.0219(11)	0.0485(15)	0.0583(16)	-0.0103(12)	0.0032(10)	-0.0021(10)
C30	0.0249(10)	0.0356(12)	0.0444(12)	-0.0029(10)	0.0052(9)	0.0010(9)
C31	0.0388(13)	0.0419(13)	0.0319(11)	-0.0011(10)	0.0017(9)	0.0028(10)
C32	0.0691(19)	0.0581(17)	0.0369(13)	-0.0075(12)	0.0129(13)	0.0036(15)
C33	0.0604(18)	0.0513(16)	0.0502(16)	0.0093(12)	0.0060(14)	-0.0012(13)
C34	0.0323(14)	0.074(2)	0.078(2)	-0.0047(17)	0.0179(13)	-0.0041(13)

The form of the anisotropic displacement parameter is:

$$\exp[-2\pi^2(h^2a^2U_{11} + k^2b^2U_{22} + l^2c^2U_{33} + 2klb^*c^*U_{23} + 2hla^*c^*U_{13} + 2hka^*b^*U_{12})]$$

Table 7. Derived Atomic Coordinates and Displacement Parameters for Hydrogen Atoms

Atom	<i>x</i>	<i>y</i>	<i>z</i>	$U_{eq}, \text{\AA}^2$
H4	-0.1791	0.1782	0.7957	0.042
H5	-0.2591	0.3364	0.8905	0.048
H6	-0.2492	0.5241	0.8138	0.042
H7	-0.1641	0.5597	0.6413	0.031
H9	-0.1369	0.0962	0.3791	0.031
H12	0.1630	0.4101	0.3368	0.039
H13	0.2444	0.4328	0.1596	0.051
H14	0.1797	0.3153	0.0007	0.052
H15	0.0322	0.1715	0.0144	0.044
H17A	-0.1120	-0.0468	0.1938	0.042
H17B	-0.0881	0.0212	0.0775	0.042
H19	-0.2506	0.1871	0.0219	0.066
H20	-0.4587	0.2211	-0.0128	0.085
H21	-0.5958	0.0972	0.0666	0.085
H22	-0.5236	-0.0605	0.1778	0.093
H23	-0.3151	-0.0925	0.2148	0.068
H25	0.3333	0.2365	0.6500	0.034
H26	0.3167	-0.0039	0.5825	0.038
H27A	0.4867	0.1021	0.7550	0.055
H27B	0.4831	-0.0342	0.7248	0.055
H28A	0.5394	0.0033	0.5384	0.061
H28B	0.6378	0.0610	0.6320	0.061
H29	0.5504	0.2458	0.5980	0.052
H30A	0.3824	0.2743	0.4598	0.042
H30B	0.3775	0.1378	0.4299	0.042
H31	0.1588	0.0288	0.6923	0.045
H32A	0.2187	0.2043	0.7855	0.065
H32B	0.3157	0.1356	0.8722	0.065
H32C	0.1730	0.1129	0.8762	0.065
H33A	0.2620	-0.1469	0.7386	0.065
H33B	0.1985	-0.0989	0.8476	0.065
H33C	0.3422	-0.0839	0.8432	0.065
H34A	0.5986	0.2811	0.4084	0.073
H34B	0.5931	0.1445	0.3798	0.073
H34C	0.6981	0.1948	0.4715	0.073

Appendix IV: X-ray Crystallographic Data for compound 59a (Chapter Three)

STRUCTURE REPORT

XCL Code: FGW1407

Date: 16 September 2014

Compound: (1*R*,2*S*,5*R*)-8-Phenylmenthyl (2*R*)-1'-methyl-3-oxo-1,2',3,3'-tetrahydro-1'*H*,2*H*-2,3'-biindole-2-carboxylate

Formula: C₃₄H₃₆N₂O₃

Supervisor: F. G. West

Crystallographer: R. McDonald

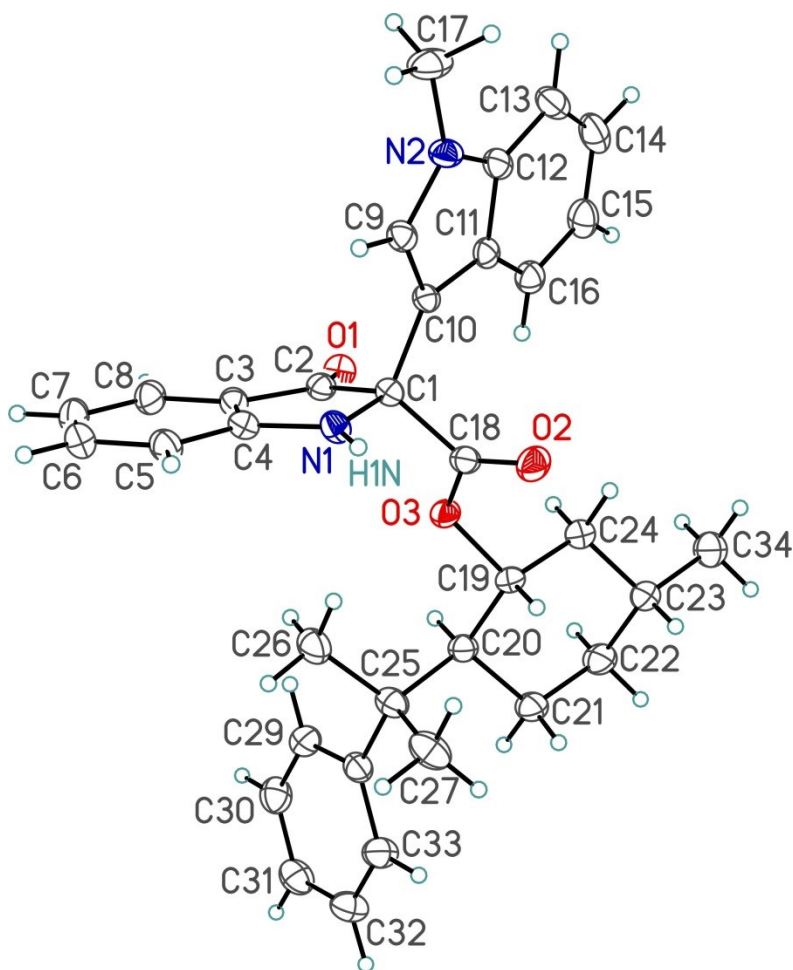
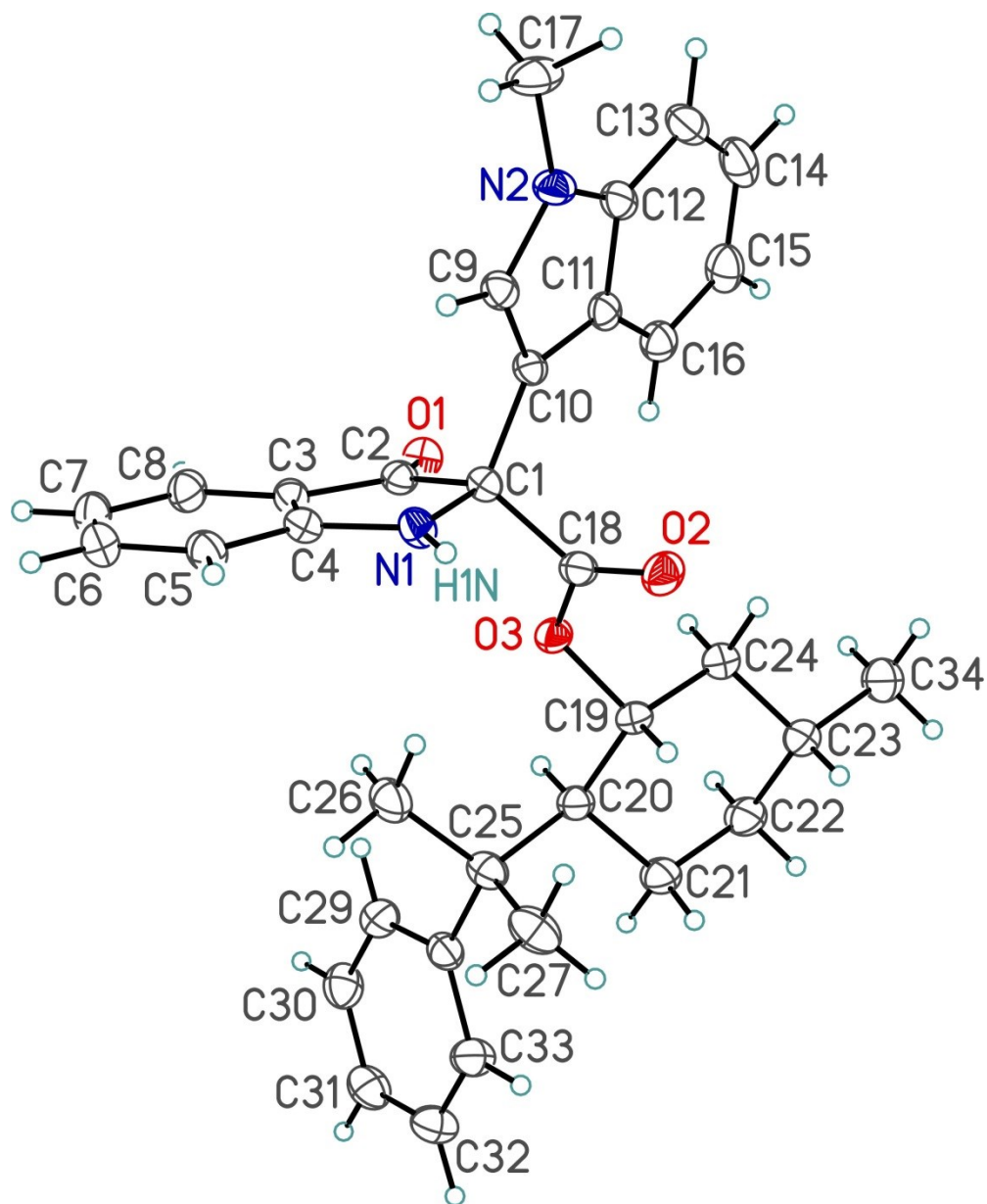
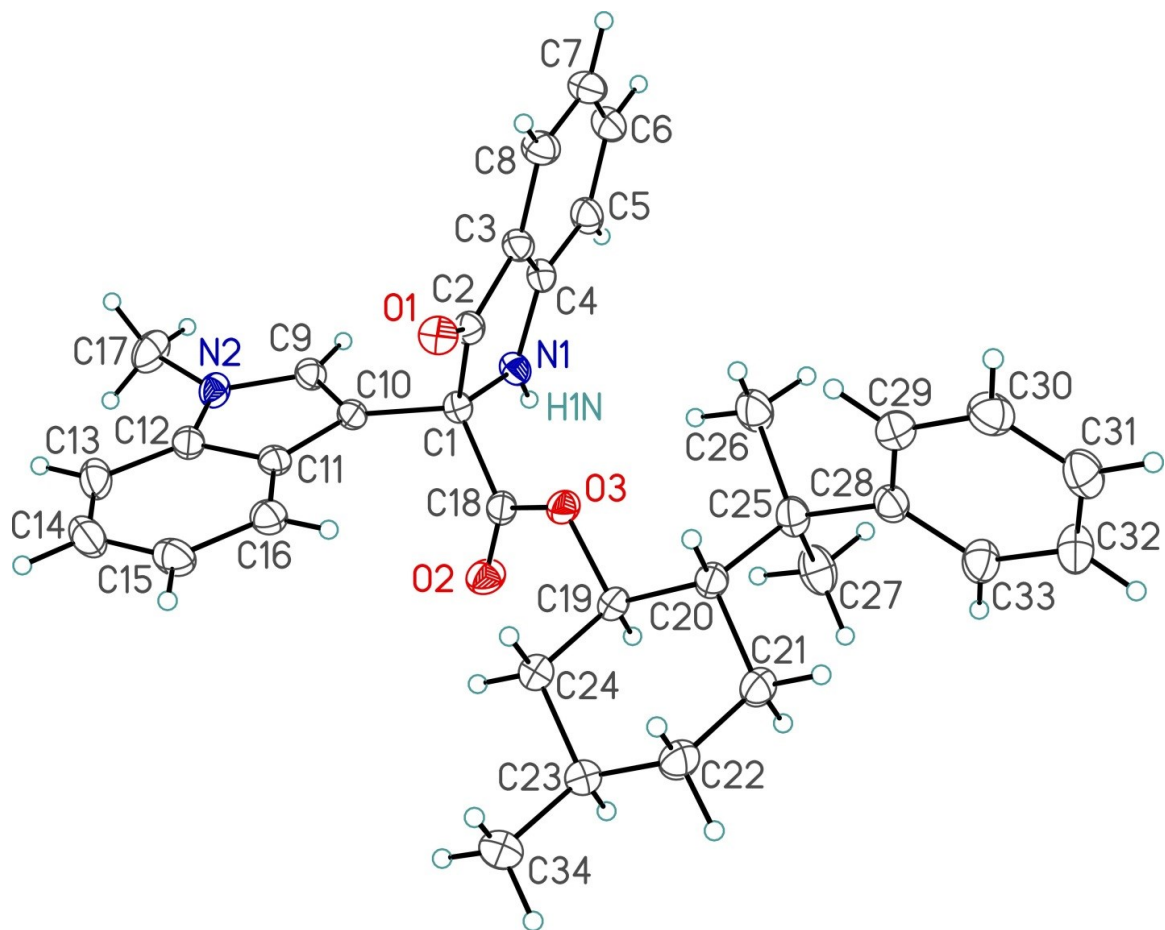


Figure Legends

Figure 1. Perspective view of the (1*R*,2*S*,5*R*)-8-phenylmenthyl (2*R*)-1'-methyl-3-oxo-1,2',3,3'-tetrahydro-1'*H*,2*H*-2,3'-biindole-2-carboxylate molecule showing the atom labelling scheme. Non-hydrogen atoms are represented by Gaussian ellipsoids at the 30% probability level. Hydrogen atoms are shown with arbitrarily small thermal parameters.

Figure 2. Alternate view of the molecule.





List of Tables

- Table 1.** Crystallographic Experimental Details
- Table 2.** Atomic Coordinates and Equivalent Isotropic Displacement Parameters
- Table 3.** Selected Interatomic Distances
- Table 4.** Selected Interatomic Angles
- Table 5.** Torsional Angles
- Table 6.** Anisotropic Displacement Parameters
- Table 7.** Derived Atomic Coordinates and Displacement Parameters for Hydrogen Atoms

Table 1. Crystallographic Experimental Details*A. Crystal Data*

formula	C ₃₄ H ₃₆ N ₂ O ₃
formula weight	520.65
crystal dimensions (mm)	0.35 × 0.15 × 0.03
crystal system	orthorhombic
space group	<i>P</i> 2 ₁ 2 ₁ 2 ₁ (No. 19)
unit cell parameters ^a	
<i>a</i> (Å)	6.2535 (2)
<i>b</i> (Å)	9.9971 (2)
<i>c</i> (Å)	45.2588 (10)
<i>V</i> (Å ³)	2829.44 (12)
<i>Z</i>	4
ρ _{calcd} (g cm ⁻³)	1.222
μ (mm ⁻¹)	0.613

B. Data Collection and Refinement Conditions

diffractometer	Bruker D8/APEX II CCD ^b
radiation (λ [Å])	Cu Kα (1.54178) (microfocus source)
temperature (°C)	-100
scan type	ω and φ scans (1.0°) (5 s exposures)
data collection 2θ limit (deg)	145.93
total data collected	19473 (-7 ≤ <i>h</i> ≤ 7, -12 ≤ <i>k</i> ≤ 12, -49 ≤ <i>l</i> ≤ 54)
independent reflections	5608 (<i>R</i> _{int} = 0.0693)
number of observed reflections (<i>NO</i>)	4795 [<i>F</i> _o ² ≥ 2σ(<i>F</i> _o ²)]
structure solution method	direct methods/dual space (<i>SHELXD</i> ^c)
refinement method	full-matrix least-squares on <i>F</i> ² (<i>SHELXL-2013</i> ^d)
absorption correction method	Gaussian integration (face-indexed)
range of transmission factors	1.0000–0.7881
data/restraints/parameters	5608 / 0 / 353
Flack absolute structure parameter ^e	-0.19(16)
goodness-of-fit (<i>S</i>) ^f [all data]	1.085
final <i>R</i> indices ^g	
<i>R</i> ₁ [<i>F</i> _o ² ≥ 2σ(<i>F</i> _o ²)]	0.0600
<i>wR</i> ₂ [all data]	0.1400
largest difference peak and hole	0.259 and -0.227 e Å ⁻³

^aObtained from least-squares refinement of 7777 reflections with 7.82° < 2θ < 142.02°.

^bPrograms for diffractometer operation, data collection, data reduction and absorption correction were those supplied by Bruker.

(continued)

Table 1. Crystallographic Experimental Details (continued)

^cSchneider, T. R.; Sheldrick, G. M. *Acta Crystallogr.* **2002**, *D58*, 1772-1779.

^dSheldrick, G. M. *Acta Crystallogr.* **2008**, *A64*, 112–122.

^eFlack, H. D. *Acta Crystallogr.* **1983**, *A39*, 876–881; Flack, H. D.; Bernardinelli, G. *Acta Crystallogr.* **1999**, *A55*, 908–915; Flack, H. D.; Bernardinelli, G. *J. Appl. Cryst.* **2000**, *33*, 1143–1148. The Flack parameter will refine to a value near zero if the structure is in the correct configuration and will refine to a value near one for the inverted configuration. The low anomalous scattering power of the atoms in this structure (none heavier than oxygen) implies that the data alone cannot be used for absolute structure assignment; indeed, the relatively large standard uncertainty indicates that the Flack results are essentially meaningless here. The absolute stereochemistry of the molecule was based on the known configuration of the (1*R*,2*S*,5*R*)-8-phenylmenthyl group.

$fS = [\sum w(F_o^2 - F_c^2)^2 / (n - p)]^{1/2}$ (n = number of data; p = number of parameters varied; $w = [\sum^2(F_o^2) + (0.0438P)^2 + 1.4685P]^{-1}$ where $P = [\text{Max}(F_o^2, 0) + 2F_c^2]/3$).

$gR_1 = \sum ||F_o| - |F_c|| / \sum |F_o|$; $wR_2 = [\sum w(F_o^2 - F_c^2)^2 / \sum w(F_o^4)]^{1/2}$.

Table 2. Atomic Coordinates and Equivalent Isotropic Displacement Parameters

Atom	<i>x</i>	<i>y</i>	<i>z</i>	$U_{\text{eq}}, \text{\AA}^2$
O1	0.6304(4)	0.4252(3)	0.17570(6)	0.0398(6)*
O2	0.2181(5)	0.1488(3)	0.13307(6)	0.0479(8)*
O3	0.4833(4)	0.2930(3)	0.12151(6)	0.0363(6)*
N1	0.0855(5)	0.4234(3)	0.15399(7)	0.0350(7)*
N2	0.0882(6)	0.2061(3)	0.23506(7)	0.0376(7)*
C1	0.2697(6)	0.3436(4)	0.16357(8)	0.0290(8)*
C2	0.4445(7)	0.4499(4)	0.16999(8)	0.0329(8)*
C3	0.3363(6)	0.5788(4)	0.16860(8)	0.0336(8)*
C4	0.1276(7)	0.5574(4)	0.15939(8)	0.0348(8)*
C5	-0.0145(7)	0.6638(4)	0.15569(9)	0.0424(10)*
C6	0.0619(9)	0.7913(4)	0.16201(10)	0.0500(11)*
C7	0.2704(9)	0.8147(4)	0.17157(10)	0.0494(11)*
C8	0.4096(8)	0.7082(4)	0.17497(9)	0.0438(10)*
C9	0.0639(6)	0.2866(4)	0.21071(8)	0.0340(8)*
C10	0.2313(6)	0.2680(3)	0.19172(8)	0.0299(8)*
C11	0.3707(6)	0.1705(4)	0.20500(8)	0.0327(8)*
C12	0.2741(7)	0.1339(4)	0.23211(9)	0.0386(9)*
C13	0.3652(9)	0.0385(4)	0.25072(10)	0.0496(12)*
C14	0.5513(9)	-0.0208(4)	0.24175(11)	0.0560(13)*
C15	0.6513(8)	0.0143(4)	0.21501(11)	0.0498(11)*
C16	0.5631(7)	0.1104(4)	0.19685(9)	0.0409(10)*
C17	-0.0505(8)	0.2085(5)	0.26106(10)	0.0561(13)*
C18	0.3201(6)	0.2483(4)	0.13795(8)	0.0343(8)*
C19	0.5445(7)	0.2105(4)	0.09590(8)	0.0354(9)*
C20	0.6694(7)	0.3007(4)	0.07448(8)	0.0357(9)*
C21	0.7639(8)	0.2090(4)	0.05009(9)	0.0460(10)*
C22	0.8897(9)	0.0899(5)	0.06211(10)	0.0514(12)*
C23	0.7573(9)	0.0049(4)	0.08259(9)	0.0506(12)*
C24	0.6746(8)	0.0927(4)	0.10748(9)	0.0419(10)*
C25	0.5392(7)	0.4192(4)	0.06058(9)	0.0412(9)*
C26	0.4658(9)	0.5213(5)	0.08391(11)	0.0591(14)*
C27	0.3372(8)	0.3662(5)	0.04466(11)	0.0563(13)*
C28	0.6867(7)	0.4929(4)	0.03884(9)	0.0394(9)*
C29	0.8461(8)	0.5777(4)	0.04912(10)	0.0501(11)*
C30	0.9815(9)	0.6464(5)	0.03003(11)	0.0539(12)*
C31	0.9613(8)	0.6316(5)	0.00000(11)	0.0537(12)*
C32	0.8073(8)	0.5458(5)	-0.01073(11)	0.0543(12)*

Table 2. Atomic Coordinates and Displacement Parameters (continued)

Atom	<i>x</i>	<i>y</i>	<i>z</i>	$U_{\text{eq}}, \text{\AA}^2$
C33	0.6721(8)	0.4779(5)	0.00853(10)	0.0486(11)*
C34	0.8857(12)	-0.1115(5)	0.09482(12)	0.0746(19)*

Anisotropically-refined atoms are marked with an asterisk (*). The form of the anisotropic displacement parameter is: $\exp[-2\pi^2(h^2a^{*2}U_{11} + k^2b^{*2}U_{22} + l^2c^{*2}U_{33} + 2klb^{*c^{*}}U_{23} + 2hla^{*c^{*}}U_{13} + 2hka^{*b^{*}}U_{12})]$.

Table 3. Selected Interatomic Distances (Å)

Atom1	Atom2	Distance	Atom1	Atom2	Distance
O1	C2	1.216(5)	C11	C16	1.394(6)
O2	C18	1.202(5)	C12	C13	1.394(6)
O3	C18	1.340(5)	C13	C14	1.368(7)
O3	C19	1.473(4)	C14	C15	1.407(7)
N1	C1	1.466(5)	C15	C16	1.379(6)
N1	C4	1.387(5)	C19	C20	1.537(5)
N2	C9	1.373(5)	C19	C24	1.525(5)
N2	C12	1.375(5)	C20	C21	1.552(5)
N2	C17	1.462(5)	C20	C25	1.569(5)
C1	C2	1.552(5)	C21	C22	1.527(6)
C1	C10	1.501(5)	C22	C23	1.505(7)
C1	C18	1.533(5)	C23	C24	1.519(6)
C2	C3	1.457(5)	C23	C34	1.519(6)
C3	C4	1.387(6)	C25	C26	1.539(6)
C3	C8	1.403(5)	C25	C27	1.548(6)
C4	C5	1.397(5)	C25	C28	1.537(6)
C5	C6	1.391(6)	C28	C29	1.389(6)
C6	C7	1.394(7)	C28	C33	1.383(6)
C7	C8	1.384(6)	C29	C30	1.391(6)
C9	C10	1.367(5)	C30	C31	1.373(7)
C10	C11	1.439(5)	C31	C32	1.378(7)
C11	C12	1.416(5)	C32	C33	1.391(6)

Table 4. Selected Interatomic Angles (deg)

Atom1	Atom2	Atom3	Angle	Atom1	Atom2	Atom3	Angle
C18	O3	C19	116.6(3)	C12	C13	C14	117.7(4)
C1	N1	C4	108.9(3)	C13	C14	C15	121.7(4)
C9	N2	C12	108.9(3)	C14	C15	C16	120.6(5)
C9	N2	C17	124.8(4)	C11	C16	C15	119.2(4)
C12	N2	C17	126.0(4)	O2	C18	O3	125.3(4)
N1	C1	C2	103.7(3)	O2	C18	C1	122.9(4)
N1	C1	C10	113.5(3)	O3	C18	C1	111.7(3)
N1	C1	C18	106.0(3)	O3	C19	C20	107.5(3)
C2	C1	C10	107.4(3)	O3	C19	C24	107.5(3)
C2	C1	C18	115.0(3)	C20	C19	C24	113.5(3)
C10	C1	C18	111.2(3)	C19	C20	C21	107.2(3)
O1	C2	C1	125.0(4)	C19	C20	C25	115.6(3)
O1	C2	C3	129.3(4)	C21	C20	C25	111.0(3)
C1	C2	C3	105.7(3)	C20	C21	C22	113.8(3)
C2	C3	C4	108.3(3)	C21	C22	C23	112.1(4)
C2	C3	C8	130.9(4)	C22	C23	C24	108.5(4)
C4	C3	C8	120.8(4)	C22	C23	C34	111.5(5)
N1	C4	C3	112.4(4)	C24	C23	C34	110.7(4)
N1	C4	C5	126.4(4)	C19	C24	C23	111.9(3)
C3	C4	C5	121.1(4)	C20	C25	C26	112.4(3)
C4	C5	C6	117.1(4)	C20	C25	C27	110.6(4)
C5	C6	C7	122.6(4)	C20	C25	C28	107.9(3)
C6	C7	C8	119.6(4)	C26	C25	C27	107.6(4)
C3	C8	C7	118.7(4)	C26	C25	C28	107.5(4)
N2	C9	C10	109.9(4)	C27	C25	C28	110.9(4)
C1	C10	C9	126.0(3)	C25	C28	C29	120.6(4)
C1	C10	C11	126.8(3)	C25	C28	C33	122.9(4)
C9	C10	C11	107.1(3)	C29	C28	C33	116.5(4)
C10	C11	C12	106.2(3)	C28	C29	C30	122.0(4)
C10	C11	C16	134.8(4)	C29	C30	C31	120.4(5)
C12	C11	C16	119.1(4)	C30	C31	C32	118.7(5)
N2	C12	C11	108.0(3)	C31	C32	C33	120.5(4)
N2	C12	C13	130.3(4)	C28	C33	C32	121.9(4)
C11	C12	C13	121.7(4)				

Table 5. Torsional Angles (deg)

Atom1	Atom2	Atom3	Atom4	Angle	Atom1	Atom2	Atom3	Atom4	Angle
C19	O3	C18	O2	-1.7(6)	C8	C3	C4	C5	1.1(6)
C19	O3	C18	C1	-179.1(3)	C2	C3	C8	C7	179.7(4)
C18	O3	C19	C20	159.4(3)	C4	C3	C8	C7	-0.7(6)
C18	O3	C19	C24	-78.1(4)	N1	C4	C5	C6	-179.1(4)
C4	N1	C1	C2	-10.3(4)	C3	C4	C5	C6	-0.8(6)
C4	N1	C1	C10	105.9(3)	C4	C5	C6	C7	0.2(7)
C4	N1	C1	C18	-131.7(3)	C5	C6	C7	C8	0.2(7)
C1	N1	C4	C3	7.4(4)	C6	C7	C8	C3	0.1(6)
C1	N1	C4	C5	-174.2(4)	N2	C9	C10	C1	-176.0(3)
C12	N2	C9	C10	0.2(4)	N2	C9	C10	C11	-0.5(4)
C17	N2	C9	C10	174.3(4)	C1	C10	C11	C12	176.1(3)
C9	N2	C12	C11	0.2(4)	C1	C10	C11	C16	-4.6(7)
C9	N2	C12	C13	-179.1(4)	C9	C10	C11	C12	0.6(4)
C17	N2	C12	C11	-173.8(4)	C9	C10	C11	C16	179.9(4)
C17	N2	C12	C13	6.9(7)	C10	C11	C12	N2	-0.5(4)
N1	C1	C2	O1	-172.2(4)	C10	C11	C12	C13	178.8(4)
N1	C1	C2	C3	9.6(4)	C16	C11	C12	N2	-179.9(3)
C10	C1	C2	O1	67.3(5)	C16	C11	C12	C13	-0.6(6)
C10	C1	C2	C3	-110.8(3)	C10	C11	C16	C15	-177.5(4)
C18	C1	C2	O1	-57.0(5)	C12	C11	C16	C15	1.7(6)
C18	C1	C2	C3	124.8(3)	N2	C12	C13	C14	178.3(4)
N1	C1	C10	C9	-12.6(5)	C11	C12	C13	C14	-0.9(6)
N1	C1	C10	C11	172.8(3)	C12	C13	C14	C15	1.3(7)
C2	C1	C10	C9	101.4(4)	C13	C14	C15	C16	-0.2(7)
C2	C1	C10	C11	-73.2(4)	C14	C15	C16	C11	-1.4(6)
C18	C1	C10	C9	-132.0(4)	O3	C19	C20	C21	171.2(3)
C18	C1	C10	C11	53.4(5)	O3	C19	C20	C25	-64.4(4)
N1	C1	C18	O2	-77.8(4)	C24	C19	C20	C21	52.5(4)
N1	C1	C18	O3	99.7(3)	C24	C19	C20	C25	176.9(3)
C2	C1	C18	O2	168.4(4)	O3	C19	C24	C23	-176.7(4)
C2	C1	C18	O3	-14.1(4)	C20	C19	C24	C23	-58.0(5)
C10	C1	C18	O2	46.1(5)	C19	C20	C21	C22	-51.9(5)
C10	C1	C18	O3	-136.4(3)	C25	C20	C21	C22	-179.0(4)
O1	C2	C3	C4	176.2(4)	C19	C20	C25	C26	64.5(5)
O1	C2	C3	C8	-4.2(7)	C19	C20	C25	C27	-55.8(5)
C1	C2	C3	C4	-5.7(4)	C19	C20	C25	C28	-177.2(3)
C1	C2	C3	C8	173.9(4)	C21	C20	C25	C26	-173.2(4)
C2	C3	C4	N1	-0.8(4)	C21	C20	C25	C27	66.5(5)
C2	C3	C4	C5	-179.2(4)	C21	C20	C25	C28	-54.9(5)
C8	C3	C4	N1	179.6(4)	C20	C21	C22	C23	56.7(5)

Table 5. Torsional Angles (continued)

Atom1	Atom2	Atom3	Atom4	Angle	Atom1	Atom2	Atom3	Atom4	Angle
C21	C22	C23	C24	-56.8(5)	C27	C25	C28	C33	-18.0(6)
C21	C22	C23	C34	-178.9(4)	C25	C28	C29	C30	-179.7(4)
C22	C23	C24	C19	57.5(5)	C33	C28	C29	C30	1.3(7)
C34	C23	C24	C19	-179.9(4)	C25	C28	C33	C32	179.9(4)
C20	C25	C28	C29	-75.7(5)	C29	C28	C33	C32	-1.0(7)
C20	C25	C28	C33	103.3(5)	C28	C29	C30	C31	-0.2(8)
C26	C25	C28	C29	45.7(6)	C29	C30	C31	C32	-1.2(8)
C26	C25	C28	C33	-135.3(5)	C30	C31	C32	C33	1.5(8)
C27	C25	C28	C29	163.0(4)	C31	C32	C33	C28	-0.3(8)

Table 6. Anisotropic Displacement Parameters (U_{ij} , Å²)

Atom	U_{11}	U_{22}	U_{33}	U_{23}	U_{13}	U_{12}
O1	0.0324(15)	0.0424(15)	0.0445(16)	-0.0008(13)	-0.0001(12)	0.0005(13)
O2	0.055(2)	0.0451(16)	0.0438(17)	-0.0075(13)	0.0036(14)	-0.0155(15)
O3	0.0420(16)	0.0361(14)	0.0307(13)	-0.0019(11)	0.0081(11)	-0.0054(12)
N1	0.0345(18)	0.0313(16)	0.0390(18)	0.0047(14)	-0.0065(14)	-0.0034(14)
N2	0.0406(19)	0.0418(18)	0.0304(16)	0.0033(14)	0.0047(14)	-0.0081(16)
C1	0.0267(19)	0.0301(17)	0.0301(18)	0.0029(14)	0.0006(14)	0.0009(16)
C2	0.035(2)	0.0338(19)	0.0298(18)	0.0015(15)	0.0024(15)	-0.0037(16)
C3	0.037(2)	0.0303(18)	0.0339(19)	0.0018(16)	0.0047(16)	-0.0008(17)
C4	0.040(2)	0.0335(19)	0.0311(19)	0.0048(15)	0.0021(16)	-0.0006(17)
C5	0.045(3)	0.040(2)	0.042(2)	0.0060(18)	0.0020(19)	0.010(2)
C6	0.068(3)	0.034(2)	0.048(3)	0.0045(18)	0.003(2)	0.006(2)
C7	0.066(3)	0.033(2)	0.050(3)	-0.0032(18)	0.006(2)	-0.006(2)
C8	0.049(3)	0.037(2)	0.046(2)	-0.0025(18)	0.005(2)	-0.008(2)
C9	0.035(2)	0.0318(19)	0.036(2)	0.0021(15)	-0.0006(15)	-0.0039(17)
C10	0.0321(19)	0.0275(17)	0.0301(18)	0.0016(14)	0.0010(14)	-0.0068(15)
C11	0.035(2)	0.0273(18)	0.036(2)	-0.0015(14)	-0.0054(16)	-0.0060(16)
C12	0.048(3)	0.0328(19)	0.035(2)	0.0019(16)	-0.0071(18)	-0.0116(19)
C13	0.064(3)	0.043(2)	0.042(2)	0.0121(18)	-0.012(2)	-0.017(2)
C14	0.068(4)	0.036(2)	0.063(3)	0.011(2)	-0.024(3)	-0.004(2)
C15	0.048(3)	0.040(2)	0.061(3)	-0.003(2)	-0.012(2)	0.009(2)
C16	0.044(2)	0.037(2)	0.042(2)	-0.0020(17)	-0.0067(19)	-0.0004(18)
C17	0.059(3)	0.073(3)	0.037(2)	-0.002(2)	0.015(2)	-0.018(3)
C18	0.038(2)	0.0355(19)	0.0289(18)	0.0028(15)	-0.0016(16)	-0.0026(17)
C19	0.043(2)	0.037(2)	0.0263(18)	-0.0015(15)	0.0043(16)	-0.0006(18)
C20	0.038(2)	0.038(2)	0.0310(19)	0.0007(16)	0.0009(16)	-0.0006(18)
C21	0.055(3)	0.048(2)	0.035(2)	0.0006(18)	0.0073(19)	0.010(2)
C22	0.062(3)	0.052(3)	0.041(2)	-0.0025(19)	0.009(2)	0.017(2)
C23	0.077(4)	0.039(2)	0.036(2)	-0.0018(18)	0.000(2)	0.010(2)
C24	0.052(3)	0.039(2)	0.035(2)	-0.0001(17)	0.0019(18)	0.002(2)
C25	0.041(2)	0.044(2)	0.039(2)	0.0084(18)	0.0050(18)	0.003(2)
C26	0.078(4)	0.047(3)	0.053(3)	0.010(2)	0.021(3)	0.019(3)
C27	0.043(3)	0.063(3)	0.064(3)	0.021(2)	-0.003(2)	0.001(2)
C28	0.042(2)	0.036(2)	0.040(2)	0.0050(17)	0.0025(18)	0.0045(18)
C29	0.065(3)	0.044(2)	0.041(2)	-0.002(2)	-0.001(2)	-0.006(2)
C30	0.055(3)	0.045(3)	0.062(3)	0.000(2)	0.003(2)	-0.009(2)
C31	0.051(3)	0.051(3)	0.059(3)	0.013(2)	0.010(2)	-0.004(2)
C32	0.059(3)	0.062(3)	0.042(2)	0.012(2)	0.002(2)	-0.005(2)

Table 6. Anisotropic Displacement Parameters (continued)

Atom	U_{11}	U_{22}	U_{33}	U_{23}	U_{13}	U_{12}
C33	0.052(3)	0.054(3)	0.040(2)	0.004(2)	-0.004(2)	-0.011(2)
C34	0.122(6)	0.047(3)	0.055(3)	0.000(2)	0.004(3)	0.029(3)

The form of the anisotropic displacement parameter is:

$$\exp[-2\pi^2(h^2a^2U_{11} + k^2b^2U_{22} + l^2c^2U_{33} + 2klb^*c^*U_{23} + 2hla^*c^*U_{13} + 2hka^*b^*U_{12})]$$

Table 7. Derived Atomic Coordinates and Displacement Parameters for Hydrogen Atoms

Atom	<i>x</i>	<i>y</i>	<i>z</i>	$U_{eq}, \text{\AA}^2$
H1N	-0.0325	0.3914	0.1461	0.042
H5	-0.1571	0.6497	0.1491	0.051
H6	-0.0318	0.8654	0.1597	0.060
H7	0.3167	0.9032	0.1757	0.059
H8	0.5522	0.7225	0.1815	0.053
H9	-0.0519	0.3464	0.2075	0.041
H13	0.3003	0.0154	0.2690	0.060
H14	0.6147	-0.0874	0.2539	0.067
H15	0.7806	-0.0285	0.2094	0.060
H16	0.6325	0.1354	0.1790	0.049
H17A	-0.0889	0.1167	0.2665	0.084
H17B	-0.1805	0.2592	0.2566	0.084
H17C	0.0251	0.2510	0.2775	0.084
H19	0.4127	0.1765	0.0859	0.042
H20	0.7919	0.3403	0.0857	0.043
H21A	0.6456	0.1753	0.0376	0.055
H21B	0.8593	0.2630	0.0373	0.055
H22A	0.9399	0.0343	0.0454	0.062
H22B	1.0171	0.1230	0.0728	0.062
H23	0.6324	-0.0313	0.0714	0.061
H24A	0.7972	0.1269	0.1191	0.050
H24B	0.5842	0.0383	0.1208	0.050
H26A	0.3711	0.4773	0.0982	0.089
H26B	0.5909	0.5573	0.0943	0.089
H26C	0.3887	0.5944	0.0742	0.089
H27A	0.2455	0.3197	0.0589	0.085
H27B	0.2584	0.4414	0.0360	0.085
H27C	0.3796	0.3040	0.0290	0.085
H29	0.8632	0.5892	0.0698	0.060
H30	1.0886	0.7038	0.0378	0.065
H31	1.0517	0.6797	-0.0131	0.064
H32	0.7935	0.5329	-0.0314	0.065
H33	0.5666	0.4196	0.0006	0.058
H34A	0.7953	-0.1647	0.1080	0.112
H34B	0.9357	-0.1678	0.0785	0.112
H34C	1.0090	-0.0773	0.1058	0.112

Appendix V: Selected NMR Spectra (Chapter Three)



Agilent Technologies

Department of Chemistry, University of Alberta

Recorded on: 4/8/05, Mon 4:28:15

File Name: 1356891.D

File Sequence: 01

Integration File: 318894.7

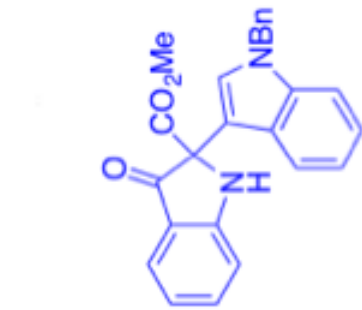
Digital Resolution: 0.39

Acquisition Format: 2.3

Resolution (ppm): 0.5

Completed Scans: 128

1356891.D is cdcd3.fid, is cdcd3.fid, temp 27.7 C, actual temp = 27.6 C, external probe



77.320
79.000
75.810
72.491
59.820
50.443

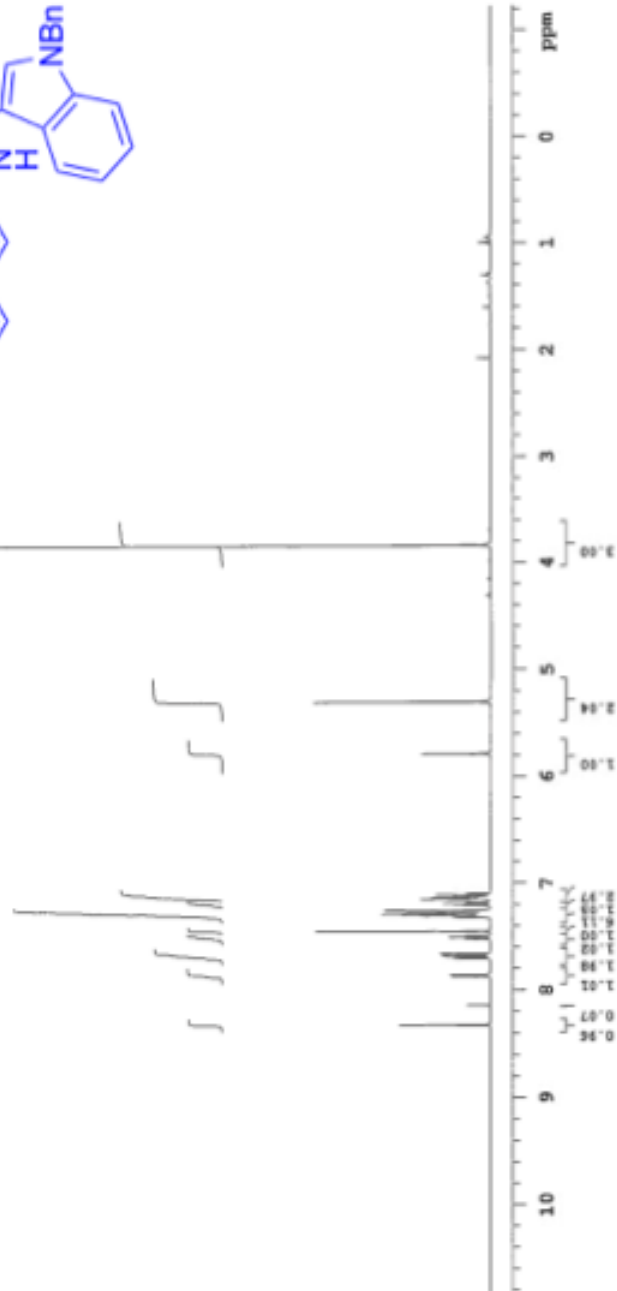
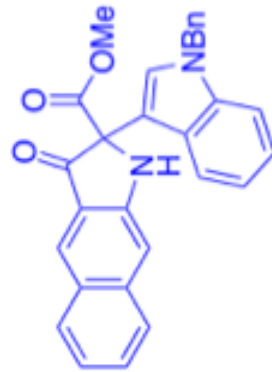
189.061
181.043
137.913
137.036
136.958
128.841
127.768
127.513
126.920
126.211
125.496
122.443
120.414
120.218
119.960
119.059
113.046
110.527
110.361

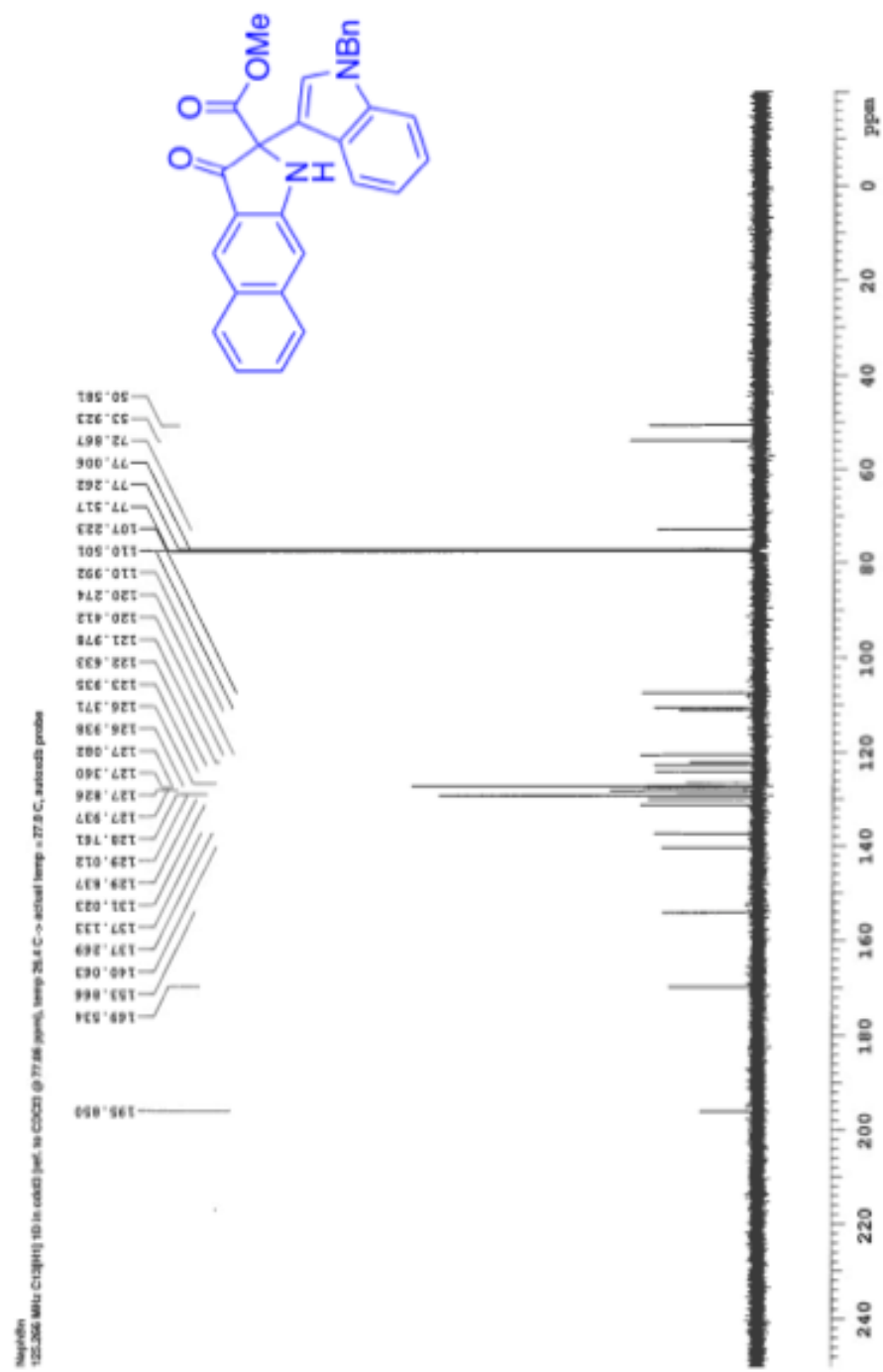
194.740



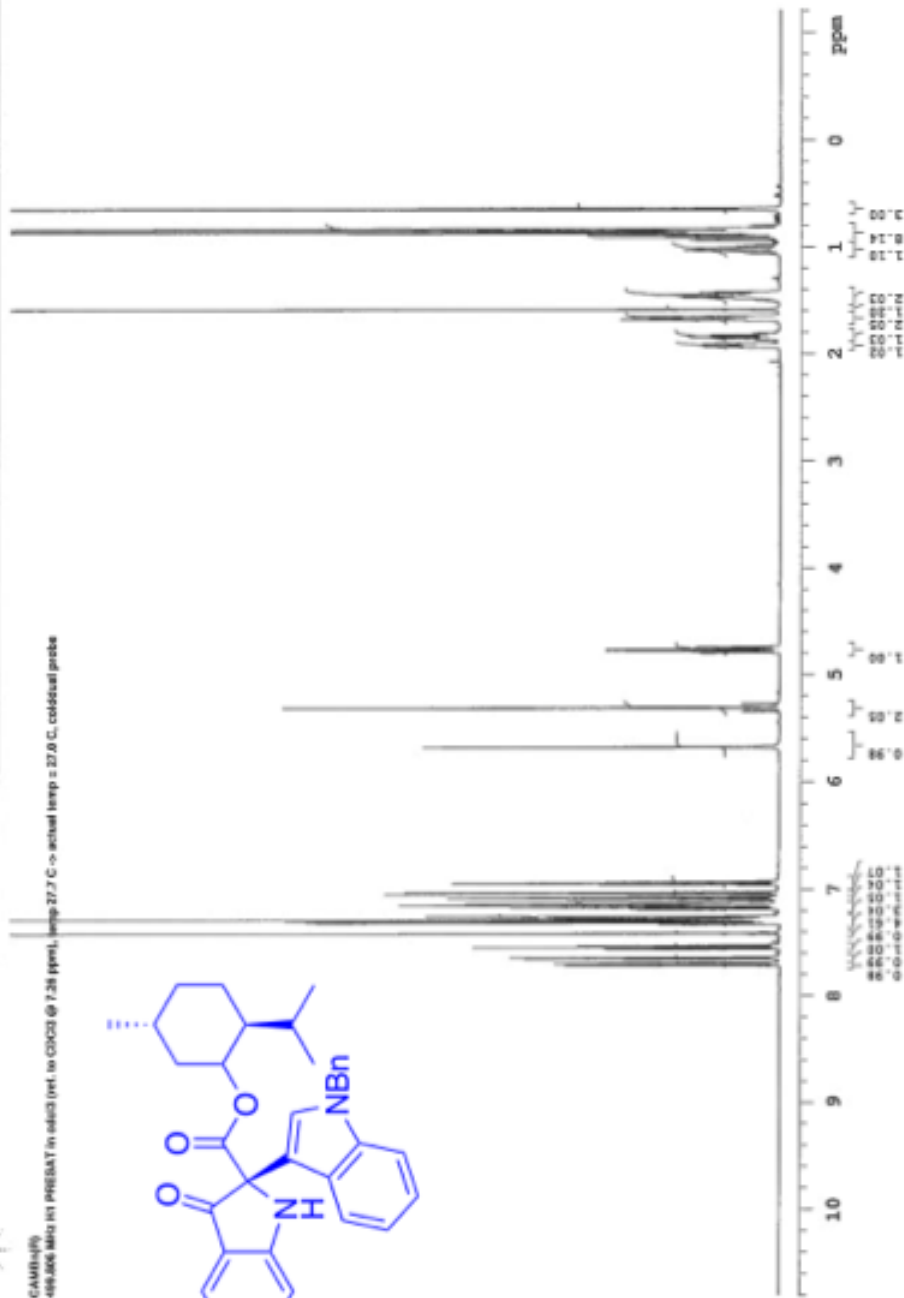
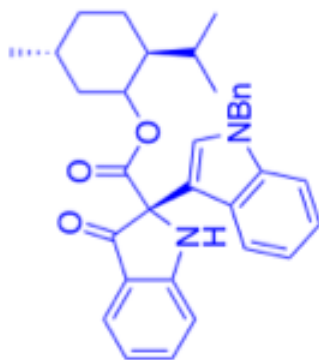


MSK118 400 MHz ¹H NMR (CDCl₃) (4.0 ppm), temp 30.4 C → actual temp is 27.8 C, autoedit proton



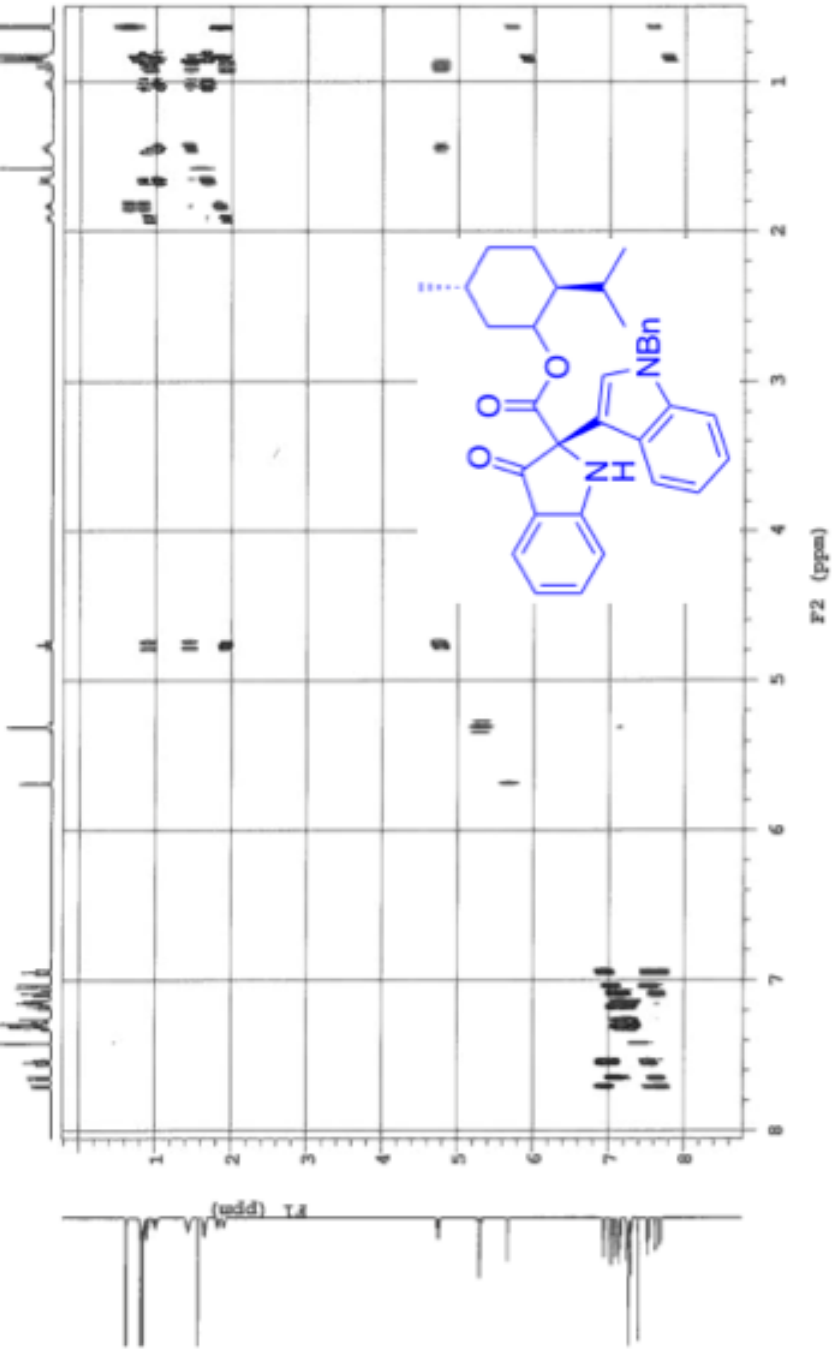


GAMBI(16)
 499.906 MHz (1) PRESAT in cdcl3 (ref. to CDCl3 @ 7.26 ppm), temp 37.7 C -> actual temp = 37.0 C, coldstart probe

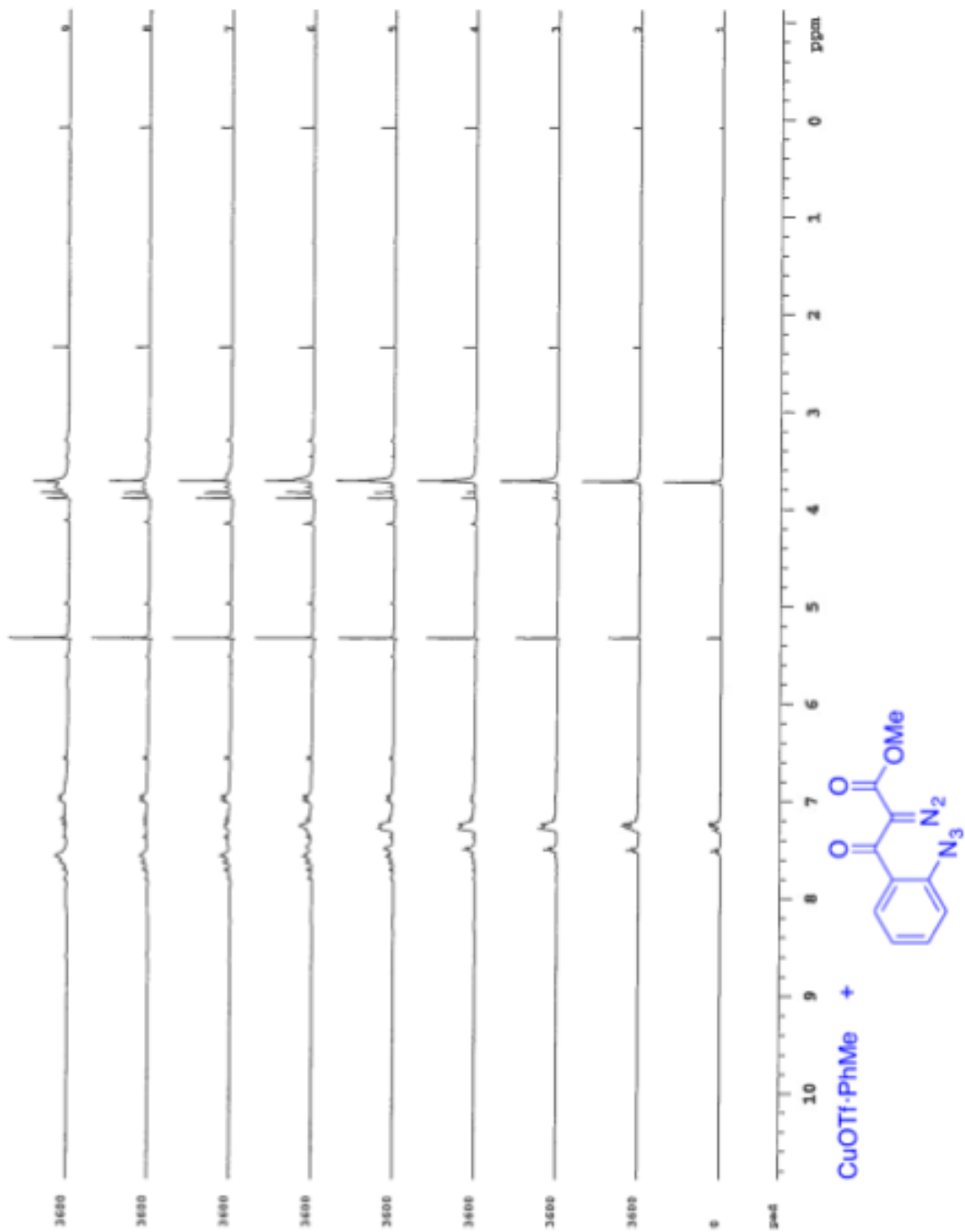




CAUTION!
651306.MU.int.gCOSY is locked (ref. to CDCl3 @ 7.26 ppm), temp 27.7 C -- actual temp is 27.8 C, cddkbaal.paste



Appendix VI: Mechanistic studies (Monitoring Decomposition of Diazo Azide in the Presence of Copper (I) catalyst, Using NMR Spectroscopy) (Chapter Three)

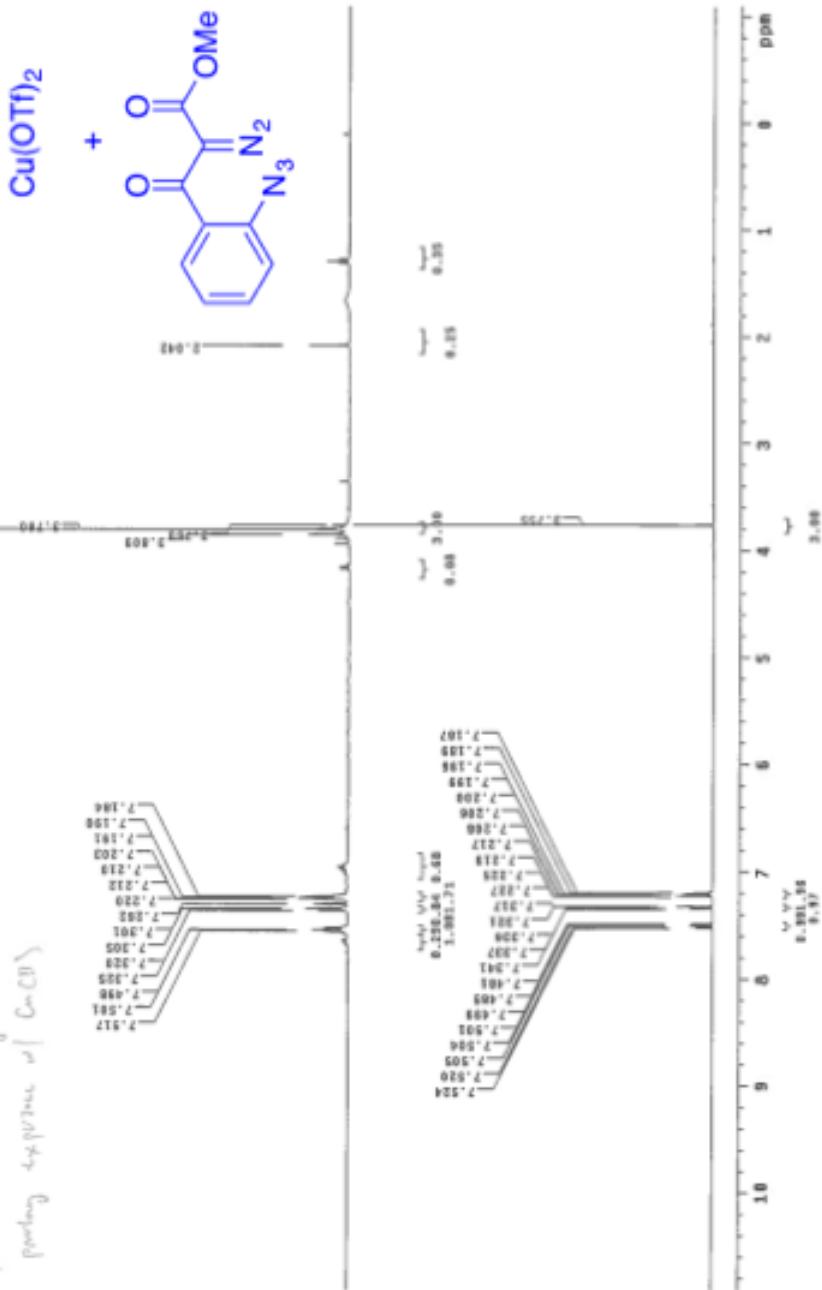


Appendix VII: Mechanistic studies (Comparison of Diazo Azide Decomposition In the Presence of Copper(II) and Copper(I) Catalyst) (Chapter Three)

TOP: Cu(II), + DIAZONIUM SUBSTRATE AFTER 9 DAYS STIRRING CDCl3 3H
BOTTOM: PURE DIAZONIUM SUBSTRATE CDCl3 3H
355.734 MHz in CDCl3 (ref. to CDCl3 @ 7.26 ppm), temp 26.5 C -> actual temp = 27.8 C, autoval probe

Pulse Sequence: zgpg30

*No substitution observed on
purity experiment w/ Cu(II)*

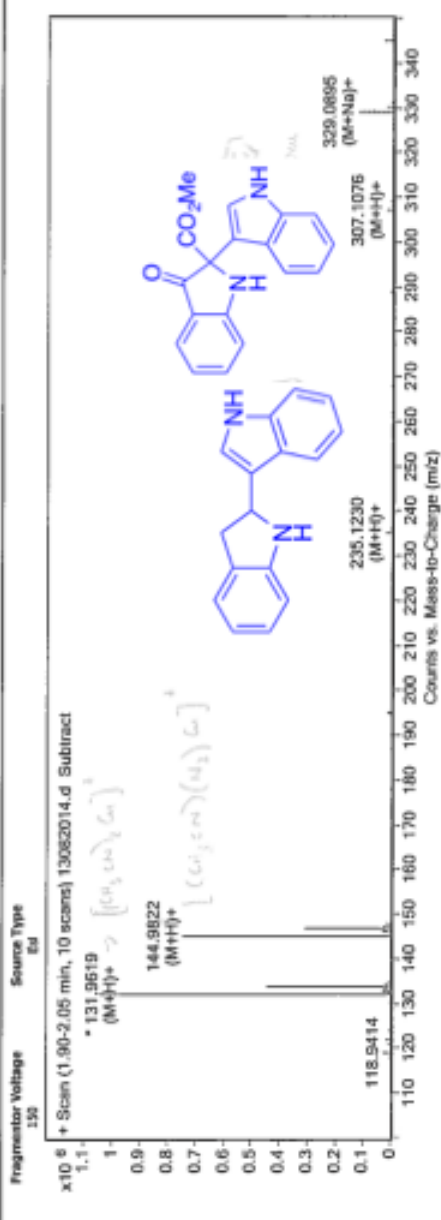


Appendix VIII: Mechanistic studies (Detection of Dimer, Indicative of Formation of Triflic Acid) (Chapter Three)

Department of Chemistry Mass Spectrometry Laboratory

Name B. Atienza, F. West **Sample Name** Cu(II+indole+1-diazazolo
Data Filename 13062014.d **Instrument Name** eaTOF6270
Position -1 **Operator** Randy
Acq Method **DA Method** DA_Low_Mass.m

User Spectra



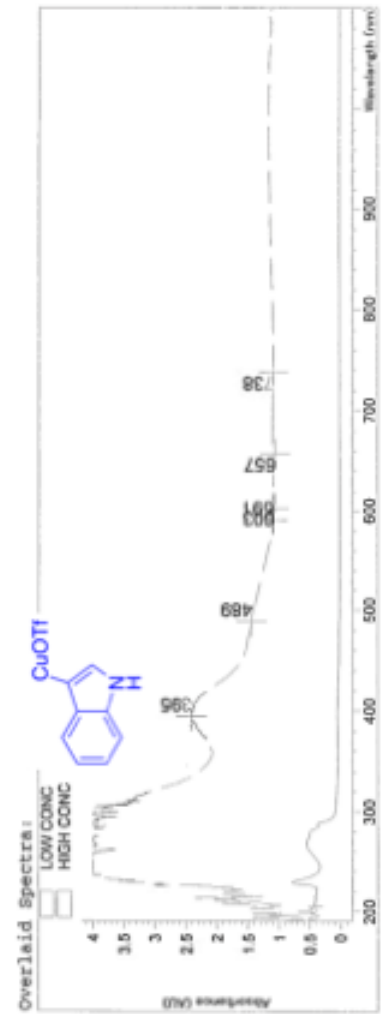
Formula Calculator Results

Formula	Ion Species	m/z	Calc. m/z	Diff (mDa)	Diff (ppm)	DBE	Ion	Score
C4 H5 Cu N2	C4 H5 Cu N2	144.9822	144.9822	-0.02	-0.14		(M+H) ⁺	96.18
C2 H2 Cu N3	C2 H3 Cu N3	131.9619	131.9617	-0.12	-0.93		(M+H) ⁺	97.21
C16 H14 N2	C16 H15 N2	235.123	235.123	-0.03	-0.15	11	(M+H) ⁺	97.89
C18 H14 N2 O3	C18 H14 N2 Na O3	329.0895	329.0897	0.2	0.64	13	(M+Na) ⁺	98.94
C18 H14 N2 O3	C18 H15 N2 O3	307.1076	307.1077	0.05	0.16	13	(M+H) ⁺	64.3

--- End Of Report ---

**Appendix IX: Mechanistic Studies (UV-VIS Detection of Copper Complex) (Chapter
Three)**

Method file : <untitled>
 Information : Default Method
 Data File : <untitled>



#	Name	Peaks (nm)	Abs (AU)	Valleys (nm)	Abs (AU)
1	LOW CONC	229.0	0.79478	590.0	1.7186E-2
1	LOW CONC	268.0	0.55188	568.0	1.7265E-2
1	LOW CONC	287.0	0.38234	596.0	1.7889E-2
2	HIGH CONC	395.0	2.43560	657.0	1.06600
2	HIGH CONC	489.0	1.44140	603.0	1.08560
2	HIGH CONC	591.0	1.09860	738.0	1.08990

**Appendix X: Determination of Diastereomeric Ratio Using HPLC
(Chapter Three)**

Include summary statistics for standard samples
 Include individual values for standard samples

Report Output
 Save report to file
 Save calibration summary
 Save unknown summary
 Print: <nothing>
 Print Calibration: <nothing>

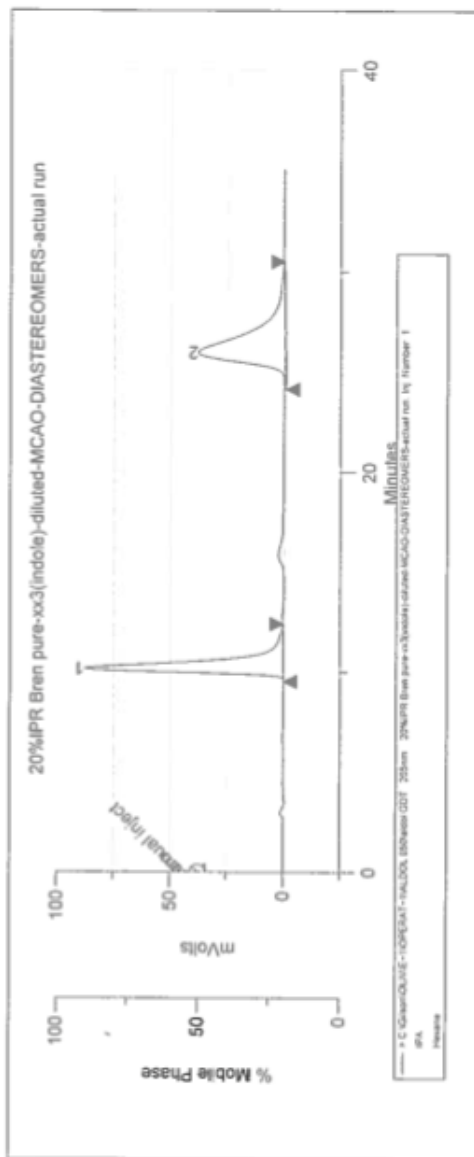
Peak Analysis Error Conditions

Background Blank Removal
 <None>

Track peak retention time

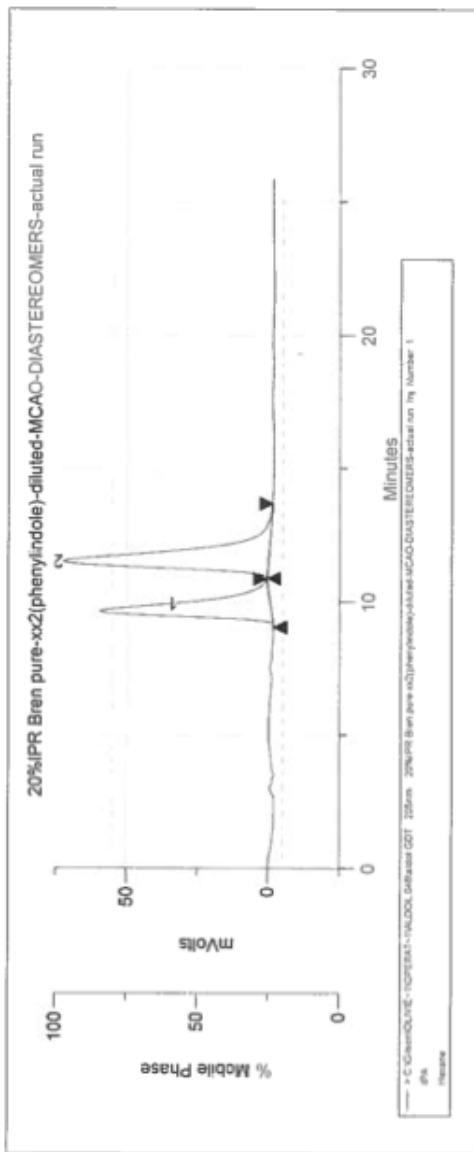
Peak Table
 <None>

Peak Detection Parameters
 Relative Error: 5 (%) Absolute Error: 0.1 (min)



Inj. Number	Peak Name	R. Time	Area	Sample Descrip.
1	*1	10.17	5364012.00	diluted-MCAC
2	*2	25.95	6361793.50	diluted-MCAC

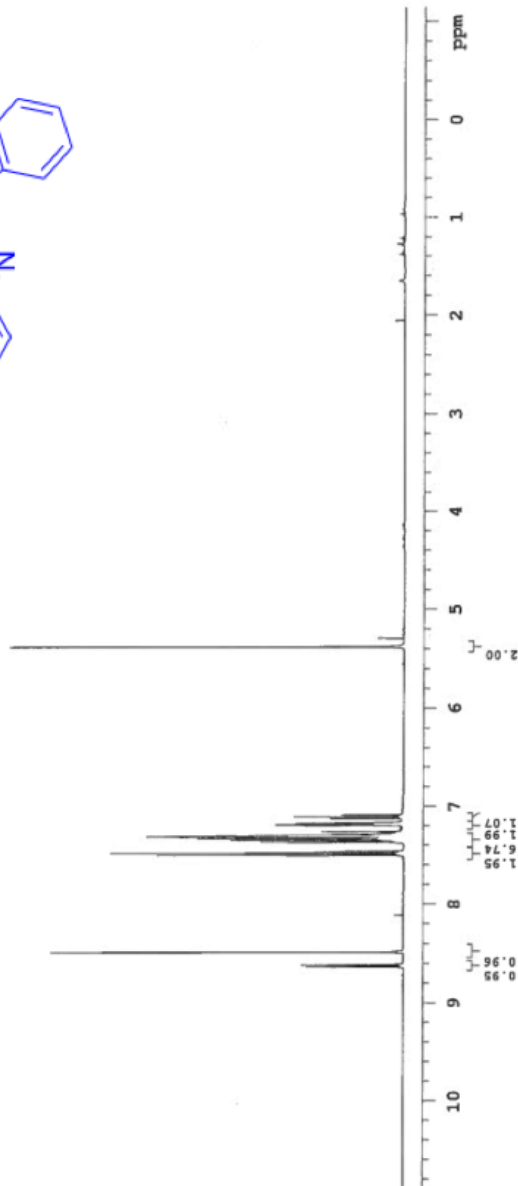
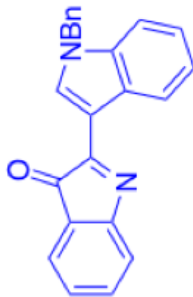
Report Output
 Save report to file
 Save calibration summary
 Save unknown summary
 Print: <nothing>
 Print Calibration: <nothing>
 Peak Analysis Error Conditions
 Background Blank Removal
 <None>
 Track peak retention time
 Peak Table
 <None>
 Peak Detection Parameters
 Relative Error: 5 (%) Absolute Error: 0.1 (min)



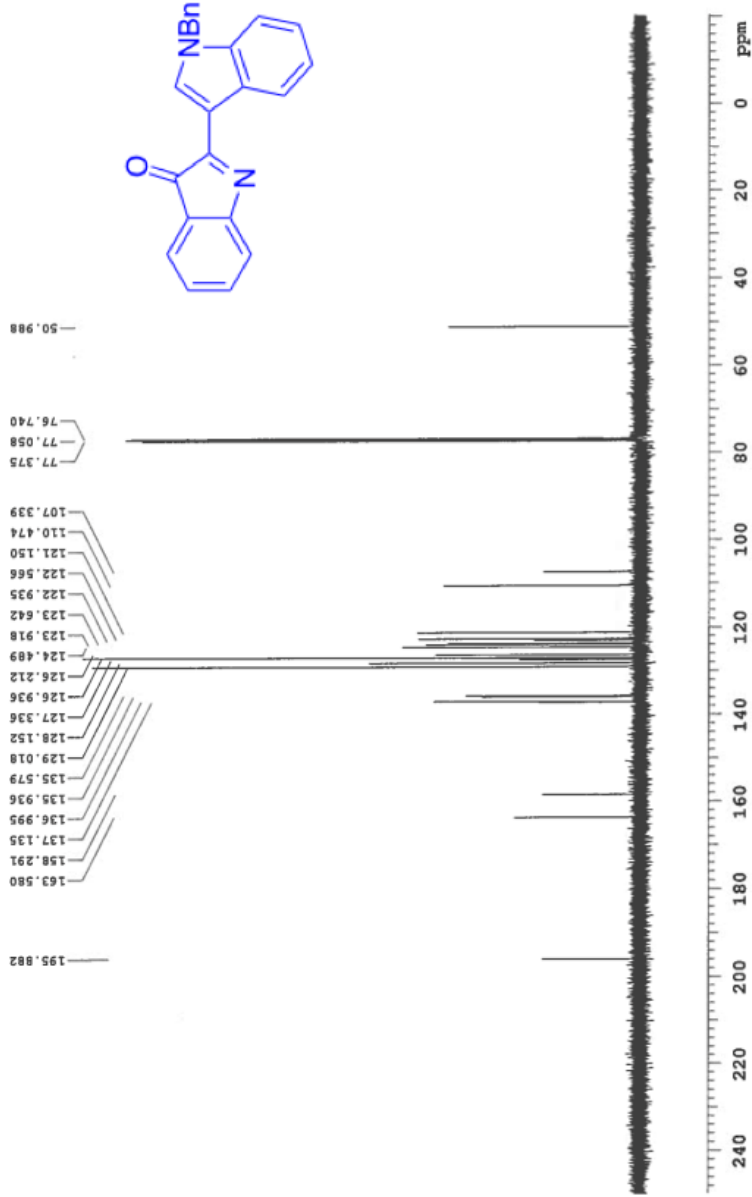
Inj. Number	Peak Name	R. Time	Area	Sample Descrip.
1	*1	9.63	3643997.25	ienylindole)-diluted-MCAO-DIA
2	*2	11.51	5086082.00	ienylindole)-diluted-MCAO-DIA

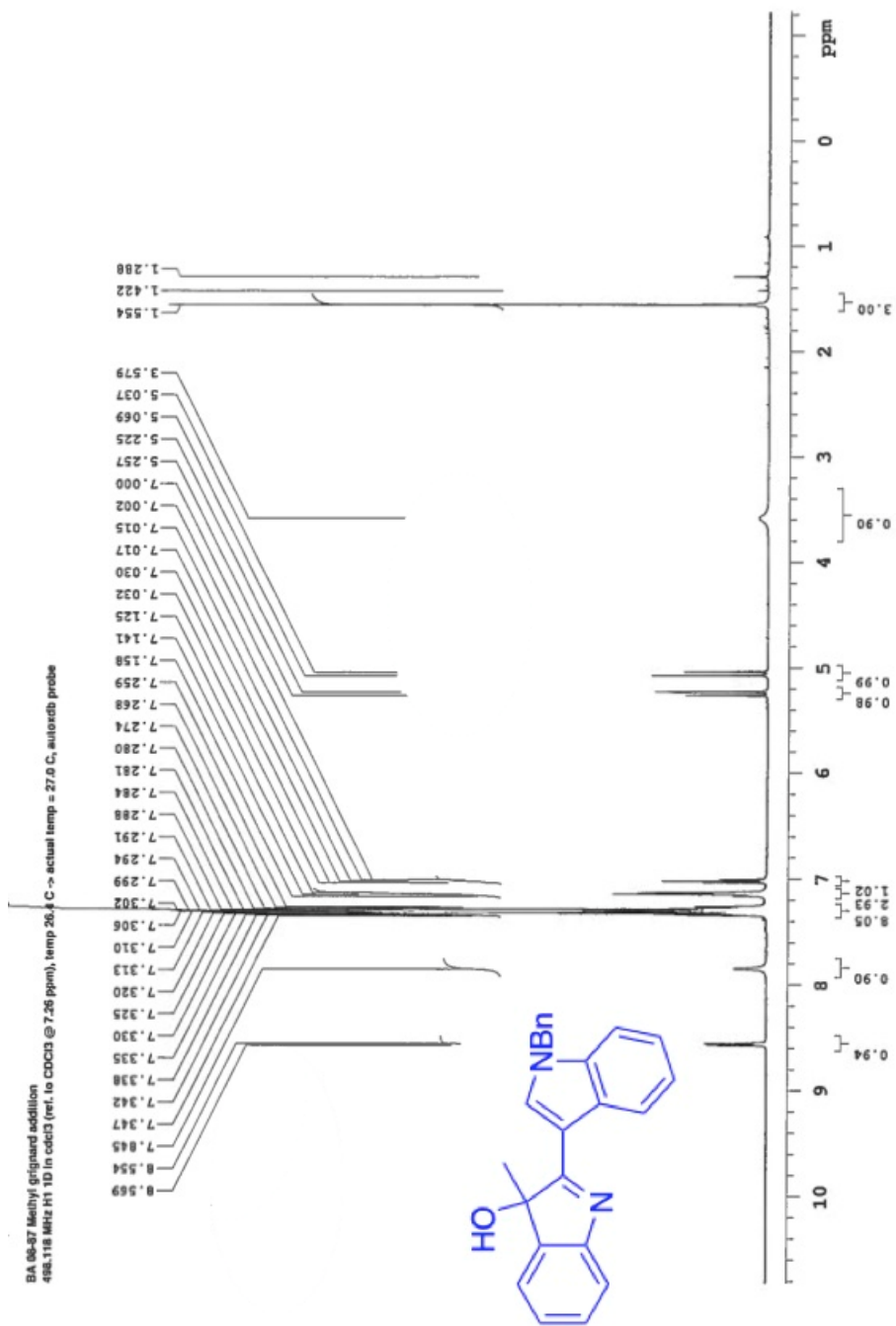
Appendix XI: Selected NMR Spectra (Chapter Four)

NBn-c-ACYLMINE
399.864 MHz H1 1D in cdcl3 (ref. to CDCl3 @ 7.26 ppm), temp 25.9 C -> actual temp = 27.0 C, oneimm probe



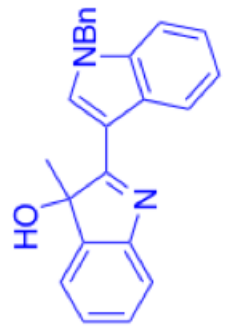
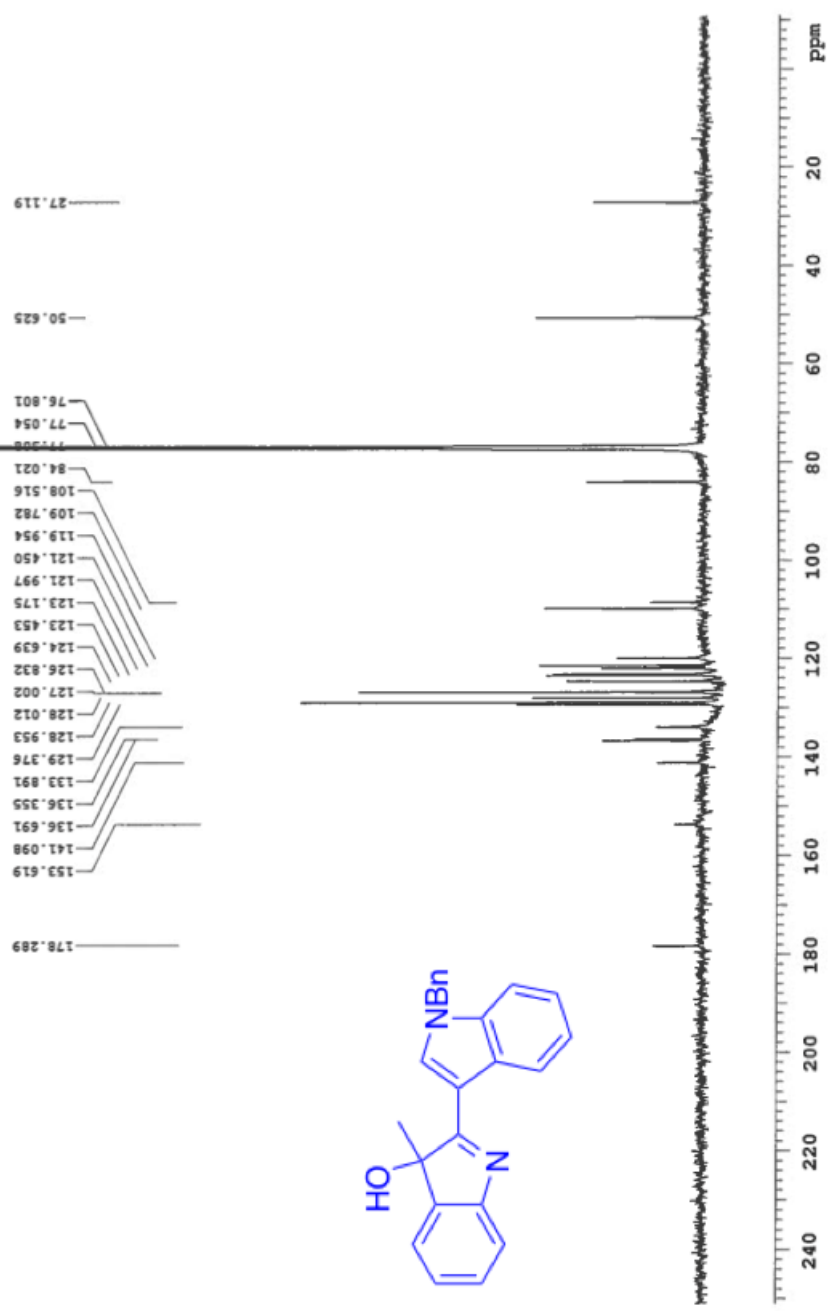
HbN C-acetylmide
100.587 MHz C13[1H] 1D in cdcl3 (ref. to CDCl3 @ 77.06 ppm), temp 25.9 C -> actual temp = 27.0 C, onemym probe



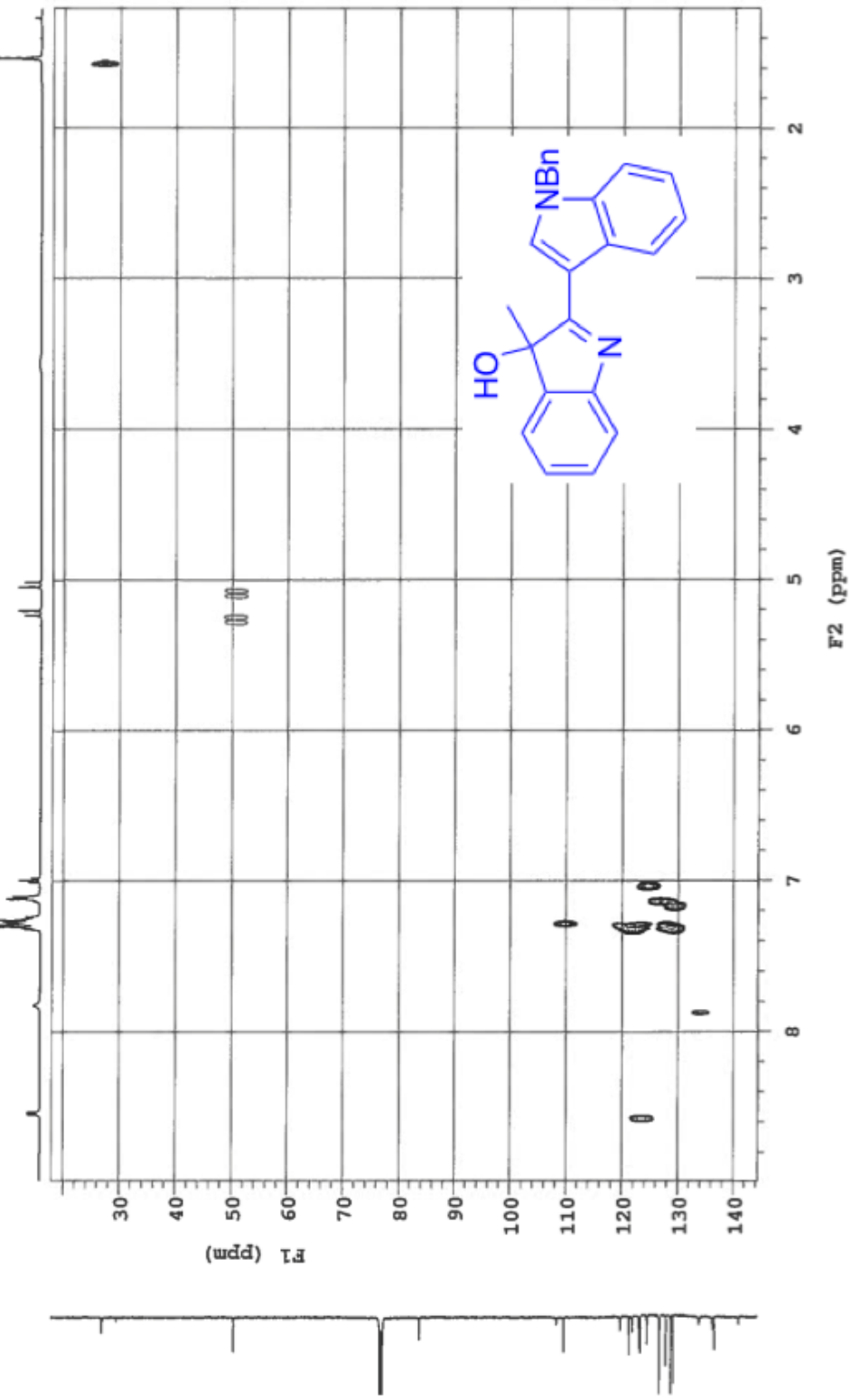


Department of Chemistry, University of Alabama
 Recorded on: **u500, Jan 28 2016** Scan: 1, 4487-13 **22042.7** Retention: 4.07 min **4.1**
 Pulse Sequence: **zgpg30** Digital Res (Hz): **0.25** Hz per amp(Hz): **137.06** Completed Scans: **120**

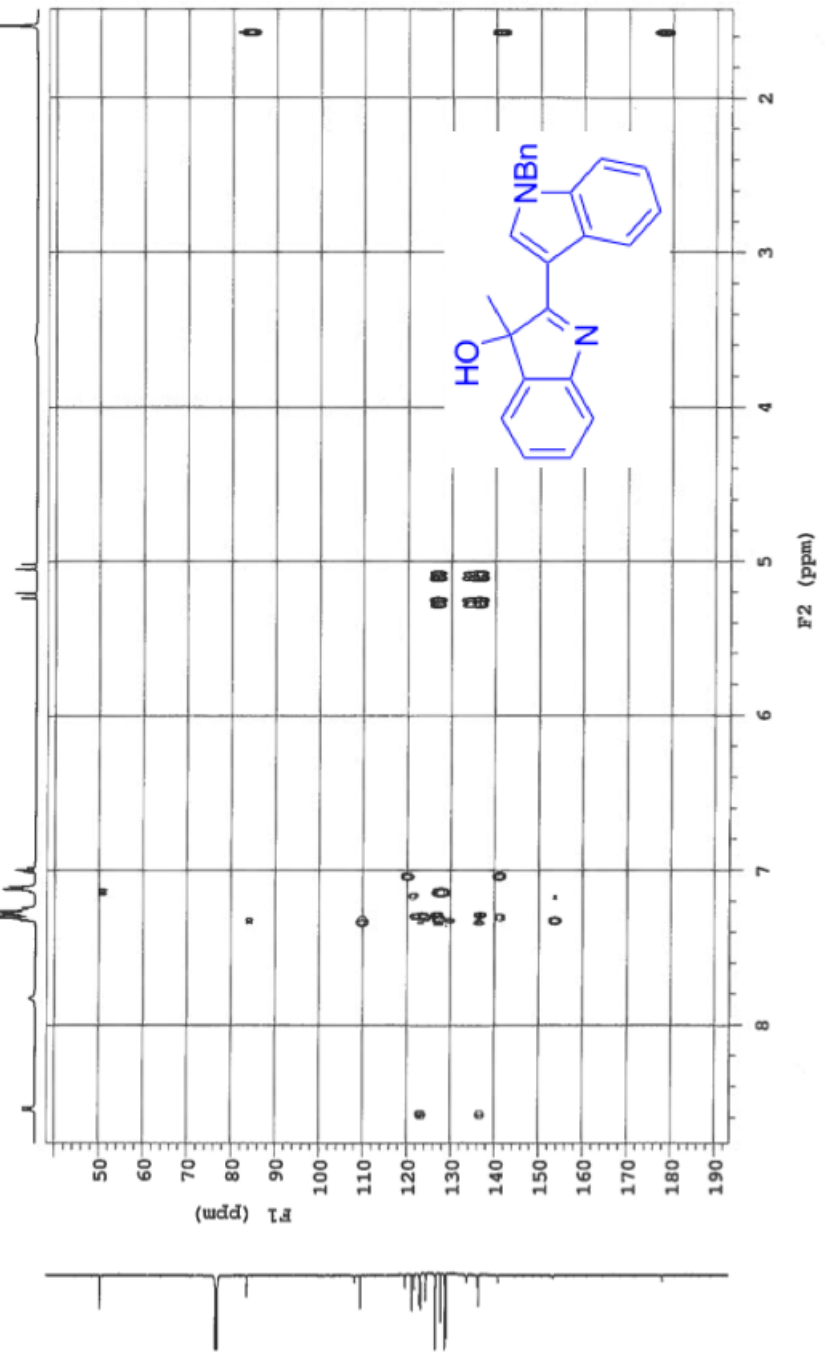
Brenn-Jordan, BA_08-86_Methyl_ergoguard_addition
 125.691 MHz C13(1H) 1D in cdcl3 (ref. to CDCl3 @ 77.06 ppm), temp 27.7 C -> actual temp = 27.0 C, collisional probe

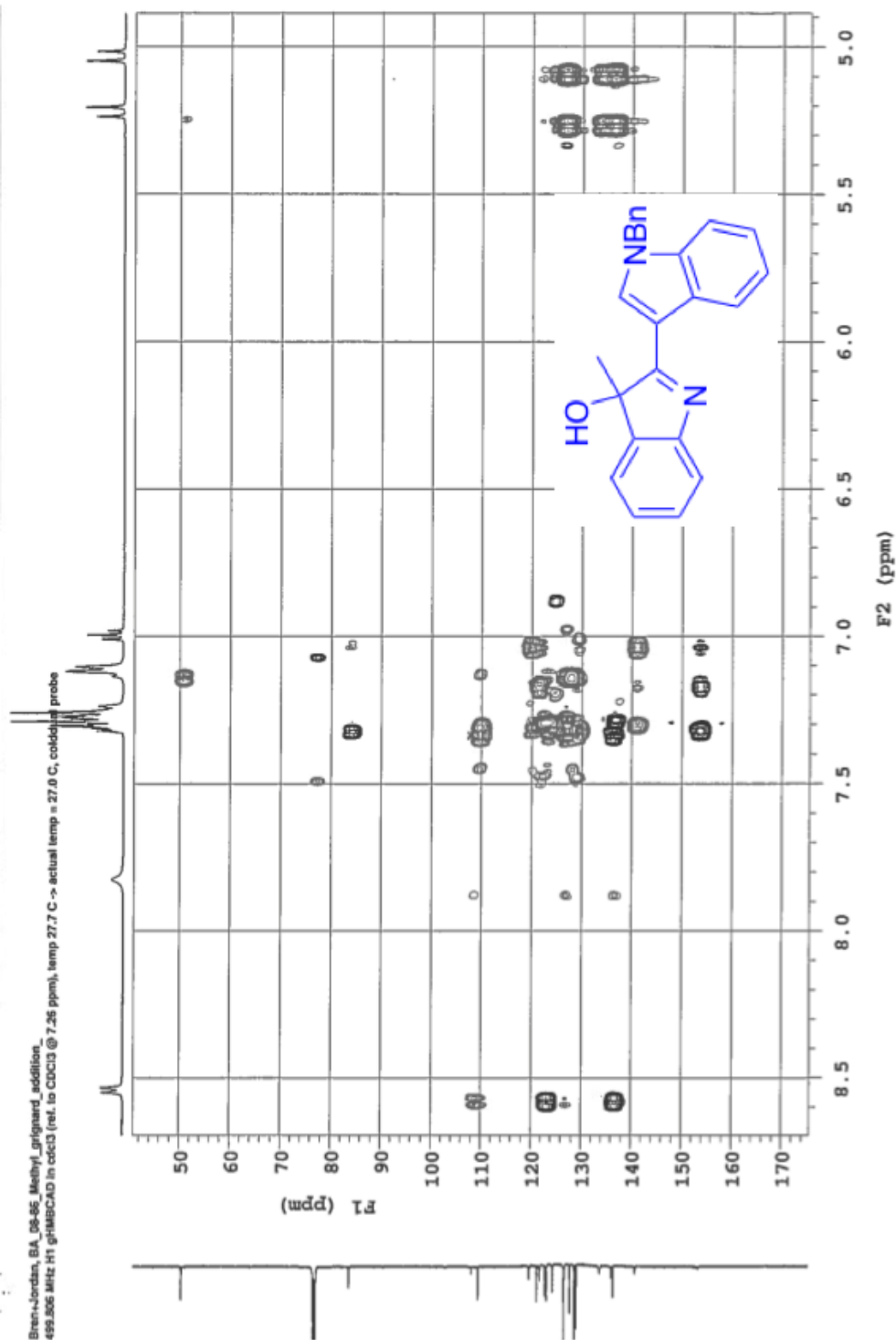


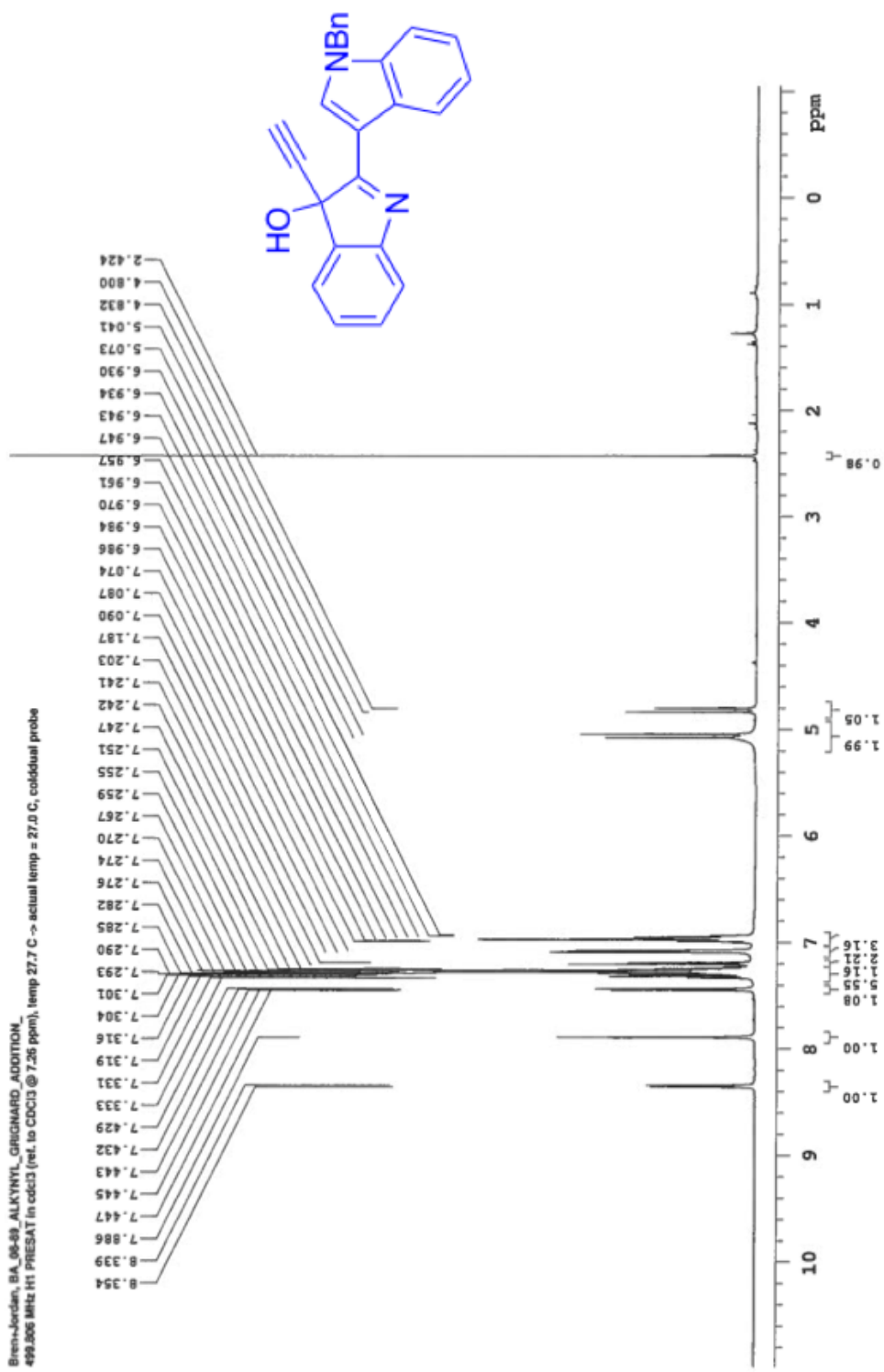
Biren-Jordan, BA_09-26_Methyl_gripward_addition_489.806 MHz 1H gHSQCAD in cdcl3 (ref. to CDCl3 @ 7.2677706 ppm), temp 27. C -> actual temp = 27.0 C, coaddidial probe



Brenn-Jordan, BA_08-05_Methyl_glnigand_addition_499.806 MHz ¹H gmsbpcad in cdcl3 (ref. to CDCl3 @ 7.26 ppm), temp 27.7 C -> actual temp = 27.8 C, coldlual probe







BA 06-9X ALKYNYL GRIGNARD ADDITION
100.587 MHz C13[1H] 1D in cdcl3 (ref. to CDCl3 @ 77.06 ppm), temp 25.9 C -> actual temp = 27.0 C, onenmr probe

